

DOCTORAL THESIS

Metabolic Characterization and Composition Control of Next Generation Probiotic Consortia

Anna Kattel

TALLINN UNIVERSITY OF TECHNOLOGY
DOCTORAL THESIS
62/2025

Metabolic Characterization and Composition Control of Next Generation Probiotic Consortia

ANNA KATTEL



TALLINN UNIVERSITY OF TECHNOLOGY

School of Science

Department of Chemistry and Biotechnology

This dissertation was accepted for the defence of the degree Doctor of Philosophy in Chemistry 08/07/2025.

Supervisor:

Professor Emeritus Raivo Vilu
Tallinn University of Technology
Tallinn, Estonia

Co-supervisor:

Dr. Ranno Nahku
TFTAK
Tallinn, Estonia

Opponents:

Dr. Stéphane Chaillou
Biosphera Graduate School
INRAE, Micalis Institute
Paris-Saclay University
Paris, France

Professor Jaak Truu
Faculty of Science and Technology
Institute of Molecular and Cell Biology
University of Tartu
Tartu, Estonia

Defence of the thesis: 10/09/2025, Tallinn

Declaration:

Hereby I declare that this doctoral thesis, my original investigation and achievement, submitted for the doctoral degree at Tallinn University of Technology has not been submitted for doctoral or equivalent academic degree.

Anna Kattel

signature



Copyright: Anna Kattel, 2025

ISSN 2585-6898 (publication)

ISBN 978-9916-80-358-5 (publication)

ISSN 2585-6901 (PDF)

ISBN 978-9916-80-359-2 (PDF)

DOI <https://doi.org/10.23658/taltech.62/2025>

Kattel, A. (2025). *Metabolic Characterization and Composition Control of Next Generation Probiotic Consortia* [TalTech Press]. <https://doi.org/10.23658/taltech.62/2025>

TALLINNA TEHNIKAÜLIKOOL
DOKTORITÖÖ
62/2025

Uue põlvkonna probiootiliste koosluste koostise kontroll ja metaboolne iseloomustus

ANNA KATTEL



Contents

List of Publications	7
Author's Contribution to the Publications	8
Introduction	9
Abbreviations	10
1 Literature Review	11
1.1 Definition and evolution of the microbiome field.....	11
1.2 Probiotics, next-generation probiotics, and synthetic consortia	12
1.3 Advantages and challenges of microbial consortia	15
1.4 Isothermal microcalorimetry	16
1.5 Short-chain fatty acids metabolism and genome-scale metabolic models	17
1.6 Viable cell quantification methods	20
2 Aims of the Study	22
3 Materials and Methods.....	23
3.1 Strains	23
3.2 Media	23
3.3 Cultivation	24
3.4 Microscopy and image analysis.....	25
3.5 Quantification of extracellular metabolites	25
3.6 Flow cytometry	26
3.7 DNA extraction	26
3.8 PMAx treatment and spike-in control.....	26
3.9 Quantitative real-time PCR	26
3.10 16S rRNA NGS.....	27
3.11 Construction of metabolic networks and flux balance analysis.....	27
4 Results and Discussion	28
4.1 Creation of the model consortium.....	28
4.2 Stability and resilience of a defined human gut microbiota consortium assessed with isothermal microcalorimetry (Publication I)	29
4.3 Evaluating diversity of 25-species model consortium (Unpublished data).....	34
4.4 Analysis of metabolism in co-cultures of <i>Anaerostipes caccae</i> and <i>Bacteroides</i> spp. (Publication II)	34
4.4.1 Screening and genome annotation analysis of candidate species	34
4.4.2 Establishing and validating co-cultures based on substrate specificity	36
4.4.3 Co-culture metabolic interactions	37
4.4.4 Species ratio determination.....	39
4.4.5 Development of co-culture bioprocess.....	40
4.4.6 Altering substrate ratios and characterizing metabolic interactions with FBA.....	41
4.5 Estimation of viable cell abundance and enumeration using PMAx and spike-in control as alternatives to traditional methods (Publication III)	44
4.5.1 Estimation of viable cell abundance using PMAx-qPCR	44
4.5.2 Bacterial enumeration using spike-in and NGS.....	47
4.5.3 Combining PMAx treatment and spike-in control.....	48
5 Conclusions	50
References	51

Acknowledgements.....	63
Abstract.....	64
Lühikokkuvõte.....	66
Appendix 1	67
Appendix 2	81
Appendix 3	95
Appendix 4	109
Curriculum vitae.....	121
Elulookirjeldus.....	123

List of Publications

The list of author's publications, on the basis of which the thesis has been prepared:

- I **Kattel, A.**, Aro, V., Lahtvee, P. J., Kazantseva, J., Jõers, A., Nahku, R., & Belouah, I. (2024). Exploring the resilience and stability of a defined human gut microbiota consortium: An isothermal microcalorimetric study. *MicrobiologyOpen*, 13(4). <https://doi.org/10.1002/mbo3.1430>
- II **Kattel, A.**, Morell, I., Aro, V., Lahtvee, P. J., Vilu, R., Jõers, A., & Nahku, R. (2023). Detailed analysis of metabolism reveals growth-rate-promoting interactions between *Anaerostipes caccae* and *Bacteroides* spp. *Anaerobe*, 79. <https://doi.org/10.1016/j.anaerobe.2022.102680>
- III Kallastu, A., Malv, E., Aro, V., Meikas, A., Vendelin, M., **Kattel, A.**, Nahku, R., & Kazantseva, J. (2023). Absolute quantification of viable bacteria abundances in food by next-generation sequencing: Quantitative NGS of viable microbes. *Current Research in Food Science*, 6(December 2022), 100443. <https://doi.org/10.1016/j.crfs.2023.100443>

Author's Contribution to the Publications

Contribution to the papers in this thesis are:

- I The author participated in the study design, experimental work and in data curation. She also participated in the editing of the manuscript.
- II The author participated in the study design and performed all the in vitro experimental work. She collected, calculated and interpreted the data, and wrote the manuscript draft. She also edited the manuscript.
- III The author participated in the experimental work and editing of the manuscript.

Introduction

The human gut microbiome plays an important role in host health, influencing various processes like nutrient digestion, immune system development and resistance to pathogens. While traditional probiotics have been used for decades to support gut health, their clinical efficiency is limited to definite strains. This has led to the emergence of next-generation probiotics (NGP), consisting of commensal microbes with targeted health benefits. However, many promising NGP candidates are strict anaerobes with poorly understood metabolic requirements, presenting significant production challenges. These may include maintaining strict anaerobic conditions, achieving consistent yields, and preserving wanted species ratios.

One potential solution is the use of defined microbial consortia – multi-strain consortia cultivated in controlled conditions, where each species is chosen with a specific purpose. Unlike monocultures, synthetic consortia can benefit from enhanced metabolic capabilities and multifunctionality through complementary metabolic functions. One species might break down complex carbohydrates, producing intermediates that support the metabolic activity of another species. This division of labour allows the processing of substrates that no single species can fully utilize on its own. At the same time, compared to multiple monoculture cultivations, co-cultivation can decrease the amount of hardware and production costs.

Co-cultivation also offers advantages in terms of stability and resilience. Microbial consortia tend to be more robust under environmental fluctuations such as changes in pH, temperature, or exposure to inhibitory compounds. Consortium members can buffer stress, compensate for lost functions, or change in abundance to maintain overall performance. Synergistic interactions, such as cross-feeding of metabolites (short-chain fatty acids such as acetate, other organic acids like lactate, vitamins), can further enhance growth and production of beneficial metabolites. Importantly, cultivating consortia instead of assembling mixed monocultures can also reduce the risk of contamination by maintaining high cell densities and ecological niches that make it harder for unwanted microbes to grow. Moreover, mimicking natural microbial ecosystems promotes stable co-existence and enables more predictable functionality in applications, from biotherapeutics to industrial fermentation.

The current thesis addresses the challenge of how to cultivate stable and controllable consortia of NGP candidate species. The main purpose of this work is to develop and validate a workflow for cultivating stable, defined microbial consortia of NGP candidates. “Unique carbon source” strategy is proposed, in which each species is provided with a carbon source that is not shared by others, thereby minimizing direct competition and enabling compositional control. Consortium growth was continuously monitored with isothermal microcalorimetry to evaluate stability, growth dynamics, and resilience under serial batch conditions. This was combined with flux balance analysis using genome-scale metabolic models to explore cross-feeding interactions. To assess viability and track species ratios, we developed microscopy-based quantification and implemented PMAxx-qPCR. Additionally, the workflow for absolute quantification of viable bacteria with next-generation sequencing was developed. The findings of this thesis have been presented at scientific seminars and conferences. Based on this work, a research service has been developed at TFTAK, which has attracted interest from international clients. Collectively, these results enhance our understanding of consortia production.

Abbreviations

<i>A. caccae</i>	<i>Anaerostipes caccae</i>
ace	Acetate pathway
<i>A. muciniphila</i>	<i>Akkermansia muciniphila</i>
<i>B. thetaiotaomicron</i>	<i>Bacteroides thetaiotaomicron</i>
but	Butyrate pathway
<i>B. vulgatus</i>	<i>Bacteroides vulgatus</i>
CDI	<i>Clostridioides difficile</i> infection
CDM	Chemically defined medium
CFU	Colony-forming unit
Cq	Quantification cycle
CRC	Colorectal cancer
FBA	Flux balance analysis
FC	Flow cytometry
FMT	Faecal microbiota transfer
<i>F. prausnitzii</i>	<i>Faecalibacterium prausnitzii</i>
GEM	Genome-scale metabolic model
glyc	Glycolysis
HPLC	High-performance liquid chromatography
IMC	Isothermal microcalorimetry
ldh	Lactate dehydrogenase
NGP	Next-generation probiotics
NGS	Next-generation sequencing
OD	Optical density
PMA	Propidium monoazide
pfl	Pyruvate formate lyase
pfr	Pyruvate ferredoxin oxidoreductase
prp	Propionate pathway
pyk	Pyruvate kinase
qPCR	Quantitative real-time PCR
SCFA	Short-chain fatty acid
suc	Succinate pathway
YCFAM	Yeast extract, casitone, fatty acids, mucin
YCM	Yeast extract, casitone, mucin

1 Literature review

1.1 Definition and evolution of the microbiome field

The study of the microbiome has evolved substantially over time. Early research between the 17th and 19th centuries laid the foundations by describing microorganisms and distinguishing microbial differences between health and disease states. A significant technological milestone in the field was the development of anaerobic cultivation techniques. Methods such as the Hungate roll-tube technique, developed in the mid-20th century, along with the later use of GasPak systems and anaerobic chambers, have been necessary for isolating and studying anaerobic microorganisms. These methods, together with the use of germ-free animal models, have been essential in highlighting the critical impact of gut microbiota on host physiology. However, they also underscore the need for continued development of cultivation techniques that enable the growth and study of diverse microbial species under laboratory conditions.

As microbiome research advanced, slightly different definitions of the microbiome began to emerge across various scientific contexts. Ecologically, the microbiome is described as an “Ecological community of commensal, symbiotic and pathogenic microorganisms within a body space or other environment” (Lederberg & Mccray, 2001). From a genomic perspective, it encompasses the full genetic material – the metagenome – of all microorganisms inhabiting a niche, such as the human gut (Nature, n.d.). In this thesis, the definition proposed by Berg et al., (2020), building upon Whipps J, 1988 is adopted: the microbiome is seen as a “characteristic microbial community occupying a reasonably well-defined habitat with distinct physio-chemical properties.” This view emphasizes that the microbiome includes not just the microorganisms themselves (such as bacteria, archaea, protozoa, fungi, and algae), but also their “theatre of activity” – a complex network of metabolites (organic acids, toxins, signalling molecules), structural components (proteins, lipids, nucleic acids), mobile genetic elements, and relic DNA. This expanded view positions the microbiome as a dynamic and integrated micro-ecosystem that both shapes and is shaped by its environment over time. When integrated within eukaryotic hosts, such as humans, the microbiome plays an essential role in maintaining host health and modulating disease risk.

Alongside growing insight into its functional importance, more precise methods have corrected earlier misconceptions about the number of microbes relative to human cells. In several scientific sources, it has been stated that microbiota outnumber human cells by a ratio of 10:1 (Pluznick, 2014; Sekirov et al., 2010; Xu et al., 2022). However, this claim has been debunked, with research suggesting that the actual ratio is closer to 1:1 (Sender et al., 2016b). It is important to note that the actual ratio is not static; it varies between individuals and can fluctuate depending on factors such as body size, gender, recent antibiotic use, and bowel habits (Sender et al., 2016a). However, revising the estimated ratio of bacteria to human cells from 10:1 to a more accurate value of approximately 1:1 does not diminish the biological significance of the microbiota.

Over the last decade the research of the microbiome in the health and well-being of a body has been remarkably accelerated. Especially the gut microbiome which has been linked to organs like brain, skin, pancreas and liver (Byrd et al., 2018; Leung et al., 2016; Sharon et al., 2016; Tripathi et al., 2018). Everyone’s gut microbiome is unique, and shaped primarily by environmental factors such as diet, medication, and lifestyle, with genetics playing only a minor role (Falony et al., 2016; Rothschild et al., 2018). This individuality

means that the composition and function of the gut microbiota can vary significantly from person to person. A diverse gut microbiome is generally considered beneficial, as it can increase resilience against pathogens and support metabolic and immune functions (Lloyd-Price et al., 2016; Lozupone et al., 2012). Conversely, reduced diversity is often linked to dysbiosis and disease. Changes in microbiome diversity and low or high abundance of species have been associated with diseases such as inflammatory bowel disease, diabetes, obesity, cardiovascular disease, and cancer (Alam et al., 2020; W.-Z. Li et al., 2020; Masheghati et al., 2024; Muscogiuri et al., 2019; Novakovic et al., 2020). Gut microbiome has been even linked to neurodegenerative diseases like Parkinson's disease (Pereira et al., 2022; Tan et al., 2021).

The concept of microbiome-based therapies dates back to fourth-century China, where fecal matter from healthy individuals was used to treat conditions such as fever, poisoning, and diarrhoea (Zhang et al., 2018). In 1958, Eisemann et al. announced the successful treatment of pseudomembranous enterocolitis with a faecal enema, now referred to as faecal microbiota transfer (FMT) (Stone, 2019). FMT is a method that has been researched in numerous clinical studies and used to treat various conditions, including ulcerative, Crohn's disease, and type 2 diabetes mellitus (Costello et al., 2019; Sokol et al., 2020; Su et al., 2022). However, clear evidence of its efficacy is currently available only for recurrent *Clostridioides difficile* infection (CDI) (Baunwall et al., 2020). While FMT has been effective for treating recurrent CDI, it has its implications. Introducing undefined live bacteria carries unpredictable risks for infections and metabolic disorders, especially in immunocompromised individuals. Although FMT is highly effective and has a good short-term safety record, it faces significant standardization challenges and potential long-term risks. Adverse events related to FMT are mostly gastrointestinal symptoms like diarrhoea, abdominal discomfort, nausea but also sore throat, rash, aspiration pneumonia and even death has been documented (Marcella et al., 2021).

Additionally, the use of postbiotics have been studied. Sterile faecal filtrates – containing bacterial debris, proteins, antimicrobial compounds, metabolic products, and DNA, but not intact microorganisms – were used to treat patients with CDI (Ott et al., 2017). In all five patients, diarrhoea and other recurrent CDI symptoms resolved, and they remained symptom-free until the end of the study, which was at least six months post-intervention. Even though the exact mechanism of action was not defined it enhances the complexity of finding treatment for different gut related diseases. For therapeutic effect it might not be necessary to transfer the entire microbiome from donor to the patient. This opens the door to rationally designed microbial therapies, such as synthetic microbial consortia, that are both safer and targeted.

1.2 Probiotics, next-generation probiotics, and synthetic consortia

Term “probiotics” refers to live microorganisms which offer health benefits upon consumption in adequate amounts (Hill et al., 2014). Probiotics can be found in traditional fermented foods (like kimchi, sauerkraut) which have a long history of consumption and are generally associated with gut health. These traditional sources contain a wide array of microorganisms, though both the quantity and composition of strains can vary considerably. Over time, specific strains have been isolated, characterized, and developed into commercially available food supplements. Decades of research have resulted in the identification of strains with targeted health benefits, some of which have undergone clinical trials and demonstrated efficacy. Probiotics are

recognized for their ability to influence the gut microbiome, and in some cases, have shown clinically validated mechanisms (Michail et al., 2006). However, effectiveness of probiotics can vary significantly depending on several factors. These include the individual's health status, the condition being targeted, the number and strain of live bacteria in the product, and whether the bacteria can survive the acidic conditions of the gastrointestinal tract. This variability makes it difficult to achieve consistent therapeutic results.

However, there are novel species with potential to have more defined therapeutic effects, specific health benefits and can become more standardized biotherapeutic products, and even drugs against diseases. These microbes, which are part of the healthy gut microbiota and have therapeutic potential are generally referred to as next-generation probiotics (NGP)(T. P. Singh & Natraj, 2021). Unlike traditional probiotics, NGP candidate species belong to diverse range of genera, have no history of use and therefore require careful safety assessments and regulations. Some promising NGP candidate species are *Akkermansia muciniphila* (*A. muciniphila*), *Bacteroides thetaiotaomicron* (*B. thetaiotaomicron*), *Faecalibacterium prausnitzii* (*F. prausnitzii*), and *Christensenella minuta* (Lalowski & Zielińska, 2024; T. P. Singh & Natraj, 2021). In addition to single species, different assembled consortia are also investigated (Clark et al., 2021; Kurt et al., 2023). NGP consortia can be customized to meet individual requirements, considering the unique composition of the microbiome and the disease being treated. While the benefits and potential have been shown in many cases, there are still many challenges to tackle. Most of the NGP candidate species are obligate anaerobes, which makes their production complicated and increases cost due to our limited knowledge of their metabolic peculiarities and the challenges associated with cultivating them (Andrade et al., 2020; Ndongo et al., 2020). And, as stated, to be classified as live biotherapeutic products, or drugs, the clinical efficacy must be proven in parallel with safety studies.

NGPs have potential applications in preventing further negative outcome of therapeutic treatments and supporting the positive effects of treatments of various conditions, including CDI, inflammatory bowel disease, colorectal cancer (CRC), and metabolic disorders (Jonkers et al., 2012). For example, it was shown in mice that *A. muciniphila* colonization significantly increased the anti-cancer effect of FOLFOX which is a combination chemotherapy regimen used to treat CRC (Hou et al., 2021). Another study investigated the effects of administering *A. muciniphila* to insulin-resistant overweight or obese human volunteers, focusing on its safety, tolerability, and impact on metabolic parameters (Depommier et al., 2019). It demonstrated that both live and pasteurized *A. muciniphila* were safe and well-tolerated over three months. *A. muciniphila* notably improved insulin sensitivity, reduced insulinemia and plasma total cholesterol. In addition, body weight, fat mass, and hip circumference decreased compared to baseline. Interestingly, pasteurized *A. muciniphila* had significantly stronger effects than live *A. muciniphila*. Observing the beneficial effect on metabolism confirms results previously shown with pasteurized *A. muciniphila* on mice (Plovier et al., 2017).

There are ongoing clinical trials testing co-cultures as biotherapeutic products for safety and efficacy. Phase I-II clinical trials have been completed to evaluate the safety and tolerability of a live biotherapeutic product comprising 11 commensal bacterial strains in combination with nivolumab for the treatment of different types of advanced or metastatic cancer including CRC (NCT04208958). Currently there are two FDA-approved microbiota-based therapeutics on the market. One of them is SER-109, which is an oral live biotherapeutic product derived from faecal microbiota, mainly consisting of purified

Firmicutes spores, which helps to prevent the recurrence of CDI (Blair, 2024). Another one is RBX2660, a live faecal microbiota suspension for rectal use, also meant for preventing recurrence of CDI (Blair, 2023). Both of them are manufactured from donated human faecal matter and the detailed mechanisms by which they are effective are unknown. No synthetically produced consortia have gained the approval of FDA.

In addition to their therapeutic potential as next-generation probiotics, defined microbial consortia also play important roles in diverse fields such as bioprocessing, fermentation, and environmental science (Chen et al., 2014; Shin et al., 2010; Wang et al., 2016). Synthetic microbial consortia are typically developed using a closed-loop design-build-test-learn cycle. Their construction commonly follows two main strategies: the bottom-up approach, which assembles consortia from individually characterized strains, and the top-down approach, which simplifies complex natural communities (Lawson et al., 2019). In practice, many designs also employ hybrid strategies that combine elements of both methods.

Synthetic microbial consortia can also be constructed based on different design principles, such as cross-feeding and trait-based selection (Liang et al., 2022). Cross-feeding is a common microbial interaction where one species produces metabolites that others consume. This strategy promotes diversity, stability, and functional specialization through metabolic division of labour. Cross-feeding can occur in unidirectional, bidirectional, or multidirectional forms and usually involves metabolites but can also involve extracellular enzymes. Various mathematical models such as generalized Lotka–Volterra equations and flux balance analysis can help predict and optimize these interactions. An example of cross-feeding-based design is the study by Ziesack et al., (2019), in which a synthetic consortium of four gut-associated bacteria was engineered for obligate amino acid cross-feeding. Each species overproduced one amino acid while depending on the others for three, resulting in increased population evenness and reduced antagonism.

However, constructing stable consortia based on cross-feeding presents several challenges. Despite their cooperative nature, these systems are vulnerable to negative effects of competition, evolutionary instability, and the emergence of strains that exploit shared resources without contributing themselves. For instance, marine bacteria *Prochlorococcus* and SAR11 exhibit a commensal cross-feeding interaction (lactate and acetate provided by *Prochlorococcus*), but their possible competition for limited sulphur compounds could destabilize the co-culture (Becker et al., 2019).

Trait-based construction of synthetic microbial consortia involves selecting species based on defined physiological or ecological characteristics, such as substrate preferences, environmental tolerances, or metabolic functions. In trait-based microbial consortia, each species is chosen to perform a specific, non-overlapping function – such as breaking down a certain substrate or producing a needed compound. This complementary role distribution reduces overlap in resource use, which minimizes direct competition among members. In contrast to cross-feeding-based consortia, which behaviour depends on metabolic exchanges between species, trait-based approaches rely on the independent functional capabilities of each member. Krieger et al., (2021) demonstrate how temperature ranges of different species can be used to adjust their abundance in a consortium. They applied temperature cycles to a consortium of *Escherichia coli* and *Pseudomonas putida* to exploit their different growth patterns at various temperatures. This approach integrates a trait-based perspective (bottom-up design) with environmental

control, which is a characteristic of a top-down approach. In another example, Clark et al., (2021) used a model-guided approach to construct synthetic human gut microbiome optimized for butyrate production. By selecting species based on traits related to growth dynamics and butyrate production, and accounting for environmental factors like pH and hydrogen sulphide levels, they successfully assembled consortia with enhanced metabolic function.

However, the effectiveness of trait-based approach depends on how reliably traits are expressed in co-culture. Microbial traits observed in monoculture may not behave similarly in complex consortia due to factors like regulatory shifts, microbial interactions, or stress responses (Lawson et al., 2019; Widder et al., 2016).

Defined microbial consortia are designed through theoretical strategies and validated with experimental models. One example of this is a study in which bottom-up design was used to select nine strains for a consortium that mimics the carbohydrate fermentation processes of a healthy human gut (Kurt et al., 2023). These bacteria were cultured together, and they formed a stable and reproducible consortium. At the same time, if grown individually, none of the strains showed increased growth but rather poor or equal growth compared to consortium growth. While it is an example of a bottom-up approach it also highlights the importance and benefits of co-cultivation and the need for novel cultivation techniques. Moreover, it was shown that consortium growth and metabolic activity differed from a mix of the same strain's monocultures. Co-cultivated consortium was found to be as effective as FMT for treating acute colitis induced by dextran sodium sulphate in mice, but the equivalent mix of individually cultured strains did not achieve the same effectiveness.

1.3 Advantages and challenges of microbial consortia

While the design of microbial consortia can be complex, they offer several advantages. Microbial consortia tend to be more resilient and resistant to stress than monocultures. Overlapping metabolic functions and having redundancy mean if one species is under stress, others can compensate for preserving functionality (Embree et al., 2015). For example, gut microbiota can withstand disturbances like antibiotics better than a single strain, because surviving members can fill the functional roles of those who were lost. Additionally, species abundances within a consortium can shift dynamically in response to environmental changes, allowing the community to maintain a stable overall function through complex feedback interactions, such as cross-feeding and substrate competition (McCarty & Ledesma-Amaro, 2019). Monocultures, lacking such internal redundancy, are more vulnerable – if the single strain fails under stress, the function is lost.

Consortia also benefit from division of labour among different microbes, enabling degradation or synthesis of compounds that no single strain could accomplish alone (Z. Li et al., 2019). In bioremediation, mixed microbial communities can break down complex pollutants (like petroleum) via sequential and cooperative metabolism, achieving degradation where monocultures cannot (Zanaroli et al., 2010). Similarly, in industrial biotechnology, co-cultures allow compartmentalization of metabolic pathways across strains, reducing the burden on any one cell and improving overall efficiency (McCarty & Ledesma-Amaro, 2019). This wide range of cooperative benefits is seen in soil consortia and plant root microbiomes. Combinations of bacteria and fungi provide enhanced nutrient cycling and stress tolerance for plants, surpassing the capabilities of single inoculants (Santoyo et al., 2021). In short, a consortium's functional

diversity allows for niche saturation, where available ecological niches and resources are fully exploited.

Furthermore, a well-established microbial consortium can protect itself against invading pathogens through competitive exclusion and production of inhibitory compounds. Diverse consortia occupy a wide array of niches and consume available nutrients, leaving little opportunity for pathogens to establish themselves. In the gut, the existing microbiome can affect whether incoming species successfully establish themselves, primarily through competitive exclusion, when both incoming and resident species rely on the same niche and resources, coexistence becomes unlikely (Le Roy et al., 2019; Maldonado-Gómez et al., 2016; Martínez et al., 2018).

These advantages can offer notable economic and operational benefits as well. Use of cheap, complex feedstocks that is possible due to division of labour. As well the overall enhanced productivity and efficiency (Roell et al., 2019). In addition, the hardware requirements for cultivating consortia in a single bioreactor are considerably lower than those needed to grow each monoculture separately, which can reduce equipment costs and save time in operational workflows.

Despite the strengths, microbial consortia can be harder to control and reliably reproduce. Complex interactions and dynamic shifts in species composition may lead to variability in performance. In industrial or clinical applications, monocultures often provide more reproducibility – a single well-characterized strain tends to behave predictably under set conditions, whereas consortia might exhibit a drift in composition and ensuring the same ratio of species can be challenging. Similarly, in cultivation processes, co-cultures require careful tuning of growth conditions, and an imbalance can lead to one species overgrowing and diminishing the consortium's intended function. Monocultures, with no inter-species competition, are simpler to optimize.

From a practical standpoint, monocultures are still essential in applications requiring precise, high-yield production of a target compound. Engineered monocultures avoid the uncertainty of interactions between species, though they sacrifice the resilience and multifunctionality of consortia. Microbial consortia offer strength in numbers – greater stress resistance, metabolic diversity, and ecological stability – while monocultures offer simplicity and predictability. Finding the right balance between these trade-offs is important, as the benefits of cooperative microbial consortia must be weighed against the need for precise control and consistent performance.

1.4 Isothermal microcalorimetry

Isothermal microcalorimetry (IMC) is a unique method that has been used for shelf-life studies, on-line monitoring of growth and metabolism of microorganisms including biofilm formation and fermentation in milk (Kabanova et al., 2009; Kütt et al., 2023; Morozova et al., 2020; Stulova et al., 2015; Sultan et al., 2022).

IMC is an extremely sensitive technique for monitoring the heat generation by metabolically active microorganisms within hermetically sealed ampoules maintained at a constant temperature. The rate of heat generation directly correlates with the rate of biomass production, and the shape of the heat production curve reflects the metabolic activities of the microorganisms (Forrest W.W. & Walker D.J., 1963).

IMC has several advantages in microbiology compared to other methods. Firstly, the sensitivity; heat generated by even a small number of microorganisms can be detected by IMC. Detectable cell concentration is starting from 2.5×10^4 and 1.0×10^5 CFU per mL which is significantly lower than detection level of spectrophotometer that measures

turbidity (10^7 – 10^8 CFU mL⁻¹)(Braissant et al., 2010). An additional advantage of IMC is its suitability for cultivation in anaerobic conditions, making it particularly useful for studying human gut microbiome species. Furthermore, heat production is unaffected by the growth medium opacity. Mucin is one of the medium ingredients that is mostly insoluble in water, but a necessary substrate for some NGP candidate species. Mucin-containing media are not transparent but biochemical reactions in them could be readily investigated using IMC.

Besides high sensitivity, IMC allows to measure heat flows changes with high accuracy – approximately 1%. This is due to instruments ability to maintain the temperature of the ampoule's within ± 0.1 °C, and measure heat flow across a large range, while having only small baseline drift, typically by only 0.2 μ W over 24 hours. In addition to this, IMC provides continuous on-line measurements which allows to observe experiments in real time. Also, the heat measurements are non-invasive, as it occurs externally without altering the samples inside the ampoules. This allows the samples to be used for additional analyses afterwards, such as quantifying organic acids, amino acids, and carbohydrates (Kattel et al., 2023, 2024).

Each method has its limitations; for IMC, samples must reach the set temperature before measurements can begin. Typical equilibration period is approximately one hour during which no data can be acquired. Secondly, only batch processes can be studied in the IMC. In the batch process, the cell concentration as well as substrate and product concentrations are changing. In serial batch format, microorganisms are inoculated into the medium and grown until stationary phase. Fraction of the grown culture is then transferred into fresh medium. This process is repeated and helps to mimic industrial production processes where several seed batches are needed to be produced as inocula for higher volume cultivations.

1.5 Short-chain fatty acids metabolism and genome-scale metabolic models

Short-chain fatty acids (SCFA) are key microbial metabolites with significant physiological roles in the human gut. Understanding how these compounds are produced, utilized, and cross-fed among microbial species requires both experimental and computational tools. Methods like IMC describe phenotypic traits but genome-scale metabolic models (GEMs) can be used to simulate metabolic behaviour and to predict interactions under various conditions.

To effectively model microbial interactions using GEMs, it is necessary to understand the diversity and metabolic roles of SCFA-producing bacteria. Metabolism of human gut microbiota species is diverse while they convert indigestible substrates into SCFA. Based on the substrate preferences or metabolism end products gut microbiota species can be categorized into several subgroups: asaccharolytic bacteria, mucin degraders, butyrate producers, lactic acid producers, succinate and propionate producers, acetate and ethanol producers. Figure 1 provides a schematic overview of the key anaerobic metabolic pathways and enzymes involved in SCFA production by different gut microbiota subgroups. SCFA play a role in modulating interactions between the host and microbiota, influencing inflammatory processes and our health overall. Among the SCFAs, acetate is the most prevalent but has received less research attention compared to propionate and butyrate, which are often regarded as more functional (Münste & Hartmann, 2025).

Butyrate is an important SCFA that serves not only as a fermentation product but also as an energy source for colonocytes through β -oxidation and the Krebs cycle (Donohoe et al., 2011). In the gut, butyrate has anti-inflammatory and immunoregulatory effects (Chang et al., 2014; Recharla et al., 2023; N. Singh et al., 2014). It also accelerates the assembly of tight junctions, which are necessary for the barrier function formation and maintenance (Peng et al., 2009).

While butyrate is an energy source for colonocytes, other SCFAs like acetate and propionate, which are not metabolized, travel to the liver with the portal vein. Once absorbed, propionate is rapidly metabolized by hepatocytes, while acetate can either be utilized in the liver or enter peripheral circulation for use by other tissues (den Besten et al., 2013). At the same time, there is SCFA and other organic acid cross-feeding in the intestine between different species. The main acetate producers can be found among several phyla like Bacteroidetes, Firmicutes, Actinobacteria, and Verrucomicrobia (Hosmer et al., 2024; Mukherjee et al., 2020). This acetate can be consumed by other Firmicutes like *Anaerostipes caccae* who utilize the acetyl-CoA pathway and convert it together with lactate into butyrate (Duncan et al., 2004; Schwartz et al., 2002). Also, succinate that is produced by Bacteroidetes can be converted into propionate by succinate-utilizers like *Phascolarctobacterium faecium* via succinate pathway (Ikeyama et al., 2020). As cross-feeding interactions can be used to design stable microbial consortia, it is important to understand the metabolism of species and characterize inter-species metabolic interactions in detail.

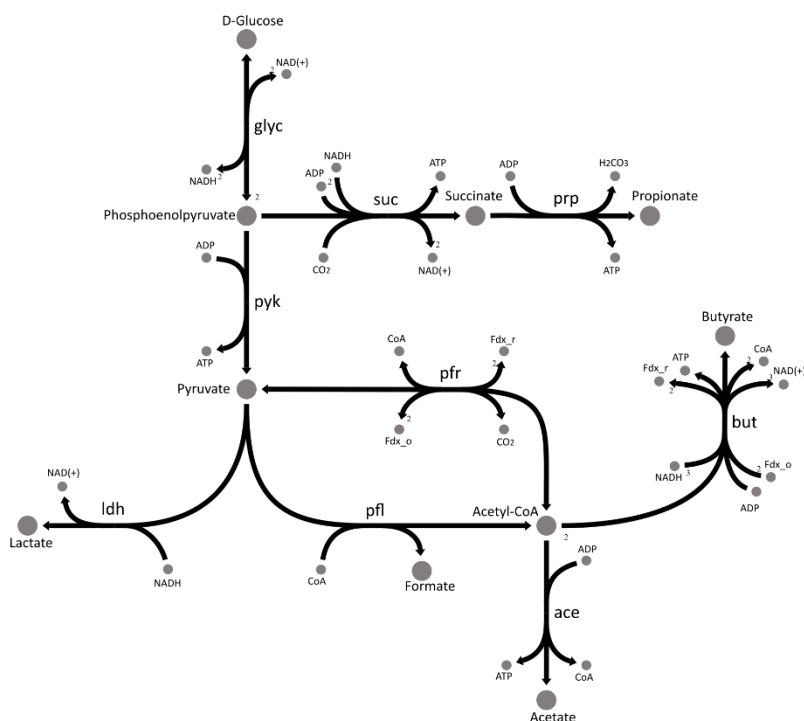


Figure 1. Anaerobic central carbon metabolism and short-chain fatty acid production. The map illustrates the flow of metabolites from glucose through glycolysis (glyc), which in this scheme includes eight enzymes: glucose-6-phosphate isomerase, 6-phosphofructokinase, fructose-bisphosphate aldolase, triose-phosphate isomerase, glyceraldehyde-3-phosphate dehydrogenase, phosphoglycerate kinase, phosphoglycerate mutase, and enolase. The final glycolytic step, conversion of phosphoenolpyruvate to pyruvate, is catalyzed by pyruvate kinase (pyk). Pyruvate is further metabolized via multiple branch points including lactate dehydrogenase (ldh), pyruvate formate lyase (pfl), and pyruvate ferredoxin oxidoreductase (pfr). Conversion of acetyl-CoA to acetate occurs via acetate kinase and phosphate acetyltransferase (ace). The butyrate production pathway (but) includes six enzymatic steps, catalyzed by acetyl-CoA C-acetyltransferase, 3-hydroxybutyryl-CoA dehydrogenase, 3-hydroxybutyryl-CoA dehydratase, butyryl-CoA dehydrogenase, butyryl-CoA phosphate butyryltransferase, and butyrate kinase. The succinate pathway (suc) includes phosphoenolpyruvate carboxykinase, malate dehydrogenase, fumarate hydratase, and fumarate reductase. The propionate pathway (prp) is a sum of reactions catalyzed by succinate-CoA ligase, methylmalonyl-CoA mutase, (S)-methylmalonyl-CoA decarboxylase, propionyl-CoA phosphate propionyltransferase, and propionate kinase. Stoichiometric coefficients are shown to indicate the number of molecules involved in each reaction step.

GEMs map out gene-protein-reaction associations for an organism's metabolic genes and use a stoichiometric matrix to predict metabolic fluxes, enabling analysis of metabolism at the whole-cell level (Thiele & Palsson, 2010). One of the advantages is that GEMs provide a detailed understanding of an organism's metabolic network, which can be used to predict metabolic fluxes and identify key metabolic pathways. GEMs serve as a platform for generating hypotheses about metabolic functions and interactions, which can then be tested experimentally. However, data quality plays an important role in the accuracy of these models. The completeness of GEMs is limited by the availability of high-quality genomic data. Both the data quality and the number of degrees of

freedom i.e. complexity of metabolism in the metabolic model significantly impacts the accuracy of the computational procedures. The outcome of calculations is also strongly affected by both the availability and reliability of genomic and protein annotation data for respective microbial species. Incomplete or poorly annotated genomes can lead to gaps in the metabolic network, reducing the model's accuracy. Outside model organisms, many reactions included in GEMs are predicted based on genomic data and have not been experimentally validated.

1.6 Viable cell quantification methods

Accurate and reliable quantification of viable microbes is essential for informed decision-making and quality control in the production of NGP and other applications. To date, plating remains the most widely accepted method for this purpose. CFU counts are specific, detection requires cells to be alive and able to reproduce, providing a definitive measure of viable organisms. Most probable number dilution assays provide a comparable alternative for viability quantification in liquid media, but they also rely on the growth of culturable organisms and use statistical calculations rather than direct cell counts (Oblinger & Koburger, 1975). While both methods are affordable and technically straightforward, they share significant limitations, especially when applied to complex microbial communities. Samples containing diverse species, such as those with NGP candidates, may require different culture media or growth conditions, making universal cultivation difficult. Furthermore, some bacteria are unculturable under standard laboratory conditions, cultivation does not provide taxonomic information, and obtaining results can take several days (Stewart, 2012).

Use of fluorescent stains that distinguish live and dead cells based on membrane integrity do not require cultivation. Dyes such as SYTO9 (penetrates all cells) and propidium iodide (penetrates only cells with compromised membranes) are used together to label intact and membrane-damaged cells (Baena-Ruano et al., 2006). Live cells fluoresce green while dead cells fluoresce red, enabling direct counts via flow cytometry (FC). FC allows thousands of individual cells to be analysed per second and is a high-throughput tool for viability assessment across fields ranging from water disinfection to food and industrial bioprocessing (Bunthof et al., 2001; Grey & Steck, 2001; Hoefel et al., 2003). However, not all dead cells immediately lose membrane integrity, so dyes can misclassify some dead cells as viable, potentially overestimating live counts (Truchado et al., 2020). Conversely, injured cells with leaky membranes might be counted as dead even if they could recover.

RNA-based methods, such as transcriptomics, offer an alternative approach for identifying only viable cells. Since RNA is an unstable molecule that is rapidly degraded after cell death, its presence indicates metabolically active live bacteria. This allows the sequencing workflow to begin directly from RNA isolation. But due to RNA's short lifespan and associated technical challenges, this method is not widely adopted. Although RNASeq offers high resolution, sensitivity, and suitability for low-biomass samples, it remains expensive and time-consuming, making it impractical for routine use.

Other modern molecular methods, including next-generation sequencing (NGS), PCR, and immunoassays, offer detailed information on the abundance of specific bacterial species (Cao et al., 2017). However, they also have certain limitations. PCR and immunoassays are designed to detect selected target microorganisms, offering rapid and quantitative results. Yet, their sensitivity often depends on prior culturing to increase the number of cells, and they are limited to detecting only those bacteria that have been

specifically predefined in the analysis. The primary advantage of NGS over these methods is its ability to uncover previously unknown microorganisms. Unlike targeted techniques, NGS does not require prior knowledge of the sample's microbial composition. 16S rRNA gene (16S) amplicon NGS offers a comprehensive profile of bacterial consortia by providing the relative abundance of all detected taxa (Adamberg, Raba, et al., 2020; Ji & Nielsen, 2015). However, obtaining absolute abundance data remains challenging due to significant variation in 16S rRNA gene copy numbers among taxa, PCR amplification biases introduced during library preparation, and complexities in data analysis like setting appropriate thresholds.

One solution is to use quantitative microbiome profiling where FC is used to normalize 16S sequencing data by estimating total bacterial load (Vandeputte et al., 2017). Alternatively, spike-in controls added during DNA extraction help account for DNA loss and improve quantification. Introducing spike-in controls at the DNA extraction stage helps to monitor the entire sequencing workflow and minimize biases. Two main types of spike-in controls have been developed: synthetic DNA molecules and whole cells (Piwoz et al., 2018; Smets et al., 2016; Tkacz et al., 2018; Zemb et al., 2020). Synthetic DNA is highly precise and flexible but does not account for biases introduced during cell lysis or DNA extraction. In contrast, spike-in cells typically comprising a mix of Gram-positive and Gram-negative bacteria better reflect processing steps but may not match the specific characteristics of the native microbial community. By combining the known quantity of spike-in material with the relative abundance data from sequencing, absolute microbial counts can be obtained.

An affordable and technically simple option for converting relative data to absolute is quantitative real-time PCR (qPCR). Standard qPCR yields absolute or relative abundance of target gene copies, but it does not differentiate live and dead cells, DNA from dead cells can persist in samples and be amplified. To address this, viability PCR techniques have been developed using photoreactive dyes like ethidium monoazide, propidium monoazide (PMA), and PMAxx (advanced version of PMA). PMAxx-qPCR involves treating a sample with PMAxx before DNA extraction. PMA penetrates cells with compromised membranes and covalently binds their DNA upon light activation, thereby inhibiting the amplification of DNA from dead bacteria. It has been successfully applied in a wide range of contexts, including probiotics research, food safety testing, and the analysis of environmental water and soil microbiomes (Alonso et al., 2014; Ditommaso et al., 2015; Scariot et al., 2018). Limitations of this method are similar to those observed with fluorescent dyes and FC, if some dead cells have intact membranes, dye might fail to enter and their DNA will be mistakenly counted as viable, leading to overestimation (Nocker et al., 2017). On the other hand, high PMA concentrations or cell membrane differences can sometimes exclude DNA from slightly damaged but recoverable cells. Given the complexity of distinguishing viable from non-viable microbes, no single method is universally sufficient for all applications. A combined, sample-dependent approach balancing accuracy and feasibility is important for reliable microbial viability assessment across research and industry settings.

2 Aims of the Study

The aim of this thesis is to develop and validate scalable workflows for the cultivation, characterization, and compositional control of defined microbial consortia, with a focus on NGP candidates. The specific aims were as follows:

- Evaluating consortium stability and resilience using isothermal calorimetry.
- Exploring metabolic interactions and cross-feeding mechanisms through co-culture experiments.
- Establishing a substrate-based strategy to control species abundance in co-cultures.
- Establishing robust viability assessment and enumeration methods.

3 Materials and Methods

Below is a summary of the methods used in this study. More details for every method are provided in Publications I–III.

3.1 Strains

The following bacterial strains were used across the three publications and in the thesis: *Akkermansia muciniphila* (DSM 22959), *Alistipes shahii* (DSM 19121), *Anaerostipes caccae* (DSM 14662), *Anaerotruncus colihominis* (DSM 17241), *Bacteroides thetaiotaomicron* (DSM 2079), *Bacteroides caccae* (DSM 19024), *Bacteroides ovatus* (DSM 1896), *Bacteroides uniformis* (DSM 6597), *Bacteroides vulgatus* (DSM 3289), *Bifidobacterium adolescentis* (DSM 20087), *Bifidobacterium longum* subsp. *infantis* (DSM 20088), *Blautia faecis* (DSM 27629), *Blautia hydrogenotrophica* (DSM 10507), *Butyricimonas faecihominis* (DSM 105721), *Christensenella minuta* (DSM 22607), *Catenibacterium mitsuokai* (DSM 15897), *Collinsella aerofaciens* (DSM 13712), *Dorea formicigenerans* (DSM 3992), *Dorea longicatena* (DSM 13814), *Eisenbergiella tayi* (DSM 26961), *Eubacterium rectale* (DSM 17629), *Faecalibacterium prausnitzii* (DSM 17677), *Odoribacter splanchnicus* (DSM 20712), *Prevotella copri* (DSM 18205), and *Roseburia faecis* (DSM 16840). All strains were obtained from the German Collection of Microorganisms and Cell Cultures (DSMZ).

Several species included in this thesis have undergone reclassification based on genomic evidence. Specifically, *Faecalibacterium prausnitzii* has been reclassified; the strain used in this thesis corresponds to *Faecalibacterium duncaniae* (Sakamoto et al., 2022). Similarly, *Eubacterium rectale* has been reclassified as *Agathobacter rectalis*, *Prevotella copri* as *Segatella copri*, and *Bacteroides vulgatus* as *Phocaeicola vulgatus* (Hahnke et al., 2016; Hitch et al., 2022; Rosero et al., 2016). For consistency with existing literature and publications this thesis is based on, historical species names have been retained in results and plots. However, the updated taxonomic names are used in the phylogenetic tree (Figure 3), which is based on the current NCBI taxonomy as retrieved using the taxize R package.

The lyophilized strains were revived in suitable media tailored for each organism (see Publication II for the medium composition). After cultivation, bacterial stocks were washed with Dulbecco's phosphate-buffered saline supplemented with 1% L-Cysteine hydrochloride. Long-term storage was carried out at -80°C in Dulbecco's phosphate-buffered saline containing 20% glycerol and 1% L-Cysteine hydrochloride.

To prepare the multi-strain stock (20 strains), the number of cells in each strain stock culture was estimated by measuring optical density at 600 nm (OD600), assuming that an OD600 of 1 corresponds approximately to 10^9 CFU per mL. From each stock, 5×10^8 cells were taken and combined into the mixture, resulting in a final OD600 of 0.98 for the mixed culture. To prepare the multi-strain stock (25 strains), from each stock, 2×10^8 cells were taken and combined into the mixture.

3.2 Media

Different types of complex and defined media were used in this thesis to describe co-culture growth. Complex yeast extract, casitone, fatty acids, mucin (YCFAM) medium was used in Publication I (composition and preparation details provided there). In Publication II, several versions of chemically defined media (CDM) were tested,

the details of which are provided in the supplementary data of that publication. For evaluating diversity of 25-species model consortium we used yeast extract, casitone, mucin (YCM) medium. YCM medium consisted of (per litre): 2.5 g casitone (Tryptone Plus, Sigma-Aldrich), 2.5 g yeast extract (NuCel 545, Bio Springer), 1 g L-cysteine HCl (Alfa Aesar), 1 mg resazurin sodium salt (Acros Organics), 2.93 g K₂HPO₄ (Sigma-Aldrich), 4.65 g KH₂PO₄ (Sigma-Aldrich), 0.9 g (NH₄)₂SO₄ (Alfa Aesar), 0.9 g NaCl (Acros Organics), 0.28 g KOH (Fluka), 1 g NaHCO₃ (Sigma-Aldrich), 10 mg hemin (Sigma-Aldrich), 10 µg biotin (Merck), 10 µg cobalamin (Fisher Bioreagents), 30 µg para-aminobenzoic acid (Sigma-Aldrich), 150 µg pyridoxamine (Carbosynth), 50 µg folate (Alfa Aesar), 0.09 g MgSO₄·7H₂O (Alfa Aesar), 0.09 g CaCl₂·H₂O (ApliChem). Mucin from porcine stomach type III (Sigma-Aldrich) was used as a substrate at concentration of 1 g L⁻¹. Sterilization was performed using the same procedure as described for the YCFAM medium (Publication I).

In all cases, media was kept overnight in an anaerobic chamber (COY box, Coy Laboratory Products Inc., Grass Lake, MI, USA) with an atmosphere of 2.5 ± 0.5% H₂, 10% CO₂, and balanced N₂.

3.3 Cultivation

Different systems were used for anaerobic cultivation throughout the thesis. Culture preparations were always done in an anaerobic chamber. Most experiments were conducted using isothermal microcalorimetry (IMC)—TAM III and TAM IV-48 (TA Instruments, New Castle, DE, USA). These included the stability and resilience study of the three-species consortium in Publication I, as well as the small-scale co-culture production and substrate validation experiments in Publication II. Except for the substrate validation and acetate/lactate supplementation study (see Table 2, Table S3, Table S4), all IMC experiments followed a serial batch design: each batch lasted 23–24 h, and 20 µL (1% v/v) of the culture was transferred into 1.98 mL of fresh medium at the start of each new batch (Figure 2). The cultivation period ranged from three to seven consecutive batches.

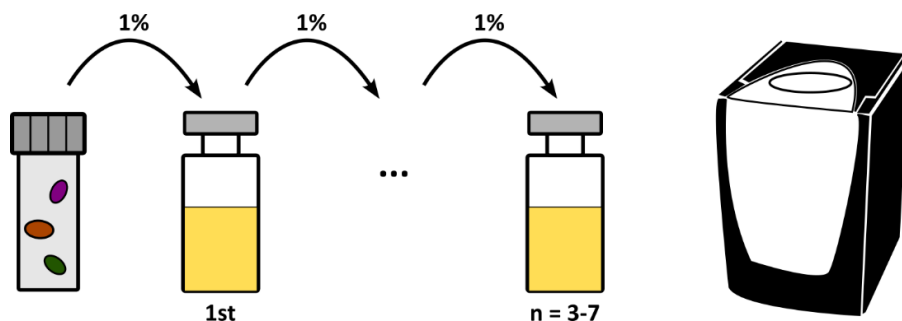


Figure 2. This figure presents the workflow scheme for serial batch cultivations using IMC, conducted with both mono- and co-cultures. Bacteria or bacterial mixtures were inoculated into glass ampoules, which were then hermetically sealed and placed into the IMC. After 23–24 hours of incubation, 1% of the culture volume was transferred into fresh medium. Depending on the experimental setup, three to seven consecutive batch cultivations were carried out.

Strain screening in chemically defined media containing glucose was performed using a BioTek Synergy H1 Multi-Mode Reader (Agilent Technologies Inc., Santa Clara, CA, USA), as described in Publication II. Upscaling from IMC conditions was carried out using 1.25 L Biobundle bioreactors (Applikon, Delft, Netherlands), with further details provided in Publication II.

3.4 Microscopy and image analysis

In Publication II we developed a microscopy image-based method to estimate the species ratios in the co-cultures. Bacterial cultures (*A. caccae*, *B. thetaiotaomicron*, *B. vulgatus*) were adjusted to an OD of 1 and vortexed to disperse the cells. Gram staining was performed using the Biogram 4 Kit (Biognost Ltd., Croatia), and samples were examined with a Nikon Eclipse E200-LED microscope (Japan) using a 100× oil immersion lens. Brightfield images were captured with a Nikon D5200 camera and analyzed in Fiji software. Cells were segmented via color thresholding to determine cell area. *B. thetaiotaomicron* and *B. vulgatus* were defined as cells under 0.85 mm², while *A. caccae* ranged from 0.85–2 mm². For clusters of *A. caccae* exceeding 2 mm², the area was divided by 1.6 mm² (average area of *A. caccae*) to estimate cell count. Each sample included 1200–8900 measured cells. Results are based on triplicate measurements and standard error was calculated accordingly.

In Publication III, a similar procedure was used to study the morphology of selected strains. The same staining protocol and microscope configuration were applied, and brightfield images were captured using the Nikon D5200 camera. No image analysis was performed in Fiji; only the images were collected.

3.5 Quantification of extracellular metabolites

For metabolite analysis (Publication I and II), fermentation samples were centrifuged at 14000 g for 5 minutes at 4 °C and the supernatant was filtered using 0.2 µm syringe filters (Millipore Millex-LG filters 13 mm Millex PTFE 0.2 µm non-sterile SLLGH13NK; Millipore Corp.). Medium samples were filtered directly without centrifugation.

Metabolite concentrations were measured using high-performance liquid chromatography (Waters 2695 HPLC system; Waters Corporation, Milford, MA, USA). The system was equipped with an HPX-87H column (Bio-Rad Laboratories, Richmond, CA, USA) and used isocratic elution with 0.005 M H₂SO₄ at a flow rate of 0.6 mL min⁻¹. The column temperature was maintained at 35 °C. Detection was performed with both refractive index (RI) and ultraviolet (UV) detectors, and quantification was based on external standard curves. The following metabolites were quantified: acetate, butyrate, citrate, ethanol, formate, isobutyrate, isovalerate, lactate, malate, propionate, succinate, valerate, D-galacturonic acid, D-sorbitol, and D-xylose.

Free amino acids were quantified from the same supernatant using a Waters UPLC-PDA system (Waters Corporation, Milford, MA, USA). Samples were derivatized with 6-aminoquinolyl-N-hydroxysuccinimidyl carbamate using the AccQ-Tag Ultra Derivatization Kit (Waters Corporation), and separated on an AccQ-Tag Ultra column using a gradient of eluents A and B. Amino acids were detected by photodiode array and analysed with Empower 3 software (Waters Corporation).

3.6 Flow cytometry

A50-Micro Flow Cytometer (Apogee Flow Systems, UK) was used to assess the viability of 20 individual strains as well as the mixed 20-strain consortia glycerol stock. Membrane integrity was assessed using a dual-staining approach. SYTO24 (SYTO™ 24 Green Fluorescent Nucleic Acid Stain, 5 mM solution in dimethyl sulfoxide; Invitrogen, USA) was used to label all bacterial cells, while propidium iodide (1.0 mg/mL solution in water; Invitrogen, USA) stained only those with compromised membranes. The sample preparation and instrument setup are described in more detail in Publication III.

3.7 DNA extraction

Genomic DNA extraction was performed using two different kits depending on the publication. In Publications I and II, DNA was extracted using the GenElute Bacterial Genomic DNA Kit (Merck, Germany), and the resulting DNA was diluted to a concentration of approximately 10 ng/μL to fit the requirements of the downstream analysis. For Publication III, genomic DNA from the 20-strain consortia samples was isolated using the ZymoBIOMICS™ DNA Miniprep Kit (Zymo Research, Irvine, CA, USA), following the manufacturer's protocol. DNA concentrations were measured using a Qubit™ 4 Fluorometer (Thermo Fisher Scientific, Waltham, MA, USA) in combination with the Qubit dsDNA BR Assay Kit (Thermo Fisher Scientific).

3.8 PMAxx treatment and spike-in control

To evaluate cell viability of twenty bacterial species as well as the 20-strain consortia, propidium monoazide (PMAxx) treatment was used prior to qPCR. Cell suspensions were mixed with PMAxx™ solution in water (Biotium, Fremont, CA, USA) to achieve a final concentration of 25 μM. The mixtures were incubated in the dark on a shaker for 10 minutes. Following incubation, the samples were exposed to blue light using the PMA-Lite™ LED Photolysis device (Biotium) for 20 minutes, with intermittent inversion to ensure even exposure. After light treatment, the samples were centrifuged at 5000 × g for 15 minutes at 4 °C. The resulting pellets were resuspended in phosphate-buffered saline. A defined number of ZymoBIOMICS™ Spike-in Control I (High Microbial Load, Zymo Research, Irvine, CA, USA) was added to the samples if relevant.

3.9 Quantitative real-time PCR

In Publication II, the relative abundances of *A. caccae*, *B. thetaiotaomicron*, and *B. vulgatus* were measured using quantitative real-time PCR (qPCR). Specific primers targeting the Peptidase S41 family gene of *B. thetaiotaomicron*, the sorbitol operon transcription regulator gene of *A. caccae*, and the 16S rRNA gene of *B. vulgatus* were used. Standard curves were constructed from genomic DNA of each species using five concentrations ranging from 0.002 to 36 ng mL⁻¹. PCR reactions were run in triplicate in a final volume of 20 μL using 5× HOT FirePol EvaGreen qPCR Mix Plus (Solis BioDyne, Estonia) and primers at 10 μM. Reactions were set up in white 96-well plates (BIOplastics, Netherlands) sealed with Opti-seal™ Optical Disposable Adhesive. Amplification was carried out with qTOWER³ (Analytik Jena GmbH, Germany) using the following thermal profile: initial denaturation at 95 °C for 15 minutes; 40 cycles of 95 °C for 15 seconds, 60 °C for 20 seconds, 72 °C for 20 seconds, one cycle of 95 °C for 5 seconds, 60 °C for 1 minute, and a melting curve from 60 °C to 97 °C.

While qPCR was also used in Publication III, additional steps were included to assess viability of 20 individual and mixed 20-strain consortium stocks. There were slight differences in the thermal protocol (see Publication III). Viability was determined using strain-specific primers and calculated from the ΔCq (based on the quantification cycle (Cq)) between PMAxx-treated and untreated samples. Viable cell percentages were calculated using the following equation:

$$\% \text{ viable} = \frac{100}{2^{\Delta Cq}}$$

3.10 16S rRNA NGS

In Publication I and III, relative abundances of the three-species consortium were determined using 16S rRNA sequencing. For 16S rRNA gene sequencing, the V4 region was amplified using primers F515 and R806, and libraries were prepared using a standard protocol. Sequencing was performed using the Illumina iSeq 100. Read identification and quantification were performed using BION-META software. In Publication I the relative abundances were normalized based on known 16S rRNA gene copy numbers (3 for *A. muciniphila*, 5 for *B. thetaiotaomicron*, and 6 for *F. prausnitzii*; (Stoddard et al., 2015)).

3.11 Construction of metabolic networks and flux balance analysis

In Publication I genome-scale metabolic networks for *A. muciniphila*, *B. thetaiotaomicron*, and *F. prausnitzii* were obtained from public database (Machado et al., 2018) and the curated with MEMOTE (Lieven et al., 2020). Intracellular flux patterns were analysed using flux balance analysis (FBA) and flux variability analysis (FVA), with biomass production (growth rate) set as the objective function.

In Publication II, metabolic networks were built for *A. caccae* and *B. thetaiotaomicron*, consisting of 371 metabolites and 490 reactions for *A. caccae*, and 447 metabolites and 584 reactions for *B. thetaiotaomicron*. These individual models were merged into a consortium-level metabolic network by introducing a shared extracellular metabolite pool and eliminating duplicate exchange reactions. The resulting consortium network included a total of 760 metabolites and 1025 reactions.

FBA model was created in Wolfram Mathematica format using in-house software developed in MATLAB (Orth et al., 2010). All calculations were carried out using Wolfram Mathematica version 8.01. The model was constrained using input flux data, and ATP production was set as the objective function. To find a feasible solution, the input flux error margin was increased stepwise by $\pm 1\%$. To evaluate how well the measured metabolite data reflected the organisms' known metabolism, a carbon mass balance analysis was also conducted. Additionally, flux variability analysis was applied to selected exchange fluxes to explore potential cross-feeding interactions between *A. caccae* and *B. thetaiotaomicron* in co-culture conditions (Mahadevan & Schilling, 2003).

4 Results and Discussion

4.1 Creation of the model consortium

Model consortium was created of 25 human gut microbiome species, many of them are also NGP candidates (Figure 3). The selection was done based on existing literature to ensure both diversity and similarity to the typical Estonian gut microbiome (Adamberg, Jaagura, et al., 2020). Additionally, the availability of the strains' genomes and their safety levels were taken into account. The model consortium includes various bacteria with distinct metabolic roles. Several species – such as *Faecalibacterium prausnitzii* (now *F. duncaniae*), *Agathobacter rectalis*, *Roseburia faecis*, *A. caccae*, *Blautia* spp., and *Butyricimonas faecihominis* – are known producers of butyrate and/or acetate, SCFAs associated with anti-inflammatory effects. *A. muciniphila* is specialized in degrading mucin, while *Bacteroides* species efficiently break down a wide range of dietary polysaccharides. Bile salt hydrolase genes, which contribute to bile acid metabolism, have been identified in genera such as *Bacteroides*, *Bifidobacterium*, *Collinsella*, and *Blautia* (Song et al., 2019). This thesis investigates the metabolic traits of selected consortium members in more detail than others, with particular attention to their roles in cross-feeding and consortium stability.

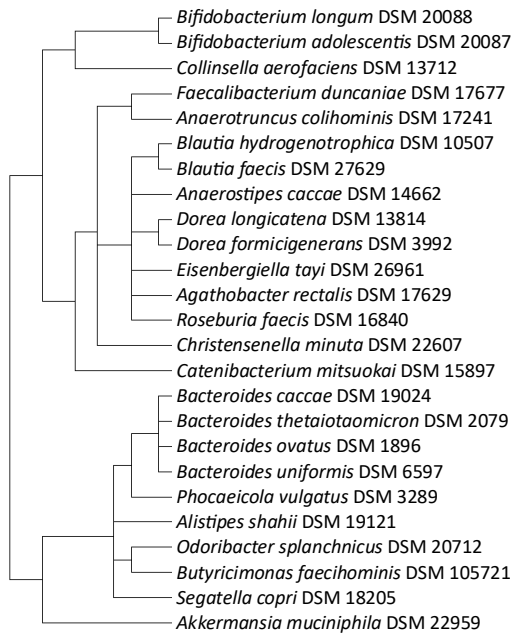


Figure 3. Phylogenetic tree of 25 human gut microbiome species constructed using NCBI taxonomy data. The tree was generated using the R package taxize (version 0.10.0) in RStudio (version 2025.05.0), based on NCBI Taxonomy IDs and visualized using R plotting functions. Tree structure reflects taxonomic relationships as defined by NCBI and is not inferred from sequence data. Four species included in this thesis have undergone taxonomic reclassification: *Faecalibacterium prausnitzii* to *Faecalibacterium duncaniae*, *Eubacterium rectale* to *Agathobacter rectalis*, *Prevotella copri* to *Segatella copri*, and *Bacteroides vulgatus* to *Phocaeicola vulgatus* (Hahnke et al., 2016; Hitch et al., 2022; Rosero et al., 2016; Sakamoto et al., 2022). The phylogenetic tree reflects the updated taxonomy, but the original names are retained throughout the thesis for consistency with publications this thesis is based on.

4.2 Stability and resilience of a defined human gut microbiota consortium assessed with isothermal microcalorimetry (Publication I)

Stability and resilience are important characteristics of consortia as they ensure consistent metabolic activity and species ratio which are essential for achieving desired biotechnological outcomes. Additionally, resilience helps in managing environmental fluctuations, providing a foundation for experimental and industrial applications. To investigate these characteristics, we employed a calorimetric approach, chosen for its wide range of advantages, and implemented serial batch cultivation. This way we can simulate conditions in production processes where multiple seed batches are required to produce inocula for larger volumes. Our consortium of choice consisted of human gut microbiota species, but these methods could be applied to other consortia as well. To simplify the 25 species model consortium and gain deeper insight into interspecies interactions, we chose three species with different metabolic types for the study: *A. muciniphila*, *B. thetaiotaomicron*, and *F. prausnitzii*. These species were characterized in both monoculture and consortium settings.

Using an isothermal microcalorimeter, we determined that the consortium's stability was achieved when the heat flow curves became reproducible over the course of seven passages. A passage was defined by the transfer of 1% (v/v) of the preceding bacterial culture into fresh YCFAM medium, plus the fermentation time (approximately 24h). Principal component analysis based on the collected heat flow data showed that the consortium and individual strains required a different number of passages to reach stability (Figure 4). *A. muciniphila* monoculture needed four passages, while *B. thetaiotaomicron* and *F. prausnitzii* monocultures needed only two passages. The consortium was stable after three passages. Stability was also confirmed by 16S rRNA sequencing, which confirmed the presence of all three species in the consortium. At the end of the seventh passage, *B. thetaiotaomicron*, *A. muciniphila*, and *F. prausnitzii* ratios were 54 ± 1 %, 31 ± 1 %, and 15 ± 0 %, respectively ($n = 3$) (Figure 5B).

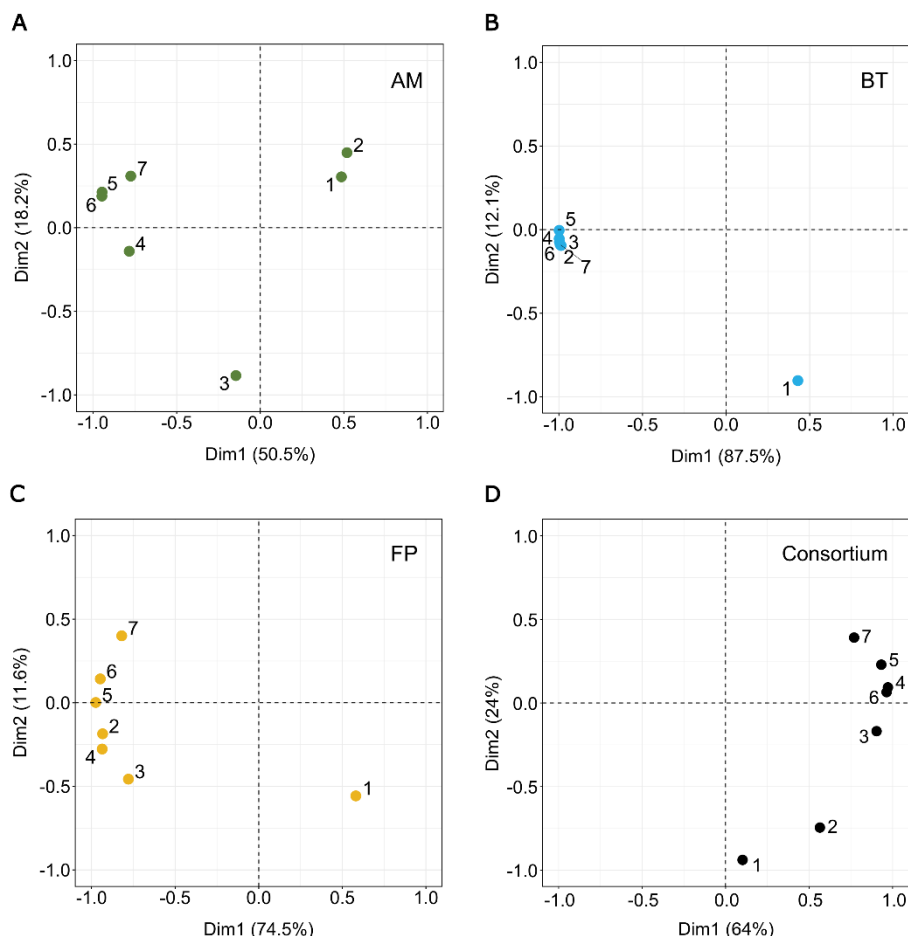


Figure 4. Stability was reached at different passage numbers for the consortium and individual strains. Principal component analysis was performed on heat flow data obtained with isothermal microcalorimetry (IMC) across seven consecutive passages (1 through 7, $n = 3$). Panels a–d represent the following: A. *muciniphila* (green), B. *thetaitaomicron* (blue), F. *prausnitzii* (yellow), and the consortium (black). Reproduced from: Kattel et al., (2024), *MicrobiologyOpen*, Wiley. Licensed under CC BY 4.0.

To further characterize the strains and their possible influence on each other, their growth rates were determined in monoculture and in the consortium. Hourly samples were taken to determine the relative abundance of each strain in the consortium using 16S rRNA sequencing. The total heat generated by the consortium was used, along with these abundances, to reconstruct the growth curves of each individual strain (Figure 5C). In case of monocultures heat data from the fifth, sixth and seventh passage were used. *A. muciniphila* specific growth rate in the monoculture was $0.57 \pm 0.02 \text{ h}^{-1}$ (Figure S1A,B), which is similar to its growth rate in consortium 0.62 h^{-1} (Figure 5C). Multiple phases were observed in the heat flow curves of *B. thetaiotaomicron* and *F. prausnitzii* monocultures (Figure S1A, C, D). The depletion of the most preferred substrate(s) likely triggered metabolic switches, which in turn slowed the growth rate during each new phase. Both strains had fast first initial growth phases, specific growth rates in

monocultures were $0.88 \pm 0.06 \text{ h}^{-1}$ and $1.00 \pm 0.08 \text{ h}^{-1}$ for *B. thetaiotaomicron* and *F. prausnitzii* respectively. Then entered a slower second ($0.20 \pm 0.01 \text{ h}^{-1}$ and $0.21 \pm 0.01 \text{ h}^{-1}$, respectively) and third phase ($0.07 \pm 0.002 \text{ h}^{-1}$ and $0.09 \pm 0.004 \text{ h}^{-1}$, respectively). The growth rates calculated from the reconstructed growth curves closely match those observed in monocultures (Figure 5C).

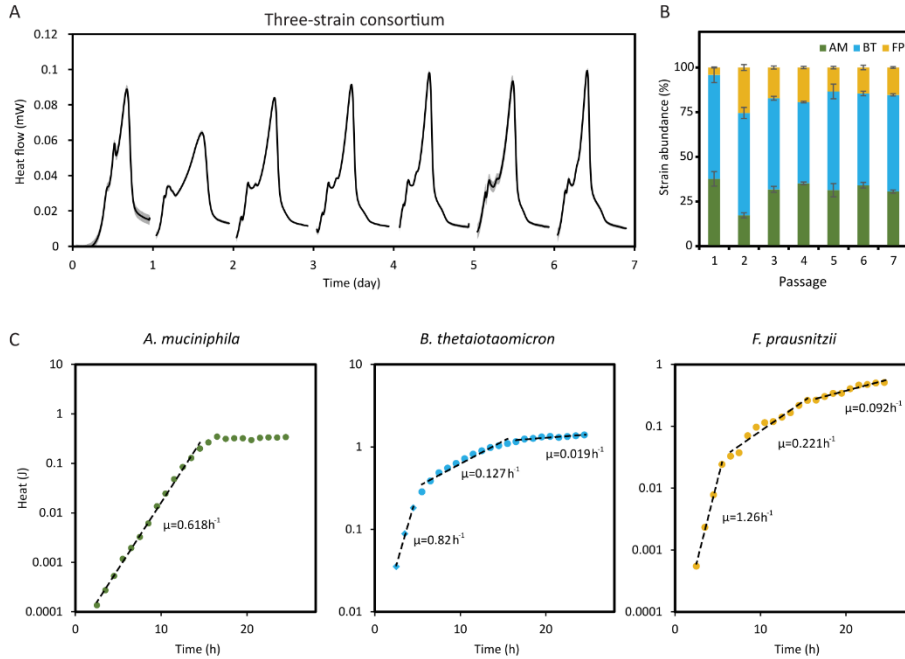


Figure 5. Stability of the consortium composition throughout serial passages. (a) Growth of the consortium was assessed in YCFAM medium across seven consecutive passages using IMC. For each passage, average heat flow and its standard deviation ($n = 3$) are illustrated by full lines and ribbon, respectively. (b) The relative abundance of each strain within the consortium was analyzed at the end of each passage via 16S rRNA gene sequencing. *A. muciniphila*, *B. thetaiotaomicron*, and *F. prausnitzii* are indicated by green, blue, and yellow bars, respectively. (c) Individual growth rates (h^{-1}) were calculated based on the total heat (J) produced by the consortium and the relative abundance of each strain within the consortium. Reproduced from: Kattel et al., (2024), *MicrobiologyOpen*, Wiley. Licensed under CC BY 4.0.

Community's ability to recover from different types of disturbances by growth, physiological, or genetic adaptation is defined as resilience (Allison & Martiny, 2008). The stability of the community can be affected by pH, medium composition, and species initial abundance over serial passages (Goldford et al., 2018; Niehaus et al., 2019). We challenged the stability of the consortium and assessed its resilience by altering the initial species abundances. Three combinations were tested, each with the concentration of one species reduced 100-fold compared to the other two species in the inoculum. At the end of all passages, species ratio was quantified using 16S rRNA sequencing. If the composition of the consortia and growth kinetics were to match the reference consortium (equal inoculation rate, Figure 5), the disturbance would be considered overcome. If this were not achieved, the consortium would not be resilient.

Firstly, the growth kinetics were assessed. Two consortia, where *A. muciniphila* and *B. thetaiotaomicron* were inoculated at a lower concentration respectively, had notably different growth kinetics than the reference consortium (Figure 6A). The consortium with a low *A. muciniphila* inoculation rate overcame the disturbance after four passages. In the case of consortia with low *B. thetaiotaomicron* and *F. prausnitzii*, two passages were sufficient to recover from the disturbance. Consistent with the heat flow data, 16S rRNA sequencing also confirmed that all three consortia were able to overcome the disturbances and return to stable composition by the end of the fifth passage (Figure 6B). The obtained consortia compositions after each passage are presented in Table S1. This indicates that there is no strong competition for growth-dependent substrate(s), and species are not heavily dependent on each other, although cross-feeding possibilities exist.

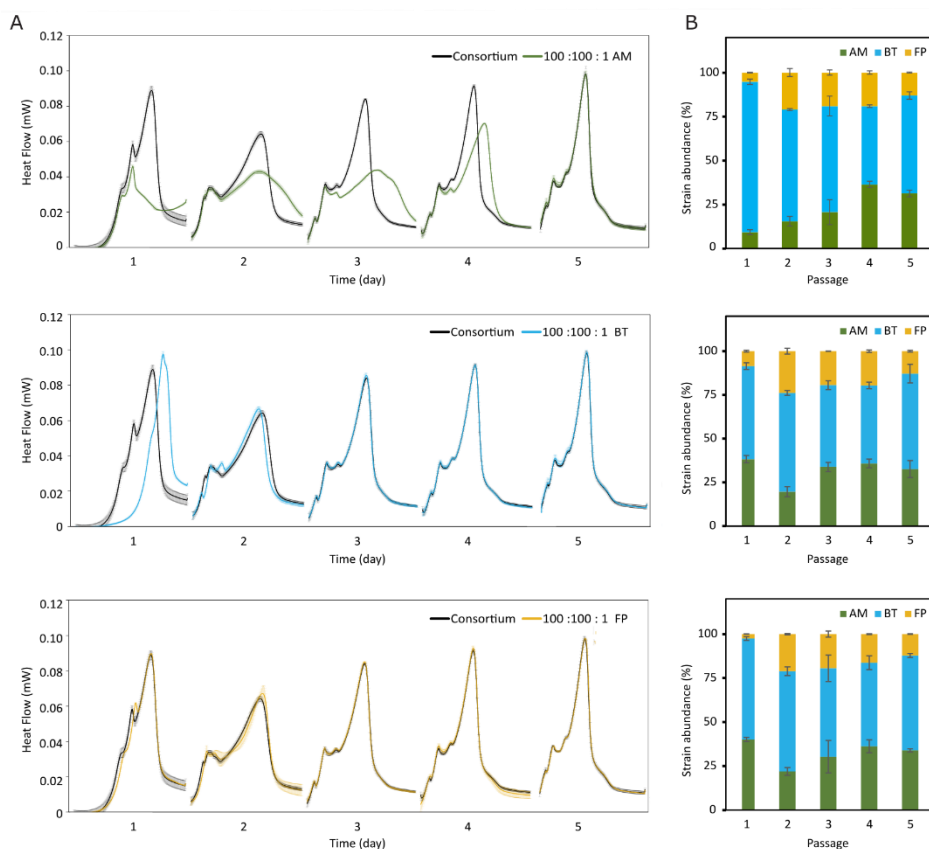


Figure 6. Resilience of the consortium. (a) To assess the resilience of the consortium, three experimental setups were designed where either *A. muciniphila* (AM), *B. thetaiotaomicron* (BT), or *F. prausnitzii* (FP) was initially inoculated at a 100-fold lower concentration than the other two strains (from top to bottom, respectively). Average heat flow and its standard deviation ($n = 3$) are shown as solid line and ribbon respectively. Resilience was considered achieved once the heat flow profile matched that of the original consortium (Figure 5). (b) The relative abundance of *A. muciniphila* (green), *B. thetaiotaomicron* (blue), and *F. prausnitzii* (yellow) was determined with 16S rRNA gene sequencing at the end of each passage ($n = 3$). Reproduced from: Kattel et al., (2024), *MicrobiologyOpen*, Wiley. Licensed under CC BY 4.0.

To further investigate the interactions in the consortium, we looked into the main metabolites (Figure 7). SCFA were quantified at the end of the fifth, sixth, and seventh passages in the consortium (equal inoculation rate) as well as the monoculture samples. Results from the three monoculture samples were summarized to allow for a better comparison with the consortium. The consortium had a significantly higher concentration of acetate, butyrate, and succinate compared to the sum of monocultures. Propionate concentration was significantly lower in the consortium than in the sum of monocultures. These results indicate that species are not completely independent of one another. As butyrate is only produced by *F. prausnitzii*, the higher concentration indicates beneficial cross-feeding with acetate producers. Despite the presence of acetate consumption, its concentration remains higher in the consortium compared to the sum of monocultures, likely due to overall increased production, suggesting complex metabolic interplay.

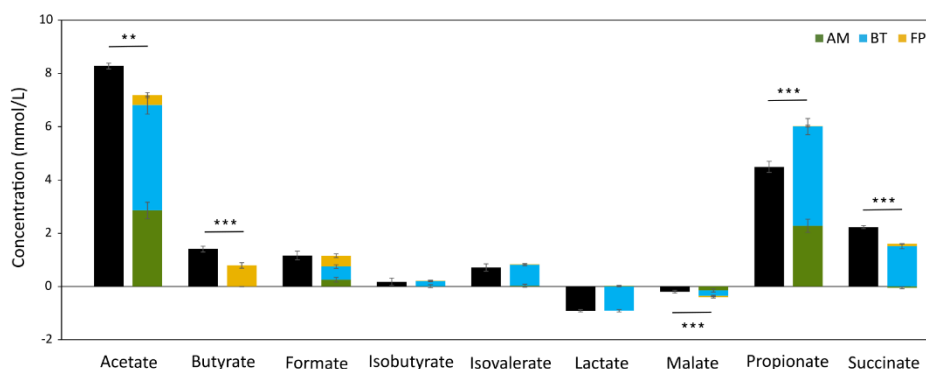


Figure 7. Production of external metabolites in monocultures and the consortium. Concentrations of organic acids (mmol/L) were measured following the fifth, sixth, and seventh passages. Green, blue, and yellow bars indicate the monocultures of *A. muciniphila* (AM), *B. thetaiotaomicron* (BT), and *F. prausnitzii* (FP), respectively, while black bars depict the consortium. To represent the expected outcome without interspecies interactions, metabolite concentrations from individual strains were stacked up. Statistical significance between consortium and the mathematical sum of monocultures was calculated with a Student's t-test (* $p < 0.05$, ** $p < 0.01$, *** $p < 0.001$). Reproduced from: Kattel et al., (2024), *MicrobiologyOpen*, Wiley. Licensed under CC BY 4.0.

Flux balance analysis (FBA) was also performed using the available data; however, many of the predictions were not confirmed by in vitro data, especially the quantification of amino acids. While FBA provides valuable hypotheses, it is limited by data quality and model-specific constraints such as steady-state growth and objective functions. In our case, the use of a complex undefined medium and the inability to quantify carbon source consumption further constrained the accuracy of FBA predictions. Our results indicate that further refinement, particularly the use of chemically defined media and dynamic sampling, will be essential to align predictions with empirical data. Nonetheless, we concluded that each strain likely had a different growth-limiting substrate, supporting the idea that each species in the consortia is limited by a different primary growth substrate.

4.3 Evaluating diversity of 25-species model consortium (Unpublished data)

As our three-species consortium was stable, we proceeded to test a more diverse model consortium. We cultivated 25 species in complex YCM medium over three passages, again using an isothermal microcalorimeter. All species except *Prevotella copri* were present after day 3, and the Shannon diversity index was 2.26. The Shannon diversity index, often referred to as the Shannon-Wiener index, quantifies community diversity by incorporating both the number of species and relative abundance of those species (Shannon, 1948). It should be noted that 16S rRNA gene sequencing could not differentiate between *Bifidobacterium adolescentis* and *Bifidobacterium longum*, as well as *Roseburia faecis* and *Eubacterium rectale*, so these species were grouped together in the analysis.

Odoribacter splanchnicus had the highest relative abundance (30.4%), while *Bacteroides* spp. accounted for a combined 44.8%. Butyrate producers, excluding *Odoribacter splanchnicus*, made up 5.4% of the consortium. Considering that the consortium consisted of strict anaerobes and often difficult-to-cultivate species, the observed diversity was relatively high, with 14 species exceeding 1% abundance.

At this stage, we lacked effective tools to selectively increase or decrease the abundance of individual species and thereby modulate overall consortium diversity. One potential strategy was to supplement the medium with additional substrates. However, without a clear understanding of how these changes would impact consortium dynamics, such modifications could lead to unpredictable and undesirable outcomes. This challenge motivated the development of a unique substrate-based approach for consortia production.

4.4 Analysis of metabolism in co-cultures of *Anaerostipes caccae* and *Bacteroides* spp. (Publication II)

Many NGP candidate species are cultivated in rich complex media due to limited knowledge of their metabolism. To enable detailed metabolic studies, we switched from complex rich media to a chemically defined medium (CDM). This approach allows precise quantification of substrates and yields more accurate data for FBA. Although we anticipated that some species might not be culturable in CDM, the resulting loss in diversity was acceptable, as the aim was not to replicate gut complexity but to develop a controlled production workflow.

4.4.1 Screening and genome annotation analysis of candidate species

We assessed the growth of 25 species in CDM, where glucose was the primary carbon source, using a microtiter plate reader. Out of the 25 species, growth was observed for 12 species (Table 1). Species with extremely slow growth rates, long lag-phases, or no detectable growth were excluded from subsequent experiments. Following the initial screening, eight species were selected for further analysis: *Anaerostipes caccae* (*A. caccae*), *Bifidobacterium longum*, *Bifidobacterium adolescentis*, *B. thetaiotaomicron*, *B. vulgatus*, *Bacteroides ovatus*, *Bacteroides caccae*, and *Bacteroides uniformis*.

Table 1. Overview of the average measured and calculated growth parameters in a glucose-containing defined medium. The following species did not exhibit measurable growth and were therefore excluded from the table: *Christensenella minuta*, *Alistipes shahii*, *Anaerotruncus colihominis*, *Blautia faecis*, *Blautia hydrogenotrophica*, *Butyrivimonas faecihominis*, *Prevotella copri*, *Eubacterium rectale*, *Akkermansia muciniphila*, *Faecalibacterium prausnitzii*, *Roseburia faecis*, *Eisenbergiella tayi*, and *Odoribacter splanchnicus*. Reported errors represent the standard error of four biological replicates. * – Growth parameters for *Catenibacterium mitsuokai* are unavailable due to cell clumping during cultivation, which resulted in unreliable OD measurements. Adapted from: Kattel et al., (2023), *Anaerobe*, Elsevier. Used under author rights.

Organism	Maximum OD at 600 nm	Lag phase, h	Specific growth rate, h ⁻¹
<i>Anaerostipes caccae</i>	0.59 ± 0.03	10.4 ± 0.1	0.59 ± 0.01
<i>Bacteroides vulgatus</i>	0.61 ± 0.01	3.6 ± 0.3	0.27 ± 0.01
<i>Bacteroides caccae</i>	0.82 ± 0.00	2.0 ± 0.1	0.37 ± 0.01
<i>Bacteroides ovatus</i>	0.66 ± 0.01	2.6 ± 0.2	0.34 ± 0.01
<i>Bacteroides thetaiotaomicron</i>	0.70 ± 0.00	2.9 ± 0.1	0.45 ± 0.00
<i>Bacteroides uniformis</i>	0.71 ± 0.01	2.4 ± 0.1	0.34 ± 0.01
<i>Bifidobacterium longum</i> subsp. <i>infantis</i>	0.35 ± 0.01	6.3 ± 0.1	0.31 ± 0.01
<i>Bifidobacterium adolescentis</i>	0.41 ± 0.01	5.3 ± 0.0	0.24 ± 0.01
<i>Collinsella aerofaciens</i>	0.32 ± 0.02	5.7 ± 0.2	0.09 ± 0.00
<i>Dorea formicigenerans</i>	0.11 ± 0.00	21.2 ± 0.6	0.05 ± 0.00
<i>Dorea longicatena</i>	1.40 ± 0.08	15.7 ± 0.5	0.39 ± 0.02
<i>Catenibacterium mitsuokai</i>		NA*	

Next, we looked into the metabolic pathways to determine the substrate utilization capabilities of these species (Table S2), focusing on monosaccharides and their derivatives such as sugar alcohols and acids. These substrates were selected due to the availability of reliable analytical methods for their quantification, which is crucial for high-quality metabolic modelling and assessing cross-feeding interactions.

The pathway analysis revealed that *Bifidobacterium longum* and *Bifidobacterium adolescentis* lacked unique degradation pathways that were not also present in *A. caccae* and the *Bacteroides* species. Therefore, *Bifidobacteria* were excluded from further experiments. In summary, among the remaining six species, pathway analysis revealed 13 different degradation pathways across 12 selected carbohydrates. Glucose was replaced with these substrates (at equimolar concentrations) in CDM, and growth profiles were recorded (Table 2). Due to the limited number of unique substrates identified among the six species, we were restricted to conducting pairwise co-culture experiments. Substrate was considered to be unique if it was exclusively consumed by single species in the co-culture.

Table 2. Validation of in silico metabolic predictions. Shown are the average growth rates (μ , h^{-1}) for six different species grown on selected substrates. Growth rates were calculated based on heat production data, with standard errors calculated from two biological replicates. AC – *A. caccae*, BC – *B. caccae*, BO – *B. ovatus*, BT – *B. thetaiotaomicron*, BU – *B. uniformis*, BV – *B. vulgatus*, ND – growth not detected. Adapted from: Kattel et al., (2023), *Anaerobe*, Elsevier. Used under author rights.

Substrate	AC	BC	BO	BT	BU	BV
D-Fructose	0.35 ± 0.01	0.51 ± 0.03	0.33 ± 0.06	0.48 ± 0.03	0.55 ± 0.08	0.57 ± 0.01
D-Galactose	0.50 ± 0.00	0.56 ± 0.02	0.43 ± 0.05	0.66 ± 0.00	0.55 ± 0.00	0.32 ± 0.01
D-Xylose	ND	0.61 ± 0.00	0.44 ± 0.02	0.56 ± 0.05	0.54 ± 0.01	0.42 ± 0.01
L-Arabinose	ND	0.53 ± 0.00	0.50 ± 0.00	0.58 ± 0.01	0.51 ± 0.02	0.56 ± 0.02
D-Galacturonic acid	ND	0.31 ± 0.02	0.19 ± 0.02	0.27 ± 0.01	0.22 ± 0.02	0.21 ± 0.02
L-Rhamnose	ND	0.14 ± 0.00	0.15 ± 0.00	0.15 ± 0.01	ND	0.30 ± 0.01
L-Fucose	ND	0.29 ± 0.01	0.12 ± 0.00	0.22 ± 0.01	ND	ND
D-Mannitol	0.08 ± 0.00	ND	0.34 ± 0.01	ND	ND	ND
D-Sorbitol	0.17 ± 0.00	ND	ND	ND	ND	ND
Dulcitol	0.05 ± 0.00	ND	ND	ND	ND	ND
Xylitol	ND	ND	ND	ND	ND	ND
D-Lyxose	ND	ND	ND	ND	ND	ND

4.4.2 Establishing and validating co-cultures based on substrate specificity

Based on the growth data (Table 2) we identified multiple unique substrate-based co-culture pairs and tested *A. caccae* (D-sorbitol; specific growth rate 0.17 h^{-1}) with *B. thetaiotaomicron* (D-xylose; 0.56 h^{-1}) and *B. vulgatus* (D-galacturonic acid; 0.21 h^{-1}). These combinations allowed us to pair the butyrate-producer *A. caccae* with succinate/propionate producers – *B. thetaiotaomicron* and *B. vulgatus*. Firstly, we needed to confirm that in multi-substrate conditions, species selectively utilized their designated unique carbon source and that there would be no consumption of the other one.

Growth medium containing a unique carbon source along with a non-utilizable carbon source for each species was prepared and used in a serial batch format. Growth kinetics of monocultures remained consistent across three consecutive batches. In D-xylose + D-sorbitol medium, total heat production by *B. thetaiotaomicron* was $0.68 \pm 0.02 \text{ J mL}^{-1}$ (day 3)(Figure 8A), and in D-galacturonic acid + D-sorbitol medium, *B. vulgatus* produced $0.44 \pm 0.04 \text{ J mL}^{-1}$ of heat on day 3 (Figure 8B). The heat produced by *A. caccae* remained unchanged whether D-sorbitol medium was supplemented with D-xylose ($0.35 \pm 0.02 \text{ J mL}^{-1}$) or D-galacturonic acid ($0.33 \pm 0.02 \text{ J mL}^{-1}$). No significant difference was observed ($p = 0.48$). Quantification of the sugars at the end of the experiments confirmed the depletion of the main carbon sources: D-sorbitol by *A. caccae*, D-xylose by *B. thetaiotaomicron*, and D-galacturonic acid by *B. vulgatus*.

We then studied co-cultures of *A. caccae* with *B. thetaiotaomicron* or *B. vulgatus* in the same dual-substrate media. Our hypothesis was that, in the absence of interactions, total heat production would equal or be similar to the sum of monocultures. However, measured heat was 1.1 to 1.5 times higher in both co-cultures across all three batches (Figure 8), suggesting positive metabolic interactions.

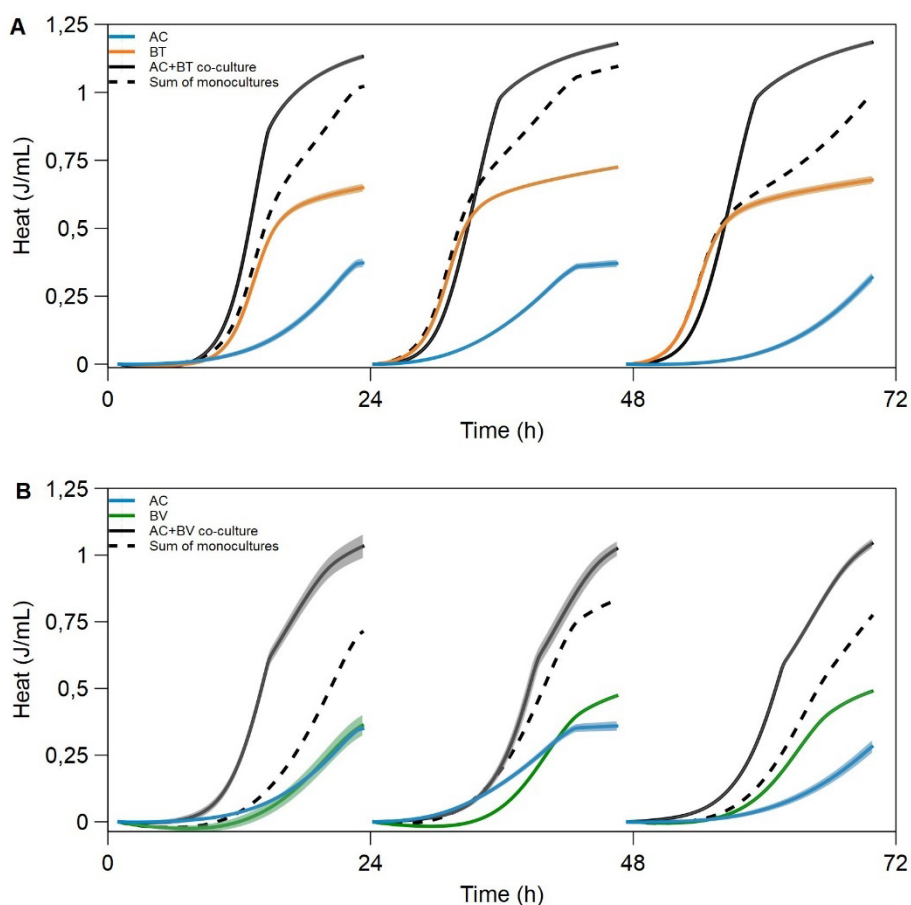


Figure 8. Monitoring of monoculture and co-culture growth kinetics using IMC. (A) Heat flow profiles for *A. caccae* (AC), *B. thetaiotaomicron* (BT), and their co-culture (AC + BT) cultivated in D-sorbitol and D-xylose medium. (B) Heat flow for AC, *B. vulgatus* (BV), and their co-culture (AC + BV) cultivated in D-sorbitol and D-galacturonic acid medium. Full line and ribbon represent the average and standard deviation of the heat, respectively ($n=3$), for each batch. The dashed line indicates the mathematical sum of the two monoculture heat profiles. Reproduced from: Kattel et al., (2023), *Anaerobe*, Elsevier. Used under author rights.

4.4.3 Co-culture metabolic interactions

Figure 8 illustrates that co-cultures generated consistently throughout three batches more heat than the sum of individual monocultures, indicating metabolic interactions. We compared final organic acid concentrations in co-cultures to the sum of monocultures (Table 3, Table 4). Significant differences were observed for acetate, butyrate, and lactate.

In the *A. caccae* + *B. thetaiotaomicron* co-culture on day 3, acetate levels were 2-fold lower and lactate 50-fold lower when compared to the sum of monoculture results (Table 3). In the co-culture, butyrate and propionate concentrations were 3.1-fold and 1.3-fold higher, respectively. Acetate and propionate were produced exclusively by *B. thetaiotaomicron*, whereas lactate and butyrate were produced solely by *A. caccae*.

Therefore, these results indicate mutual metabolic benefits likely via cross-feeding of acetate for butyrate synthesis (Chia et al., 2018; Duncan et al., 2004; Falony et al., 2006).

A. caccae + *B. vulgatus* co-culture had similar changes regarding the metabolite concentrations (Table 4). When comparing the day 3 results, acetate and lactate levels in the co-culture were 1.4-fold and 6-fold lower, respectively, than the combined values from the *A. caccae* and *B. vulgatus* monocultures. In contrast, concentrations of butyrate and propionate were higher 2.9-fold and 2-fold, respectively in the co-culture.

To assess the potential growth-promoting effects of acetate on *A. caccae* and lactate on *B. thetaiotaomicron*, supplementation experiments were conducted in the IMC. A range of acetate and lactate concentrations (0 to 20 mM) was tested. When grown on D-sorbitol without acetate, *A. caccae* exhibited a specific growth rate of $0.24 \pm 0.00 \text{ h}^{-1}$. The addition of 2 mM acetate significantly increased specific growth rate up to $0.74 \pm 0.00 \text{ h}^{-1}$ ($p < 0.001$). Increasing acetate concentrations further (4 to 20 mM) produced an additional though smaller effect, with maximal specific growth rates ranging from 0.85 to 1.05 h^{-1} ($p < 0.001$).

Regardless of the acetate concentration, all D-sorbitol ($5.5 \pm 0.1 \text{ mM}$) was consumed by *A. caccae* (Table S3). When 6 mM of acetate or more was in the medium, approximately $4.2 \pm 0.2 \text{ mM}$ of acetate was taken up. At lower acetate concentrations (2 mM and 4 mM), acetate was depleted. This corresponds to a molar consumption ratio of acetate to D-sorbitol of roughly 0.8:1. The conversion of acetate to butyrate requires one NADH molecule per reaction via a non-bifurcative pathway (KEGG, Kanehisa & Goto, 2000), whereas converting D-sorbitol to butyrate yields one NADH per molecule of D-sorbitol. Theoretically, the expected molar ratio of acetate to D-sorbitol should be 1:1. The observed deviation from this ratio likely comes from the consumption of free amino acids and the potential utilization of bifurcative butyrate synthesis pathways, both of which reduce intracellular NADH levels (F. Li et al., 2008). Additionally, as the acetate concentration in the medium was increased, lactate production decreased (Table S3). When added acetate concentrations were 6 mM or higher, steep decrease in lactate production was observed, implying that limited NADH availability may limit acetate uptake.

The effect of lactate supplementation on the growth of *B. thetaiotaomicron* was evaluated across a same range of concentrations: 2 mM, 4 mM, 6 mM, 8 mM, 10 mM, and 20 mM. Despite varying lactate levels, the effect on specific growth rate remained relatively consistent. Without lactate, *B. thetaiotaomicron* exhibited a specific growth rate of $0.38 \pm 0.00 \text{ h}^{-1}$, which increased to 0.53 – 0.56 h^{-1} upon lactate addition ($p < 0.01$). The maximum observed lactate consumption was $3.2 \pm 0.0 \text{ mM}$, while $4.7 \pm 0.0 \text{ mM}$ of D-xylose was metabolized, resulting in a lactate to D-xylose molar consumption ratio of 0.7:1 (Table S4). Under anaerobic conditions, converting lactate to pyruvate is not energetically favourable and requires a bifurcative pathway involving reduced ferredoxin with a low redox potential as a co-substrate (Weghoff et al., 2015). This conversion yields two NADH molecules. Given that pyruvate ferredoxin oxidoreductase is the primary source of reduced ferredoxin in succino- and propionigenic bacteria, lactate consumption is likely constrained by the availability of reduced ferredoxin (Blaschkowski et al., 1982). The NADH generated from concentration dependent lactate uptake is subsequently channeled into the production of succinate and propionate. As lactate concentrations in the medium increase, the molar ratio of these acids to consumed D-xylose also rises from 0.4:1 to 0.7:1. These findings strongly suggest that the extent of cross-feeding between the species is limited by intracellular availability of NADH and/or reduced ferredoxin.

Table 3. Production of major metabolites on day 3 in the co-culture (*A. caccae* + *B. thetaiotaomicron*) and in the respective monocultures (*A. caccae*, *B. thetaiotaomicron*). Average values (mM) \pm standard errors (n = 3) are presented. Statistical significance between the co-culture and the combined monocultures was determined using Student's t-test (*p < 0.05, **p < 0.01, *p < 0.001). ND – not detected. Adapted from: Kattel et al., (2023), Anaerobe, Elsevier. Used under author rights.**

	acetate	butyrate	formate	lactate	propionate	succinate
<i>A. caccae</i>	ND	1.32 \pm 0.02	0.73 \pm 0.03	4.68 \pm 0.06	ND	ND
<i>B. thetaiotaomicron</i>	2.53 \pm 0.01	ND	0.60 \pm 0.01	ND	1.53 \pm 0.01	1.95 \pm 0.01
<i>A. caccae</i> + <i>B. thetaiotaomicron</i> co-culture	1.38 \pm 0.01***	4.49 \pm 0.01***	0.41 \pm 0.00***	0.10 \pm 0.00***	2.00 \pm 0.01***	1.73 \pm 0.00***
Sum of <i>A. caccae</i> and <i>B. thetaiotaomicron</i>	2.53 \pm 0.01	1.32 \pm 0.02	1.33 \pm 0.04	4.68 \pm 0.06	1.53 \pm 0.01	1.95 \pm 0.01

Table 4. Production of major metabolites on day 3 in the co-culture (*A. caccae* + *B. vulgatus*) and in the respective monocultures (*A. caccae*, *B. vulgatus*). Average values (mM) \pm standard errors (n = 3) are presented. Statistical significance between the co-culture and the combined monocultures was determined using Student's t-test (*p < 0.05, **p < 0.01, *p < 0.001). ND – not detected. Adapted from: Kattel et al., (2023), Anaerobe, Elsevier. Used under author rights.**

	acetate	butyrate	formate	lactate	propionate	succinate
<i>A. caccae</i>	ND	1.19 \pm 0.01	0.7 \pm 0.03	4.28 \pm 0.15	ND	ND
<i>B. vulgatus</i>	4.29 \pm 0.01	ND	0.24 \pm 0.00	ND	0.57 \pm 0.00	0.99 \pm 0.00
<i>A. caccae</i> + <i>B. vulgatus</i> co-culture	3.12 \pm 0.02***	3.73 \pm 0.03***	0.61 \pm 0.01**	1.03 \pm 0.06***	1.04 \pm 0.01***	1.11 \pm 0.01**
Sum of <i>A. caccae</i> and <i>B. vulgatus</i>	4.29 \pm 0.01	1.19 \pm 0.01	0.94 \pm 0.03	4.28 \pm 0.15	0.57 \pm 0.00	0.99 \pm 0.00

4.4.4 Species ratio determination

Accurately determining species ratios is critical for understanding co-culture dynamics, as the ratio of the species can determine the overall functionality of the co-culture. While 16S sequencing and qPCR are commonly used in research, extracting DNA from different species presents challenges, and it is important to evaluate and optimize protocols specifically for the species of interest (Clark et al., 2021; Oba et al., 2020). We tested DNA extraction and qPCR protocol using artificial mixes of *A. caccae*, *B. thetaiotaomicron*, and *B. vulgatus*. In an equal mix (ratio based on OD measurements), *B. thetaiotaomicron* and *B. vulgatus* were overestimated (47% \pm 2% and 41% \pm 1%), and *A. caccae* was underestimated (12% \pm 1%)(Table S5). A second test mix, where the expected OD-based ratio was 80% *A. caccae*, 10% *B. thetaiotaomicron*, and 10% *B. vulgatus*, yielded 52% *A. caccae*, 27% *B. thetaiotaomicron*, and 21% *B. vulgatus*. In these test experiments, we used the GenElute™ Bacterial Genomic DNA Kit (Merck, Germany) for DNA extraction. We also evaluated an alternative kit, the ZymoBIOMICS™ DNA Miniprep Kit, (Zymo Research, Irvine, CA, USA); however, this did not improve the extraction yield for *A. caccae* (data not shown). Alternative primers were also designed for all three strains; however, consistent with previous results, *A. caccae* was still underestimated (data not shown).

A potential reason for this bias is the difference in cell wall structures: *A. caccae* is gram-variable, while the *Bacteroides* spp. are gram-negative (Schwiertz et al., 2002; Weiss & Rettger, 1937). These differences likely affect DNA extraction efficiency. Therefore, DNA-based methods may not reliably quantify species ratios but can be used to determine stability in co-cultivation experiments.

The qPCR analysis confirmed that the strain ratios remained consistent throughout the serial batch experiment (Table S6). However, we needed a method that could measure the species ratio as the goal was to also change the ratio later and only using metabolome data would not have been sufficient. To determine cell ratios more accurately, we developed a microscopy-based image analysis method leveraging the distinct morphologies of *A. caccae* and *Bacteroides* spp. At the end of the serial batch experiment (day 3), microscopy image analysis showed average species ratios of 49:51 ($\pm 3\%$) for *A. caccae*:*B. thetaiotaomicron* and 37:63 ($\pm 1\%$) for *A. caccae*:*B. vulgatus*, indicating that both species were present in approximately equal cell concentrations in both co-cultures.

4.4.5 Development of co-culture bioprocess

IMC is a good method for screening experiments but for more technical control and additional analysis we developed high density processes in Applikon bioreactors. Now we had an opportunity to perform through growth gas analysis and elevate both carbon source and amino acid concentrations three to five times for higher biomass densities. Final OD values for monocultures were consistent: 2.3 ± 0.0 for *A. caccae*, 2.1 ± 0.1 for *B. thetaiotaomicron*, and 1.6 ± 0.1 for *B. vulgatus*. Co-cultures showed nearly doubled biomass: 4.1 ± 0.2 for *A. caccae* + *B. thetaiotaomicron* and 3.5 ± 0.1 for *A. caccae* + *B. vulgatus*.

The *A. caccae* + *B. vulgatus* co-culture had a similar specific growth rate ($0.52 \pm 0.02 \text{ h}^{-1}$) with *A. caccae* + *B. thetaiotaomicron* co-culture ($0.48 \pm 0.05 \text{ h}^{-1}$). As in IMC experiments, co-cultures showed higher butyrate and propionate levels, and lower acetate and lactate levels, than monocultures (Table 5). Since qPCR could not be used to determine the species ratio, microscopy images were taken from samples at the end of fermentation. Based on cell size, *Bacteroides* spp. and *A. caccae* were differentiated. Microscopy confirmed species ratios: 43:57 (*A. caccae*:*B. thetaiotaomicron*) and 49:51 (*A. caccae*:*B. vulgatus*), demonstrating maintained control upon scale-up.

Table 5. Production of major metabolites was determined in monocultures of *A. caccae*, *B. thetaiotaomicron*, and *B. vulgatus*, as well as in their respective two-species co-cultures in bioreactor experiments. Average concentrations (mM) \pm standard errors ($n \geq 2$) are shown. A Student's *t*-test was used to assess statistical significance between co-culture values and the sum of monoculture values (* $p < 0.05$, ** $p < 0.01$, * $p < 0.001$). ND – not detected. Adapted from: Kattel et al., (2023), *Anaerobe*, Elsevier. Used under author rights.**

	acetate	butyrate	formate	lactate	propionate	succinate
<i>A. caccae</i>	ND	4.31 \pm 0.03	0.45 \pm 0.01	13.40 \pm 0.29	ND	ND
<i>B. thetaiotaomicron</i>	9.24 \pm 0.10	ND	3.71 \pm 0.15	0.35 \pm 0.18	1.22 \pm 0.05	6.96 \pm 0.04
<i>B. vulgatus</i>	16.68 \pm 0.68	ND	2.74 \pm 0.04	0.05 \pm 0.05	0.62 \pm 0.01	2.78 \pm 0.22
<i>A. caccae</i> + <i>B. thetaiotaomicron</i> co-culture	3.11 \pm 0.34**	9.51 \pm 0.51**	2.52 \pm 0.11**	8.58 \pm 0.69**	1.85 \pm 0.21	5.48 \pm 0.62
<i>A. caccae</i> + <i>B. vulgatus</i> co-culture	6.11 \pm 1.02***	14.06 \pm 0.50***	4.82 \pm 1.17	3.80 \pm 0.59***	1.10 \pm 0.09***	2.03 \pm 0.23
Sum of <i>A. caccae</i> and <i>B. thetaiotaomicron</i>	9.24 \pm 0.10	4.31 \pm 0.03	4.17 \pm 0.15	13.76 \pm 0.34	1.22 \pm 0.05	6.96 \pm 0.04
Sum of <i>A. caccae</i> and <i>B. vulgatus</i>	16.68 \pm 0.68	4.31 \pm 0.03	3.20 \pm 0.04	13.45 \pm 0.30	0.62 \pm 0.01	2.78 \pm 0.22

4.4.6 Altering substrate ratios and characterizing metabolic interactions with FBA

One key aspect of the workflow was the ability to control species ratios. This is essential when product efficacy depends on specific ratio. Initially, we used a 50:50 (percentage wise) substrate ratio (D-sorbitol:D-xylose), expecting corresponding species ratios. To demonstrate substrate-based control, we altered the ratio to 80:20 and 20:80 while keeping the ratio in the inoculum same as before: 50:50 (*A. caccae*:*B. thetaiotaomicron*).

For the 80:20 substrate ratio we increased the target concentration of D-sorbitol (*A. caccae* substrate) to 66.8 mM and maintained the target concentration of D-xylose (substrate for *B. thetaiotaomicron*) at 16.7 mM. These concentrations were based on values set during experimental design and the actual concentrations measured by HPLC showed some deviation, as expected. Under these conditions, we observed a longer lag phase, likely due to insufficient acetate production by *B. thetaiotaomicron*. Acetate remained undetectable until 12.4 h and previously observed high growth rate was not reached. We monitored hydrogen production throughout the growth as an indicator of *A. caccae*'s metabolic activity. Microscopy at the end showed an 82:18 ratio (*A. caccae*:*B. thetaiotaomicron*).

Subsequently, we reversed the substrate concentrations, increasing the target concentration of D-xylose (substrate for *B. thetaiotaomicron*) to 66.8 mM while maintaining the D-sorbitol (substrate for *A. caccae*) target concentration at 16.7 mM. This also resulted in a significantly longer lag-phase compared to the 50:50 substrate ratio. Hydrogen production ceased at 17.8 h, indicating the depletion of D-sorbitol and the onset of the asaccharolytic phase for *A. caccae*. At the end of fermentation, based on microscopy images, the cell ratio was 29:71 (*A. caccae*:*B. thetaiotaomicron*).

For metabolic modelling, the organisms' growth was separated into two main phases: saccharolytic and asaccharolytic. Model calculations indicated that the computationally

estimated metabolomes differed from experimental observations by 2–5%, leading to a surplus in carbon balance ranging from 1–4%. Flux variability analysis showed obligatory cross-feeding under several experimental scenarios (Figure 9). Based on exometabolome data, acetate was conclusively cross-fed by *A. caccae* in the saccharolytic phase of the 80:20 (D-sorbitol:D-xylose) setup, while *B. thetaiotaomicron* exhibited lactate cross-feeding during the asaccharolytic phase. Additionally, in the 20:80 (D-sorbitol:D-xylose) setup, *A. caccae* also displayed lactate cross-feeding in the asaccharolytic phase, therefore confirming metabolic interactions between the two species in the co-culture.

One of the earlier studies also looked into interactions between *A. caccae* and *B. thetaiotaomicron*, reporting metabolite changes such as lactate depletion and reductions in acetate and malate levels in co-cultures compared to monocultures (Chia et al., 2020). In agreement with these observations, we detected declines in short-chain fatty acids, specifically acetate and lactate, both substrates utilized by *A. caccae* (Duncan et al., 2004; Schwieritz et al., 2002). Although acetate utilization by *B. thetaiotaomicron* has been documented, lactate metabolism had not previously been demonstrated. Conversely, study with a different *B. thetaiotaomicron* strain (LMG 11262) indicated an inability to metabolize lactate (Falony et al., 2009). Additionally, we measured a significant increase in butyrate and propionate concentrations in our cultivation experiments, indicating mutual benefits from co-cultivation, with butyrate produced only by *A. caccae* and propionate only by *B. thetaiotaomicron*.

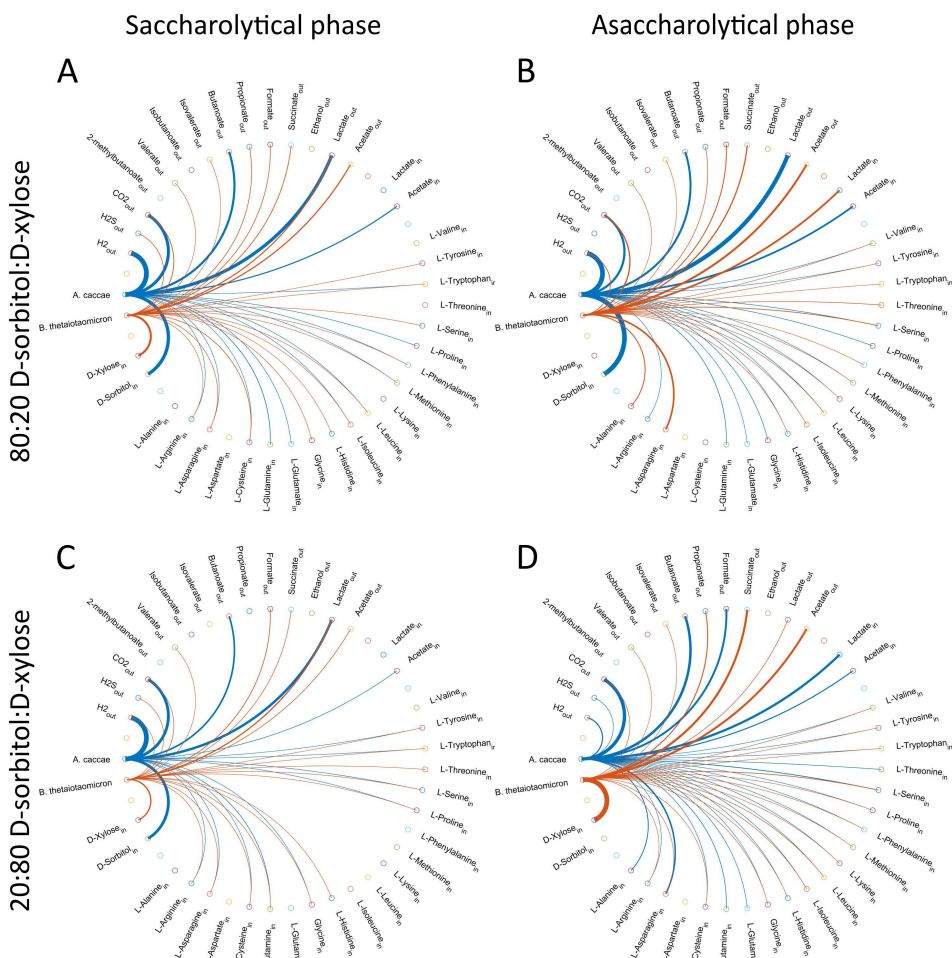


Figure 9. Metabolic cross-feeding between *A. caccae* and *B. thetaiotaomicron* in co-culture. After depletion of the primary carbon sources, both species continued growth, therefore growth was divided into saccharolytic and asaccharolytic phases. Varying the initial carbon source concentrations resulted in different metabolic scenarios. Metabolic flux distributions are shown for the 80:20 (D-sorbitol:D-xylose) setup, where both species are saccharolytic (A), and where BT transitions to the asaccharolytic phase (B). In this phase, BT consumes lactate produced by AC, while AC predominantly utilizes D-sorbitol and acetate. In the 20:80 (D-sorbitol:D-xylose) setup, panel C illustrates a scenario where both species remain in saccharolytic phase, while panel D depicts a condition in which AC is in asaccharolytic phase. In the asaccharolytic phase, AC consumes lactate and acetate, while BT mainly utilizes D-xylose. Orange and blue lines represent metabolic fluxes from AC and BT, respectively, with line thickness correlating with the corresponding flux value. Compounds labelled as “in” are consumed, and those labelled as “out” are produced. Adapted from: Kattel et al., (2023), Anaerobe, Elsevier. Used under author rights.

4.5 Estimation of viable cell abundance and enumeration using PMAXx and spike-in control as alternatives to traditional methods (Publication III)

4.5.1 Estimation of viable cell abundance using PMAXx-qPCR

Accurate viability assessment is critical for evaluating the biological functionality of microbial products. Specifically, their ability to perform intended metabolic roles and for ensuring the quality and consistency of synthetic microbial consortia. Traditional plating methods, while commonly used, are limited by their low throughput, labour intensiveness, and lack of species-level taxonomic information without further downstream analysis such as MALDI-TOF or PCR. Additionally, not all bacteria are culturable or grow on very specific medium. These limitations are especially pronounced in complex consortia where precise species-level viability data are crucial.

To address these challenges, we implemented a combination of propidium monoazide (PMAXx) and qPCR for viability assessment (Emerson et al., 2017; Navarro et al., 2020). PMAXx is a photo-reactive dye that selectively penetrates dead cells with compromised membranes and binds covalently to DNA upon exposure to light, thereby inhibiting its amplification in subsequent PCR reactions. By comparing the qPCR amplification of PMAXx-treated samples to untreated controls, we could estimate the proportion of viable cells within the sample. Strain specific primers were used to carry out the qPCR.

Flow cytometry (FC) was used to benchmark the PMAXx-qPCR results. Using SYTO24 and propidium iodide staining, we assessed the viability of each of the 20 individual strains as well as the viability of the mixed 20-strain consortia glycerol stock. The viability values obtained from FC varied significantly among individual strains, with viability ranging from 4% (*Bacteroides caccae*) to 96% (*Butyricimonas faecihominis*) (Table 6). The viability of the mixed 20-strain consortium was 68%. Importantly, PMAXx-qPCR results showed strong correlation with FC data (Figure 10) ($R^2 = 0.884$ when outliers were excluded), validating the accuracy of the method.

Table 6. The viability of 20 bacterial strains was evaluated using both FC and qPCR. *- Universal primers targeting the 16S rRNA gene V4 region were used instead of specific ones. Adapted from: Kallastu et al., (2023), *Current Research in Food Science, Elsevier*. Licensed under CC BY 4.0.

Species (acronym)	Gram stain	Viability by FC, %	Viability by qPCR, %
<i>Akkermansia muciniphila</i> (AM)	negative	66.11 ± 0.03	81.22 ± 13.47
<i>Alistipes shahii</i> (AS)	negative	62.40 ± 7.63	78.51 ± 12.18
<i>Anaerostipes caccae</i> (AC)	variable	60.69 ± 9.86	90.01 ± 5.02
<i>Anaerotruncus colihominis</i> (ACo)	positive	23.35 ± 0.90	40.15 ± 13.87
<i>Bacteroides caccae</i> (BC)	negative	3.76 ± 2.16	9.28 ± 0.26
<i>Bacteroides thetaiotaomicron</i> (BT)	negative	63.88 ± 8.26	56.87 ± 2.51
<i>Bacteroides uniformis</i> (BU)	negative	88.59 ± 1.82	100.00 ± 8.84
<i>Bifidobacterium adolescentis</i> (BA)	positive	83.72 ± 1.55	90.26 ± 7.07
<i>Blautia hydrogenotrophica</i> (BH)	positive	35.06 ± 14.86	24.63 ± 1.62
<i>Butyrivibrio faecihominis</i> (BF)	negative	95.88 ± 0.85	92.47 ± 27.24
<i>Catenibacterium mitsuokai</i> (CM)	positive	6.14 ± 1.86	0.46 ± 0.01
<i>Christensenella minuta</i> (ChM)	negative	40.40 ± 0.46	34.66 ± 7.18
<i>Collinsella aerofaciens</i> (CA)	positive	4.31 ± 0.13	11.25 ± 1.51
<i>Dorea formicigenerans</i> (DF)	positive	81.80 ± 1.19	90.18 ± 8.42
<i>Dorea longicatena</i> (DL)	positive	14.91 ± 1.49	22.70 ± 0.89
<i>Eisenbergiella tayi</i> (ET)	positive but Gram-stain negative	8.95 ± 1.57	43.96 ± 2.16
<i>Faecalibacterium prausnitzii</i> (FP)	positive	72.23 ± 5.40	74.70 ± 14.27
<i>Odoribacter splanchnicus</i> (OS)	negative	87.06 ± 0.54	93.38 ± 4.83
<i>Prevotella copri</i> (PC)	negative	32.88 ± 4.00	73.56 ± 21.67
<i>Roseburia faecis</i> (RF)	negative or variable	67.84 ± 4.32	87.07 ± 2.16
Mix of 20 strains		68.41 ± 0.18	60.92 ± 3.98*

However, some discrepancies between the two approaches were observed. For example, in the case of *Catenibacterium mitsuokai*, FC showed several-fold higher viability than qPCR, whereas in the case of *Eisenbergiella tayi*, the opposite was observed. Both FC and PMAxx-qPCR have distinct advantages and limitations. FC allows rapid detection of membrane integrity using fluorescent dyes, although its throughput is limited by sample preparation and instrument settings. It struggles with species exhibiting atypical morphologies, forming long chains or aggregates (like *Dorea longicatena*), which complicate gating strategies and can lead to underestimation or misclassification. Additionally, FC cannot provide taxonomic resolution unless paired with fluorescent in situ hybridization or other markers.

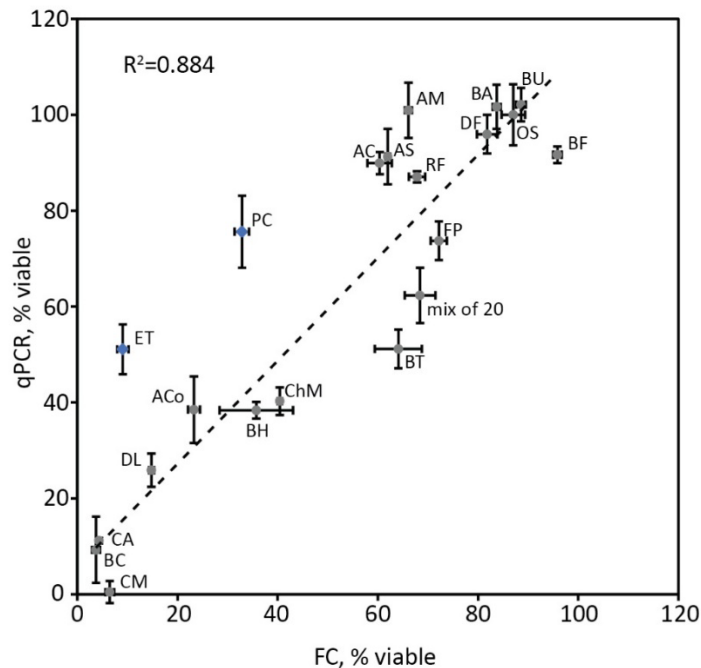


Figure 10. Scatterplot showing cell viability results obtained by FC and qPCR using strain-specific primers. The dotted line shows the regression trendline, with R^2 representing correlation strength. Grey circles are included in the regression analysis; blue squares are outliers. Acronyms for bacterial strains are provided in the Table 6. Reproduced from: Kallastu et al., (2023), *Current Research in Food Science*, Elsevier. Licensed under CC BY 4.0.

PMAxx-qPCR, in contrast, offers high taxonomic specificity by using strain-specific primers, making it suitable for studying complex microbial consortia. PMAxx-qPCR is compatible with plate-based and automated workflows, enhancing scalability in both research and industrial contexts. Nonetheless, PMAxx-qPCR is not without limitations. Its accuracy depends heavily on consistent and efficient DNA extraction, which may vary significantly between strains due to differences in cell wall structure. Gram-positive and Gram-variable species, such as *A. cacciae*, may yield lower DNA quantities, leading to an underestimation of viability. Also, the primer specificity and PCR efficiency play an important role in getting accurate results. The effectiveness of PMAxx also relies on light exposure and the optical clarity of the suspension. In coloured or turbid matrices, the efficiency of dye-DNA crosslinking may decrease, potentially allowing dead cell DNA to be amplified. Furthermore, both FC and PMAxx-qPCR rely on the differential permeability of fluorescent dyes, introducing a potential bias if dye uptake is inconsistent between species.

Overall, qPCR in combination with PMAxx showed higher levels of viable cells than FC. To further understand the discrepancies between two methods, microscopy analysis was done selectively to visually confirm species morphology and cellular arrangement. Based on FC and PMAxx-qPCR results, we selected representative species to investigate whether structural characteristics such as clumping could explain the differences in viability estimates. Some selected species showed agreement between both methods and others had clear discrepancies. Figure 11B shows that species with discrepancies between FC and qPCR data tend to form clusters and fiber-like structures. These formations can impact

cloud formation and complicate the analysis of FC data. In conclusion, PMAxx dye offers a reliable approach for distinguishing viable from dead microbial cells when used in combination with qPCR. This combination provides species-level resolution and improved accuracy in viability assessments, particularly in complex microbial communities.

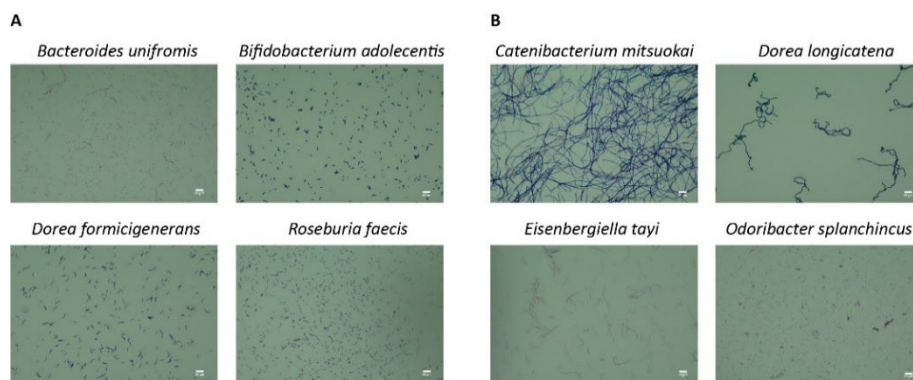


Figure 11. Microscopy images of bacterial strains: (A) examples where FC and qPCR data were similar, and (B) examples where FC and qPCR data differed. The white scale bar in the bottom right corner indicates 10 μm . Reproduced from: Kallastu et al., (2023), *Current Research in Food Science*, Elsevier. Licensed under CC BY 4.0.

4.5.2 Bacterial enumeration using spike-in and NGS

In some cases, the composition of microbial consortia is unknown. In such situations, NGS is a suitable alternative to PCR as it provides taxonomic information on all the species present in the sample. When combined with PMAxx, it can also distinguish between viable and non-viable cells. Additionally, incorporating a spike-in control allows for quantification of the total bacterial load not only relative abundance of bacteria.

To estimate the number of bacteria in our mixed 20-strain consortium stock, a spike-in control was incorporated prior to DNA extraction. We picked out the commercially available High-load Spike-in control (ZymoResearch) which contains a known quantity of two rarely occurring bacterial strains: *Allobacillus halotolerans* and *Imtechella halotolerans*. These strains underwent the entire NGS workflow alongside the sample and knowing the precise quantity of the spike-in strains allowed us to estimate the number of all bacteria in each sample. It is important to add the spike-in cells before the DNA extraction, so that they undergo the same experimental workflow as the target cells, ensuring methodological consistency.

To confirm that the number of added spike-in cells correlates with their NGS read counts linearly, we added them at different concentrations. As expected, varying the spike-in concentration resulted in a linear correlation with the total bacterial count (Pearson correlation coefficient, $r = 0.9981$). Therefore, for reliable estimation of microbial cell numbers, it is not required to add spike-in at an exact amount.

Based on OD600 measurement, our 20-strain mix sample taken for analysis had approximately 1.50×10^9 cells. Spike-in control reads, and species reads were used to estimate the total cell count of the mix sample using NGS. With the exact spike-in cell numbers known, we calculated the number of total cells in our sample (Table 7). Across different spike-in concentrations (0.5, 1.0, and 2.5%), the average calculated number of total cells was $1.55 \pm 0.18 \times 10^9$ which is similar to the theoretical value based on OD600 measurement (1.50×10^9 cells).

Table 7. Using spike-in for absolute quantification of total cells in 20 strain mix sample. NA – not available. Adapted from: Kallastu et al., (2023), *Current Research in Food Science*, Elsevier. Licensed under CC BY 4.0.

		20 st mix	20 st mix 0.5%	20 st mix 1%	20 st mix 2.5%
Number of added spike-in cells		0.00	7.50×10^6	1.50×10^7	3.75×10^7
Calculated abundance of added spike-in, %	<i>Allobacillus halotolerans</i>	0.00	0.25	0.72	1.13
	<i>Imtechella halotolerans</i>	0.00	0.18	0.35	1.28
SUM of spike-in, %		0.00	0.43	1.07	2.42
Calculated abundance of 20 strains, %		100	99.57	98.93	97.58
Calculated number of total cells in 20 strain mix sample		NA	1.74×10^9	1.39×10^9	1.51×10^9

As mentioned before, spike-in control should be added before DNA extraction. However, this is not always feasible or the quantitative information about bacterial load is needed retrospectively. In such cases, the only option is by measuring microbial gDNA concentration. Real-time quantitative PCR is a widely accepted method for obtaining quantitative DNA data, as the concentration of microbial gDNA is directly proportional to the number of bacterial cells. We decided to test it by performing qPCR with degenerate primers targeting the conserved 16S V4 region. Using a calibration curve, the microbial gDNA concentration was converted into an estimated total bacterial cell count of $1.16 \pm 0.12 \times 10^9$ cells. When compared to the theoretical value, the total cell count estimated with the qPCR was of the same order of magnitude but slightly lower.

According to our findings, the application of a spike-in control resulted in highly accurate enumeration of microbes, yielding results comparable to those obtained with FC, while qPCR-based estimation was slightly lower. Similar observations were made by Zemb et al., (2020), who reported that qPCR underestimated bacterial counts by approximately 1.9-fold compared to values obtained using an artificial internal spike-in standard.

4.5.3 Combining PMAxx treatment and spike-in control

Next, we combined PMAxx treatment with a spike-in control to assess both total and viable bacterial populations. Cells were either left untreated or treated with PMAxx, followed by the addition of the spike-in control. The complete 16S amplicon sequencing workflow was then performed. To quantify viable bacteria, three parallel analyses were conducted (20St 0.5PMA, 20St 1PMA, 20St 2.5PMA), each differing in the concentration of spike-in control added. Sequencing results confirmed the presence of all 20 bacterial species (Figure 12). The taxonomic profiles of viable bacteria across the three replicates were consistent with one another but differed from the total bacteria profile. For example, *Catenibacterium mitsuokai* and *Collinsella aerofaciens* were found in total consortia, but not among viable cells, aligning well with results from FC and qPCR (Figure 12, Table 6). Overall, the viability determined by NGS showed strong agreement with FC and qPCR data.

To express the results in absolute cell numbers, the data was normalized using either spike-in or qPCR quantification (Figure 12B). The total number of bacteria detected via spike-in control was $1.55 \pm 0.18 \times 10^9$, closely matching the FC result of $1.56 \pm 0.17 \times 10^9$ and aligning with the theoretical estimate (Table 8). In terms of viable cells, spike-in

quantification yielded $1.05 \pm 0.12 \times 10^9$ cells per sample, while qPCR yielded a lower count of $7.03 \pm 0.25 \times 10^8$ cells. FC viability results were consistent with the spike-in data, reporting $1.06 \pm 0.17 \times 10^9$ viable cells in the sample. Across all methods, calculated viability ranged between 61% and 68% (Table 8).

Table 8. Total and viable cell counts obtained with different methods. Mean values (cells) \pm standard deviations ($n = 3$) are presented. Adapted from: Kallastu et al., (2023), *Current Research in Food Science, Elsevier*. Licensed under CC BY 4.0.

Sample	Cell number	Viability, %
20 st mix theoretical	1.50×10^9	
20 st mix FC	$1.56 \pm 0.17 \times 10^9$	68.41 ± 0.18
20 st mix FC alive	$1.06 \pm 0.17 \times 10^9$	
20 st spike-in	$1.55 \pm 0.18 \times 10^9$	67.79 ± 8.19
20 st spike-in alive	$1.05 \pm 0.12 \times 10^9$	
20 st mix qPCR	$1.16 \pm 0.12 \times 10^9$	60.92 ± 3.98
20 st mix qPCR alive	$7.03 \pm 0.25 \times 10^8$	

In summary, cell number estimates for both total and viable cells were closely aligned between the FC and spike-in control combined with NGS, whereas qPCR consistently yielded lower counts. This integrated approach, combining a viability reagent with either spike-in control and NGS analysis or qPCR, proved effective for characterizing microbial consortia. Although applied here to a bacterial mixture with a known composition, the method is versatile and can be extended to a range of microbial samples, including those derived from food, environmental, or clinical sources.

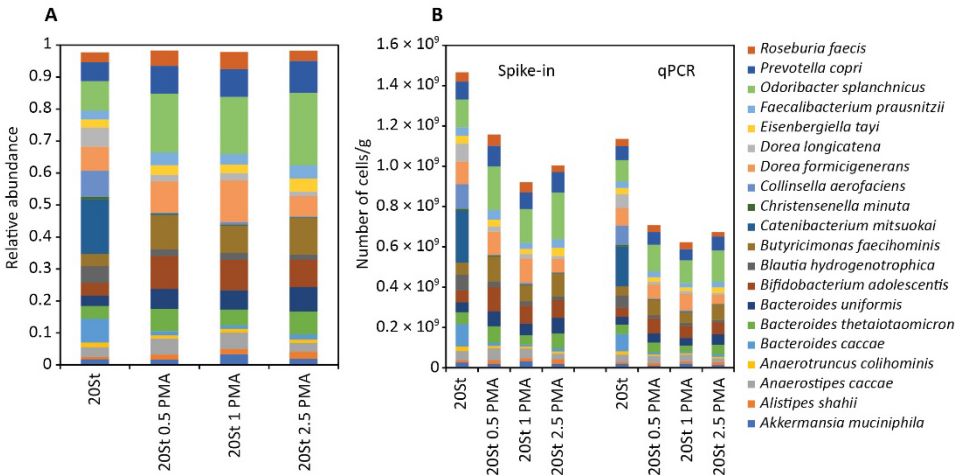


Figure 12. Identification of bacterial composition in total (20St) and viable (20St 0.5PMA, 20St 1PMA, 20St 2.5PMA) consortia samples using 16S V4 amplicon NGS. (A) Distribution of bacterial relative abundance. (B) Normalized NGS data using either spike-in control or qPCR-based quantification. Reproduced from: Kallastu et al., (2023), *Current Research in Food Science, Elsevier*. Licensed under CC BY 4.0.

5 Conclusions

This thesis set out to develop and validate scalable methodologies for cultivating, characterizing, and controlling defined microbial consortia composed of next-generation probiotic candidates. While traditional probiotic applications have focused on single-strain cultures, the complexity of gut microbiota and the emerging role of strict anaerobes in health and disease necessitate co-culture approaches. This work provides insights into designing robust consortia by combining trait-based design principles, isothermal calorimetry, and genome-scale metabolic modelling. The main conclusions that can be drawn from this work are:

- A three-species model consortium (*A. muciniphila*, *B. thetaiotaomicron*, *F. prausnitzii*) maintained stable composition across serial passages and showed resilience when initial species ratios were notably altered. The consortium recovered its original composition, demonstrating robustness and compositional stability during serial batch cultivation.
- Metabolic interactions, such as cross-feeding, were observed through changes in SCFA profiles and confirmed that co-cultivation can enhance metabolite production compared to monocultures. Notably, butyrate concentrations were significantly higher in consortia, suggesting beneficial interactions.
- Genome-scale metabolic models and flux balance analysis were used to support experimental findings. In Publication I, model accuracy was limited by data quality due to complex media. However, in Publication II, defined media and metabolite measurements enabled more accurate metabolic modelling, confirming single substrate utilization and confirming cross-feeding interactions.
- An approach based on unique carbon sources was implemented to control species abundance in co-culture. Each species was provided with a carbon source not shared by others, reducing competition and allowing stable co-cultivation. This compositional control strategy was validated using isothermal microcalorimetry, bioreactors, flux balance analysis, and microscopy-based species ratio analysis.
- Viability quantification method PMAxx-qPCR was adapted for strict anaerobes, enabling accurate assessment of species viability in mixed cultures. In addition, the workflow for absolute quantification of viable bacteria with next-generation sequencing was developed by adding PMAxx reagent and spike-in control. This method can be used for defined microbial consortia as well as for unknown samples.

In summary, this thesis outlines a workflow for the cultivation and control of defined microbial consortia composed of strict anaerobes. While the developed methodologies offer a step forward in the field of synthetic gut microbiota, further work is needed to improve scale-up strategies, and functionality validation under relevant conditions.

References

- Adamberg, K., Jaagura, M., Aaspõllu, A., Nurk, E., & Adamberg, S. (2020). The composition of faecal microbiota is related to the amount and variety of dietary fibres. *International Journal of Food Sciences and Nutrition*, 71(7), 845–855. <https://doi.org/10.1080/09637486.2020.1727864>
- Adamberg, K., Raba, G., & Adamberg, S. (2020). Use of Changestat for Growth Rate Studies of Gut Microbiota. *Frontiers in Bioengineering and Biotechnology*, 8. <https://doi.org/10.3389/fbioe.2020.00024>
- Alam, M. T., Amos, G. C. A., Murphy, A. R. J., Murch, S., Wellington, E. M. H., & Arasaradnam, R. P. (2020). Microbial imbalance in inflammatory bowel disease patients at different taxonomic levels. *Gut Pathogens*, 12(1). <https://doi.org/10.1186/s13099-019-0341-6>
- Allison, S. D., & Martiny, J. B. H. (2008). *Resistance, resilience, and redundancy in microbial communities*. www.pnas.org/cgi/content/full/
- Alonso, J. L., Amorós, I., & Guy, R. A. (2014). Quantification of viable *Giardia* cysts and *Cryptosporidium* oocysts in wastewater using propidium monoazide quantitative real-time PCR. *Parasitology Research*, 113(7), 2671–2678. <https://doi.org/10.1007/s00436-014-3922-9>
- Andrade, J. C., Almeida, D., Domingos, M., Seabra, C. L., Machado, D., Freitas, A. C., & Gomes, A. M. (2020). Commensal obligate anaerobic bacteria and health: Production, storage, and delivery strategies. In *Frontiers in Bioengineering and Biotechnology* (Vol. 8, pp. 1–23). Frontiers Media S.A. <https://doi.org/10.3389/fbioe.2020.00550>
- Baena-Ruano, S., Jiménez-Ot, C., Santos-Dueñas, I. M., Cantero-Moreno, D., Barja, F., & García-García, I. (2006). Rapid method for total, viable and non-viable acetic acid bacteria determination during acetification process. *Process Biochemistry*, 41(5), 1160–1164. <https://doi.org/10.1016/j.procbio.2005.12.016>
- Baunwall, S. M. D., Lee, M. M., Eriksen, M. K., Mullish, B. H., Marchesi, J. R., Dahlerup, J. F., & Hvas, C. L. (2020). Faecal microbiota transplantation for recurrent *Clostridioides difficile* infection: An updated systematic review and meta-analysis. *EClinicalMedicine*, 29–30. <https://doi.org/10.1016/j.eclinm.2020.100642>
- Becker, J. W., Hogle, S. L., Rosendo, K., & Chisholm, S. W. (2019). Co-culture and biogeography of *Prochlorococcus* and SAR11. *ISME Journal*, 13(6), 1506–1519. <https://doi.org/10.1038/s41396-019-0365-4>
- Berg, G., Rybakova, D., Fischer, D., Cernava, T., Vergès, M. C. C., Charles, T., Chen, X., Cocolin, L., Eversole, K., Corral, G. H., Kazou, M., Kinkel, L., Lange, L., Lima, N., Loy, A., Macklin, J. A., Maguin, E., Mauchline, T., McClure, R., ... Schlöter, M. (2020). Microbiome definition re-visited: old concepts and new challenges. In *Microbiome* (Vol. 8, Issue 1). BioMed Central Ltd. <https://doi.org/10.1186/s40168-020-00875-0>
- Blair, H. A. (2023). RBX2660 (REBYOTA®) in preventing recurrence of *Clostridioides difficile* infection: a profile of its use in the USA. *Drugs and Therapy Perspectives*, 39(10), 331–338. <https://doi.org/10.1007/s40267-023-01023-y>
- Blair, H. A. (2024). SER-109 (VOWST™): A Review in the Prevention of Recurrent *Clostridioides difficile* Infection. *Drugs*. <https://doi.org/10.1007/s40265-024-02006-7>

- Blaschkowski, H. P., Neuer, G., Ludwig-Festl, M., & Knappe, J. (1982). Routes of Flavodoxin and Ferredoxin Reduction in *Escherichia coli* CoA-Acylating Pyruvate: Flavodoxin and NADPH: Flavodoxin Oxidoreductases Participating in the Activation of Pyruvate Formate-Lyase. *European Journal of Biochemistry*, 123(3), 563–569. <https://doi.org/10.1111/j.1432-1033.1982.tb06569.x>
- Braissant, O., Wirz, D., Göpfert, B., & Daniels, A. U. (2010). Use of isothermal microcalorimetry to monitor microbial activities. In *FEMS Microbiology Letters* (Vol. 303, Issue 1, pp. 1–8). Blackwell Publishing Ltd. <https://doi.org/10.1111/j.1574-6968.2009.01819.x>
- Bunthof, C. J., Van Schalkwijk, S., Meijer, W., Abee, T., & Hugenholtz, J. (2001). Fluorescent Method for Monitoring Cheese Starter Permeabilization and Lysis. *Applied and Environmental Microbiology*, 67(9), 4264–4271. <https://doi.org/10.1128/AEM.67.9.4264-4271.2001>
- Byrd, A. L., Belkaid, Y., & Segre, J. A. (2018). The human skin microbiome. In *Nature Reviews Microbiology* (Vol. 16, Issue 3, pp. 143–155). Nature Publishing Group. <https://doi.org/10.1038/nrmicro.2017.157>
- Cao, Y., Fanning, S., Proos, S., Jordan, K., & Srikumar, S. (2017). A review on the applications of next generation sequencing technologies as applied to food-related microbiome studies. In *Frontiers in Microbiology* (Vol. 8, Issue SEP). Frontiers Media S.A. <https://doi.org/10.3389/fmicb.2017.01829>
- Chang, P. V., Hao, L., Offermanns, S., & Medzhitov, R. (2014). The microbial metabolite butyrate regulates intestinal macrophage function via histone deacetylase inhibition. *Proceedings of the National Academy of Sciences of the United States of America*, 111(6), 2247–2252. <https://doi.org/10.1073/pnas.1322269111>
- Chen, Y., Li, C., Zhou, Z., Wen, J., You, X., Mao, Y., Lu, C., Huo, G., & Jia, X. (2014). Enhanced biodegradation of alkane hydrocarbons and crude oil by mixed strains and bacterial community analysis. *Applied Biochemistry and Biotechnology*, 172(7), 3433–3447. <https://doi.org/10.1007/s12010-014-0777-6>
- Chia, L. W., Hornung, B. V. H., Aalvink, S., Schaap, P. J., de Vos, W. M., Knol, J., & Belzer, C. (2018). Deciphering the trophic interaction between *Akkermansia muciniphila* and the butyrogenic gut commensal *Anaerostipes caccae* using a metatranscriptomic approach. *Antonie van Leeuwenhoek, International Journal of General and Molecular Microbiology*, 111(6), 859–873. <https://doi.org/10.1007/s10482-018-1040-x>
- Chia, L. W., Mank, M., Blijenberg, B., Aalvink, S., Bongers, R. S., Stahl, B., Knol, J., & Belzer, C. (2020). *Bacteroides thetaiotaomicron* fosters the growth of butyrate-producing *anaerostipes caccae* in the presence of lactose and total human milk carbohydrates. *Microorganisms*, 8(10), 1–13. <https://doi.org/10.3390/microorganisms8101513>
- Clark, R. L., Connors, B. M., Stevenson, D. M., Hromada, S. E., Hamilton, J. J., Amador-Noguez, D., & Venturelli, O. S. (2021). Design of synthetic human gut microbiome assembly and butyrate production. *Nature Communications*, 12(1), 1–16. <https://doi.org/10.1038/s41467-021-22938-y>

- Costello, S. P., Hughes, P. A., Waters, O., Bryant, R. V., Vincent, A. D., Blatchford, P., Katsikeros, R., Makanyanga, J., Campaniello, M. A., Mavrangelos, C., Rosewarne, C. P., Bickley, C., Peters, C., Schoeman, M. N., Conlon, M. A., Roberts-Thomson, I. C., & Andrews, J. M. (2019). Effect of Fecal Microbiota Transplantation on 8-Week Remission in Patients with Ulcerative Colitis: A Randomized Clinical Trial. *JAMA - Journal of the American Medical Association*, 321(2), 156–164. <https://doi.org/10.1001/jama.2018.20046>
- den Besten, G., van Eunen, K., Groen, A. K., Venema, K., Reijngoud, D. J., & Bakker, B. M. (2013). The role of short-chain fatty acids in the interplay between diet, gut microbiota, and host energy metabolism. In *Journal of Lipid Research* (Vol. 54, Issue 9, pp. 2325–2340). <https://doi.org/10.1194/jlr.R036012>
- Depommier, C., Everard, A., Druart, C., Plovier, H., Van Hul, M., Vieira-Silva, S., Falony, G., Raes, J., Maiter, D., Delzenne, N. M., de Barse, M., Loumaye, A., Hermans, M. P., Thissen, J. P., de Vos, W. M., & Cani, P. D. (2019). Supplementation with *Akkermansia muciniphila* in overweight and obese human volunteers: a proof-of-concept exploratory study. *Nature Medicine*, 25(7), 1096–1103. <https://doi.org/10.1038/s41591-019-0495-2>
- Ditommaso, S., Ricciardi, E., Giacomuzzi, M., Arauco Rivera, S. R., & Zotti, C. M. (2015). Legionella in water samples: How can you interpret the results obtained by quantitative PCR? *Molecular and Cellular Probes*, 29(1), 7–12. <https://doi.org/10.1016/j.mcp.2014.09.002>
- Donohoe, D. R., Garge, N., Zhang, X., Sun, W., O'Connell, T. M., Bunger, M. K., & Bultman, S. J. (2011). The microbiome and butyrate regulate energy metabolism and autophagy in the mammalian colon. *Cell Metabolism*, 13(5), 517–526. <https://doi.org/10.1016/j.cmet.2011.02.018>
- Duncan, S. H., Louis, P., & Flint, H. J. (2004). Lactate-utilizing bacteria, isolated from human feces, that produce butyrate as a major fermentation product. *Applied and Environmental Microbiology*, 70(10), 5810–5817. <https://doi.org/10.1128/AEM.70.10.5810-5817.2004>
- Embree, M., Liu, J. K., Al-Bassam, M. M., & Zengler, K. (2015). Networks of energetic and metabolic interactions define dynamics in microbial communities. *Proceedings of the National Academy of Sciences of the United States of America*, 112(50), 15450–15455. <https://doi.org/10.1073/pnas.1506034112>
- Emerson, J. B., Adams, R. I., Román, C. M. B., Brooks, B., Coil, D. A., Dahlhausen, K., Ganz, H. H., Hartmann, E. M., Hsu, T., Justice, N. B., Paulino-Lima, I. G., Luongo, J. C., Lymperopoulou, D. S., Gomez-Silvan, C., Rothschild-Mancinelli, B., Balk, M., Huttenhower, C., Nocker, A., Vaishampayan, P., & Rothschild, L. J. (2017). Schrödinger's microbes: Tools for distinguishing the living from the dead in microbial ecosystems. In *Microbiome* (Vol. 5, Issue 1, p. 86). <https://doi.org/10.1186/s40168-017-0285-3>
- Falony, G., Calmeyer, T., Leroy, F., & De Vuyst, L. (2009). Coculture fermentations of bifidobacterium species and bacteroides thetaiotaomicron reveal a mechanistic insight into the prebiotic effect of inulin-type fructans. *Applied and Environmental Microbiology*, 75(8), 2312–2319. <https://doi.org/10.1128/AEM.02649-08>

- Falony, G., Joossens, M., Vieira-Silva, S., Wang, J., Darzi, Y., Faust, K., Kurilshikov, A., Bonder, M. J., Valles-Colomer, M., Vandeputte, D., Tito, R. Y., Chaffron, S., Rymenans, L., Verspecht, C., De Sutter, L., Lima-Mendez, G., D'hoë, K., Jonckheere, K., Homola, D., ... Raes, J. (2016). Population-level analysis of gut microbiome variation. *American Association for the Advancement of Science*, 352(6285), 560–564. <https://doi.org/10.1126/science.aad3503>
- Falony, G., Vlachou, A., Verbrugghe, K., & De Vuyst, L. (2006). Cross-feeding between *Bifidobacterium longum* BB536 and acetate-converting, butyrate-producing colon bacteria during growth on oligofructose. *Applied and Environmental Microbiology*, 72(12), 7835–7841. <https://doi.org/10.1128/AEM.01296-06>
- Forrest W.W., & Walker D.J. (1963). Calorimetric measurements of energy of maintenance of *Streptococcus faecalis*. *Biochemical and Biophysical Research Communications*, 13(3), 217–222.
- Goldford, J. E., Lu, N., Bajić, D., Estrela, S., Tikhonov, M., Sanchez-Gorostiaga, A., Segrè, D., Mehta, P., & Sanchez, A. (2018). *Emergent simplicity in microbial community assembly*. <https://doi.org/10.1126/science.aat1168>
- Grey, B., & Steck, T. R. (2001). Concentrations of Copper Thought to Be Toxic to *Escherichia coli* Can Induce the Viable but Nonculturable Condition. *Applied and Environmental Microbiology*, 67(3–12), 5325–5327. <https://doi.org/10.1128/aem.67.11.5325-5327.2001>
- Hahnke, R. L., Meier-Kolthoff, J. P., García-López, M., Mukherjee, S., Huntemann, M., Ivanova, N. N., Woyke, T., Kyrpides, N. C., Klenk, H. P., & Göker, M. (2016). Genome-based taxonomic classification of Bacteroidetes. *Frontiers in Microbiology*, 7(DEC). <https://doi.org/10.3389/fmicb.2016.02003>
- Hill, C., Guarner, F., Reid, G., Gibson, G. R., Merenstein, D. J., Pot, B., Morelli, L., Canani, R. B., Flint, H. J., Salminen, S., Calder, P. C., & Sanders, M. E. (2014). The international scientific association for probiotics and prebiotics consensus statement on the scope and appropriate use of the term probiotic. *Nature Reviews Gastroenterology and Hepatology*, 11(8), 506–514. <https://doi.org/10.1038/nrgastro.2014.66>
- Hitch, T. C. A., Bisdorf, K., Afrizal, A., Riedel, T., Overmann, J., Strowig, T., & Clavel, T. (2022). A taxonomic note on the genus *Prevotella*: Description of four novel genera and emended description of the genera *Hallella* and *Xylanibacter*. *Systematic and Applied Microbiology*, 45(6). <https://doi.org/10.1016/j.syapm.2022.126354>
- Hoefel, D., Grooby, W. L., Monis, P. T., Andrews, S., & Saint, C. P. (2003). Enumeration of water-borne bacteria using viability assays and flow cytometry: A comparison to culture-based techniques. *Journal of Microbiological Methods*, 55(3), 585–597. [https://doi.org/10.1016/S0167-7012\(03\)00201-X](https://doi.org/10.1016/S0167-7012(03)00201-X)
- Hosmer, J., McEwan, A. G., & Kappler, U. (2024). Bacterial acetate metabolism and its influence on human epithelia. In *Emerging Topics in Life Sciences* (Vol. 8, Issue 1, pp. 1–13). Portland Press Ltd. <https://doi.org/10.1042/ETLS20220092>
- Hou, X., Zhang, P., Du, H., Chu, W., Sun, R., Qin, S., Tian, Y., Zhang, Z., & Xu, F. (2021). *Akkermansia muciniphila* Potentiates the Antitumor Efficacy of FOLFOX in Colon Cancer. *Frontiers in Pharmacology*, 12. <https://doi.org/10.3389/fphar.2021.725583>

- Ikeyama, N., Murakami, T., Toyoda, A., Mori, H., Iino, T., Ohkuma, M., & Sakamoto, M. (2020). Microbial interaction between the succinate-utilizing bacterium *Phascolarctobacterium faecium* and the gut commensal *Bacteroides thetaiotaomicron*. *MicrobiologyOpen*, 9(10). <https://doi.org/10.1002/mbo3.1111>
- Ji, B., & Nielsen, J. (2015). From next-generation sequencing to systematic modeling of the gut microbiome. In *Frontiers in Genetics* (Vol. 6, Issue JUN). Frontiers Media S.A. <https://doi.org/10.3389/fgene.2015.00219>
- Jonkers, D., Penders, J., Masclee, A., & Pierik, M. (2012). Probiotics in the management of inflammatory bowel disease: A systematic review of intervention studies in adult patients. *Drugs*, 72(6), 803–823. <https://doi.org/10.2165/11632710-000000000-00000>
- Kabanova, N., Kazarjan, A., Stulova, I., & Vilu, R. (2009). Microcalorimetric study of growth of *Lactococcus lactis* IL1403 at different glucose concentrations in broth. *Thermochimica Acta*, 496(1–2), 87–92. <https://doi.org/10.1016/j.tca.2009.07.003>
- Kallastu, A., Malv, E., Aro, V., Meikas, A., Vendelin, M., Kattel, A., Nahku, R., & Kazantseva, J. (2023). Absolute quantification of viable bacteria abundances in food by next-generation sequencing: Quantitative NGS of viable microbes. *Current Research in Food Science*, 6(December 2022), 100443. <https://doi.org/10.1016/j.crfs.2023.100443>
- Kanehisa, M., & Goto, S. (2000). KEGG: Kyoto Encyclopedia of Genes and Genomes. *Nucleic Acids Research*, 28(1), 27–30. <https://doi.org/10.3892/ol.2020.11439>
- Kattel, A., Aro, V., Lahtvee, P. J., Kazantseva, J., Jöers, A., Nahku, R., & Belouah, I. (2024). Exploring the resilience and stability of a defined human gut microbiota consortium: An isothermal microcalorimetric study. *MicrobiologyOpen*, 13(4). <https://doi.org/10.1002/mbo3.1430>
- Kattel, A., Morell, I., Aro, V., Lahtvee, P. J., Vilu, R., Jöers, A., & Nahku, R. (2023). Detailed analysis of metabolism reveals growth-rate-promoting interactions between *Anaerostipes caccae* and *Bacteroides* spp. *Anaerobe*, 79. <https://doi.org/10.1016/j.anaerobe.2022.102680>
- Krieger, A. G., Zhang, J., & Lin, X. N. (2021). Temperature regulation as a tool to program synthetic microbial community composition. *Biotechnology and Bioengineering*, 118(3), 1381–1392. <https://doi.org/10.1002/bit.27662>
- Kurt, F., Leventhal, G. E., Spalinger, M. R., Anthamatten, L., Rogalla von Bieberstein, P., Menzi, C., Reichlin, M., Meola, M., Rosenthal, F., Rogler, G., Lacroix, C., & de Wouters, T. (2023). Co-cultivation is a powerful approach to produce a robust functionally designed synthetic consortium as a live biotherapeutic product (LBP). *Gut Microbes*, 15(1). <https://doi.org/10.1080/19490976.2023.2177486>
- Kütt, M. L., Orgusaar, K., Stulova, I., Priidik, R., Pismennõi, D., Vaikma, H., Kallastu, A., Zhogoleva, A., Morell, I., & Kriščiunaite, T. (2023). Starter culture growth dynamics and sensory properties of fermented oat drink. *Heliyon*, 9(5). <https://doi.org/10.1016/j.heliyon.2023.e15627>
- Lalowski, P., & Zielińska, D. (2024). The Most Promising Next-Generation Probiotic Candidates—Impact on Human Health and Potential Application in Food Technology. *Fermentation*, 10(9), 444. <https://doi.org/10.3390/fermentation10090444>

- Lawson, C. E., Harcombe, W. R., Hatzenpichler, R., Lindemann, S. R., Löffler, F. E., O'Malley, M. A., García Martín, H., Pfleger, B. F., Raskin, L., Venturelli, O. S., Weissbrodt, D. G., Noguera, D. R., & McMahon, K. D. (2019). Common principles and best practices for engineering microbiomes. In *Nature Reviews Microbiology* (Vol. 17, Issue 12, pp. 725–741). Nature Publishing Group. <https://doi.org/10.1038/s41579-019-0255-9>
- Le Roy, T., Debédat, J., Marquet, F., Da-Cunha, C., Ichou, F., Guerre-Millo, M., Kapel, N., Aron-Wisnewsky, J., & Clément, K. (2019). Comparative evaluation of microbiota engraftment following fecal microbiota transfer in mice models: Age, kinetic and microbial status matter. *Frontiers in Microbiology*, 10(JAN). <https://doi.org/10.3389/fmicb.2018.03289>
- Lederberg, J., & McCray, A. T. (2001). 'Ome Sweet 'Omics-A Genealogical Treasury of Words. *The Scientist*, 15(8), 8–8. www.ics.com
- Leung, C., Rivera, L., Furness, J. B., & Angus, P. W. (2016). The role of the gut microbiota in NAFLD. In *Nature Reviews Gastroenterology and Hepatology* (Vol. 13, Issue 7, pp. 412–425). Nature Publishing Group. <https://doi.org/10.1038/nrgastro.2016.85>
- Li, F., Hinderberger, J., Seedorf, H., Zhang, J., Buckel, W., & Thauer, R. K. (2008). Coupled ferredoxin and crotonyl coenzyme A (CoA) reduction with NADH catalyzed by the butyryl-CoA dehydrogenase/Etf complex from *Clostridium kluyveri*. *Journal of Bacteriology*, 190(3), 843–850. <https://doi.org/10.1128/JB.01417-07>
- Li, W.-Z., Stirling, K., Yang, J.-J., & Zhang, L. (2020). Gut microbiota and diabetes: From correlation to causality and mechanism. *World Journal of Diabetes*, 11(7), 293–308. <https://doi.org/10.4239/wjd.v11.i7.293>
- Li, Z., Wang, X., & Zhang, H. (2019). Balancing the non-linear rosmarinic acid biosynthetic pathway by modular co-culture engineering. *Metabolic Engineering*, 54, 1–11. <https://doi.org/10.1016/j.ymben.2019.03.002>
- Liang, Y., Ma, A., & Zhuang, G. (2022). Construction of Environmental Synthetic Microbial Consortia: Based on Engineering and Ecological Principles. In *Frontiers in Microbiology* (Vol. 13). Frontiers Media S.A. <https://doi.org/10.3389/fmicb.2022.829717>
- Lieven, C., Beber, M. E., Olivier, B. G., Bergmann, F. T., Ataman, M., Babaei, P., Bartell, J. A., Blank, L. M., Chauhan, S., Correia, K., Diener, C., Dramp, A., Ebert, B. E., Edirisinghe, J. N., Faria, P., Feist, A. M., Fengos, G., T Fleming, R. M., Garcamp, B., ... Zhang, C. (2020). MEMOTE for standardized genome-scale metabolic model testing. *Nature Biotechnology*, 38, 272–276. <https://doi.org/10.5281/zenodo.2636858>
- Lloyd-Price, J., Abu-Ali, G., & Huttenhower, C. (2016). The healthy human microbiome. In *Genome Medicine* (Vol. 8, Issue 1). BioMed Central Ltd. <https://doi.org/10.1186/s13073-016-0307-y>
- Lozupone, C. A., Stombaugh, J. I., Gordon, J. I., Jansson, J. K., & Knight, R. (2012). Diversity, stability and resilience of the human gut microbiota. In *Nature* (Vol. 489, Issue 7415, pp. 220–230). <https://doi.org/10.1038/nature11550>
- Machado, D., Andrejev, S., Tramontano, M., & Patil, K. R. (2018). Fast automated reconstruction of genome-scale metabolic models for microbial species and communities. *Nucleic Acids Research*, 46(15), 7542–7553. <https://doi.org/10.1093/nar/gky537>

- Mahadevan, R., & Schilling, C. H. (2003). The effects of alternate optimal solutions in constraint-based genome-scale metabolic models. *Metabolic Engineering*, 5(4), 264–276. <https://doi.org/10.1016/j.ymben.2003.09.002>
- Maldonado-Gómez, M. X., Martínez, I., Bottacini, F., O’Callaghan, A., Ventura, M., van Sinderen, D., Hillmann, B., Vangay, P., Knights, D., Hutkins, R. W., & Walter, J. (2016). Stable Engraftment of *Bifidobacterium longum* AH1206 in the Human Gut Depends on Individualized Features of the Resident Microbiome. *Cell Host and Microbe*, 20(4), 515–526. <https://doi.org/10.1016/j.chom.2016.09.001>
- Marcella, C., Cui, B., Kelly, C. R., Ianiro, G., Cammarota, G., & Zhang, F. (2021). Systematic review: the global incidence of faecal microbiota transplantation-related adverse events from 2000 to 2020. In *Alimentary Pharmacology and Therapeutics* (Vol. 53, Issue 1, pp. 33–42). Blackwell Publishing Ltd. <https://doi.org/10.1111/apt.16148>
- Martinez, I., Maldonado-Gomez, M. X., Gomes-Neto, J. C., Kittana, H., Ding, H., Schmaltz, R., Joglekar, P., Cardona, R. J., Marsteller, N. L., Kembel, S. W., Benson, A. K., Peterson, D. A., Ramer-Tait, A. E., & Walter, J. (2018). Experimental evaluation of the importance of colonization history in early-life gut microbiota assembly. *Elife*. <https://doi.org/10.7554/eLife.36521.001>
- Masheghati, F., Asgharzadeh, M. R., Jafari, A., Masoudi, N., & Maleki-Kakelar, H. (2024). The role of gut microbiota and probiotics in preventing, treating, and boosting the immune system in colorectal cancer. In *Life Sciences* (Vol. 344). Elsevier Inc. <https://doi.org/10.1016/j.lfs.2024.122529>
- McCarty, N. S., & Ledesma-Amaro, R. (2019). Synthetic Biology Tools to Engineer Microbial Communities for Biotechnology. In *Trends in Biotechnology* (Vol. 37, Issue 2, pp. 181–197). Elsevier Ltd. <https://doi.org/10.1016/j.tibtech.2018.11.002>
- Michail, S., Sylvester, F., Fuchs, G., & Issenman, R. (2006). Clinical efficacy of probiotics: Review of the evidence with focus on children. In *Journal of Pediatric Gastroenterology and Nutrition* (Vol. 43, Issue 4, pp. 550–557). <https://doi.org/10.1097/01.mpg.0000239990.35517.bf>
- Morozova, K., Bulbarello, A., Schaefer, C., Funda, E., Porta, F., & Scampicchio, M. (2020). Novel isothermal calorimetry approach to monitor micronutrients stability in powder forms. *LWT*, 117. <https://doi.org/10.1016/j.lwt.2019.108594>
- Mukherjee, A., Lordan, C., Ross, R. P., & Cotter, P. D. (2020). Gut microbes from the phylogenetically diverse genus *Eubacterium* and their various contributions to gut health. In *Gut Microbes* (Vol. 12, Issue 1). Taylor and Francis Inc. <https://doi.org/10.1080/19490976.2020.1802866>
- Münste, E., & Hartmann, P. (2025). The Role of Short-Chain Fatty Acids in Metabolic Dysfunction-Associated Steatotic Liver Disease and Other Metabolic Diseases. In *Biomolecules* (Vol. 15, Issue 4). Multidisciplinary Digital Publishing Institute (MDPI). <https://doi.org/10.3390/biom15040469>
- Muscogiuri, G., Cantone, E., Cassarano, S., Tuccinardi, D., Barrea, L., Savastano, S., & Colao, A. (2019). Gut microbiota: a new path to treat obesity. *International Journal of Obesity Supplements*, 9(1), 10–19. <https://doi.org/10.1038/s41367-019-0011-7>
- Nature. (n.d.). *Microbiome*. Retrieved December 12, 2024, from URL: <https://www.nature.com/subjects/microbiome>
- Navarro, Y., Torija, M. J., Mas, A., & Beltran, G. (2020). Viability-PCR allows monitoring yeast population dynamics in mixed fermentations including viable but non-culturable yeasts. *Foods*, 9(10). <https://doi.org/10.3390/foods9101373>

- Ndongo, S., Khelaifia, S., Lagier, J. C., & Raoult, D. (2020). From anaerobes to aerointolerant prokaryotes. In *Human Microbiome Journal* (Vol. 15). Elsevier Ltd. <https://doi.org/10.1016/j.humic.2019.100068>
- Niehaus, L., Boland, I., Liu, M., Chen, K., Fu, D., Henckel, C., Chaung, K., Miranda, S. E., Dyckman, S., Crum, M., Dedrick, S., Shou, W., & Momeni, B. (2019). Microbial coexistence through chemical-mediated interactions. *Nature Communications*, 10(1). <https://doi.org/10.1038/s41467-019-10062-x>
- Nocker, A., Cheswick, R., Dutheil de la Rochere, P. M., Denis, M., Léziart, T., & Jarvis, P. (2017). When are bacteria dead? A step towards interpreting flow cytometry profiles after chlorine disinfection and membrane integrity staining. *Environmental Technology (United Kingdom)*, 38(7), 891–900. <https://doi.org/10.1080/09593330.2016.1262463>
- Novakovic, M., Rout, A., Kingsley, T., Kirchoff, R., Singh, A., Verma, V., Kant, R., & Chaudhary, R. (2020). Role of gut microbiota in cardiovascular diseases. In *World Journal of Cardiology* (Vol. 12, Issue 4, pp. 110–122). Baishideng Publishing Group Co. <https://doi.org/10.4330/wjc.v12.i4.110>
- Oba, S., Sunagawa, T., Tanihiro, R., Awashima, K., Sugiyama, H., Odani, T., Nakamura, Y., Kondo, A., Sasaki, D., & Sasaki, K. (2020). Prebiotic effects of yeast mannan, which selectively promotes *Bacteroides thetaiotaomicron* and *Bacteroides ovatus* in a human colonic microbiota model. *Scientific Reports*, 10(1), 1–11. <https://doi.org/10.1038/s41598-020-74379-0>
- Oblinger, J. L., & Koburger, J. A. (1975). Understanding and Teaching the Most Probable Number Technique. *Journal of Food Protection*, 38(9), 540–545.
- Orth, J. D., Thiele, I., & Palsson, B. O. (2010). What is flux balance analysis? In *Nature Biotechnology* (Vol. 28, Issue 3, pp. 245–248). <https://doi.org/10.1038/nbt.1614>
- Ott, S. J., Waetzig, G. H., Rehman, A., Moltzau-Anderson, J., Bharti, R., Grasis, J. A., Cassidy, L., Tholey, A., Fickenscher, H., Seegert, D., Rosenstiel, P., & Schreiber, S. (2017). Efficacy of Sterile Fecal Filtrate Transfer for Treating Patients With *Clostridium difficile* Infection. *Gastroenterology*, 152(4), 799–811.e7. <https://doi.org/10.1053/j.gastro.2016.11.010>
- Peng, L., Li, Z. R., Green, R. S., Holzman, I. R., & Lin, J. (2009). Butyrate enhances the intestinal barrier by facilitating tight junction assembly via activation of AMP-activated protein kinase in Caco-2 cell monolayers. *Journal of Nutrition*, 139(9), 1619–1625. <https://doi.org/10.3945/jn.109.104638>
- Pereira, P. A. B., Trivedi, D. K., Silverman, J., Duru, I. C., Paulin, L., Auvinen, P., & Scheperjans, F. (2022). Multiomics implicate gut microbiota in altered lipid and energy metabolism in Parkinson's disease. *Npj Parkinson's Disease*, 8(1). <https://doi.org/10.1038/s41531-022-00300-3>
- Piwoz, K., Shabarova, T., Tomasch, J., Šimek, K., Kopejtká, K., Kahl, S., Pieper, D. H., & Koblížek, M. (2018). Determining lineage-specific bacterial growth curves with a novel approach based on amplicon reads normalization using internal standard (ARNIS). *ISME Journal*, 12(11), 2640–2654. <https://doi.org/10.1038/s41396-018-0213-y>
- Plovier, H., Everard, A., Druart, C., Depommier, C., Van Hul, M., Geurts, L., Chilloux, J., Ottman, N., Duparc, T., Lichtenstein, L., Myridakis, A., Delzenne, N. M., Klievink, J., Bhattacharjee, A., Van Der Ark, K. C. H., Aalvink, S., Martinez, L. O., Dumas, M. E., Maiter, D., ... Cani, P. D. (2017). A purified membrane protein from *Akkermansia muciniphila* or the pasteurized bacterium improves metabolism in obese and diabetic mice. *Nature Medicine*, 23(1), 107–113. <https://doi.org/10.1038/nm.4236>

- Pluznick, J. L. (2014). Gut microbes and host physiology: What happens when you host billions of guests? In *Frontiers in Endocrinology* (Vol. 5, Issue JUN). Frontiers Research Foundation. <https://doi.org/10.3389/fendo.2014.00091>
- Recharla, N., Geesala, R., & Shi, X. Z. (2023). Gut Microbial Metabolite Butyrate and Its Therapeutic Role in Inflammatory Bowel Disease: A Literature Review. In *Nutrients* (Vol. 15, Issue 10). Multidisciplinary Digital Publishing Institute (MDPI). <https://doi.org/10.3390/nu15102275>
- Roell, G. W., Zha, J., Carr, R. R., Koffas, M. A., Fong, S. S., & Tang, Y. J. (2019). Engineering microbial consortia by division of labor. In *Microbial Cell Factories* (Vol. 18, Issue 1). BioMed Central Ltd. <https://doi.org/10.1186/s12934-019-1083-3>
- Rosero, J. A., Killer, J., Sechovcová, H., Mrázek, J., Benada, O., Fliegerová, K., Havlík, J., & Kopečný, J. (2016). Reclassification of *Eubacterium rectale* (Hauduroy et al. 1937) prévôt 1938 in a new genus *agathobacter* gen. nov. as *Agathobacter rectalis* comb. nov., and description of *Agathobacter ruminis* sp. nov., isolated from the rumen contents of sheep and cows. *International Journal of Systematic and Evolutionary Microbiology*, 66(2), 768–773. <https://doi.org/10.1099/ijsem.0.000788>
- Rothschild, D., Weissbrod, O., Barkan, E., Kurilshikov, A., Korem, T., Zeevi, D., Costea, P. I., Godneva, A., Kalka, I. N., Bar, N., Shilo, S., Lador, D., Vila, A. V., Zmora, N., Pevsner-Fischer, M., Israeli, D., Kosower, N., Malka, G., Wolf, B. C., ... Segal, E. (2018). Environment dominates over host genetics in shaping human gut microbiota. *Nature*, 555(7695), 210–215. <https://doi.org/10.1038/nature25973>
- Sakamoto, M., Sakurai, N., Tanno, H., Iino, T., Ohkuma, M., & Endo, A. (2022). Genome-based, phenotypic and chemotaxonomic classification of *Faecalibacterium* strains: proposal of three novel species *Faecalibacterium duncaniae* sp. nov., *Faecalibacterium hattorii* sp. nov. and *Faecalibacterium gallinarum* sp. nov. *International Journal of Systematic and Evolutionary Microbiology*, 72(4). <https://doi.org/10.1099/ijsem.0.005379>
- Santoyo, G., Guzmán-Guzmán, P., Parra-Cota, F. I., de los Santos-Villalobos, S., Orozco-Mosqueda, M. D. C., & Glick, B. R. (2021). Plant growth stimulation by microbial consortia. In *Agronomy* (Vol. 11, Issue 2). MDPI AG. <https://doi.org/10.3390/agronomy11020219>
- Scariot, M. C., Venturelli, G. L., Prudêncio, E. S., & Arisi, A. C. M. (2018). Quantification of *Lactobacillus paracasei* viable cells in probiotic yoghurt by propidium monoazide combined with quantitative PCR. *International Journal of Food Microbiology*, 264, 1–7. <https://doi.org/10.1016/j.ijfoodmicro.2017.10.021>
- Schwartz, A., Hold, G. L., Duncan, S. H., Gruhl, B., Collins, M. D., Lawson, P. A., Flint, H. J., & Blaut, M. (2002). *Anaerostipes caccae* gen. nov., sp. nov., a new saccharolytic, acetate-utilising, butyrate-producing bacterium from human faeces. *Systematic and Applied Microbiology*, 25(1), 46–51. <https://doi.org/10.1078/0723-2020-00096>
- Sekirov, I., Russell, S. L., Caetano, L., Antunes, M., & Finlay, B. B. (2010). *Gut Microbiota in Health and Disease*. <https://doi.org/10.1152/physrev.00045.2009>.-Gut
- Sender, R., Fuchs, S., & Milo, R. (2016a). Are We Really Vastly Outnumbered? Revisiting the Ratio of Bacterial to Host Cells in Humans. *Cell*, 164(3), 337–340. <https://doi.org/10.1016/j.cell.2016.01.013>
- Sender, R., Fuchs, S., & Milo, R. (2016b). Revised Estimates for the Number of Human and Bacteria Cells in the Body. *PLoS Biology*, 14(8), 1–14. <https://doi.org/10.1371/journal.pbio.1002533>

- Shannon, C. E. (1948). A Mathematical Theory of Communication. *The Bell System Technical Journal*, 27(3), 379–423.
- Sharon, G., Sampson, T. R., Geschwind, D. H., & Mazmanian, S. K. (2016). The Central Nervous System and the Gut Microbiome. In *Cell* (Vol. 167, Issue 4, pp. 915–932). Cell Press. <https://doi.org/10.1016/j.cell.2016.10.027>
- Shin, H. D., McClendon, S., Vo, T., & Chen, R. R. (2010). Escherichia coli binary culture engineered for direct fermentation of hemicellulose to a biofuel. *Applied and Environmental Microbiology*, 76(24), 8150–8159. <https://doi.org/10.1128/AEM.00908-10>
- Singh, N., Gurav, A., Sivaprakasam, S., Brady, E., Padia, R., Shi, H., Thangaraju, M., Prasad, P. D., Manicassamy, S., Munn, D. H., Lee, J. R., Offermanns, S., & Ganapathy, V. (2014). Activation of Gpr109a, receptor for niacin and the commensal metabolite butyrate, suppresses colonic inflammation and carcinogenesis. *Immunity*, 40(1), 128–139. <https://doi.org/10.1016/j.immuni.2013.12.007>
- Singh, T. P., & Natraj, B. H. (2021). Next-generation probiotics: a promising approach towards designing personalized medicine. In *Critical Reviews in Microbiology* (Vol. 47, Issue 4, pp. 479–498). Taylor and Francis Ltd. <https://doi.org/10.1080/1040841X.2021.1902940>
- Smets, W., Leff, J. W., Bradford, M. A., McCulley, R. L., Lebeer, S., & Fierer, N. (2016). A method for simultaneous measurement of soil bacterial abundances and community composition via 16S rRNA gene sequencing. *Soil Biology and Biochemistry*, 96, 145–151. <https://doi.org/10.1016/j.soilbio.2016.02.003>
- Sokol, H., Landman, C., Seksik, P., Berard, L., Montil, M., Nion-Larmurier, I., Bourrier, A., Le Gall, G., Lalande, V., De Rougemont, A., Kirchgessner, J., Dagueneil, A., Cachanado, M., Rousseau, A., Drouet, É., Rosenzweig, M., Hagege, H., Dray, X., Klatzman, D., ... Simon, T. (2020). Fecal microbiota transplantation to maintain remission in Crohn's disease: A pilot randomized controlled study. *Microbiome*, 8(1), 1–14. <https://doi.org/10.1186/s40168-020-0792-5>
- Song, Z., Cai, Y., Lao, X., Wang, X., Lin, X., Cui, Y., Kalavagunta, P. K., Liao, J., Jin, L., Shang, J., & Li, J. (2019). Taxonomic profiling and populational patterns of bacterial bile salt hydrolase (BSH) genes based on worldwide human gut microbiome. *Microbiome*, 7(1). <https://doi.org/10.1186/s40168-019-0628-3>
- Stewart, E. J. (2012). Growing unculturable bacteria. In *Journal of Bacteriology* (Vol. 194, Issue 16, pp. 4151–4160). <https://doi.org/10.1128/JB.00345-12>
- Stoddard, S. F., Smith, B. J., Hein, R., Roller, B. R. K., & Schmidt, T. M. (2015). rrnDB: Improved tools for interpreting rRNA gene abundance in bacteria and archaea and a new foundation for future development. *Nucleic Acids Research*, 43(D1), D593–D598. <https://doi.org/10.1093/nar/gku1201>
- Stone, L. (2019). Faecal microbiota transplantation for Clostridioides difficile infection. *Nature Milestones*.
- Stulova, I., Kabanova, N., Kriščiunaite, T., Adamberg, K., Laht, T. M., & Vilu, R. (2015). Microcalorimetric study of the growth of Streptococcus thermophilus in renneted milk. *Frontiers in Microbiology*, 6(FEB). <https://doi.org/10.3389/fmicb.2015.00079>
- Su, L., Hong, Z., Zhou, T., Jian, Y., Xu, M., Zhang, X., Zhu, X., & Wang, J. (2022). Health improvements of type 2 diabetic patients through diet and diet plus fecal microbiota transplantation. *Scientific Reports*, 12(1), 1–12. <https://doi.org/10.1038/s41598-022-05127-9>

- Sultan, A. R., Tavakol, M., Lemmens-Den Toom, N. A., Croughs, P. D., Verkaik, N. J., Verbon, A., & van Wamel, W. J. B. (2022). Real time monitoring of *Staphylococcus aureus* biofilm sensitivity towards antibiotics with isothermal microcalorimetry. *PLoS ONE*, 17(2 February). <https://doi.org/10.1371/journal.pone.0260272>
- Tan, A. H., Chong, C. W., Lim, S. Y., Yap, I. K. S., Teh, C. S. J., Loke, M. F., Song, S. L., Tan, J. Y., Ang, B. H., Tan, Y. Q., Kho, M. T., Bowman, J., Mahadeva, S., Yong, H. Sen, & Lang, A. E. (2021). Gut Microbial Ecosystem in Parkinson Disease: New Clinicobiological Insights from Multi-Omics. *Annals of Neurology*, 89(3), 546–559. <https://doi.org/10.1002/ana.25982>
- Thiele, I., & Palsson, B. (2010). A protocol for generating a high-quality genome-scale metabolic reconstruction. *Nature Protocols*, 5(1), 93–121. <https://doi.org/10.1038/nprot.2009.203>
- Tkacz, A., Hortal, M., & Poole, P. S. (2018). Absolute quantitation of microbiota abundance in environmental samples. *Microbiome*, 6(1). <https://doi.org/10.1186/s40168-018-0491-7>
- Tripathi, A., Debelius, J., Brenner, D. A., Karin, M., Lomaba, R., Schnabl, B., & Knight, R. (2018). The gut-liver axis and the intersection with the microbiome. In *Nature Reviews Gastroenterology and Hepatology* (Vol. 15, Issue 7, pp. 397–411). Nature Publishing Group. <https://doi.org/10.1038/s41575-018-0011-z>
- Truchado, P., Gil, M. I., Larrosa, M., & Allende, A. (2020). Detection and Quantification Methods for Viable but Non-culturable (VBNC) Cells in Process Wash Water of Fresh-Cut Produce: Industrial Validation. *Frontiers in Microbiology*, 11. <https://doi.org/10.3389/fmicb.2020.00673>
- Vandeputte, D., Kathagen, G., D’Hoe, K., Vieira-Silva, S., Valles-Colomer, M., Sabino, J., Wang, J., Tito, R. Y., De Commer, L., Darzi, Y., Vermeire, S., Falony, G., & Raes, J. (2017). Quantitative microbiome profiling links gut community variation to microbial load. *Nature*, 551(7681), 507–511. <https://doi.org/10.1038/nature24460>
- Wang, E. X., Ding, M. Z., Ma, Q., Dong, X. T., & Yuan, Y. J. (2016). Reorganization of a synthetic microbial consortium for one-step vitamin C fermentation. *Microbial Cell Factories*, 15(1). <https://doi.org/10.1186/s12934-016-0418-6>
- Weghoff, M. C., Bertsch, J., & Müller, V. (2015). A novel mode of lactate metabolism in strictly anaerobic bacteria. *Environmental Microbiology*, 17(3), 670–677. <https://doi.org/10.1111/1462-2920.12493>
- Weiss, J. E., & Rettger, L. F. (1937). The Gram-negative *Bacteroides* of the intestine. *Journal of Bacteriology*, 3, 423–434.
- Whipps J, Lewis K, & Cooke R. (1988). Mycoparasitism and plant disease control. In M. Burge (Ed.), *Fungi in Biological Control Systems* (pp. 161–187). Manchester University Press.
- Widder, S., Allen, R. J., Pfeiffer, T., Curtis, T. P., Wiuf, C., Sloan, W. T., Cordero, O. X., Brown, S. P., Momeni, B., Shou, W., Kettle, H., Flint, H. J., Haas, A. F., Laroche, B., Kreft, J. U., Rainey, P. B., Freilich, S., Schuster, S., Milferstedt, K., ... Wilmes, P. (2016). Challenges in microbial ecology: Building predictive understanding of community function and dynamics. In *ISME Journal* (Vol. 10, Issue 11, pp. 2557–2568). Springer Nature. <https://doi.org/10.1038/ismej.2016.45>
- Xu, Y., Zhong, F., Zheng, X., Lai, H. Y., Wu, C., & Huang, C. (2022). Disparity of Gut Microbiota Composition Among Elite Athletes and Young Adults With Different Physical Activity Independent of Dietary Status: A Matching Study. *Frontiers in Nutrition*, 9(March). <https://doi.org/10.3389/fnut.2022.843076>

- Zanaroli, G., Toro, S. Di, Todaro, D., Varese, G. C., Bertolotto, A., & Fava, F. (2010). *Characterization of two diesel fuel degrading microbial consortia enriched from a non acclimated, complex source of microorganisms*. <http://www.microbialcellfactories.com/content/9/1/10>
- Zemb, O., Achard, C. S., Hamelin, J., De Almeida, M. L., Gabinaud, B., Cauquil, L., Verschuren, L. M. G., & Godon, J. J. (2020). Absolute quantitation of microbes using 16S rRNA gene metabarcoding: A rapid normalization of relative abundances by quantitative PCR targeting a 16S rRNA gene spike-in standard. *MicrobiologyOpen*, 9(3). <https://doi.org/10.1002/mbo3.977>
- Zhang, F., Cui, B., He, X., Nie, Y., Wu, K., Fan, D., Feng, B., Chen, D., Ren, J., Deng, M., Li, N., Zheng, P., Cao, Q., Yang, S., Liu, Y., Zhou, Y., Nie, Y., Ji, G., & Li, P. (2018). Microbiota transplantation: concept, methodology and strategy for its modernization. In *Protein and Cell* (Vol. 9, Issue 5, pp. 462–473). Higher Education Press. <https://doi.org/10.1007/s13238-018-0541-8>
- Ziesack, M., Gibson, T., Oliver, J. K. W., Shumaker, A. M., Hsu, B. B., Riglar, D. T., Giessen, T. W., Dibenedetto, N. V., Bry, L., Way, J. C., Silver, P. A., & Gerber, G. K. (2019). *Engineered Interspecies Amino Acid Cross-Feeding Increases Population Evenness in a Synthetic Bacterial Consortium*. <https://journals.asm.org/journal/msystems>

Acknowledgements

Financial support was provided by the European Regional Development Fund through the project “High throughput platform for growth improvement of microorganisms” (NSP137, 2014–2020.4.02.17-0104), funded by SA Archimedes. This work was also partially supported by the “TUT Institutional Development Program for 2016–2022” Graduate School in Biomedicine and Biotechnology, receiving funding from the European Regional Development Fund under the ASTRA program (2014–2020.4.01.16-0032) in Estonia.

This work was conducted at AS TFTAK, an innovative research centre where I had the opportunity to grow both professionally and personally. This research would not have been possible without the visionary leadership of Raivo Vilu. Over the course of my work there, I gained valuable experience in scientific research, bioprocess development, and collaborative problem-solving. I am grateful to my supervisor, Ranno Nahku, for his guidance and support. I enjoyed the scientific journey we shared and the many projects we worked on together. Kudos to Jekaterina Kazantseva for the guidance in the thesis writing process.

My sincere thanks go to entire Bioprocess group at TFTAK for being awesome colleagues. Special thanks to Isma Belouah and Mariann Vendelin for the insightful discussions and tea breaks that helped me get through even the toughest days. I am also thankful to my colleagues at TalTech Kuressaare College for their support during the thesis writing process.

Lastly, I extend my deepest gratitude to my partner Siim, mother Pille, sister Leena, and brother Aleksander. Thank you for your long-lasting support and motivational talks throughout my studies. To my late father, thank you for everything. I hope this makes you proud.

Abstract

Metabolic characterization and composition control of next generation probiotic consortia

The human gut microbiome plays an important role in host health, contributing to digestion, immune function, and pathogen resistance. While traditional probiotics have long been used to support gut health, their effectiveness is often limited to specific strains and conditions. This has led to growing interest in next-generation probiotics, which include strictly anaerobic commensals with demonstrated health benefits but also complex cultivation requirements. One promising strategy to overcome these limitations is the use of defined microbial consortia, where multiple strains are co-cultivated under controlled conditions to improve stability, and reduce production complexity. However, challenges remain in achieving reproducible growth, maintaining and controlling species ratio, and assessing cell viability in these systems. This thesis addresses these challenges by developing and testing workflows for cultivating and controlling NGP-based consortia with the goal of achieving stability and compositional control.

The main aim of this thesis was to develop and validate workflows for the cultivation, characterization, and compositional control of synthetic consortia composed of next-generation probiotics candidate strains. This work combines experimental and computational methodologies, including isothermal microcalorimetry (IMC), genome-scale metabolic modelling (GEM), flux balance analysis (FBA), microscopy-based image analysis, and quantitative viability assays using PMAxx-qPCR as well as next-generation sequencing (NGS) combined with both PMAxx treatment and spike-in controls. Together, these methods were used to explore the stability, resilience, and cross-feeding among microbial consortia under batch cultivation conditions.

Results were obtained through three publications and an additional set of unpublished data. First, a simplified three-species model consortium (*Akkermansia muciniphila*, *Bacteroides thetaiotaomicron*, and *Faecalibacterium prausnitzii*) was used to explore consortium stability and resilience over serial batch passages using IMC. The consortium exhibited stable heat flow profiles and consistent species ratios. The consortium was also resilient to initial compositional disturbances, returning to its original state within two to four passages.

To extend these findings, a more complex 25-species model consortium was cultivated under anaerobic conditions in serial batch format. Despite achieving high diversity after third passage (Shannon index = 2.26), precise compositional control remained a challenge. To address this, unique substrate approach was proposed and tested, wherein each species was provided a unique carbon source. This trait-based design reduced competition and enabled control of species abundance. Stable two-species co-cultures including *Anaerostipes caccae* with either *Bacteroides thetaiotaomicron* or *Bacteroides vulgatus* were validated using IMC, microscopy, and metabolite analysis. Cross-feeding interactions enhanced butyrate and propionate production. Furthermore, defined media allowed a more accurate application of FBA. While modelling in complex media (Publication I) remained limited due to insufficient data, the combined use of GEMs and empirical validation in Publication II helped to identify key cross-feeding mechanisms, especially involving short-chain fatty acids such as acetate and butyrate.

In Publication III, we evaluated the viability of 20 individual strains and their combined consortia using both PMAxx-qPCR and flow cytometry. PMAxx-qPCR, which selectively

quantifies cells with intact membranes, proved to be a rapid and effective alternative to traditional methods. It provided reliable viability assessments for both individual strains and a 20-strain mixture. However, when the composition of a consortium is unknown, qPCR is not feasible. To address this, we used NGS in combination with PMAxx treatment and spike-in controls, making possible both viability determination and absolute enumeration. Together, these approaches offer alternatives for monitoring cell viability and abundance during cultivation and long-term storage of defined microbial consortia. Moreover, they are adaptable to various types of consortia, including those with unknown composition or greater complexity.

The methodologies developed in this thesis offer a framework for building scalable microbial consortia for industrial use. Nevertheless, limitations remain in extending these workflows to more diverse consortia. Future work should focus on improving compositional control in larger consortia and optimizing media for broader strain coverage. In summary, this thesis demonstrates that co-cultivation using a unique substrate approach can be a scalable method to produce defined consortium. The combination of experimental and modelling approaches provides new insights into microbial interactions and supports the rational design of stable and resilient microbial consortia.

Lühikokkuvõte

Uue põlvkonna probiootiliste koosluste koostise kontroll ja metaboolne iseloomustus

Inimese soolestiku mikrobioomil on oluline roll, aidates kaasa seedimisele, immuunfunktsioonile ja patogeenide resistentsusele. Kuigi traditsioonilisi probiootikume on soolestiku tervise toetamiseks juba pikka aega kasutatud, piirdub nende efektiivsus sageli teatud tüvede ja haigusseisunditega. See on toonud kaasa kasvava huvi järgmise põlvkonna probiootikumide vastu, mis hõlmavad rangelt anaeroobseid baktereid. Neil on tõestatud tervisele kasulik mõju, kuid nende kultiveerimine on keeruline. Üks potentsiaalne strateegia on nende kasvatamine kooslusena, et parandada stabiilsust ja imiteerida nende kasvukeskkonda. Siiski on endiselt probleeme reprodutseeritava kasvu saavutamise, liikide suhte säilitamise ja kontrollimisega ning rakkude elujõulisuse hindamisega. See doktoritöö käsitleb neid probleeme, arendades ja testides töövooge koosluste kultiveerimiseks ja kontrollimiseks eesmärgiga saavutada stabiilsus ja koostise kontroll. Selleks kasutati mitmeid eksperimentaalseid ja arvutuslike meetodeid, sealhulgas isotermaalset kalorimeetriat (IMC), genoomi skaalal ainevahetuse modelleerimist (GEM), voobalansi analüüsi (FBA), mikroskoopiat ning PMAx-qPCR meetodit koos *spike-in* kontrolliga, et hinnata rakkude elumust ja hulka.

Doktoritöö raames näidati, et kolmeliikmeline mudelkooslus (*Akkermansia muciniphila*, *Bacteroides thetaiotaomicron*, *Faecalibacterium prausnitzii*) säilitab stabiilse koostise järjestikustes annuskultiveerimistes ning rakkude suhe on võimeline taastuma, kui inokulumis on rakkude suhet muudetud. Nende tulemuste põhjal kultiveeriti 25-liikmelist kooslust järjestikustes annuskultuurides isotermaalses mikrokalorimeetris. Kolmanda annuskultuuri lõpus oli koosluse mitmekesisus kõrge (Shannoni indeks 2.26), kuid liikmete suhtelise arvukuse muutmine oli piiratud. Sellest tulenevalt töötati välja unikaalsete substraatide lähenemine, kus igale liigile oli keskkonnas ainult nende poolt tarbitav peamine süsinikuallikas. Selline lähenemine vähendas konkurentsi ning võimaldas reguleerida liikide suhteid substraadikontsentratsioonide abil. Metaboliitide kvantitatiivne analüüs kinnitas, et testitud kooslused olid stabiilsed ning tõenäoliselt toimub liikide vahel rist-toitumine. Kuna kasutati defineeritud söödet, siis oli lisaks võimalik viia läbi FBA, mis omakorda kinnitas rist-toitumise.

Kolmandas publikatsioonis hinnati PMAx-qPCR meetodi sobivust rakkude elumuse hindamiseks. Analüüsiti 20 erinevat tüve ning nendest koosnevat kooslust ja saadud tulemusi võrreldi voolutsütomeetriaga saadud andmetega. PMAx reagent seondub kovalentselt rakkudega, mille membraan on kompromiteeritud, inhibeerides seeläbi PCR reaktsiooni. Nii voolutsütomeetria kui ka PMAx-qPCR andsid võrreldavaid tulemusi, mis kinnitab viimase sobivust elumuse hindamiseks nii monokultuurides kui ka kooslustes. Siiski, juhtudel kui koosluse täpne koostis pole teada, pole qPCR rakendatav. Selliste proovide jaoks on sobiv kasutada järgmise põlvkonna sekveneerimist, mida kombineeriti käesolevas töös PMAx ja *spike-in* kontrolliga, et hinnata nii rakkude elumust kui ka koguarvu. Tulemused korreleerusid hästi voolutsütomeetria andmetega. Väljatöötatud meetodeid on võimalik rakendada nii koosluste bioprotsesside arendamisel ja säilivuskatsetet biotehnoloogias kui ka muudes valdkondades nagu toit või põllumajandus.

Appendix 1

Supplemental materials

Supplementary Tables
Supplementary tables to Publication I

Table S1. Consortium resilience evaluation by modifying the initial concentration of one species at a time in the inoculum. At the end of each passage (1-5), the relative abundances of *A. muciniphila* (AM), *B. thetaiotaomicron* (BT), and *F. prausnitzii* (FP) was determined. Relative abundances were quantified using 16S rRNA sequencing (n=3). The consortium conditions rAM+BT+FP, AM+rBT+FP, and AM+BT+rFP indicate that the initial concentration of *A. muciniphila*, *B. thetaiotaomicron*, and *F. prausnitzii*, respectively, were reduced (r) at the start of the experiment. Adapted from: Kattel et al., (2024), *MicrobiologyOpen*, Wiley. Licensed under CC BY 4.0.

Condition I		rAM+BT+FP			
Passage	1	2	3	4	5
AM	8.88 ± 1.38	15.09 ± 2.73	25.37 ± 10.11	36.03 ± 1.25	31.02 ± 1.9
BT	85.95 ± 1.54	63.81 ± 0.5	55.44 ± 9.74	44.74 ± 0.57	55.98 ± 2.1
FP	5.17 ± 0.27	21.1 ± 2.26	19.19 ± 1.02	19.23 ± 0.69	13 ± 0.32
Condition II		AM+rBT+FP			
Passage	1	2	3	4	5
AM	38.21 ± 2.04	19.64 ± 2.84	33.74 ± 2.64	35.78 ± 2.53	32.56 ± 4.84
BT	53.18 ± 1.91	56.47 ± 1.41	46.81 ± 2.56	44.64 ± 1.9	54.6 ± 5.32
FP	8.61 ± 0.52	23.88 ± 1.64	19.45 ± 0.08	19.59 ± 0.66	12.84 ± 0.53
Condition III		AM+BT+rFP			
Passage	1	2	3	4	5
AM	40.02 ± 1.16	21.97 ± 2.21	30.33 ± 9.25	36.26 ± 3.67	33.9 ± 0.94
BT	57.51 ± 1.05	56.96 ± 2.54	50.24 ± 7.52	47.46 ± 3.88	53.98 ± 1.15
FP	2.48 ± 0.12	21.07 ± 0.33	19.43 ± 1.74	16.29 ± 0.21	12.12 ± 0.21

Supplementary tables to Publication II

Table S2. Predicted metabolic capabilities with percentage indicating the completeness level of each specific pathway. Adapted from: Kattel et al., (2023), *Anaerobe*, Elsevier. Used under author rights.

Metabolite	Direction	KEGG/ PubChem code	<i>B. adolescentis</i>	<i>B. longum</i>	<i>B. thetaiotaomicron</i>	<i>B. caccae</i>	<i>B. ovatus</i>	<i>B. uniformis</i>	<i>B. vulgatus</i>	<i>A. caccae</i>
			DSM 20087	DSM 20088	DSM 2079	DSM 19024	DSM 1896	DSM 6597	DSM 3289	DSM 14662
Glycogen	deg	C00182	100%	100%	100%	100%	100%	100%	100%	100%
Amylose	deg	C00718	100%	100%	100%	100%	100%	100%	100%	0%
Amylopectin	deg	C00317	100%	0%	100%	100%	100%	100%	100%	0%
Maltodextrin	deg	C01935	100%	100%	100%	100%	100%	100%	100%	0%
Pullulan	deg	C00480	100%	0%	100%	100%	100%	100%	100%	0%
Dextrin	deg	C00721	100%	0%	100%	100%	100%	100%	100%	0%
Pectin	deg	C00714	0%	38%	91%	82%	91%	82%	91%	50%
Rhamnogalacturonan	deg	C131801240	10%	20%	90%	80%	90%	50%	70%	20%
Xylan	deg	C00707	75%	50%	100%	100%	100%	100%	100%	50%
Glucuronoarabinoxylan	deg	C405238131	67%	50%	100%	83%	100%	83%	100%	33%
Sucrose	deg	C00089	100%	100%	100%	50%	50%	100%	50%	100%
Lactose	deg	C00243	86%	100%	86%	86%	86%	86%	71%	100%
Maltose	deg	C00208	100%	100%	100%	100%	100%	100%	67%	100%
Raffinose	deg	C00492	100%	100%	100%	67%	67%	100%	67%	100%
Melibiose	deg	C05402	100%	100%	100%	100%	100%	100%	50%	100%
Trehalose	deg	C01083	50%	50%	50%	50%	50%	100%	50%	50%

Turanose	deg	C19636	100%	100%	100%	100%	100%	100%	67%	67%
Cellobiose	deg	C00185	0%	0%	0%	0%	0%	0%	0%	100%
Melezitose	deg	C08243	0%	0%	0%	0%	0%	0%	0%	0%
D-Glucose	deg	C00031	100%	100%	100%	100%	100%	100%	100%	100%
L-Glucose	deg	C10954115	0%	0%	0%	0%	0%	17%	17%	0%
D-Mannose	deg	C00159	0%	0%	100%	100%	100%	100%	100%	100%
D-Galactose	deg	C00124	80%	100%	80%	80%	80%	80%	80%	100%
D-Allose	deg	C01487	33%	33%	33%	33%	33%	33%	33%	33%
D-Fructose	deg	C00095	0%	0%	100%	100%	100%	100%	100%	100%
D-Tagatose	deg	C00795	0%	0%	0%	0%	0%	0%	0%	0%
D-Allulose	deg	C06468	50%	50%	50%	50%	50%	50%	50%	50%
L-Sorbose	deg	C00247	0%	0%	0%	0%	0%	0%	0%	100%
D-Glucuronate	deg	C00191	0%	60%	100%	100%	100%	100%	80%	80%
D-Mannuronate	deg	C02024	0%	0%	0%	0%	0%	0%	0%	0%
D-Galacturonate	deg	C00333	0%	20%	100%	100%	100%	100%	100%	60%
D-Fructuronate	deg	C00905	0%	50%	100%	100%	100%	100%	75%	75%
D-Methylgalacturonate	deg	Cp7195798	0%	17%	83%	83%	83%	83%	83%	50%
D-Gluconate	deg	C00257	100%	50%	100%	100%	100%	100%	100%	67%
L-Gluconate	deg	C38988608	0%	0%	0%	0%	0%	20%	20%	0%
D-Mannonate	deg	C00514	0%	33%	100%	100%	100%	100%	100%	67%
D-Galactonate	deg	C00880	0%	0%	0%	0%	0%	0%	0%	0%
L-Galactonate	deg	C15930	0%	0%	80%	80%	80%	80%	80%	40%
D-Altronate	deg	C00817	0%	0%	100%	100%	100%	100%	100%	67%

D-Idonate	deg	C44457530	0%	0%	0%	0%	0%	33%	33%	0%
L-Idonate	deg	C00770	33%	0%	33%	33%	33%	33%	33%	67%
L-Gulonate	deg	C00800	0%	40%	80%	80%	80%	80%	60%	60%
D-Glucarate	deg	C00818	0%	0%	0%	0%	0%	0%	0%	25%
Galactarate	deg	C00879	0%	0%	33%	33%	33%	33%	33%	25%
D-Glucosamine	deg	C00329	0%	100%	100%	100%	100%	100%	100%	100%
NAc-D-Glucosamine	deg	C00140	0%	100%	100%	100%	100%	50%	100%	100%
D-Galactosamine	deg	C02262	0%	0%	33%	33%	33%	33%	33%	67%
NAc-D-Galactosamine	deg	C01132	43%	71%	71%	71%	71%	57%	71%	57%
NAc-Neuraminate	deg	C00270	0%	80%	60%	80%	80%	60%	80%	60%
L-Rhamnose	deg	C00507	20%	20%	100%	80%	100%	80%	100%	20%
D-Fucose	deg	C01018	0%	0%	0%	0%	0%	0%	0%	0%
L-Fucose	deg	C01019	20%	40%	100%	100%	100%	40%	67%	20%
D-Sorbitol	deg	C00794	100%	50%	100%	50%	100%	50%	100%	100%
D-Mannitol	deg	C00392	0%	0%	0%	0%	0%	0%	0%	100%
Galactitol	deg	C01697	0%	0%	0%	0%	0%	0%	0%	100%
D-Altritol	deg	C21524	0%	0%	0%	0%	0%	0%	0%	0%
D-myo-Inositol	deg	C00137	0%	22%	56%	56%	56%	56%	33%	86%
D-Ribose	deg	C00121	100%	100%	100%	100%	100%	100%	100%	100%
D-Arabinose	deg	C00216	50%	50%	100%	100%	100%	100%	100%	63%
L-Arabinose	deg	C00259	100%	0%	100%	100%	100%	100%	100%	33%
D-Xylose	deg	C00181	100%	50%	100%	100%	100%	100%	100%	100%
L-Xylose	deg	C01510	0%	0%	0%	0%	0%	0%	0%	0%

[illegible]

[illegible]

L-Serine	deg	C00065	100%	100%	100%	100%	100%	100%	100%	100%
L-Threonine	syn	C00188	100%	100%	100%	100%	100%	100%	100%	100%
L-Threonine	deg	C00188	100%	100%	100%	100%	100%	100%	100%	100%
L-Tryptophan	syn	C00078	100%	100%	100%	100%	100%	100%	100%	100%
L-Tryptophan	deg	C00078	13%	13%	100%	0%	100%	100%	13%	10%
L-Tyrosine	syn	C00082	100%	100%	100%	100%	100%	100%	100%	100%
L-Tyrosine	deg	C00082	20%	20%	40%	40%	40%	40%	40%	20%
L-Valine	syn	C00183	100%	100%	100%	100%	100%	100%	100%	100%
L-Valine	deg	C00183	33%	33%	100%	100%	100%	100%	100%	44%
D-Alanine	syn	C00133	100%	100%	100%	100%	100%	100%	100%	100%
D-Alanine	deg	C00133	100%	100%	100%	100%	100%	100%	100%	100%
D-Arginine	syn	C00792	0%	0%	0%	0%	0%	0%	0%	0%
D-Arginine	deg	C00792	0%	0%	0%	0%	0%	0%	0%	0%
D-Aspartate	syn	C00402	100%	0%	0%	0%	0%	0%	0%	0%
D-Aspartate	deg	C00402	100%	0%	0%	0%	0%	0%	0%	0%
D-Cysteine	syn	C00793	0%	0%	0%	0%	0%	0%	0%	0%
D-Cysteine	deg	C00793	0%	0%	0%	0%	0%	0%	0%	0%
D-Glutamine	syn	C00819	0%	0%	0%	0%	0%	0%	0%	0%
D-Glutamine	deg	C00819	100%	100%	100%	100%	100%	100%	100%	100%
D-Glutamate	syn	C00217	100%	100%	100%	100%	100%	100%	100%	100%
D-Glutamate	deg	C00217	100%	100%	100%	100%	100%	100%	100%	100%
D-Lysine	syn	C00739	0%	0%	0%	0%	0%	0%	0%	0%
D-Lysine	deg	C00739	0%	0%	0%	0%	0%	0%	0%	0%

D-Ornithine	syn	C00515	0%	0%	0%	0%	0%	0%	0%	0%
D-Ornithine	deg	C00515	0%	0%	0%	0%	0%	0%	0%	0%
D-Proline	syn	C00763	0%	0%	0%	0%	0%	0%	0%	0%
D-Proline	deg	C00763	0%	0%	0%	0%	0%	0%	0%	0%
D-Serine	syn	C00740	0%	0%	0%	0%	0%	0%	0%	0%
D-Serine	deg	C00740	0%	0%	0%	0%	0%	0%	0%	0%
Beta-alanine	syn	C00099	50%	50%	100%	100%	100%	100%	100%	100%
Beta-alanine	deg	C00099	0%	0%	0%	0%	0%	0%	0%	0%

Table S3. Consumption and production of metabolites by *A. caccae*. The data represent the average consumption/production (mM) \pm standard error (n = 3). Adapted from: Kattel et al., (2023), *Anaerobe*, Elsevier. Used under author rights.

Amount of acetate in the medium	Sorbitol	Acetate	Butyrate	Ethanol	Formate	Lactate	Malate	Propionate	Succinate
0 mM	-5.87 \pm 0.00	ND	1.46 \pm 0.01	0.66 \pm 0.21	0.03 \pm 0.01	5.24 \pm 0.04	ND	ND	ND
2 mM	-5.34 \pm 0.00	-2.15 \pm 0.00	3.85 \pm 0.02	0.63 \pm 0.04	0.17 \pm 0.01	2.78 \pm 0.01	ND	ND	ND
4 mM	-5.30 \pm 0.00	-4.26 \pm 0.03	6.06 \pm 0.01	0.51 \pm 0.16	0.47 \pm 0.01	0.45 \pm 0.01	ND	ND	ND
6 mM	-5.51 \pm 0.00	-4.20 \pm 0.01	6.85 \pm 0.01	0.74 \pm 0.04	0.74 \pm 0.02	0.08 \pm 0.01	ND	ND	ND
8 mM	-5.61 \pm 0.00	-3.83 \pm 0.03	6.59 \pm 0.03	0.58 \pm 0.02	0.80 \pm 0.01	0.12 \pm 0.03	ND	ND	ND
10 mM	-5.40 \pm 0.00	-4.39 \pm 0.03	6.88 \pm 0.05	0.94 \pm 0.05	0.97 \pm 0.01	0.08 \pm 0.00	ND	ND	ND
20 mM	-5.36 \pm 0.00	-4.44 \pm 0.05	6.56 \pm 0.03	0.73 \pm 0.14	1.04 \pm 0.01	0.14 \pm 0.00	ND	ND	ND

Table S4. Consumption and production of metabolites by *B. thetaiotaomicron*. The data represent the average consumption/production (mM) \pm standard error ($n = 3$). * - Formate concentration could not be determined due to signal interference from the lactate peak. NA – not available, ND – not detected. Adapted from: Kattel et al., (2023), *Anaerobe*, Elsevier. Used under author rights.

Amount of lactate in the medium	Xylose	Acetate	Butyrate	Ethanol	Formate	Lactate	Malate	Propionate	Succinate
0 mM	-4.98 \pm 0.00	2.72 \pm 0.01	ND	-0.13 \pm 0.14	0.08 \pm 0.02	ND	ND	0.62 \pm 0.01	1.18 \pm 0.01
2 mM	-4.45 \pm 0.00	3.46 \pm 0.02	ND	-0.05 \pm 0.02	0.25 \pm 0.01	-1.77 \pm 0.00	ND	1.24 \pm 0.02	1.73 \pm 0.01
4 mM	-4.41 \pm 0.00	4.16 \pm 0.04	ND	-0.28 \pm 0.24	0.28 \pm 0.01	-3.01 \pm 0.04	ND	1.52 \pm 0.02	1.79 \pm 0.01
6 mM	-4.88 \pm 0.00	3.97 \pm 0.01	ND	-0.31 \pm 0.07	0.46 \pm 0.00	-2.16 \pm 0.01	ND	1.38 \pm 0.00	1.88 \pm 0.00
8 mM	-4.57 \pm 0.00	4.15 \pm 0.03	ND	-0.20 \pm 0.03	0.39 \pm 0.01	-2.84 \pm 0.03	ND	1.47 \pm 0.01	1.91 \pm 0.02
10 mM	-4.84 \pm 0.00	4.17 \pm 0.00	ND	-0.15 \pm 0.03	0.67 \pm 0.02	-2.62 \pm 0.04	ND	1.48 \pm 0.01	1.91 \pm 0.01
20 mM	-4.76 \pm 0.00	4.49 \pm 0.00	ND	0.05 \pm 0.08	NA*	-3.21 \pm 0.03	ND	1.56 \pm 0.01	2.19 \pm 0.00

Table S5. Expected gDNA ratios based on optical density measurements and experimentally determined values from qPCR. The data represent the average gDNA ratio \pm standard error ($n = 3$). Adapted from: Kattel et al., (2023), Anaerobe, Elsevier. Used under author rights.

Sample	gDNA ratio, %		
	<i>A. caccae</i>	<i>B. thetaiotaomicron</i>	<i>B. vulgatus</i>
theoretical ratio	33%	33%	33%
1st mixture	12% \pm 1%	47% \pm 2%	41% \pm 1%
theoretical ratio	80%	10%	10%
2nd mixture	52% \pm 2%	27% \pm 1%	21% \pm 1%
theoretical ratio	10%	80%	10%
3rd mixture	4% \pm 0%	87% \pm 1%	10% \pm 0%
theoretical ratio	10%	10%	80%
4th mixture	4% \pm 0%	15% \pm 1%	81% \pm 1%

Table S6. gDNA ratios were measured at the end of each batch using qPCR. Values represent the average gDNA ratio \pm standard error ($n = 3$). Adapted from: Kattel et al., (2023), Anaerobe, Elsevier. Used under author rights.

Sample	gDNA ratio, %		
	<i>A. caccae</i>	<i>B. thetaiotaomicron</i>	<i>B. vulgatus</i>
Day 1 <i>A. caccae</i> + <i>B. thetaiotaomicron</i>	5% \pm 1%	95% \pm 1%	
Day 2 <i>A. caccae</i> + <i>B. thetaiotaomicron</i>	5% \pm 0%	95% \pm 0%	
Day 3 <i>A. caccae</i> + <i>B. thetaiotaomicron</i>	4% \pm 1%	96% \pm 1%	
Day 1 <i>A. caccae</i> + <i>B. vulgatus</i>	6% \pm 1%		94% \pm 1%
Day 2 <i>A. caccae</i> + <i>B. vulgatus</i>	10% \pm 1%		90% \pm 1%
Day 3 <i>A. caccae</i> + <i>B. vulgatus</i>	8% \pm 1%		92% \pm 1%

Supplementary figures to Publication I

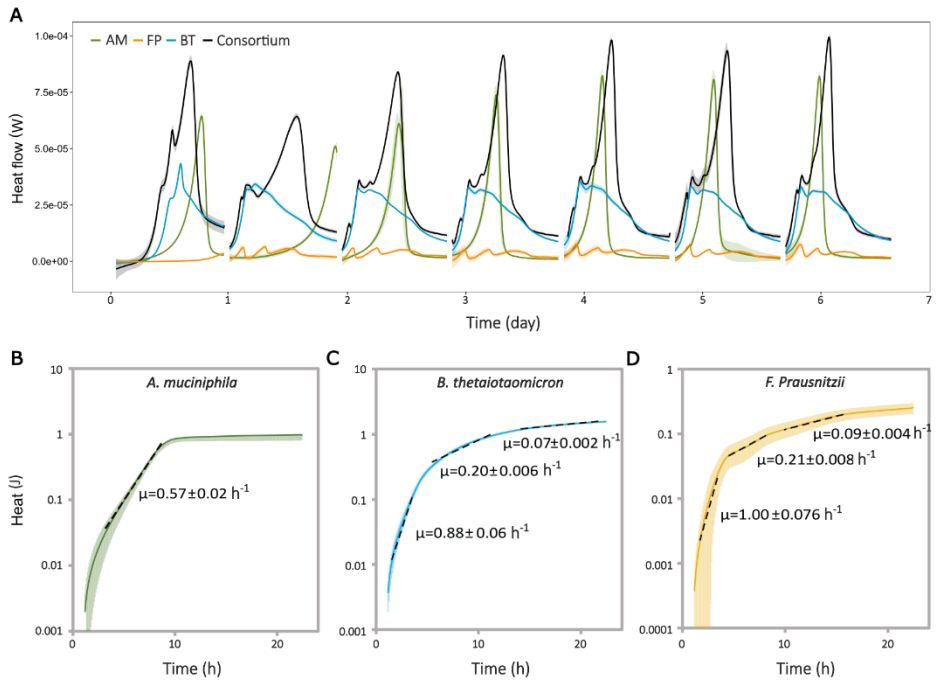


Figure S1. Growth kinetics of the monoculture and the consortium in the YCFAM medium. (A) Heat flow (W) released by monocultures and consortium. Growth was monitored over seven serial passages using the IMC. Full line and ribbon represent the average and standard deviation of the heat flow, respectively ($n=3$), for each passage. *A. muciniphila*, *B. thetaiotaomicron*, *F. prausnitzii*, and the consortium are represented by the green, blue, yellow, and black lines, respectively. (B-D) The specific growth rate(s) for each strain were calculated based on heat (J) data collected from the fifth, sixth, and seventh batch cultivations. The full line and ribbon represent the average and standard deviation, respectively, ($n = 3$). Reproduced from: Kattel et al., (2024), *MicrobiologyOpen*, Wiley. Licensed under CC BY 4.0.

Appendix 2

Publication I

Kattel, A., Aro, V., Lahtvee, P. J., Kazantseva, J., Jöers, A., Nahku, R., & Belouah, I. (2024). Exploring the resilience and stability of a defined human gut microbiota consortium: An isothermal microcalorimetric study. *MicrobiologyOpen*, 13(4).
<https://doi.org/10.1002/mbo3.1430>

Exploring the resilience and stability of a defined human gut microbiota consortium: An isothermal microcalorimetric study

Anna Kattel^{1,2} | Valter Aro^{1,3} | Petri-Jaan Lahtvee³ | Jekaterina Kazantseva² |
Arvi Jõers³ | Ranno Nahku² | Isma Belouah^{2,3} 

¹Department of Chemistry and Biotechnology, Tallinn University of Technology, Tallinn, Estonia

²Bioprocess Optimization, Center of Food and Fermentation Technologies, Tallinn, Estonia

³Cell Biology, University of Tartu, Institute of Technology, Tartu, Estonia

Correspondence

Isma Belouah, Mäealuse 2/4, 12618, Tallinn, Estonia.

Email: isma.belouah@tftak.eu

Funding information

Sihtasutus Archimedes,
Grant/Award Number:
2014-2020.4.02.17-0104

Abstract

The gut microbiota significantly contributes to human health and well-being. The aim of this study was to evaluate the stability and resilience of a consortium composed of three next-generation probiotics (NGPs) candidates originally found in the human gut. The growth patterns of *Akkermansia muciniphila*, *Bacteroides thetaiotaomicron*, and *Faecalibacterium prausnitzii* were studied both individually and consortium. The growth kinetics of *Akkermansia muciniphila* (*A. muciniphila*), *Bacteroides thetaiotaomicron* (*B. thetaiotaomicron*), and *Faecalibacterium prausnitzii* (*F. prausnitzii*) were characterized both individually and in consortium using isothermal microcalorimetry and 16S ribosomal RNA next-generation sequencing. The consortium reached stability after three passages and demonstrated resilience to changes in its initial composition. The concentration of butyrate produced was nearly twice as high in the consortium compared to the monoculture of *F. prausnitzii*. The experimental conditions and methodologies used in this article are a solid foundation for developing further complex consortia.

KEYWORDS

consortium, gut microbiota, isothermal microcalorimetry, mucin, resilience, stability

1 | INTRODUCTION

The term “microbiota” has commonly been defined as the collection of microorganisms (bacteria, fungi, viruses, etc.) growing in a singular environment. For example, the gut microbiota is the collection of microorganisms colonizing and symbiotically existing within the gastrointestinal tract. Its composition plays an active role in the prevalence of various diseases (Type 2 diabetes mellitus, cancer, obesity, mental health) (Fan & Pedersen, 2021; Wang et al., 2017). The comparison of the gut microbiota from healthy and unhealthy

individuals helped identify health-beneficial phyla such as Firmicutes, Bacteroidetes, and Actinobacteria (Derrien & Veiga, 2017; Fan & Pedersen, 2021; Flint et al., 2012; Lopez-Siles et al., 2017; Manor et al., 2020). In these phyla, some strains are currently considered potential next-generation probiotics (NGPs) (Cani & Vos, 2017; Chang et al., 2019; Wrzosek et al., 2015) that could become an alternative or support to the faecal transplant (ClinicalTrials.gov identifier: NCT04208958, NCT03106844). To make this a reality, NGP strains should be characterized individually in vitro for specific attributes that would be preserved and improved in a complex functional NGP

This is an open access article under the terms of the [Creative Commons Attribution](https://creativecommons.org/licenses/by/4.0/) License, which permits use, distribution and reproduction in any medium, provided the original work is properly cited.

© 2024 The Author(s). *MicrobiologyOpen* published by John Wiley & Sons Ltd.

consortium. NGPs are looked upon for their capability to produce health-beneficial molecules such as aromatic lactic acids, including indole-lactate, and short-chain fatty acids (SCFAs), including butyrate, propionate, acetate, and succinate (Gatto & Shliaha, 2013; Laursen et al., 2021; Rowland et al., 2018). SCFAs have anti-inflammatory effects, innate immune functions, participate in intestinal homeostasis maintenance and epithelial barrier function, and serve as an energy source for the host epithelial cells and gut bacteria (Venegas et al., 2019). One of the most discussed SCFAs is butyrate (Coppola et al., 2021; Panebianco et al., 2022; Zhang et al., 2021). One butyrate-producing bacteria is the *Faecalibacterium prausnitzii* within the *Faecalibacterium* genus (Zhu et al., 2021). *F. prausnitzii* preferentially consumes monosaccharides (glucose, rhamnose, fucose, galactose), disaccharides (cellobiose, lactose), amino sugars (N-acetylglucosamine (N-AcGam), N-acetylgalactosamine (N-AcGal)) and certain polysaccharides (pectin, starch) (Hu et al., 2022; Lopez-Siles et al., 2012). Some of these carbohydrates (fucose, galactose, N-AcGam, N-AcGal) are the building blocks of mucin, a key component of the intestinal mucus that protects the gastrointestinal epithelium. The mucus layer serves as a functional barrier, protecting the epithelium from mechanical stresses and direct contact with pathogens. Additionally, it lubricates the passage of food and ensures the diffusion of small molecules (nutrients, ions, water and gases) (Paone & Cani, 2020). Mucin is a complex glycoprotein with a peptide backbone of repeated segments of proline-threonine-serine domains decorated with O-glycans (galactose, N-AcGam, N-AcGal) chains (Ince et al., 2022) capped with sialic acid, sulfate, and fucose. To be used as substrates by *F. prausnitzii*, mucin has to be cleaved by gut microbiota members expressing specific carbohydrate-activated enzymes (glycoside hydrolases, sialidases, sulfatases and esterases) (Raba & Luis, 2023). In their extensive genomic analysis of gut microbiota strains, Glover et al. (2022) confirmed the presence of mucin O-glycan-degrading hydrolases in *Akkermansia muciniphila* and *Bacteroides thetaiotaomicron* genome and their ability to grow using mucin as the sole carbon source in a chemically defined medium (ZMB1) (Glover et al., 2022; Kostopoulos et al., 2021). Additionally, *B. thetaiotaomicron* and *A. muciniphila* are established acetate-producers that individually enhance the production of butyrate (by *F. prausnitzii* for example) in coculture (Chia et al., 2018; Kattel et al., 2023; Miner-Williams et al., 2009; Paone & Cani, 2020; Wrzosek et al., 2013). However, there are no in vitro studies describing the stability and resilience of a consortium consisting of *A. muciniphila*, *B. thetaiotaomicron*, and *F. prausnitzii*.

A. muciniphila, *B. thetaiotaomicron*, and *F. prausnitzii* are regarded as obligate anaerobes. They are usually operated in anaerobic chambers which, besides the cost, are limited in space and require dexterity from the operator. These constraints intensify during continuous processes with extensive manual manipulations, like monitoring the growth. The most conventional method consists of using a spectrophotometer (600 nm) to track changes in the optical density (OD) over time. The sensitivity of this method reaches its limitations at high cell density and with solid, opaque, or non-translucent media components, such as fibers (mucin, dietary fibers). Moreover, a spectrophotometer won't differentiate between metabolically active

cells and nonviable ones. An alternative approach is the isothermal microcalorimetry (IMC). IMC is a non-destructive, highly sensitive and high-throughput method, with the possibility to monitor simultaneously up to 48 independent samples (Bayode et al., 2022; Braissant et al., 2015; Gaisford, 2016; Kabanova et al., 2012). The complexity of the samples is theoretically limitless (solid to liquid matrices, endothermic to exothermic processes). Each sample is placed in a glass ampoule and then hermetically sealed. The ampoule is then lowered into a heated sink maintained at the chosen temperature. A thermopile sensor, in contact with both the sample and heat sink (HS), detects the transfer of heat over time in both directions (sample-to-HS and HS-to-sample) (Braissant et al., 2015; Gaisford, 2016). The sensor measures continuously the heat flow released by metabolically active microorganisms. The heat flow is mathematically transformed into total heat, which is used to determine the specific growth rate. IMC becomes relevant in describing metabolic changes in systems where microbes interact with each other within a complex environment (mucin, dietary components).

To the best of our knowledge, this study is the first to monitor *A. muciniphila*, *B. thetaiotaomicron*, and *F. prausnitzii* consortium growth kinetics by IMC and 16S ribosomal RNA next-generation sequencing (16S rRNA NGS), attesting to a robust and stable composition over time regardless of the initial consortium composition. Flux balance analysis (FBA) was tested to identify potential dependencies in their metabolisms in a complex environment. The authors are aware that the consortium used in the current study doesn't represent the huge complexity existing in the gut microbiome. Nonetheless, this study highlights the potential that exists in the continuous monitoring of NGP consortia for biotechnology advances and applications.

2 | MATERIALS AND METHODS

2.1 | Strains

A. muciniphila (DSM 22959), *B. thetaiotaomicron* (DSM 2079), and *F. prausnitzii* (DSM 17677) were ordered from DSMZ (German Collection of Microorganisms and Cell Cultures GmbH) and stored in 20% glycerol and PBS solution (pH 6.8) at -80°C . The *F. prausnitzii* genome was recently proposed as *Faecalibacterium duncaniae* sp. nov. (DSM 17677) (Sakamoto et al., 2022).

2.2 | Preparation of yeast extract, casitone, fatty acids, and mucin culture medium (YCFAM)

The composition of the medium (if not stated otherwise) was as follows (per litre): 10 g casitone (Tryptone Plus, Sigma-Aldrich), 2.5 g yeast extract (NuCel 545, Bio Springer), 4 g L-cysteine HCl (Alfa Aesar), 1 mg resazurin sodium salt (Acros Organics), 2.93 g K_2HPO_4 (Sigma-Aldrich), 4.65 g KH_2PO_4 (Sigma-Aldrich), 0.9 g $(\text{NH}_4)_2\text{SO}_4$ (Alfa Aesar), 0.9 g NaCl (Acros Organics), 0.28 g KOH (Fluka), 1 g NaHCO_3 (Sigma-Aldrich), 10 mg hemin (Sigma-Aldrich), 10 μg biotin

(Merck), 10 µg cobalamin (Fisher Bioreagents), 30 µg para-aminobenzoic acid (Sigma-Aldrich), 150 µg pyridoxamine (Carbosynth), 50 µg folate (Alfa Aesar), 0.09 g MgSO₄·7H₂O (Alfa Aesar), 0.09 g CaCl₂·H₂O (ApliChem). The medium was completed with a 1 mM concentration of acetaldehyde (Fluka) and SCFA, including acetate (Honeywell), propionate (Sigma-Aldrich), valerate (Alfa Aesar), isovalerate (Acros Organics), isobutyrate (Acros Organics), formate (Fluka), lactate (Sigma-Aldrich), L-malate (Fluka), citrate (Sigma-Aldrich), and fumarate (Fluka). Mucin from porcine stomach type III (Sigma-Aldrich) was used as a substrate and included at 1.25 g L⁻¹. SCFAs, vitamins, and hemin solution were filter-sterilized and freshly added the day before the experiment. Mucin was sterilized at 115°C for 5 min before being added to the medium. The pH of the medium was adjusted to 7.1 using a 3 M NaOH solution. The final medium, called YCFAM, was kept overnight in an anaerobic chamber (COY box, Coy Laboratory Products Inc.) filled with 5% H₂, 10% CO₂, and 85% N₂ to remove traces of oxygen.

2.3 | Culture growth conditions

Precultures were grown overnight in an anoxic YCFAM medium with 0.5% (w/v) glucose. Before inoculation, the cell culture stock was centrifuged at 14,000g for 1 min and resuspended in an anoxic YCFAM medium at a final OD (600 nm) of 0.62. All fermentations were performed under anaerobic conditions in microcalorimetry ampoules (2 mL working volume) containing YCFAM medium inoculated with bacterial culture (1% v/v). After inoculation, the ampoules were hermetically sealed and lowered into isothermal microcalorimeter channels (TAM III and TAM IV-48, TA Instruments) set at 37°C. For each passage, 1% (v/v) of the culture (20 µL) from the prior batch was transferred into a new ampoule containing fresh YCFAM medium (1.98 mL). The growth profile was determined by continuously measuring the heat difference between the IMC control temperature (37°C) and the heat released by the bacterial metabolic activity. For the consortium fermentation, bacteria were prepared as described above. Heat curves from three biological replicates, from three independent IMC vials, were used to determine the mean and standard deviation of all the growth rates. Unless mentioned otherwise, the YCFAM medium was inoculated with 1% (v/v) of each bacterial culture. Each passage was performed as described above. At the end of the fermentation, for both individual strains and the consortium, the supernatant was collected after centrifugation (14,000g, 5 min, 4°C), culture composition was determined, and OD was measured.

2.4 | Quantification of extracellular metabolites

Samples were centrifuged at 14,000g for 5 min at 4°C. The supernatant was transferred into a new tube and filtered through 0.2 µm syringe filters (Millipore Millex-LG filters 13 mm Philic PTFE 0.2 µm non-sterile SLLGH13NK; Millipore Corp.). The concentrations of acetate, citrate, butyrate, formate, isobutyrate, isovalerate, lactate, malate, propionate, and succinate were determined using high-performance

liquid chromatography (Waters 2695 HPLC system; Waters Corporation). The elution was done isocratically with 0.005 M H₂SO₄ solution at 0.6 mL min⁻¹ using a 300 × 7.8 mm Aminex HPX-87H column (Bio-Rad), with precolumn 30 × 4.6 mm Micro-Guard Cation H Refill Ca (Bio-Rad). A 50/50 milliQ/MeOH (v/v) seal wash, 10/90 acetonitrile/milliQ (v/v) needle wash, autosampler temperature of 10°C, column temperature of 35°C, and injection volume of 20 µL were used. Refractive index (RI) and ultraviolet (UV) detectors (210 nm) (Waters Corporation) were used to detect and quantify metabolites using external standard curves. Standards were prepared by performing serial dilutions with milliQ water: 1x, 2x, 4x, 8x, 16x, 32x, 64x, and 128x.

2.5 | DNA extraction and 16S rRNA NGS

The extraction of genomic DNA was done from the biomass pellet using a Sigma-Aldrich GenElute Bacterial Genomic DNA kit and diluted to 10 ng µL⁻¹. For library preparation, the V4 hypervariable region of the 16S rRNA gene was amplified with forward primer F515 5'-GTGCCAGCMGCGCGGTAA-3' and reverse primer R806 5'-GGACTACHVGGGTWCTAAT-3' (Caporaso et al., 2011) following a standard library preparation pipeline. The libraries were pooled at equimolar concentration and sequenced using the iSeq. 100 Sequencing System (Illumina) following a 2 × 150 cycles paired-end sequencing protocol. Identification and quantification of the reads were done using BION-META software (McDonald et al., 2016). The number of reads for each strain was normalized by the copy number of the 16S rRNA gene (3, 5, and 6 copies for *A. muciniphila*, *B. thetaiotaomicron*, and *F. prausnitzii*, respectively) (Stoddard et al., 2015).

2.6 | Free amino acid quantification

The concentration of free amino acids was determined as described by Kivima et al. (2021) with a few modifications. Samples were thawed, vortexed and centrifuged (21,000g, 5 min, RT). Centrifuged samples were filtrated (Millipore Millex-LG filters 13 mm Philic PTFE 0.2 µm non-sterile SLLGH13NK; Millipore Corp.) and the supernatant was diluted 10 times with milliQ water. The free amino acids from the diluted supernatant were derivatized, separated with an AccQ-Tag Ultra RP 1.7 µm (2.1 × 100 mm) column and quantified using a Waters UPLC-PDA system (Waters). For derivatization, 6-aminoquinolyl-N-hydroxysuccinimidyl carbamate (Synchem UG & Co) was used. The elution was carried out using a gradient of AccQTag Ultra eluents A and B (Waters). The data were processed with Empower 2 software (Waters).

2.7 | Genome-scale metabolic model (GEM)

2.7.1 | GEM source

The GEMs of *A. muciniphila*, *B. thetaiotaomicron*, and *F. prausnitzii* were collected from a public database published by Machado et al.

(2018) (https://github.com/cdanielmachado/embl_gems). The GEMs were further curated using MEMOTE (metabolites formula, H⁺-unbalanced reactions, duplicated reactions, unfeasible reactions, and futile cycles) until a consistency score higher than 95% was achieved (Lieven et al., 2020). For each strain, the biomass reaction was modified to integrate deoxyribonucleotides and ribonucleotides. In addition, the growth-related ATP maintenance coefficient was adjusted. Amino acid transport reactions were added when missing. Mucin consumption was modeled by allowing the consumption of mucin-derived monosaccharides (N-AcGal, N-AcGam, galactose, and fucose). With this approach, the energy expenditure associated with the cleavage of mucin was not accounted for. The consumption of mucin by *A. muciniphila* and *B. thetaiotaomicron* was supported by literature and validated experimentally (Degnan & Macfarlane, 1995; Derrien et al., 2004; Ottman et al., 2016). The exchange reactions associated with mucin-derived monosaccharides were all set to zero in *F. Prausnitzii* GEM. Vitamins, ions (metals and salts), ribonucleotides, deoxyribonucleotides, and amino acids were not considered limited because of the presence of yeast extract in the medium. A summary of the GEMs can be found in Table S1. GEMs are provided in the supporting information section.

The GEMs were constrained using uptake and production rates calculated based on the difference in metabolite concentrations between the beginning and the end of fermentation, assuming most changes occurred before the stationary phase. Finally, the concentration difference was expressed per gDW and multiplied by the growth rate to obtain a rate (mmol (gDW h)⁻¹). Data from the fifth to seventh passages were used to calculate an average and standard deviation (SD). The depletion of a metabolite from the medium was mimicked by constraining its exchange reaction to zero. A metabolite was considered growth-limiting when its depletion led to a significant decrease in the predicted growth rate.

2.7.2 | GEM analysis

The pattern of intracellular fluxes was described using FBA and flux variance analysis (FVA) using the COBRA and RAVEN Toolbox (Becker et al., 2007) in MATLAB (The MathWorks Inc.), Gurobi solver (Gurobi Optimization Inc.), and by optimizing biomass production (growth rate). Both FBA and flux variability analysis (FVA; $n = 5000$ samples, 90% of maximal growth rate) were done using constraint-based models. Experimental data obtained from the cultivations were used to constrain the model if not stated otherwise.

2.8 | Data analysis

Quantification of extracellular metabolites was carried out with Empower software (Waters Corporation). Principal component analysis (PCA) was performed using R studio (v4.2.0) on centered and scaled data. For other analyzes, data were processed using Excel v20.04 (Microsoft Corporation). Figures were prepared using Inkscape (v1.2.1).

3 | RESULTS AND DISCUSSION

3.1 | Specific and reproductive growth pattern

In the current study, *A. muciniphila*, *B. thetaiotaomicron*, and *F. prausnitzii* were initially characterized in monoculture and then in the consortium, with the prior data sets used as references for the consortium.

The characterization of the strains started by assessing their growth stability over several passages. A passage was defined by the transfer of 1% (v/v) of the preceding bacterial culture into fresh YCFAM medium, plus the fermentation time (usually 24 h). Passages were conducted daily and under strictly anaerobic conditions over 7 days. Numbers 1–7 are used in figures to refer to the passages, first to last. The growth kinetics of individual strains and the consortium were monitored using an isothermal microcalorimeter. The heat flow (W) data measured over the seven passages were summarized using a PCA (Figure 1). According to the PCA, the number of passages needed to reach stability (i.e. reproducibility in heat flow curves between passages), varied between individual strains and the consortium. The consortium required three passages to reach stability, while two passages were sufficient for *B. thetaiotaomicron* and *F. prausnitzii* monocultures (Figure 1b–d). At least four passages were needed before *A. muciniphila* monoculture showed stabilized growth kinetics (Figure 1a). From the fifth passage onward, the stability of the heat flow measurement was observed under all conditions. The heat flow from the fifth to seventh passages was used, after transformation into heat (J), to calculate growth rates. The existence of a linear relationship between heat and biomass was additionally confirmed before any growth rate calculations were made (Table S2).

The growth kinetics of *A. muciniphila* were characterized by a rapid increase of heat flow in the first 10 h after inoculation with a specific growth rate of $0.57 \pm 0.02 \text{ h}^{-1}$ (Figure S1A,B). This specific growth rate was slightly higher than the highest growth rate in basal medium reported by Noora et al. (2017) ($0.41 \pm 0.05 \text{ h}^{-1}$). This difference could be attributed to the presence of yeast extract and casitone in our medium, as well as the higher concentration of mucin, which has been shown to trigger and modulate gene expression (Liu et al., 2021). The heat flow curves of *B. thetaiotaomicron* and *F. prausnitzii* showed multiple phases (Figure S1A,C,D). These phases were likely caused by metabolic switches triggered by the depletion of the most favorable substrate(s), thus reducing the growth rate at each new phase. For both *B. thetaiotaomicron* and *F. prausnitzii*, the highest growth rate occurred in the first few hours after inoculation ($0.88 \pm 0.06 \text{ h}^{-1}$ and $1.00 \pm 0.08 \text{ h}^{-1}$, respectively) followed by a second growth phase ($0.20 \pm 0.01 \text{ h}^{-1}$ and $0.21 \pm 0.01 \text{ h}^{-1}$, respectively) and a third phase ($0.07 \pm 0.002 \text{ h}^{-1}$ and $0.09 \pm 0.004 \text{ h}^{-1}$, respectively). Prior genomic sequencing studies confirmed the presence and expression of mucin-associated hydrolases and catabolizing pathways in *B. thetaiotaomicron* (Glover et al., 2022; Martens et al., 2011; Ravcheev et al., 2013). Moreover, Martens et al. (2011) already observed complicated polyphasic growth profiles with *B. thetaiotaomicron*. In mineral medium (ZBW1), *B. thetaiotaomicron* growth rate was $0.015 \pm 0.002 \text{ h}^{-1}$.

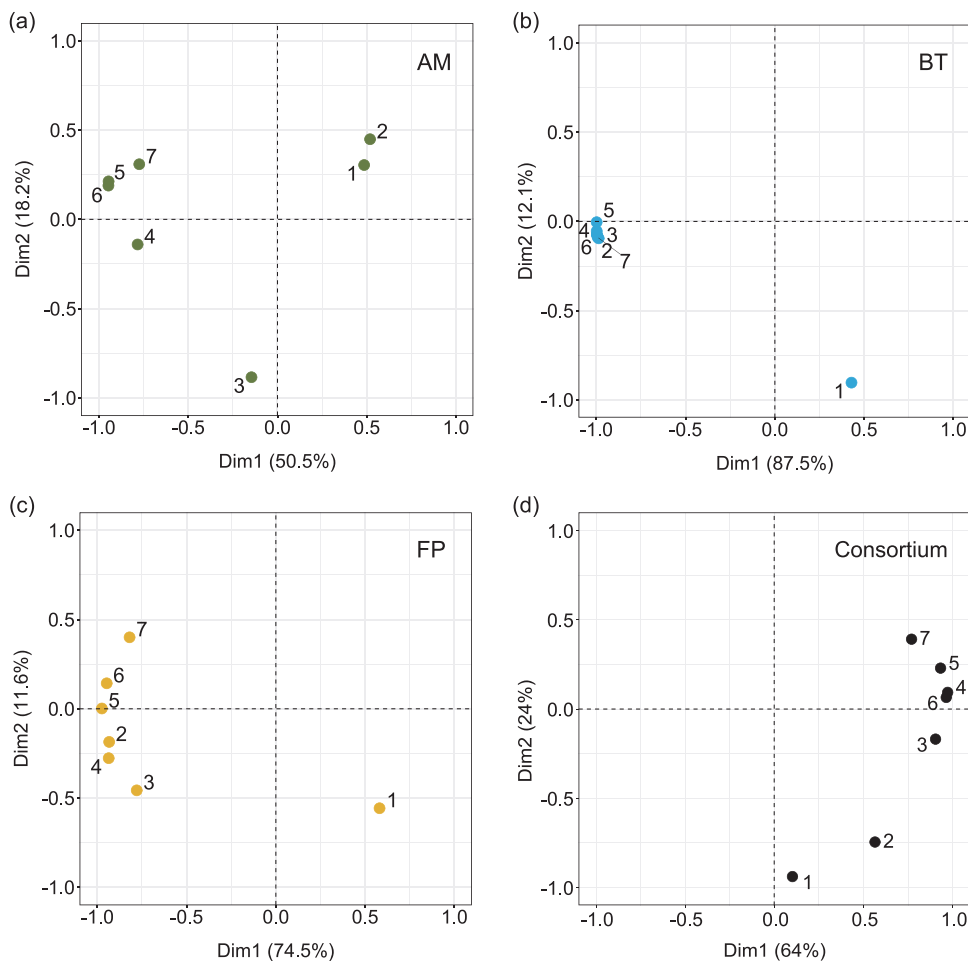


FIGURE 1 Three serial passages are required to reach consortium stability. Principal component analysis (PCA) was conducted using the heat flow monitored by IMC ($n = 3$) over seven successive passages (numbered from 1 to 7). Panels a–d correspond to *Akkermansia muciniphila* (green), *Bacteroides thetaiotaomicron* (blue), *Faecalibacterium prausnitzii* (yellow), and the consortium (black), respectively.

This growth rate was seven times lower than the lowest measured in our YCFAM medium. This difference was most certainly explained by the consumption of other components (casitone, yeast extract) present in the YCFAM medium. In Lopez-Siles et al. (2012) study, *F. prausnitzii* was unable to grow with mucin as a carbon source while in our YCFAM medium, its growth rate ranged from $0.09 \pm 0.004 \text{ h}^{-1}$ to $1.00 \pm 0.08 \text{ h}^{-1}$. The comparison between our and Lopez-Siles et al. (2012) medium showed that ours contained an additional six SCFAs, had a higher concentration of L-cysteine and included phosphate buffers. Interestingly, growth rates obtained in the YCFAM medium were more consistent with those reported in the presence of mucin-derived monosaccharides, such as N-AcGam, glucosamine, or glucose (Duncan et al., 2002; Lopez-Siles et al., 2012).

After individually characterizing each strain, *A. muciniphila*, *B. thetaiotaomicron*, and *F. prausnitzii* were co-inoculated in the YCFAM

medium, starting with the same initial cell density. The three-strain consortium growth was monitored by IMC over seven passages and compared to the individual strains (Figure S1A). In accordance with PCA (Figure 1d), the robustness of the consortium composition improved with the number of passages. From the fourth passage, the consortium heat flow curves were comparable to the combination of the curves from individual strains (Figure S1A). To confirm that the heat flow released by the consortium originated from the metabolic activities of all three strains, their presence was confirmed by 16S rRNA sequencing (Figure 2b). *B. thetaiotaomicron*, *A. muciniphila*, and *F. prausnitzii* represented $52 \pm 2\%$, $34 \pm 2\%$, and $13 \pm 1\%$ of the final consortium, respectively (Table S3).

As a further step in consortium characterization, the growth rate of individual strains within the consortium was determined. The abundance of each strain within the consortium was quantified hourly over 24 h

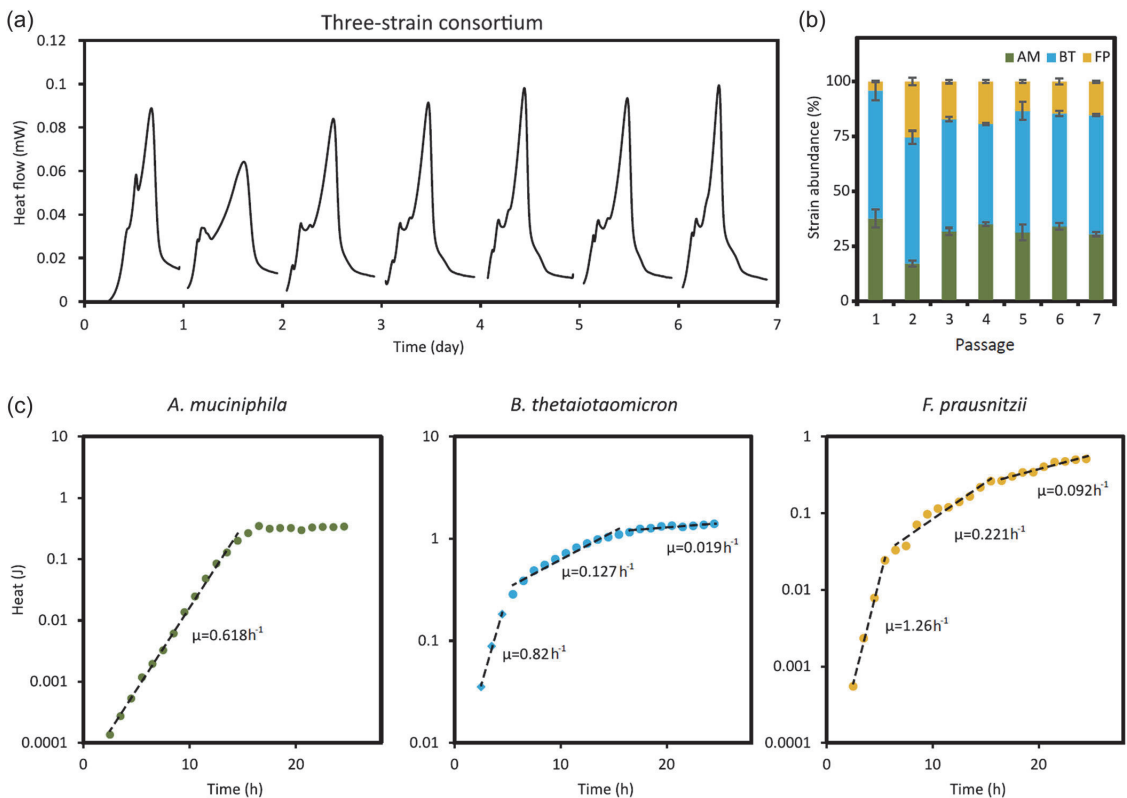


FIGURE 2 Robustness of consortium composition over serial passages. (a) The consortium growth was monitored in YCFAM over seven serial passages using the IMC. For each passage, the average and standard deviation of the heat flow ($n = 3$ replicates) are represented by a full line and ribbon, respectively. (b) At the end of passage cultivation, the consortium composition was determined using 16S rRNA sequencing. *A. muciniphila*, *B. thetaiotaomicron*, and *F. prausnitzii* are shown as green, blue, and yellow bars, respectively. (c) The growth rate (h^{-1}) of the individual strains was calculated using the heat (J) released by the consortium and the abundance of each strain within the consortium. For 16S rRNA sequencing, samples were collected hourly over 24 h. rRNA, ribosomal RNA.

using 16S rRNA amplicon sequencing. These abundances were used to reconstruct the growth curve of individual strains from the total heat generated by the consortium. Regardless of the strain, the growth rates calculated from the reconstructed curves resembled those obtained with monoculture cultivations (above paragraph and Figure 2c). In this condition, the results suggested that *B. thetaiotaomicron*, *A. muciniphila*, and *F. prausnitzii* stably coexist in the YCFAM medium.

3.2 | Evaluation of consortium resilience through growth kinetics and 16S rRNA NGS

In their work, Allison and Martiny (2008) defined resilience as the ability of a community to quickly recover from a disturbance whether by growth, physiological, or genetic adaptation. Recent works suggested that pH, medium composition, taxonomic group, and species initial abundance influence community stability over serial passages (Goldford et al., 2018; Segura Munoz et al., 2022; Zegeye et al., 2019).

To assess the resilience of our consortium, the effect of species' initial abundance was tested across three combinations (Figure 3). In each combination, one strain was inoculated at a concentration a hundred times lower than the other two strains. The composition of the consortia was evaluated at the end of each passage. Resilience was achieved when the growth kinetics and composition of a combination closely resembled the reference (Figure 3a).

The growth kinetics were significantly altered from the reference consortium when the initial concentration of BT and AM were lowered (Figure 3a, first two panels). A similar growth kinetics to the reference was retrieved after the second and fifth passages, respectively. Similarly to *B. thetaiotaomicron*, two passages were also sufficient for *F. prausnitzii* (Figure 3a, third panel). In coherence with the heat flow, a return to the former consortium composition was also obtained by 16S rRNA sequencing at the end of the fifth passage (Figure 3b [passage 5] and Figure 2b [passages 5–7]). The composition of the consortia from passages 1–5 is reported in Table S4.

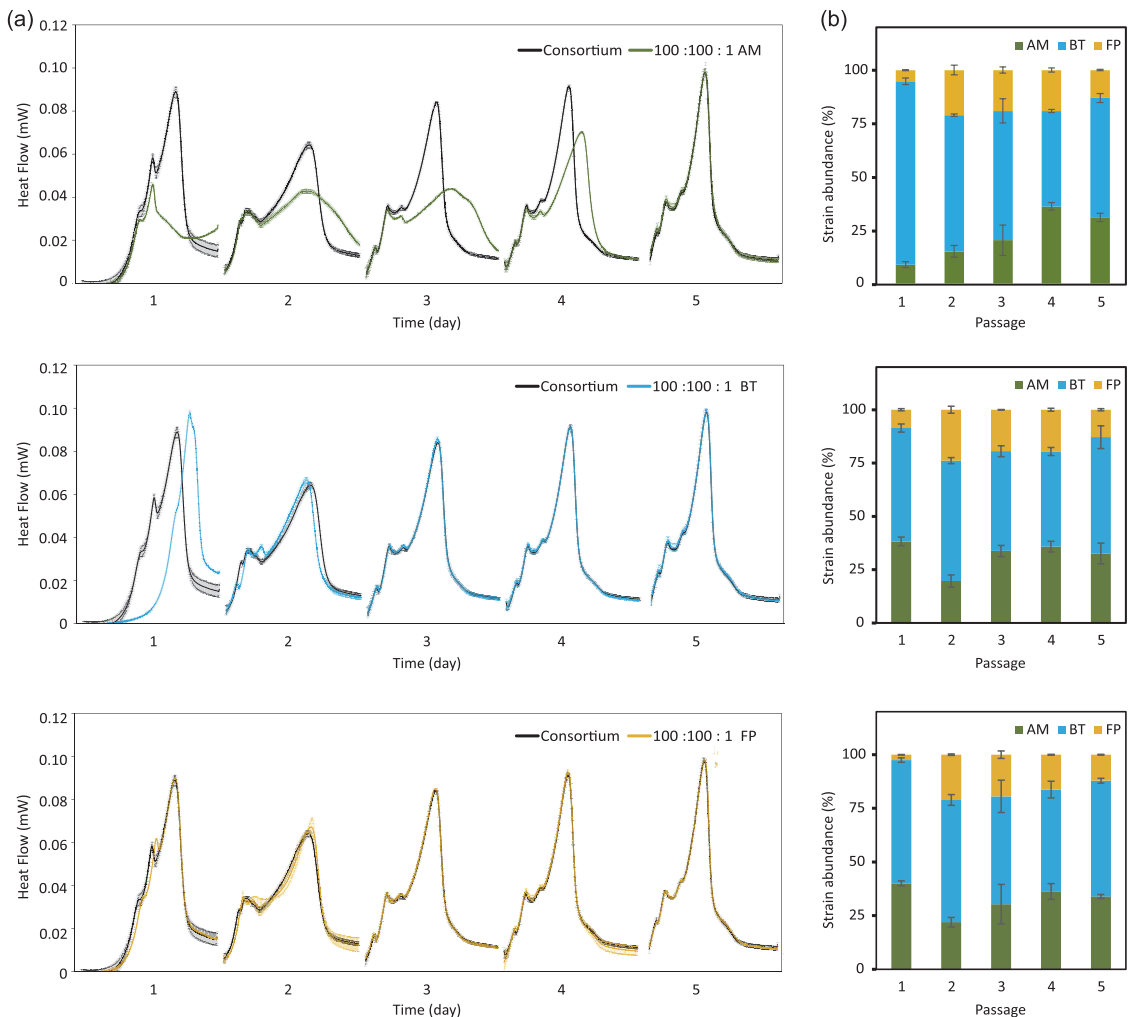


FIGURE 3 Resilience of the consortium community. (a) The resilience of the consortium was tested across three combinations. In each combination, *A. muciniphila*, *B. thetaiotaomicron*, or *F. prausnitzii* strain was inoculated at a 100-fold lower concentration compared to the two others (top to down, respectively). The full line and ribbon represent the average and standard deviation of the heat flow monitored in triplicates. The resilience was reached when the original heat flow (black, Figure 2a) was recovered. (b) The abundance of *A. muciniphila* (green), *B. thetaiotaomicron* (blue), and *F. prausnitzii* (yellow) was determined using 16S rRNA sequencing at the end of every passage ($n = 3$). rRNA, ribosomal RNA.

This return could not be achieved in the event of drastic competition for growth-dependent substrate(s).

3.3 | A slight interaction is suggested by changes in organic acid concentrations

Although the three strains proved able to thrive in the consortium, some metabolic changes may have been necessary to maintain the stability. To evaluate this hypothesis, the production and consumption of

extracellular organic acids were quantified at the end of monoculture and consortium cultivations (Table S5). As reported in the literature, *F. prausnitzii* was characterized by the secretion of butyrate and formate (Figure 4) (D'hoë et al., 2018; Lopez-Siles et al., 2012; Wrzosek et al., 2013). However, the consumption of acetate by *F. prausnitzii* was not confirmed in our study. *B. thetaiotaomicron* and *A. muciniphila* showed similar excretion profiles, with significant production of acetate and propionate, and consumption of malate (Das et al., 2018; Noora et al., 2017; van der Ark et al., 2018). The secretion of both isovaleric and isobutyrate and the consumption of lactate were measured only with

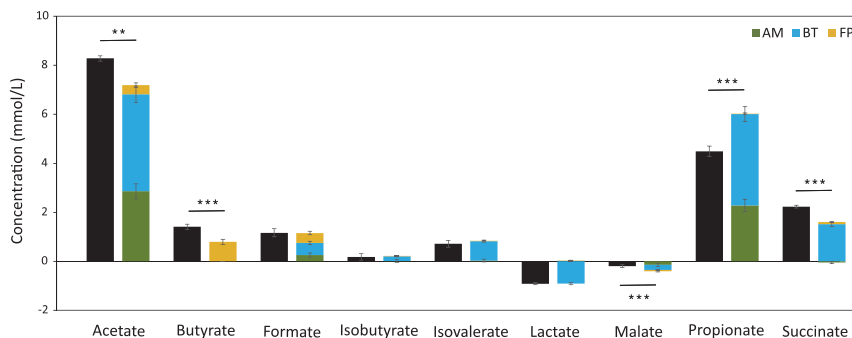


FIGURE 4 External metabolite production in monocultures and the consortium. Organic acids (mmol/L) were quantified at the end of the fifth, sixth, and seventh passages. Green, blue, and yellow bars represent individual cultures—*A. muciniphila*, *B. thetaiotaomicron*, and *F. prausnitzii* respectively, and black bars represent the consortium. The concentrations from individual strains were stacked up to visualize the expected concentrations in the consortium in the absence of interactions between the species. Statistical significance between the consortium and the sum of individual cultures is calculated with a Student's *t*-test (* $p < 0.05$, ** $p < 0.01$, *** $p < 0.001$).

B. thetaiotaomicron. The consortium had a significantly higher concentration of acetate, butyrate, and succinate compared to the combination of concentrations produced by individual strains (Figure 4; Table S5). The higher production of butyrate in the consortium was not correlated with the expected decrease in acetate concentration suggested by Wrzosek et al. (2013). However, at the end of the consortium fermentation, the concentration of acetate was eight times higher compared to *F. prausnitzii* monoculture in YCFAM, which could have enhanced butyrate production by *F. prausnitzii* (Figure 4).

3.4 | Free amino acid consumption in the consortium is mainly influenced by *B. thetaiotaomicron*

In addition to organic acids, the concentrations of 20 free amino acids were assessed at the end of the fifth, sixth, and seventh passages.

The difference in secretion and consumption of free amino acids between individual strains and consortium was examined using PCA and including the initial medium composition as a reference. The first and second components (PCs) explained 99.9% of the variability (Figure S2). The consortium and *B. thetaiotaomicron* were separated from *F. prausnitzii*, *A. muciniphila* and the medium samples in PC2. This result suggested that in the consortium the free amino acids consumption in the consortium was mainly driven by *B. thetaiotaomicron*. At the end of *A. muciniphila* and *F. prausnitzii* cultivations, the concentration of the free amino acids was comparable to the reference, suggesting either a negligible or no consumption of any free amino acids (Table S6). This observation differed greatly from the net consumption and excretion of 10 amino acids by *F. prausnitzii* reported by Heinken et al. (2014). In addition, our data did not confirm threonine consumption by *A. muciniphila* as predicted by Noora et al. (2017) and reported by van der Ark et al. (2018) (Table S6). At the end of *B. thetaiotaomicron* cultivation, over half of the measured free amino acids had increased in the medium (Table S6). Phenylalanine and tryptophan concentrations remained unchanged. In comparison to the reference, the abundances

of proline and glutamine were higher. Furthermore, aspartate and asparagine were depleted. Data reported by Catlett et al. (2020) suggested that *B. thetaiotaomicron* uses L-asparagine hydrolase (EC 3.5.1.1; BT_0526, BT_2404, BT2757) to convert asparagine to aspartate. Aspartate can then enter the TCA cycle as oxaloacetate (EC 2.6.1.1; BT_2415), resulting in the generation of ATP and cofactor (NADPH). From the overflow in the TCA cycle, the succinate that is produced by succinyl-CoA ligase (EC 6.2.1.5; BT_0788, BT_0787) is either secreted and/or mobilized in the respiratory chain to generate the proton gradient required for ATP production (Catlett et al., 2020). In addition to asparagine and aspartate, serine was also consumed and can be converted into pyruvate (EC 4.3.1.17; BT_4678).

3.5 | Metabolic modeling suggests distinct growth-limiting substrates for individual strains

In this study, FBA was used to identify strain-specific and shared carbon sources. It was assumed that all strains could uptake and catabolize amino acids and that *F. prausnitzii* was the only strain unable to cleave, and thus consume, mucin-derived monosaccharides. *A. muciniphila*, *B. thetaiotaomicron*, and *F. prausnitzii* genome-scale metabolic models (GEMs) consisted of 1308, 1491, and 1137 metabolic reactions, respectively (Table S1). GEMs were constrained using experimental rates (Table S7, Section 2.7.1). The analysis looked for the flux distributions for which the production of biomass, i.e., specific growth rate, was the most optimized (Tables S8–S10). It is important to mention that an average experimental growth rate was calculated and used to constrain GEMs for *B. thetaiotaomicron* and *F. prausnitzii*. Growth of *A. muciniphila* was predicted to be mainly sustained by threonine and N-AcGam consumption (Figure 5a). Threonine was predicted to enter the TCA cycle as succinyl-CoA to generate ATP. In addition, threonine was converted to glycine and serine. These predictions were not confirmed experimentally (Table S6).

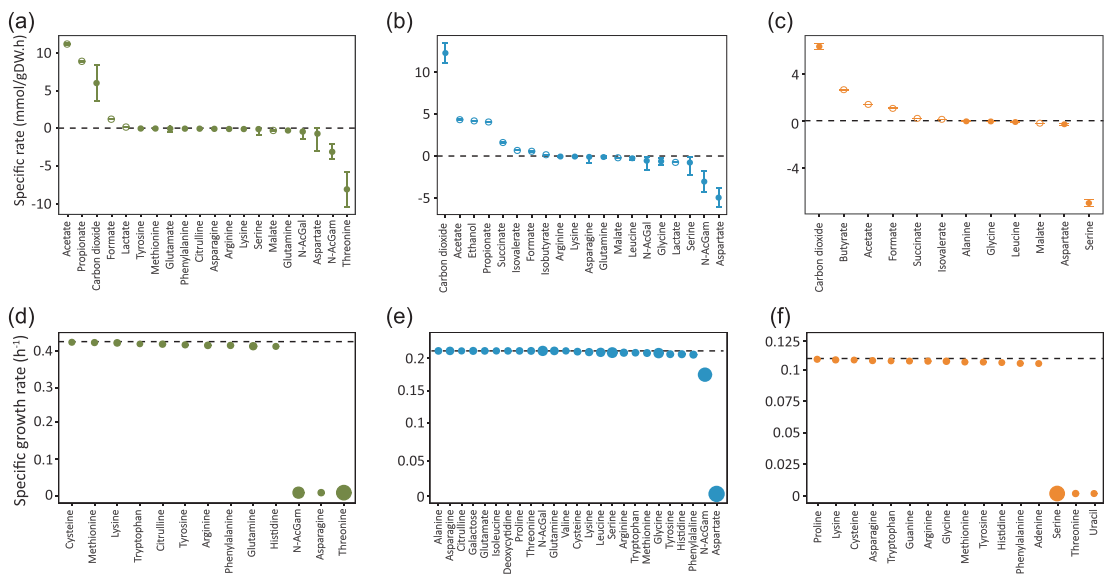


FIGURE 5 Predicted metabolic consumption and production rates for *A. muciniphila*, *B. thetaiotaomicron*, and *F. prausnitzii*. (a–c) Production and consumption rates predicted by FBA for *A. muciniphila* (a), *B. thetaiotaomicron* (b), and *F. prausnitzii* (c). Open circles show fluxes predicted by FBA, while plain circles represent fluxes that were calculated from experimental data and used to constrain respective models. Production and consumption are represented by positive and negative rates, respectively. Fluxes with absolute values lower than 0.1 were considered negligible and omitted. Specific rates were averaged, and standard deviations were calculated after flux variability analysis ($n = 5000$ samples). (d–f) Effect of substrate depletion on specific growth rates of *A. muciniphila*, *B. thetaiotaomicron*, and *F. prausnitzii*. To mimic the depletion of a substrate from the medium, the lower bound of its exchange reaction was set to zero. The dashed line represents the optimal growth rate without limitation. The size of the dots is relative to the priorly predicted uptake rates. FBA, flux balance analysis.

B. thetaiotaomicron was predicted to consume preferentially aspartate and N-AcGlc (Figure 5b). As described in Section 3.3 for *B. thetaiotaomicron*, aspartate entered the TCA cycle to generate ATP, leading to the excretion of succinate and propionate. For both *A. muciniphila* and *B. thetaiotaomicron*, N-AcGlc entered glycolysis as fructose 6-phosphate in three metabolic reactions. The energy (ATP) required to grow was generated by glycolytic enzymes (pyruvate kinase PYK, phosphoglycerate kinase PGK) and TCA enzyme (succinyl-CoA synthetase SUCOAS) (Tables S8–S10). In *A. muciniphila* metabolism, ATP was actively used by formate tetrahydrofolate ligase (FTHFLI) and phosphofructokinase (PFK). For *B. thetaiotaomicron*, the prediction showed that ATP turnover was highest for N-acetylglucosamine kinase (ACGAMK) and glucose-1-phosphate adenyllyl transferase (GLGC). In the absence of evidence suggesting that *F. prausnitzii* could cleave mucin and thus consume any of the monosaccharides, FBA predicted serine to be the main carbon source for *F. prausnitzii* (Figure 5c). Serine was predicted to enter central carbon metabolism after being converted by L-serine ammonia-lyase (SERD_L) to pyruvate. This result was consistent with the data reported in Auger et al. (2022), showing a higher expression of serine/threonine transporter (SstT) at an early stage of fermentation. However, the depletion or consumption of serine by *F. prausnitzii* was not experimentally confirmed (Table S6). Acetate kinase reaction (ACKr) was predicted as an almost unique ATP source for *F. prausnitzii*, with

one ATP produced per acetate catabolized. The limited use of the glycolysis pathway to generate ATP was due to the absence of mucin-derived monosaccharides consumption.

The following step aimed to determine which of the predicted carbon sources were essential to sustain growth and which were potentially shared by species (Table S11). The depletion of a substrate from the medium was mimicked by setting the consumption rate to zero while optimizing biomass production. In the case of *A. muciniphila*, the depletion of N-AcGlc, asparagine, or threonine entirely stopped the growth, while the other substrates had only a slight effect on the predicted growth rate (Figure 5d). These results were coherent with a previous study where N-AcGlc and L-threonine were essential for the growth of *A. muciniphila* in a minimal medium (van der Ark et al., 2018). Although asparagine was not shown as an essential nutrient, its consumption was confirmed in a BHI medium supplemented with mucin (Liu et al., 2021). *B. thetaiotaomicron*, the most robust strain, had the widest range of substrates and was slightly affected by the depletion of most of its carbon sources (Figure 5e). Only the depletion of aspartate or N-AcGlc had a significant effect on its growth rate. For *F. prausnitzii*, serine, threonine, and uracil turned out to be essential for its growth in this specific condition (Figure 5f). Interestingly, the omission of serine, threonine, and uracil in the defined medium used by Heinken et al., (2014) still allowed the growth of *F. prausnitzii*. Nonetheless, the growth in this

medium was described by the authors as poor and inconsistent (lower than 0.13 h^{-1}). Although predicting fluxes using a complex medium is controversial, our results suggested that threonine and N-AcGam were the common substrates that strains could compete for within the consortium via which they could alter each other's growth.

4 | CONCLUSION

This study demonstrates the stability, reproducibility, and resilience of a potential NGP consortium. Our results showed that a stable and reproducible composition was reached within several passages and could be maintained thereafter. Despite significant disturbances in its original composition, the resilience of the consortium could be demonstrated by recovering its expected growth kinetics and composition. The production of acetate and propionate by *A. muciniphila* and *B. thetaiotaomicron* was confirmed. The secretion of butyrate by *F. prausnitzii* was higher when grown in a consortium, likely due to the increased concentration of acetate available in the medium. In silico analysis predicted that all three species preferred mucin-derived saccharides (N-AcGAM and N-AcGal) as substrates. This competition was most likely compensated in nutrient-rich YCFAM medium to allow all strains to thrive in consortium. To the best of our knowledge, this is the first time that the resilience of these NGP candidates has been dynamically monitored and confirmed by 16S rRNA NGS analysis. Continuous monitoring throughout fermentation was made possible using IMC confirming the high potential of the device, even in an opaque environment. IMC represents an alternative methodology that responds to the demand for continuous monitoring of bacterial growth kinetics (Lebas et al., 2020). These methodologies could be further used for more complex consortia with additional environmental disturbances (pH, temperature, nutrients).

AUTHOR CONTRIBUTIONS

Anna Kattel: Data curation; methodology; writing—review and editing (equal). **Valter Aro:** Data curation; methodology; writing—original draft (equal). **Petri-Jaan Lahtvee:** Funding acquisition; investigation; supervision (equal). **Jekaterina Kazantseva:** Writing—review and editing (equal). **Arvi Jõers:** Conceptualization; funding acquisition; investigation; project administration; supervision (equal). **Ranno Nahku:** Conceptualization; data curation; funding acquisition; methodology; project administration; resources; writing—review and editing; supervision (equal). **Isma Belouah:** Data curation; formal analysis; methodology; visualization; writing—review and editing; writing—original draft (equal).

ACKNOWLEDGMENTS

The authors would like to thank Mary-Liis Kütt for her contributions in writing the project proposal. The authors would like to acknowledge the expertise and contributions of those people providing the analytical data at the Center of Food and Fermentation Technologies. This work was supported by the European Regional Development Fund ("High throughput platform for growth improvement of

microorganisms"; NSP137, 2014-2020.4.02.17-0104). The funding organization is SA Archimedes.

CONFLICT OF INTEREST STATEMENT

None declared.

DATA AVAILABILITY STATEMENT

The data that support the findings of this study are openly available in FastMicro at <https://github.com/Tftak-IB/FastMicro.git>. Additional supporting information, including supplemental tables, figures and GEMs, can be found on GitHub: <https://github.com/Tftak-nIB/FastMicro.git>.

ETHICS STATEMENT

None required.

ORCID

Isma Belouah  <http://orcid.org/0000-0003-4451-8365>

REFERENCES

- Allison, S. D., & Martiny, J. B. H. (2008). Resistance, resilience, and redundancy in microbial communities. *Proceedings of the National Academy of Sciences*, 105, 11512–11519.
- van der Ark, K. C. H., Aalvink, S., Suarez-Diez, M., Schaap, P. J., de Vos, W. M., & Belzer, C. (2018). Model-driven design of a minimal medium for Akkermansia muciniphila confirms mucus adaptation. *Microbial Biotechnology*, 11, 476–485.
- Auger, S., Mournetas, V., Chiapello, H., Loux, V., Langella, P., & Chatel, J. M. (2022). Gene co-expression network analysis of the human gut commensal bacterium Faecalibacterium prausnitzii in R-Shiny. *PLoS One*, 17, e0271847.
- Bayode, M. T., Alabi, M. A., Babatunde, O. J., Sadibo, M. E., Lawani, B. T., Okiti, A. F., Elabiyi, M. O., & Lawrence, D. I. (2022). Isothermal microcalorimetry (IMC) calcreener: Automated peculiarities of antimicrobial therapy and metabolism depth of multidrug resistant bacteria. *Bulletin of the National Research Centre*, 46, 149.
- Becker, S. A., Feist, A. M., Mo, M. L., Hannum, G., Palsson, B. Ø., & Herrgard, M. J. (2007). Quantitative prediction of cellular metabolism with constraint-based models: The COBRA toolbox. *Nature Protocols*, 2, 727–738.
- Braissant, O., Keiser, J., Meister, I., Bachmann, A., Wirz, D., Göpfert, B., Bonkat, G., & Wadsö, I. (2015). Isothermal microcalorimetry accurately detects bacteria, tumorous microtissues, and parasitic worms in a label-free well-plate assay. *Biotechnology Journal*, 10, 460–468.
- Cani, P. D., & Vos, W. M. D. (2017). Next-Generation Beneficial Microbes: The Case of Akkermansia muciniphila. 8, 1–8.
- Caporaso, J. G., Lauber, C. L., Walters, W. A., Berg-Lyons, D., Lozupone, C. A., Turnbaugh, P. J., Fierer, N., & Knight, R. (2011). Global patterns of 16S rRNA diversity at a depth of millions of sequences per sample. *Proceedings of the National Academy of Sciences*, 108, 4516–4522.
- Catlett, J. L., Catazaro, J., Cashman, M., Carr, S., Powers, R., Cohen, M. B., & Buan, N. R. (2020). Metabolic feedback inhibition influences metabolite secretion by the human gut symbiont bacteroides thetaiotaomicron. *mSystems*, 5, e00252–20.
- Chang, C. J., Lin, T. L., Tsai, Y. L., Wu, T. R., Lai, W. F., Lu, C. C., & Lai, H. C. (2019). Next generation probiotics in disease amelioration. *Journal of Food and Drug Analysis*, 27, 615–622.
- Chia, L. W., Hornung, B. V. H., Aalvink, S., Schaap, P. J., de Vos, W. M., Knol, J., & Belzer, C. (2018). Deciphering the trophic interaction

- between *Akkermansia muciniphila* and the butyrogenic gut commensal *Anaerostipes caccae* using a metatranscriptomic approach. *Antonie Van Leeuwenhoek*, 111, 859–873.
- Coppola, S., Avagliano, C., Calignano, A., & Berni Canani, R. (2021). The protective role of butyrate against obesity and obesity-related diseases. *Molecules*, 26, 682.
- Das, P., Ji, B., Kovatcheva-Datchary, P., Bäckhed, F., & Nielsen, J. (2018). In vitro co-cultures of human gut bacterial species as predicted from co-occurrence network analysis. *PLoS One*, 13, e0195161.
- Degnan, B. A., & Macfarlane, G. T. (1995). Arabinogalactan utilization in continuous cultures of bifidobacterium longum: Effect of co-culture with bacteroides thetaiotaomicron. *Anaerobe*, 1, 103–112.
- Derrien, M., Vaughan, E. E., Plugge, C. M., & de Vos, W. M. (2004). *Akkermansia muciniphila* gen. nov., sp. nov., a human intestinal mucin-degrading bacterium. *International Journal of Systematic and Evolutionary Microbiology*, 54, 1469–1476.
- Derrien, M., & Veiga, P. (2017). Rethinking diet to aid human–microbe symbiosis. *Trends in Microbiology*, 25, 100–112.
- D'hoel, K., Vet, S., Faust, K., Moens, F., Falony, G., Gonze, D., Lloréns-Rico, V., Gelens, L., Danckaert, J., De Vuyst, L., & Raes, J. (2018). Integrated culturing, modeling and transcriptomics uncovers complex interactions and emergent behavior in a three-species synthetic gut community. *Elife*, 7, e37090.
- Duncan, S. H., Hold, G. L., Harmsen, H. J. M., Stewart, C. S., Flint, H. J., & Duncan, S. H. (2002). Growth requirements and fermentation products of fusobacterium prausnitzii, and a proposal to reclassify it as faecalibacterium prausnitzii gen. nov., comb. nov. *International Journal of Systematic and Evolutionary Microbiology*, 52, 2141–2146.
- Fan, Y., & Pedersen, O. (2021). Gut microbiota in human metabolic health and disease. *Nature Reviews Microbiology*, 19, 55–71.
- Flint, H. J., Scott, K. P., Louis, P., & Duncan, S. H. (2012). The role of the gut microbiota in nutrition and health. *Nature Reviews Gastroenterology & Hepatology*, 9, 577–589.
- Gaisford, S. (2016). Isothermal Microcalorimetry. 389–409.
- Gatto, L., & Shliaha, P. V. (2013). Optimising identification and quantitation by combining data using the synapter package. 1–27.
- Glover, J. S., Ticer, T. D., & Engevik, M. A. (2022). Characterizing the mucin-degrading capacity of the human gut microbiota. *Scientific Reports*, 12, 8456.
- Goldford, J. E., Lu, N., Bajić, D., Estrela, S., Tikhonov, M., Sanchez-Gorostiaga, A., Segrè, D., Mehta, P., & Sanchez, A. (2018). Emergent simplicity in microbial community assembly. *Science*, 361, 469–474.
- Heinken, A., Khan, M. T., Paglia, G., Rodionov, D. A., Harmsen, H. J. M., & Thiele, I. (2014). Functional metabolic map of faecalibacterium prausnitzii, a beneficial human gut microbe. *Journal of Bacteriology*, 196, 3289–3302.
- Hu, W., Gao, W., Liu, Z., Fang, Z., Zhao, J., Zhang, H., Lu, W., & Chen, W. (2022). Biodiversity and physiological characteristics of novel faecalibacterium prausnitzii strains isolated from human feces. *Microorganisms*, 10, 297.
- Ince, D., Lucas, T. M., & Malaker, S. A. (2022). Current strategies for characterization of mucin-domain glycoproteins. *Current Opinion in Chemical Biology*, 69, 102174.
- Kabanova, N., Stulova, I., & Vilu, R. (2012). Microcalorimetric study of the growth of bacterial colonies of lactococcus lactis IL1403 in agar gels. *Food Microbiology*, 29, 67–79.
- Kattel, A., Morell, I., Aro, V., Lahtvee, P. J., Vilu, R., Jöers, A., & Nahku, R. (2023). Detailed analysis of metabolism reveals growth-rate-promoting interactions between anaerostipes caccae and bacteroides spp. *Anaerobe*, 79, 102680.
- Kivima, A., Tanilas, K., Martverk, K., Rosensvald, S., Timberg, L., & Laos, K. (2021). The composition, physicochemical properties, antioxidant activity, and sensory properties of Estonian honeys. *Foods*, 10, 511.
- Kostopoulos, I., Aalvink, S., Kovatcheva-Datchary, P., Nijse, B., Bäckhed, F., Knol, J., de Vos, W. M., & Belzer, C. (2021). A continuous battle for host-derived glycans between a mucus specialist and a glycan generalist in vitro and in vivo. *Frontiers in Microbiology*, 12, 632454.
- Laursen, M. F., Sakanaka, M., von Burg, N., Mörbé, U., Andersen, D., Moll, J. M., Pekmez, C. T., Rivollier, A., Michaelsen, K. F., Mølgaard, C., Lind, M. V., Dragsted, L. O., Katayama, T., Frandsen, H. L., Vinggaard, A. M., Bahl, M. I., Brix, S., Agace, W., Licht, T. R., & Roager, H. M. (2021). Bifidobacterium species associated with breastfeeding produce aromatic lactic acids in the infant gut. *Nature Microbiology*, 6, 1367–1382.
- Lebas, M., Garault, P., Carrillo, D., Codoñer, F. M., & Derrien, M. (2020). Metabolic response of faecalibacterium prausnitzii to cell-free supernatants from lactic acid bacteria. *Microorganisms*, 8, 1528.
- Lieven, C., Beber, M. E., Olivier, B. G., Bergmann, F. T., Ataman, M., Babaei, P., Bartell, J. A., Blank, L. M., Chauhan, S., Correia, K., Diener, C., Dräger, A., Ebert, B. E., Edirisinghe, J. N., Faria, J. P., Feist, A. M., Fengos, G., Fleming, R. M. T., García-Jiménez, B., ... Zhang, C. (2020). MEMOTE for standardized genome-scale metabolic model testing. *Nature Biotechnology*, 38, 272–276.
- Liu, X., Zhao, F., Liu, H., Xie, Y., Zhao, D., & Li, C. (2021). Transcriptomics and metabolomics reveal the adaption of *Akkermansia muciniphila* to high mucin by regulating energy homeostasis. *Scientific Reports*, 11, 9073.
- Lopez-Siles, M., Duncan, S. H., Garcia-Gil, L. J., & Martinez-Medina, M. (2017). Faecalibacterium prausnitzii: From microbiology to diagnostics and prognostics. *The ISME journal*, 11, 841–852.
- Lopez-Siles, M., Khan, T. M., Duncan, S. H., Harmsen, H. J. M., Garcia-Gil, L. J., & Flint, H. J. (2012). Cultured representatives of two major phylogroups of human colonic faecalibacterium prausnitzii can utilize pectin, uronic acids, and host-derived substrates for growth. *Applied and Environmental Microbiology*, 78, 420–428.
- Machado, D., Andrejev, S., Tramontano, M., & Patil, K. R. (2018). Fast automated reconstruction of genome-scale metabolic models for microbial species and communities. *Nucleic Acids Research*, 46, 7542–7553.
- Manor, O., Dai, C. L., Kornilov, S. A., Smith, B., Price, N. D., Lovejoy, J. C., Gibbons, S. M., & Magis, A. T. (2020). Health and disease markers correlate with gut microbiome composition across thousands of people. *Nature Communications*, 11, 5206.
- Martens, E. C., Lowe, E. C., Chiang, H., Pudlo, N. A., Wu, M., McNulty, N. P., Abbott, D. W., Henrissat, B., Gilbert, H. J., Bolam, D. N., & Gordon, J. I. (2011). Recognition and degradation of plant cell wall polysaccharides by two human gut symbionts. *PLoS Biology*, 9, e1001221.
- McDonald, J. E., Larsen, N., Pennington, A., Connolly, J., Wallis, C., Rooks, D. J., Hall, N., McCarthy, A. J., & Allison, H. E. (2016). Characterising the canine oral microbiome by direct sequencing of reverse-transcribed rRNA molecules. *PLoS One*, 11, e0157046.
- Miner-Williams, W., Moughan, P. J., & Fuller, M. F. (2009). Methods for mucin analysis: A comparative study. *Journal of Agricultural and Food Chemistry*, 57, 6029–6035.
- Ottman, N., Davids, M., Suarez-Diez, M., Boeren, S., Schaap, P. J., Martins Dos Santos, V. A. P., Smidt, H., Belzer, C., & de Vos, W. M. (2017). Genome-scale model and omics analysis of metabolic capacities of *Akkermansia muciniphila* reveal a preferential mucin-degrading lifestyle. *Am Soc Microbiol*, 83, e01014–e01017.
- Ottman, N., Huuskonen, L., Reunanen, J., Boeren, S., Klievink, J., Smidt, H., Belzer, C., & de Vos, W. M. (2016). Characterization of outer membrane proteome of *Akkermansia muciniphila* reveals sets of novel proteins exposed to the human intestine. *Frontiers in Microbiology*, 7, 1157.
- Panebianco, C., Villani, A., Pisati, F., Orsenigo, F., Ulaszewska, M., Latiano, T. P., Potenza, A., Andolfo, A., Terracciano, F., Tripodo, C., Perri, F., & Paziienza, V. (2022). Butyrate, a postbiotic of intestinal bacteria, affects pancreatic cancer and gemcitabine response in vitro and in vivo models. *Biomedicine & Pharmacotherapy*, 151, 113163.

- Paone, P., & Cani, P. D. (2020). Mucus barrier, mucins and gut microbiota: The expected slimy partners? *Gut*, 69, 2232–2243.
- Parada Venegas, D., De La Fuente, M. K., Landskron, G., González, M. J., Quera, R., Dijkstra, G., Harmsen, H. J. M., Faber, K. N., & Hermoso, M. A. (2019). Short chain fatty acids (SCFAs)-mediated gut epithelial and immune regulation and its relevance for inflammatory bowel diseases. *Frontiers in Immunology*, 10, 277.
- Raba, G., & Luis, A. S. (2023). Mucin utilization by gut microbiota: Recent advances on characterization of key enzymes. *Essays in Biochemistry*, 67, 345–353.
- Ravcheev, D. A., Godzik, A., Osterman, A. L., & Rodionov, D. A. (2013). Polysaccharides utilization in human gut bacterium bacteroides thetaiotaomicron: Comparative genomics reconstruction of metabolic and regulatory networks. *BMC Genomics*, 14, 873.
- Segura Munoz, R. R., Mantz, S., Martínez, I., Li, F., Schmaltz, R. J., Pudlo, N. A., Urs, K., Martens, E. C., Walter, J., & Ramer-Tait, A. E. (2022). Experimental evaluation of ecological principles to understand and modulate the outcome of bacterial strain competition in gut microbiomes. *The ISME journal*, 16, 1594–1604.
- Stoddard, S. F., Smith, B. J., Hein, R., Roller, B. R. K., & Schmidt, T. M. (2015). rrnDB: Improved tools for interpreting rRNA gene abundance in bacteria and archaea and a new foundation for future development. *Nucleic Acids Research*, 43, D593–D598.
- Wang, B., Yao, M., Lv, L., Ling, Z., & Li, L. (2017). The human microbiota in health and disease. *Engineering*, 3, 71–82.
- Wrzosek, L., Miquel, S., Noordine, M.-L., Bouet, S., Chevalier-Curt, M. J., Robert, V., et al. (2015). Bacteroides thetaiotaomicron and faecalibacterium prausnitzii shape the mucus production and mucin O-glycosylation in colon epithelium. *Gastroenterology*, 144, S–59.
- Wrzosek, L., Miquel, S., Noordine, M. L., Bouet, S., Chevalier-Curt, M. J., Robert, V., Philippe, C., Bridonneau, C., Cherbuy, C., Robbe-Masselot, C., Langella, P., & Thomas, M. (2013). Bacteroides thetaiotaomicron and faecalibacterium prausnitzii influence the production of mucus glycans and the development of goblet cells in the colonic epithelium of a gnotobiotic model rodent. *BMC Biology*, 11, 61.
- Zegeye, E. K., Brislawn, C. J., Farris, Y., Fansler, S. J., Hofmockel, K. S., Jansson, J. K., Wright, A. T., Graham, E. B., Naylor, D., McClure, R. S., & Bernstein, H. C. (2019). Selection, succession, and stabilization of soil microbial consortia. *mSystems*, 4, e00055–19.
- Zhang, L., Liu, C., Jiang, Q., & Yin, Y. (2021). Butyrate in energy metabolism: There is still more to learn. *Trends in Endocrinology & Metabolism*, 32, 159–169.
- Zhu, L.-B., Zhang, Y.-C., Huang, H.-H., & Lin, J. (2021). Prospects for clinical applications of butyrate-producing bacteria. *World Journal of Clinical Pediatrics*, 10, 84–92.

SUPPORTING INFORMATION

Additional supporting information can be found online in the Supporting Information section at the end of this article.

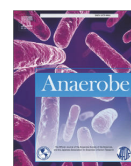
How to cite this article: Kattel, A., Aro, V., Lahtvee, P.-J., Kazantseva, J., Jöers, A., Nahku, R., & Belouah, I. (2024). Exploring the resilience and stability of a defined human gut microbiota consortium: An isothermal microcalorimetric study. *MicrobiologyOpen*, 13, e1430. <https://doi.org/10.1002/mbo3.1430>

Appendix 3

Publication II

Kattel, A., Morell, I., Aro, V., Lahtvee, P. J., Vilu, R., Jöers, A., & Nahku, R. (2023). Detailed analysis of metabolism reveals growth-rate-promoting interactions between *Anaerostipes caccae* and *Bacteroides* spp. *Anaerobe*, 79.

<https://doi.org/10.1016/j.anaerobe.2022.102680>



Detailed analysis of metabolism reveals growth-rate-promoting interactions between *Anaerostipes caccae* and *Bacteroides* spp.

Anna Kattel^{a, b}, Indrek Morell^c, Valter Aro^{a, c}, Petri-Jaan Lahtvee^{a, c}, Raivo Vilu^{a, b},
Arvi Jõers^c, Ranno Nahku^{b, *}

^a Tallinn University of Technology, Department of Chemistry and Biotechnology, Akadeemia tee 15, 12618, Tallinn, Estonia

^b Center of Food and Fermentation Technologies, Mäealuse 2/4, 12618, Tallinn, Estonia

^c University of Tartu, Institute of Technology, Nooruse 1, 50411, Tartu, Estonia

ARTICLE INFO

Article history:

Received 21 September 2022

Received in revised form

30 November 2022

Accepted 1 December 2022

Available online xxx

Keywords:

Gut bacteria

Next-generation probiotics

Live therapeutics manufacturing

Isothermal microcalorimetry

Serial batch

Flux balance analysis

ABSTRACT

Introduction: Human gut microbiota species which are next-generation probiotics (NGPs) candidates are of high interest as they have shown the potential to treat intestinal inflammation and other diseases. Unfortunately, these species are often not robust enough for large-scale cultivation, especially in maintaining diversity in co-culture production.

Objectives: In this study, we describe interactions between human gut microbiota species in the cultivation process with unique substrates. We also demonstrated that it is possible to change the species ratio in co-culture by changing the ratio of carbon sources.

Methods: We screened 25 different bacterial species based on their metabolic capabilities. After evaluating unique substrate possibilities, we chose *Anaerostipes caccae* (*A. caccae*), *Bacteroides thetaiotaomicron* (*B. thetaiotaomicron*), and *Bacteroides vulgatus* (*B. vulgatus*) as subjects for further study. D-sorbitol, D-xylose, and D-galacturonic acid were selected as substrates for *A. caccae*, *B. thetaiotaomicron*, and *B. vulgatus* respectively. All three species were cultivated as both monocultures and in co-cultures in serial batch fermentations in an isothermal microcalorimeter.

Results: Positive interactions were detected between the species in both co-cultures (*A. caccae* + *B. thetaiotaomicron*; *A. caccae* + *B. vulgatus*) resulting in higher heat production compared to the sum of the monocultures. The same positive cross-feeding interactions took place in larger-scale cultivation experiments. We confirmed acetate and lactate cross-feeding between *A. caccae* and *B. thetaiotaomicron* with flux balance analysis (FBA).

Conclusion: Changing the ratio of the selected carbon sources in the medium changed the species ratio accordingly. Such robustness is the basis for developing more efficient industrial co-culture processes including the production of NGPs.

© 2022 Elsevier Ltd. All rights reserved.

1. Introduction

Several probiotic products containing *Bifidobacteria*, *Lactobacilli*, and other lactic acid bacteria have been on the market for decades [1]. Developments in sequencing and culturing methodologies for human microbiota have sparked interest in new species with

potential health benefits [2,3]. The development of next-generation probiotics, which target diseases and have specific health benefits, is becoming ever closer to reality. Commensals who are part of the gut microbiota and have the potential to address different health problems are commonly introduced as NGPs [4]. Compared to traditional probiotics, NGP candidate species that belong to diverse genera do not have a history of safe use [4].

There is an increasing interest in the production of NGPs, and by 2026 the market is expected to reach over 91 billion US dollars (<https://www.marketsandmarkets.com/PressReleases/probiotics.asp>). Obesity, Crohn's disease, and inflammatory bowel disease are among those that could be tackled with NGPs [5–7]. For example, *Akkermansia muciniphila* was administered orally for three months

Abbreviations: NGP, Next-generation probiotics; *A. caccae*, *Anaerostipes caccae*; *B. thetaiotaomicron*, *Bacteroides thetaiotaomicron*; *B. vulgatus*, *Bacteroides vulgatus*; IMC, Isothermal microcalorimetry; FBA, Flux balance analysis; CDM, Chemically defined medium.

* Corresponding author.

E-mail address: ranno@tftak.eu (R. Nahku).

<https://doi.org/10.1016/j.anaerobe.2022.102680>

1075-9964/© 2022 Elsevier Ltd. All rights reserved.

to overweight/obese insulin-resistant participants, and results showed that it was safe and tolerated well [8]. Pasteurized *Akkermansia muciniphila* was shown to improve insulin sensitivity and reduce insulinemia, in addition to slightly decreasing body weight, fat mass, and hip circumference [8]. Also, there has been success with fecal microbiota transplants, but several risks are associated with this, including the introduction of unrecognized pathogens to the patient [9]. Furthermore, fecal material is collected from various donors, which affects the reproducibility and effectiveness of fecal microbiota transplants. As a solution, defined synthetic microbial consortia could be developed and produced. Kurt et al. [10] successfully designed a consortium of nine anaerobic intestinal bacteria with a continuous cultivation approach for production. In addition, they showed that while individually some of the strains are not cultivable or grew poorly as a monoculture, they thrive in co-culture. This co-cultivation phenomenon has also been reported before [11]. Traditionally, microorganisms are grown in monocultures because it allows the use of optimized conditions for one specific strain. Unfortunately, this might not be the optimal approach for producing NGPs, for which many strains go into single product. Additionally, it has been shown in a mouse model that mixed monocultures do not have the same therapeutic effect for treating acute dextran sulfate sodium colitis that a co-cultivated consortium of the same species does [10].

In terms of clinical trials, there are already some that test the safety and efficacy of co-cultures as biotherapeutic products. For example, a consortium of purified Firmicute bacteria in spore form effectively reduces the risk of recurrence of *Clostridioides difficile* infection and has a positive response from phase three studies (ClinicalTrials.gov identifier: NCT02437487) [12]. Furthermore, live biotherapeutic product containing 11 commensal bacterial strains is used in combination with nivolumab and is under phase 1 clinical trial for treatment of advanced or metastatic cancer (ClinicalTrials.gov identifier: NCT04208958) [13].

In terms of cultivating anaerobes, isothermal microcalorimetry (IMC) is a unique method that offers various benefits compared to optical density measurements. IMC is a highly sensitive method that measures the heat produced by metabolically active microorganisms in hermetically sealed ampoules. The emitted heat rate correlates with biomass production rate, and the heat production curve is dependent on the metabolic activity [14]. Regarding the benefits, heat production is not adversely affected by the opacity of the growth environment and clumping of cells [15]. In addition, IMC can detect cell concentrations around 2.5×10^4 – 1.0×10^5 bacteria mL⁻¹, which are not detectable with a spectrophotometer [16]. Another advantage is that the heat measurement is external and does not affect the samples inside the ampoules [16]. This means that after IMC measurements, the samples can be used for other analyses, for example, quantification of organic acids and sugars.

Human gut microbiota species are quite diverse with respect to their metabolism and can be roughly divided into several subgroups, such as butyrate producers, mucin degraders, lactic acid producers, succinate and propionate producers, acetate, and ethanol producers, and asaccharolytic bacteria. Butyrate producers mostly ferment sugars (both poly- and monosaccharides) into butyrate, lactate, and formate, while also forming hydrogen gas and carbon dioxide in significant quantities. It has also been shown that *Eubacterium hallii* and *A. caccae* can produce butyrate while growing asaccharolytically on acetate and lactate [17]. This ability enables such butyrate-producing bacteria to establish cross-feeding interactions with common acetate and lactate producers like *Bacteroides*, *Blautia*, *Dorea*, etc. Additionally, the *Bacteroides* genus is also known for its wide range of polysaccharide utilization [18,19]. As a result, they produce acetate, propionate, succinate, formate,

and carbon dioxide [20], which all, except for propionate, can be utilized via different cross-feeding mechanisms to produce propionate or butyrate as the end product of anaerobic fermentation. In addition, some acetate producers, such as *Blautia*, can perform *de novo* acetogenesis [21] from formate and carbon dioxide, which enables the conversion of these low-value metabolic end products to acetate and, ultimately, to butyrate.

In the current study, we set out to develop a co-culturing approach that would allow us to control the abundances of single species and analyze their metabolism. We hypothesized that unique carbon sources that are exclusively utilized by single species contribute to consortium stability. Such substrate level control potentially eliminates species domination in the co-culture. In addition, we quantitatively described cross-feeding between species using FBA. This limited us to use chemically defined media because rich and complex media introduce too many unknown substrates that complicate data interpretation. We started with 25 species that represent a model consortium of the human gut microbiome. The species were selected based on literature to achieve diversity and similarity to the average Estonian gut microbiome, but we also considered the availability of the strains' genomes and their safety levels (up to biosafety level two) [22]. To mimic a production process in which several seed batches are needed to produce inoculum for higher volumes, we used serial batch cultivation. The serial batch method allows us to evaluate the stability of the growth, as well as to detect growth rate changes [23]. Here we present a novel pipeline to determine combinations of species for co-producing human gut microbiota species using unique substrates and quantitatively describe cross-feeding between *A. caccae* and *B. thetaiotaomicron*. Finally, we demonstrate that it is possible to change the species ratio by changing the amount of unique carbon source.

2. Materials and methods

2.1. Strains

Akkermansia muciniphila (DSM 22959), *Alistipes shahii* (DSM 19121), *Anaerostipes caccae* (DSM 14662), *Anaerotruncus colihominis* (DSM 17241), *Bacteroides thetaiotaomicron* (DSM 2079), *Bacteroides caccae* (DSM 19024), *Bacteroides ovatus* (DSM 1896), *Bacteroides uniformis* (DSM 6597), *Bacteroides vulgatus* (DSM 3289), *Bifidobacterium adolescentis* (DSM 20087), *Bifidobacterium longum* subsp. *infantis* (DSM 20088), *Blautia faecis* (DSM 27629), *Blautia hydrogenotrophica* (DSM 10507), *Butyrivibrio faecihominis* (DSM 105721), *Christensenella minuta* (DSM 22607), *Catenibacterium mitsuokai* (DSM 15897), *Collinsella aerofaciens* (DSM 13712), *Dorea formicigenerans* (DSM 3992), *Dorea longicatena* (DSM 13814), *Eisenbergiella tayi* (DSM 26961), *Eubacterium rectale* (DSM 17629), *Faecalibacterium prausnitzii* (DSM 17677), *Odoribacter splanchnicus* (DSM 20712), *Prevotella copri* (DSM 18205), and *Roseburia faecis* (DSM 16840) were purchased from DSMZ (German Collection of Microorganisms and Cell Cultures GmbH). Lyophilized cultures were grown in various rich media. Media details for each strain can be found in Table S1. Stock cultures were washed with PBS solution containing 1% L-Cysteine hydrochloride and stored in PBS solution containing 20% glycerol and 1% L-Cysteine hydrochloride at –80 °C.

2.2. Media

Defined media were used for all experiments. Amino acid compositions and concentrations were set according to Adamberg et al. [24] and raised 2.5-fold so that the sugar:amino acid (excluding L-Cysteine) ratio would be 1:1. L-Cysteine hydrochloride (1 g/L) was added as a sulfur source and reducing agent. Mineral

composition and concentrations were based on Adamberg et al. [24]. Vitamin composition and concentrations were set according to M3 medium (excluding myo-inositol and L-glutathione reduced [25]). The final media compositions can be found in Table S2. The media were filter-sterilized (0.22 µm) and kept overnight in an anaerobic chamber (COY box, Coy Laboratory Products Inc., Grass Lake, MI, USA) with an atmosphere of $2.5 \pm 0.5\%$ H₂, 10% CO₂, and balanced N₂. Before the experiment, the pH of the medium in the anaerobic chamber was adjusted to 7.0 ± 0.1 using 3M NaOH.

2.3. Screening of the strains in the chemically defined medium

Preparations regarding the culture for all experiments were made in an anaerobic chamber. Stock cultures of the 25 strains were centrifuged at 14,000 g for 3 min and then resuspended in PBS solution containing 1% L-Cysteine hydrochloride. 198 µL of media was pipetted into the wells of a microtiter plate followed by 2 µL of culture. All strains were grown as monocultures. The plate was sealed with a transparent adhesive seal (Opti-seal™ Optical Disposable Adhesive, BIOplastics, Netherlands) and transferred out of the anaerobic chamber into the BioTek Synergy H1 Multi-Mode Reader (Agilent Technologies Inc., Santa Clara, CA, USA). The temperature was set to 37 °C. Every 15 min plate was shaken orbitally at slow speed for 15 s and then an OD (600 nm) measurement was taken. The experiment was run for 48 h, or for a shorter time if the stationary phase was reached before.

The end of the lag phase was defined as a time point at which the measured OD was higher than the maximal value of the blank media samples. The average specific growth rate was calculated between two time points: end-of-lag-phase OD value and maximal OD value.

2.4. Genome analysis

After screening the strains in the defined medium, genome data was obtained for the eight best performing species based on short lag-phase and maximum OD. Genomes of *A. caccae* (DSM 14662), *B. thetaiotaomicron* (DSM 2079), *Bacteroides caccae* (DSM 19024), *Bacteroides ovatus* (DSM 1896), *Bacteroides uniformis* (DSM 6597), *B. vulgatus* (DSM 3289), *Bifidobacterium adolescentis* (DSM 20087), and *Bifidobacterium longum* subsp. *infantis* (DSM 20088) were downloaded from the public NCBI database and uploaded into the PATRIC workspace, where annotated genomes were obtained [26]. The existence of different carbohydrate degradation pathways (Table S3) were analyzed based on the information available in the public databases KEGG [27] and MetaCyc [28] to elucidate the potential degradative capabilities of the eight chosen bacterial species (Table S4).

2.5. Validation of unique substrates

Stock cultures (*A. caccae*, *B. thetaiotaomicron*, *B. vulgatus*, *Bacteroides ovatus*, *Bacteroides caccae*, *Bacteroides uniformis*) were centrifuged at 14,000 g for 3 min and then resuspended in PBS solution containing 1% L-Cysteine hydrochloride for a final OD (600 nm) value of 1.35. For each sample, 1.98 mL of medium was pipetted into the vial followed by 20 µL (1% (v/v)) of inoculum. Vials were sealed hermetically and positioned in an isothermal microcalorimeter (TAM III and TAM IV-48, TA Instruments, New Castle, DE, USA) where the temperature was set to 37 °C. TAM systems need an hour to stabilize before data can be collected. In a batch setup, the experiment was run for 90 h, or for a shorter time if the stationary phase was reached before.

2.6. Small-scale co-culture production

Stock cultures (*A. caccae*, *B. thetaiotaomicron*, and *B. vulgatus*) were centrifuged at 14,000 g for 3 min and then resuspended in PBS solution containing 1% L-Cysteine hydrochloride. The number of viable cells in the stock cultures was adjusted to an equal level (1.2×10^9 cfu/mL). The inoculum for co-culture was mixed of two monocultures in equal volumes, and the inoculum for monocultures was diluted to match the viable cell number in the co-culture inoculum. For each sample, 1.98 mL of medium was pipetted into the vial followed by 20 µL (1% (v/v)) of inoculum. Vials were sealed hermetically and positioned in an isothermal microcalorimeter (TAM III and TAM IV-48, TA Instruments) as described above. In a serial batch setup, each batch lasted 23 h and at the end of the batch, 20 µL (1% (v/v)) of the culture was transferred into a new vial with 1.98 mL of fresh medium. The experiment was finished after three consecutive batches. After each batch, the remaining sample (after inoculation of the next batch) was transferred from the IMC ampoule to the Eppendorf tube and centrifuged at 14,000 g for 5 min at 4 °C. The supernatant was transferred into a clean tube and stored at −20 °C alongside the pellet until further analysis.

2.7. Determination of cell ratios

2.7.1. Quantitative real-time PCR (qPCR)

Fresh *A. caccae*, *B. thetaiotaomicron*, and *B. vulgatus* cultures (grown as monocultures until stationary phase in chemically defined medium (CDM) containing glucose, OD adjusted to 0.6) were mixed in different volumes: 300 µL *A. caccae*, 300 µL *B. thetaiotaomicron*, 300 µL *B. vulgatus*; 800 µL *A. caccae*, 100 µL *B. thetaiotaomicron*, 100 µL *B. vulgatus*; 100 µL *A. caccae*, 800 µL *B. thetaiotaomicron*, 100 µL *B. vulgatus*; 100 µL *A. caccae*, 100 µL *B. thetaiotaomicron*, 800 µL *B. vulgatus*. Mixtures were centrifuged at 14,000 g for 5 min at 4 °C and pellets were stored at −20 °C until analysis. Fermentation samples from small-scale co-culture and scale-up experiments were centrifuged at 14,000 g for 5 min at 4 °C. Pellets were stored at −20 °C until analysis. DNA was extracted using a GenElute™ Bacterial Genomic DNA Kit (Merck, Germany) and diluted to 7–10 ng/µL to fit the standard curve. Primers targeting the Peptidase S41 family gene of *B. thetaiotaomicron* (FW TGGCGCAATATCTGCCTGAA; RV AGCTTACCGTCCGTGTCTGT; 175 bp product), sorbitol operon transcription regulator gene of *A. caccae* (FW CCATTGTATGCGGCTCAGGA; RV CAATAATCGGTGCGGCCCT; 186 bp product) and 16 S rRNA gene of *B. vulgatus* (FW AACATC-CATCTACGCTCCCT; RV GGTATGGATACCCGTTTGCA; 130 bp product) were used for quantification. Standard curves were prepared from the DNA of each bacterium with five concentrations between 0.002 and 36 ng/µL. PCRs were performed in triplicate with 5x HOT FirePol EvaGreen qPCR Mix Plus (Solis BioDyne, Estonia) in a total volume of 20 µL with primers at 10 µM in white 96-well plates (BIOplastics) closed with Opti-seal™ Optical Disposable Adhesive (BIOplastics). Amplification was performed with qTOWER³ (Analytik Jena GmbH, Germany) with the following protocol: one cycle of 95 °C for 15 min; 40 cycles of 95 °C for 15 s, 60 °C for 20 s, 72 °C for 20 s; one cycle of 95 °C for 5 s, 60 °C for 1 min, melting curve from 60 °C to 97 °C.

2.7.2. Microscopy and image analysis

The bacterial samples were diluted to OD 1 and vortexed to separate the cells from each other. Microscope slides were prepared by Gram staining according to the manufacturer's instructions (Biogram 4 Kit; Biognost Ltd., Croatia). The slides were mounted on a Nikon Eclipse E200-LED (Japan) microscope equipped with a 100-fold oil immersion objective and brightfield images were taken

with a Nikon D5200 camera (Japan). The images were then analyzed using Fiji software [29]. The bacteria were segmented with a color threshold and the apparent area of each detected cell was recorded. *B. thetaiotaomicron* was counted as cells smaller than $0.85 \mu\text{m}^2$, while *A. caccae* was in the range of $0.85\text{--}2 \mu\text{m}^2$. Some *A. caccae* cells tended to form small clusters; thus, areas larger than $2 \mu\text{m}^2$ were divided by the average area of an *A. caccae* cell ($1.6 \mu\text{m}^2$), approximating the additional *A. caccae* counts in the clusters. The total number of counted cells for each sample was in the range 1200–8900. Standard error was calculated based on three replicates.

2.8. Co-culture process development in the bioreactors

The system for batch cultivation consisted of a 1.25 L Biobundle bioreactor (Applikon Biotechnology B.V., Schiedam, Netherlands) controlled by an ezControl or my-Control biocoordinator (Applikon Biotechnology B.V.) and a cultivation control program “BioXpert V2 version 2.96.128b05” (Applikon Biotechnology B.V.). The system was equipped with *in situ* pH (Applikon Biotechnology B.V.), redox (Applikon Biotechnology B.V.), temperature (Applikon Biotechnology B.V.), and turbidity (optek-Danulat GmbH, Germany) sensors, and online CO_2 and H_2 (BlueSens gas sensor GmbH, Germany) sensors.

To achieve 95% N_2 and 5% CO_2 in the bioreactor, the system was flushed with pure N_2 (95 mL/min) and pure CO_2 (10 mL/min). There was one exception to this; in the experiment in which substrate control was demonstrated, we wanted to achieve 99% N_2 and 1% CO_2 in the bioreactor for more accurate CO_2 production measurement (Fig. 3). Therefore, the system was flushed with pure N_2 (380 mL/min) and an 80%:20% N_2 : CO_2 gas mix (20 mL/min). The temperature was kept at 37°C and pH was maintained at 7.0 with the automatic addition of 3 M NaOH supplemented with 1 g/L of sodium ascorbate. The cultivation working volume was 600 mL and the stirrer was set to 200 rpm.

2.9. Quantification of extracellular metabolites

Fermentation samples were centrifuged at 14,000 g for 5 min at 4°C . The supernatant was transferred into a clean tube and filtered ($0.2 \mu\text{m}$). Medium samples were only filtered. Acetate, butyrate, ethanol, formate, D-galacturonic acid, isovalerate, lactate, propionate, D-sorbitol, succinate, valerate, and D-xylose concentrations were determined using high-performance liquid chromatography (Waters 2695 HPLC system; Waters Corporation, Milford, MA, USA). We used an HPX-87H column (Bio-Rad Laboratories, Richmond, CA, USA) and isocratic elution mode with 0.005 M H_2SO_4 solution at 0.6 mL/min (column temperature 35°C). The system was equipped with RI and UV detectors (Waters Corporation) and quantification was done against the external standard curves.

Sample preparation for quantification of free amino acids was the same as described above for organic acids. Free amino acids were quantified from the supernatant with LC-UV methodology (AccQ-Tag™ Ultra Derivatization Kit; Waters Corporation). AccQ-Fluor reagent (6-aminoquinolyl-N-hydroxysuccinimidyl carbamate) was used for derivatizing, and then samples were loaded on an AccQ-Tag Ultra column. The gradient of AccQ-Tag Ultra eluents A and B was used for the separation of amino acids. Amino acids were detected with a photodiode array detector, and data were processed with Empower 2 software [30].

2.10. Metabolic modeling

2.10.1. Construction of metabolic networks

Metabolic networks were constructed for *A. caccae* and

B. thetaiotaomicron. Sub-genome-size metabolic networks for gut bacteria *A. caccae* and *B. thetaiotaomicron* were constructed using information from the public databases MetaCyc and KEGG (reactions in pathways and their reversibility) and experimental evidence gathered during this work. Overall, individual metabolic networks consisted of 371 metabolites and 490 reactions for *A. caccae*, and 447 metabolites and 584 reactions for *B. thetaiotaomicron* (Table S5.1, Table S5.2).

A consortium type metabolic network was generated out of two metabolic networks representing single bacteria by assigning a common metabolite pool outside of the intracellular space and removing duplicate exchange fluxes. The relative amounts (weights) of different species in consortia manifest through modified stoichiometric coefficients of transport reactions of respective bacteria that exchange matter between intracellular space and the common metabolite pool. The final metabolic network consisted of 760 metabolites and 1025 reactions.

2.10.2. Biomass

Biomass synthesis in the model was described with separate consumption fluxes (sinks) for major biomass monomers. The biomass composition was simplified and contained only major biomass components – amino acids, (deoxy)ribonucleotides, peptidoglycan, and membrane lipids. The potential existence of glycogen, lipo- and exopolysaccharides, and other specific components in the biomass were ignored, since their significance in the overall carbon balance is small and, thus, the effect on calculations is not significant.

Protein and RNA content in biomass were set at 50% and 12%, respectively [31], and average ribonucleotide distribution was estimated to be identical to that of rRNA of *A. caccae* and *B. thetaiotaomicron*. The amino acid distribution was calculated from proteome data, which was obtained as described by Mumm et al. [32]. The number of deoxyribonucleotides was calculated assuming the presence of one chromosome per cell. Acquired values in mmol/gDW were used as model inputs. As determined by microscopy, the model cell shape for both species was set as a cylinder with spherical caps, with a height/radius ratio of 10 for *A. caccae* and 3 for *B. thetaiotaomicron* (Table S6.2). The amount of lipids and peptidoglycan needed to produce 1 g of biomass were calculated from cell size and shape (Table S6.3 and Table S6.4). Cell ratios of different species for model input were determined from the experimental D-sorbitol and D-xylose consumption for *A. caccae* and *B. thetaiotaomicron* respectively (Table S6.1). The measured OD was converted to biomass amount per liter with the following formula: $\text{gDW/L} = \text{OD}_{600} \times 0.3$ [33]. The OD values for the last data points were estimated using simplified carbon balance, since an OD decrease was monitored near the end of the experiment (Table S7). Exometabolome concentration values (mM) were calculated per gram of dry weight for model input (Table S8).

2.10.3. Flux balance analysis

The FBA [34] model was generated in Wolfram Mathematica format using in-house software built in MatLab. Calculations were performed using Wolfram Mathematica 8.01 on a laptop computer with a six-core Intel i7-8750H processor and 24 GB RAM.

FBA input data (exchange fluxes, specific growth rate, Table S8) were used to constrain the model, and calculations were performed with an increasing automatic error step of $\pm 1\%$ to input fluxes until a feasible solution was found to maximize ATP production as an objective function. Carbon mass balance analysis was performed to assess the physiological relevance of the measured metabolome with respect to the metabolic background of the given organisms (Table S9). Finally, flux variability analysis was run on selected exchange fluxes to computationally verify the potential existence of

different cross-feeding mechanisms between *A. caccae* and *B. thetaiotaomicron* in co-culture (Table S9) [35].

3. Results and discussion

The main objectives of this study were (1) to show that it is possible to find unique carbon sources to control co-culture species ratio, and (2) to quantitatively describe possible cross-feeding between species. The study was divided into four stages: 1) species screening in the CDM using glucose as the initial carbon source, 2) genome analysis for unique carbon source candidates, 3) confirmation of the unique substrates for selected species, and 4) study of metabolic cross-feeding and co-culture production process development. Chemically defined media do not always support the growth of NGP species without extensive development. For us, quantification of the consumption of carbon and nitrogen sources was important even though there might be a reduction in species diversity. We started with the screening of 25 species from the four different phyla (Firmicutes, Bacteroidetes, Actinobacteria, and Verrucomicrobia) and finished with the production process for two pairs (*A. caccae* + *B. thetaiotaomicron*; *A. caccae* + *B. vulgatus*).

3.1. Species screening in a chemically defined medium

The first step was to find out which species have adequate growth in the chosen CDM. Using a microtiter plate reader, we studied 25 species in the CDM with glucose as the main carbon source. Growth was detected for 12 species out of 25 (Table 1). Based on this experiment, we filtered out species which did not grow at all, or growth was extremely slow or delayed. As a result of this screening, we proceeded with eight species: *A. caccae*, *Bifidobacterium longum*, *Bifidobacterium adolescentis*, *B. thetaiotaomicron*, *B. vulgatus*, *Bacteroides ovatus*, *Bacteroides caccae*, and *Bacteroides uniformis*.

NGP species are known for their special requirements for growth media and conditions [25]. Usually, such species are cultivated in rich media that are suitable for describing growth dynamics. However, for studying metabolism in fine detail the quantification of all consumed substrates and metabolic by-products produced are important. Therefore, only species growing in the defined medium were included in this metabolic study.

3.2. Genome analysis and validation of in silico results

We analyzed the genomes of the eight fast-growing species to

determine their metabolizing capabilities of different substrates (Table S4). Monosugars, sugar alcohols, and sugar acids were preferred, since analytical methods are already established for these, and quantification is more accurate than it would be for polymers. Accurate quantification is crucial for metabolic modeling and metabolic cross-feeding quantitation. *Bifidobacterium longum* and *Bifidobacterium adolescentis* genomes did not contain unique substrate degradation pathways that are not present in the *A. caccae* and the *Bacteroides* species. Therefore, the *Bifidobacteria* were excluded from the subsequent screening experiments. Genome analysis of the remaining six species revealed 13 different substrate degradation pathways for the 12 selected carbohydrates. We replaced glucose with the alternative substrates in the equimolar concentration in the CDM and collected growth profiles (Table 2). Overall, there were only few unique substrates among these six species and this limited us to two-species co-cultures.

3.3. Co-culture experiments using an IMC

Based on the growth data (Table 2), there were several options for unique substrate-based co-culture pairs. We tested the combination of *A. caccae* (D-sorbitol; μ 0.17 h⁻¹) with *B. thetaiotaomicron* (D-xylose; μ 0.56 h⁻¹) or with *B. vulgatus* (D-galacturonic acid; μ 0.21 h⁻¹). This way we had species with two different metabolism types: butyrate producer *A. caccae* paired with a succinate/propionate producer – *B. thetaiotaomicron* or *B. vulgatus*. *B. thetaiotaomicron* was chosen as the most extensively studied member of the *Bacteroides* genus, whereas *B. vulgatus* is one of the most commonly reported species from human feces [18,36].

We started our experiments by making sure that in monocultures the main carbon source consumption remained the same in multi-substrate conditions. Growth medium containing a unique carbon source and a carbon source that the species does not degrade was prepared and used in serial batch format. Growth kinetics of monocultures were consistent throughout three consecutive batches. The total heat produced by *B. thetaiotaomicron* in D-xylose medium supplemented with D-sorbitol was 0.68 ± 0.02 J/mL (Fig. 1). For *B. vulgatus*, the total heat produced was 0.44 ± 0.04 J/mL in the D-galacturonic acid medium supplemented with D-sorbitol. Total heat produced by *A. caccae* did not differ ($p = 0.48$) regardless of whether the D-sorbitol medium was supplemented with D-xylose (0.35 ± 0.02 J/mL) or D-galacturonic acid (0.33 ± 0.02 J/mL). Substrate analysis at the end of the experiments confirmed that the main carbon source was depleted: D-sorbitol by *A. caccae*, D-xylose by *B. thetaiotaomicron*, and D-galacturonic acid

Table 1
Summary of average measured and calculated growth parameters in a defined medium with glucose. No growth was detected for the following species and so they are not included in the table: *Christensenella minuta*, *Alistipes shahii*, *Anaerotruncus colihominis*, *Blautia faecis*, *Blautia hydrogenotrophica*, *Butyrivibrio faecihominis*, *Prevotella copri*, *Eubacterium rectale*, *Akkermansia muciniphila*, *Faecalibacterium prausnitzii*, *Roseburia faecis*, *Eisenbergiella tayi*, *Odoribacter splanchnicus*. Errors are the standard error of biological quadruplicates.

Organism	Maximum OD at 600 nm	Lag phase, h	Specific growth rate, h ⁻¹
<i>Anaerostipes caccae</i>	0.59 ± 0.03	10.4 ± 0.1	0.59 ± 0.01
<i>Bacteroides vulgatus</i>	0.61 ± 0.01	3.6 ± 0.3	0.27 ± 0.01
<i>Bacteroides caccae</i>	0.82 ± 0.00	2.0 ± 0.1	0.37 ± 0.01
<i>Bacteroides ovatus</i>	0.66 ± 0.01	2.6 ± 0.2	0.34 ± 0.01
<i>Bacteroides thetaiotaomicron</i>	0.70 ± 0.00	2.9 ± 0.1	0.45 ± 0.00
<i>Bacteroides uniformis</i>	0.71 ± 0.01	2.4 ± 0.1	0.34 ± 0.01
<i>Bifidobacterium longum</i> subsp. <i>infantis</i>	0.35 ± 0.01	6.3 ± 0.1	0.31 ± 0.01
<i>Bifidobacterium adolescentis</i>	0.41 ± 0.01	5.3 ± 0.0	0.24 ± 0.01
<i>Collinsella aerofaciens</i> ^a	0.32 ± 0.02	5.7 ± 0.2	0.09 ± 0.00
<i>Dorea formicigenerans</i> ^a	0.11 ± 0.00	21.2 ± 0.6	0.05 ± 0.00
<i>Dorea longicatena</i> ^b	1.40 ± 0.08	15.7 ± 0.5	0.39 ± 0.02
<i>Catenibacterium mitsuokai</i> ^c	NA [*]		

^{*} – Growth parameters are not available for *Catenibacterium mitsuokai* due to the formation of clumps during growth which affected the OD measurements. ^a – excluded from later experiments due to low growth rate. ^b – excluded from later experiments due to long lag-phase. ^c – excluded from later experiments due to lack of growth parameters.

Table 2

Validation of *in silico* genome analysis results. Summary of average growth rates (μ , h^{-1}) on different substrates for six species. The growth rate is calculated based on heat production. Errors are the standard error of biological duplicates. ND – growth not detected.

Substrate	<i>Bacteroides thetaiotaomicron</i>	<i>Bacteroides caccae</i>	<i>Bacteroides ovatus</i>	<i>Bacteroides uniformis</i>	<i>Bacteroides vulgatus</i>	<i>Anaerostipes caccae</i>
D-Fructose	0.48 \pm 0.03	0.51 \pm 0.03	0.33 \pm 0.06	0.55 \pm 0.08	0.57 \pm 0.01	0.35 \pm 0.01
D-Galactose	0.66 \pm 0.00	0.56 \pm 0.02	0.43 \pm 0.05	0.55 \pm 0.00	0.32 \pm 0.01	0.50 \pm 0.00
D-Xylose	0.56 \pm 0.05	0.61 \pm 0.00	0.44 \pm 0.02	0.54 \pm 0.01	0.42 \pm 0.01	ND
L-Arabinose	0.58 \pm 0.01	0.53 \pm 0.00	0.50 \pm 0.00	0.51 \pm 0.02	0.56 \pm 0.02	ND
D-Galacturonic acid	0.27 \pm 0.01	0.31 \pm 0.02	0.19 \pm 0.02	0.22 \pm 0.02	0.21 \pm 0.02	ND
L-Rhamnose	0.15 \pm 0.01	0.14 \pm 0.00	0.15 \pm 0.00	ND	0.30 \pm 0.01	ND
L-Fucose	0.22 \pm 0.01	0.29 \pm 0.01	0.12 \pm 0.00	ND	ND	ND
D-Mannitol	ND	ND	0.34 \pm 0.01	ND	ND	0.08 \pm 0.00
D-Sorbitol	ND	ND	ND	ND	ND	0.17 \pm 0.00
Dulcitol	ND	ND	ND	ND	ND	0.05 \pm 0.00
Xylitol	ND	ND	ND	ND	ND	ND
D-Lyxose	ND	ND	ND	ND	ND	ND

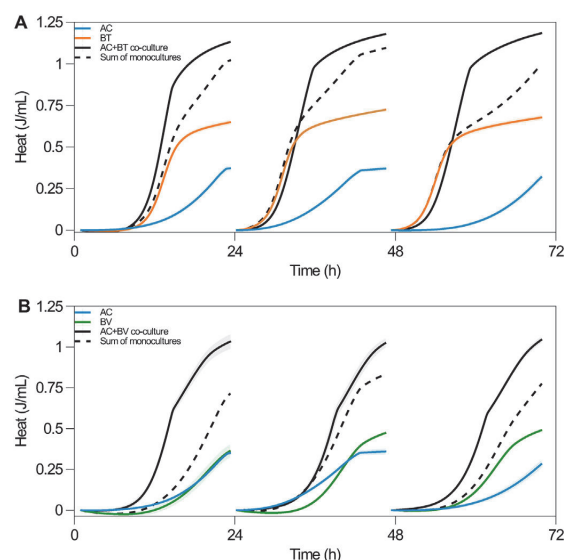


Fig. 1. Growth kinetics of mono- and co-cultures measured by IMC. (A) Growth kinetics of *A. caccae* (AC) and *B. thetaiotaomicron* (BT) monocultures and AC + BT co-culture in the D-sorbitol and D-xylose medium. (B) AC and *B. vulgatus* (BV) monocultures and AC + BV co-culture in the D-sorbitol and D-galacturonic acid medium. For each batch, the average and standard deviation of the heat ($n = 3$ replicates) are represented by a full line and ribbon, respectively. The dashed line represents the mathematical sum of heat of two monocultures.

by *B. vulgatus*.

The next step was to study the same media in co-cultures (*A. caccae* + *B. thetaiotaomicron* and *A. caccae* + *B. vulgatus*) in which both strains had their unique carbon source present. It was expected that when there is no interaction between the species, the total heat produced by co-culture is similar to the sum of the two corresponding monocultures. In both co-culture experiments, the measured total heat was higher (ranging from 1.1-fold to 1.5-fold) throughout all three consecutive batches than the sum of monocultures (Fig. 1). This indicates positive interactions between the species.

3.4. Metabolic interactions in co-culture

As can be seen in Fig. 1, the total heat produced by co-cultures was higher than that produced by two individual monocultures

growing in the same medium. This indicates a possible metabolic interaction. To investigate it further, we compared the final organic acid concentration of co-cultures with the sum of this for monocultures (Table 3). There were major differences observed in acetate, butyrate, and lactate concentrations. When we compared day 3 results from the serial batch experiment, acetate concentrations in the co-culture were 2-fold lower and lactate concentrations 50-fold lower than the sum of the *A. caccae* and *B. thetaiotaomicron* monoculture results. On the other hand, butyrate and propionate concentrations were 3.1-fold and 1.3-fold higher, respectively, in co-culture. It is important to note that acetate and propionate were only produced by *B. thetaiotaomicron*, and lactate and butyrate only produced by *A. caccae*. This indicates the possibility of mutually positive interactions between the species through metabolic by-products. Altogether, the preference of *B. thetaiotaomicron* towards acetate production [20,37,38] and the ability of *A. caccae* to convert this organic acid into butyrate [39–41] indicate that these species benefit from each other.

Similar changes in metabolite concentrations were also detected in the *A. caccae* + *B. vulgatus* co-cultures (Table 4). Again, comparing the day 3 results, acetate concentrations in the co-culture were 1.4-fold lower and lactate concentrations 6-fold lower than the sum of *A. caccae* and *B. vulgatus* monoculture results. At the same time, butyrate and propionate concentrations were respectively 2.9-fold and 2-fold higher in the co-culture.

In order to quantify the possible positive effects of acetate on *A. caccae* and lactate on *B. thetaiotaomicron*, supplementation experiments were performed in the IMC. Different concentrations of acetate and lactate were added, ranging from 0 mM to 20 mM. The growth rate of *A. caccae* on D-sorbitol without added acetate was $0.24 \pm 0.00 \text{ h}^{-1}$. Even 2 mM of acetate had a significant effect on the growth rate, increasing it up to $0.74 \pm 0.00 \text{ h}^{-1}$ ($p < 0.001$). Further increase of acetate (4 mM, 6 mM, 8 mM, 10 mM, 20 mM) had an additional, but smaller effect; maximal specific growth rate remained between 0.85 and 1.05 h^{-1} ($p < 0.001$).

All the D-sorbitol ($5.5 \pm 0.1 \text{ mM}$) was utilized regardless of acetate concentration (Table S10.1). However, when the concentration of acetate was 6 mM or higher, then around $4.2 \pm 0.2 \text{ mM}$ of acetate was consumed. In the case of lower acetate concentrations (2 mM and 4 mM), acetate was depleted. This gives acetate/D-sorbitol a consumed molar ratio of around 0.8:1. Converting acetate to butyrate consumes one NADH molecule per net reaction via a non-bifurcative pathway (KEGG; Kanehisa & Goto, 2000). Converting D-sorbitol to butyrate yields one NADH per D-sorbitol consumed, which gives a theoretical acetate/D-sorbitol molar ratio of 1:1. The deviation of the experimental acetate/D-sorbitol consumption ratio probably arises from free amino acid consumption and possible utilization of bifurcative butyrate synthesis

Table 3

Production of major metabolites in the co-culture (*A. caccae* + *B. thetaiotaomicron*) and monocultures (*A. caccae*, *B. thetaiotaomicron*). Average values (mM) \pm standard errors (n = 3) throughout three consecutive batches are presented. Statistical significance between co-culture and the sum of monocultures was calculated with a Student's *t*-test (**p* < 0.05, ***p* < 0.01, ****p* < 0.001). ND – not detected.

	acetate	butyrate	formate	lactate	propionate	succinate
Day 1 <i>A. caccae</i>	ND	1.48 \pm 0.04	0.55 \pm 0.03	5.44 \pm 0.11	ND	ND
Day 2 <i>A. caccae</i>	ND	1.47 \pm 0.01	0.82 \pm 0.02	5.48 \pm 0.01	ND	ND
Day 3 <i>A. caccae</i>	ND	1.32 \pm 0.02	0.73 \pm 0.03	4.68 \pm 0.06	ND	ND
Day 1 <i>B. thetaiotaomicron</i>	2.33 \pm 0.03	ND	0.47 \pm 0.05	ND	1.31 \pm 0.01	1.86 \pm 0.02
Day 2 <i>B. thetaiotaomicron</i>	2.62 \pm 0.01	ND	0.60 \pm 0.01	ND	1.54 \pm 0.01	2.04 \pm 0.00
Day 3 <i>B. thetaiotaomicron</i>	2.53 \pm 0.01	ND	0.60 \pm 0.01	ND	1.53 \pm 0.01	1.95 \pm 0.01
Day 1 <i>A. caccae</i> + <i>B. thetaiotaomicron</i> co-culture	1.25 \pm 0.01***	4.28 \pm 0.05***	0.36 \pm 0.00**	0.13 \pm 0.00***	1.86 \pm 0.00***	1.82 \pm 0.01
Day 2 <i>A. caccae</i> + <i>B. thetaiotaomicron</i> co-culture	1.18 \pm 0.08**	4.26 \pm 0.28**	0.37 \pm 0.02***	0.06 \pm 0.00***	1.88 \pm 0.12	1.65 \pm 0.11
Day 3 <i>A. caccae</i> + <i>B. thetaiotaomicron</i> co-culture	1.38 \pm 0.01***	4.49 \pm 0.01***	0.41 \pm 0.00***	0.10 \pm 0.00***	2.00 \pm 0.01***	1.73 \pm 0.00***
Day 1 Sum of <i>A. caccae</i> and <i>B. thetaiotaomicron</i>	2.33 \pm 0.03	1.48 \pm 0.04	1.02 \pm 0.06	5.44 \pm 0.11	1.31 \pm 0.01	1.86 \pm 0.02
Day 2 Sum of <i>A. caccae</i> and <i>B. thetaiotaomicron</i>	2.62 \pm 0.01	1.47 \pm 0.01	1.41 \pm 0.02	5.48 \pm 0.01	1.54 \pm 0.01	2.04 \pm 0.00
Day 3 Sum of <i>A. caccae</i> and <i>B. thetaiotaomicron</i>	2.53 \pm 0.01	1.32 \pm 0.02	1.33 \pm 0.04	4.68 \pm 0.06	1.53 \pm 0.01	1.95 \pm 0.01

Table 4

Production of major metabolites in the co-culture (*A. caccae* + *B. vulgatus*) and monocultures (*A. caccae*, *B. vulgatus*). Average values (mM) \pm standard errors (n = 3) throughout three consecutive batches are presented. Statistical significance between co-culture and the sum of monocultures is calculated with a Student's *t*-test (**p* < 0.05, ***p* < 0.01, ****p* < 0.001). ND – not detected.

	acetate	butyrate	formate	lactate	propionate	succinate
Day 1 <i>A. caccae</i>	ND	1.45 \pm 0.02	0.63 \pm 0.04	5.38 \pm 0.03	ND	ND
Day 2 <i>A. caccae</i>	ND	1.46 \pm 0.02	0.75 \pm 0.01	5.34 \pm 0.01	ND	ND
Day 3 <i>A. caccae</i>	ND	1.19 \pm 0.01	0.70 \pm 0.03	4.28 \pm 0.15	ND	ND
Day 1 <i>B. vulgatus</i>	3.60 \pm 0.02	ND	0.20 \pm 0.00	ND	0.34 \pm 0.00	0.73 \pm 0.01
Day 2 <i>B. vulgatus</i>	4.15 \pm 0.05	ND	0.24 \pm 0.01	ND	0.55 \pm 0.01	0.92 \pm 0.01
Day 3 <i>B. vulgatus</i>	4.29 \pm 0.01	ND	0.24 \pm 0.00	ND	0.57 \pm 0.00	0.99 \pm 0.00
Day 1 <i>A. caccae</i> + <i>B. vulgatus</i> co-culture	2.63 \pm 0.03***	4.17 \pm 0.05***	0.54 \pm 0.05*	0.51 \pm 0.04***	0.92 \pm 0.01***	1.04 \pm 0.01***
Day 2 <i>A. caccae</i> + <i>B. vulgatus</i> co-culture	3.01 \pm 0.01**	3.83 \pm 0.13**	0.57 \pm 0.03**	0.92 \pm 0.09***	1.01 \pm 0.02***	1.07 \pm 0.00**
Day 3 <i>A. caccae</i> + <i>B. vulgatus</i> co-culture	3.12 \pm 0.02***	3.73 \pm 0.03***	0.61 \pm 0.01**	1.03 \pm 0.06***	1.04 \pm 0.01***	1.11 \pm 0.01**
Day 1 Sum of <i>A. caccae</i> and <i>B. vulgatus</i>	3.60 \pm 0.02	1.45 \pm 0.02	0.83 \pm 0.04	5.38 \pm 0.03	0.34 \pm 0.00	0.73 \pm 0.01
Day 2 Sum of <i>A. caccae</i> and <i>B. vulgatus</i>	4.15 \pm 0.05	1.46 \pm 0.02	0.99 \pm 0.02	5.34 \pm 0.01	0.55 \pm 0.01	0.92 \pm 0.01
Day 3 Sum of <i>A. caccae</i> and <i>B. vulgatus</i>	4.29 \pm 0.01	1.19 \pm 0.01	0.94 \pm 0.03	4.28 \pm 0.15	0.57 \pm 0.00	0.99 \pm 0.00

mechanisms [42], which both lower NADH levels in the cell. Furthermore, the production of lactate is inversely proportional to the amount of acetate added into the medium. Lactate production drastically decreased when 6 mM or more of acetate was added, indicating that NADH deficiency could limit acetate uptake (Table S10.1).

The effect of lactate on the growth of *B. thetaiotaomicron* was determined. The added lactate concentrations were 2 mM, 4 mM, 6 mM, 8 mM, 10 mM, and 20 mM. The effect on growth rate was similar across different concentrations. The growth rate of *B. thetaiotaomicron* on D-xylose without lactate was $0.38 \pm 0.00 \text{ h}^{-1}$ and the addition of lactate increased this to $0.53\text{--}0.56 \text{ h}^{-1}$ (*p* < 0.01). The maximum consumption of lactate observed was $3.2 \pm 0.0 \text{ mM}$, while $4.7 \pm 0.0 \text{ mM}$ of D-xylose was consumed, giving a lactate/D-xylose consumption molar ratio of 0.7:1 (Table S10.2). The anaerobic oxidation of lactate to pyruvate is energetically unfavorable [43] and can only proceed via a bifurcative mechanism utilizing low redox potential reduced ferredoxin as a co-substrate. Conversion of lactate to pyruvate results in the formation of two NADH molecules. Since pyruvate ferredoxin oxidoreductase is the principal source of reduced ferredoxin in succino- and propionigenic bacteria [44], the limiting factor for lactate consumption is probably the availability of reduced ferredoxin needed to oxidize lactate to pyruvate. The accumulating NADH from the concentration-dependent intake of lactate is directed into the synthesis of succinate and propionate, whose molar ratio to consumed D-xylose rises steadily with an increasing concentration of lactate in the medium from 0.4:1 to 0.7:1. In

conclusion, it is highly likely that the cross-feeding in both organisms is limited by the NADH and/or reduced ferredoxin availability in the cell.

3.4.1. Determining the species ratio in co-cultures

An important parameter in co-culture growth is the ratio of species. DNA-based methods such as 16 S sequencing or qPCR are used to determine species ratios in consortia [45–47]. Since DNA extraction from different species is not straightforward, careful testing of the methods with the species of interest is necessary [48]. For testing the qPCR method, we mixed the three species (*A. caccae*, *B. thetaiotaomicron*, *B. vulgatus*) in different ratios based on OD (OD of all the cultures was 0.6 at 600 nm), extracted the DNA, and then performed the qPCR analysis. In a test sample in which *A. caccae*, *B. thetaiotaomicron*, and *B. vulgatus* were mixed in equal ODs, we were expecting to see roughly 33% of each species. Results showed an underestimation of *A. caccae* ($12\% \pm 1\%$) and overestimation of *B. thetaiotaomicron* ($47\% \pm 2\%$) and *B. vulgatus* ($41\% \pm 1\%$). Similarly, in an *A. caccae* (80%): *B. thetaiotaomicron* (10%): *B. vulgatus* (10%) mixture, qPCR showed $52\% \pm 2\%$ of *A. caccae*, $27\% \pm 1\%$ of *B. thetaiotaomicron*, $21\% \pm 1\%$ of *B. vulgatus* (Table S11.1). We tested another DNA extraction kit (ZymoBIOMICS™ DNA Miniprep Kit; Zymo research, Irvine, CA, USA) but the yield of *A. caccae* did not improve with this (data not shown). In the literature, *A. caccae* is described as gram-variable, while *B. thetaiotaomicron* and *B. vulgatus* are gram-negative, which might be the reason why DNA extraction is less efficient for *A. caccae* [49,50]. Because of this, the DNA ratios determined with qPCR are probably biased but can be

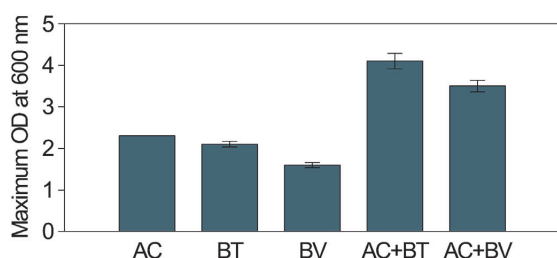


Fig. 2. Final OD values of monocultures of *A. caccae* (AC), *B. thetaiotaomicon* (BT), and *B. vulgatus* (BV) and two species co-cultures in bioreactor experiments. Error bars represent the standard error of the maximum OD ($n \geq 2$ replicates).

used to confirm that there is stability in the co-culture serial batch experiment. Indeed, the qPCR analysis showed that the strain ratios did not change during the serial batch experiment (Table S11.2).

To get additional information about cell ratios in the co-culture serial batch experiment, the microscopy image analysis method was developed. The latter was possible since *A. caccae* and

Bacteroides spp. have very different morphologies (Table S6.2). Microscopy image analysis showed that at the end of the experiment (day 3), the average *A. caccae*:*B. thetaiotaomicon* ratio was 49:51 ($\pm 3\%$), while the *A. caccae*:*B. vulgatus* ratio was 37:63 ($\pm 1\%$). This shows that both species are present in roughly equal cell concentrations.

3.5. Co-culture bioprocess development

To perform gas analysis and control the growth environment, a higher culture density bioreactor co-culture process was developed. For this, we used Applikon 1 L bioreactors. This allowed us to elevate sugar and free amino acid concentrations three to five times and reach higher biomass densities (Table S2). Final OD values of monocultures were similar for all species: 2.3 ± 0.0 for *A. caccae*, 2.1 ± 0.1 for *B. thetaiotaomicon*, and 1.6 ± 0.1 for *B. vulgatus* (Fig. 2). As expected, co-cultures had final OD values almost twice as high: 4.1 ± 0.2 for *A. caccae* + *B. thetaiotaomicon* and 3.5 ± 0.1 for *A. caccae* + *B. vulgatus* (Fig. 2). The growth rate of the *A. caccae* + *B. vulgatus* co-culture was slightly higher ($0.52 \pm 0.02 \text{ h}^{-1}$) than for the *A. caccae* + *B. thetaiotaomicon* co-culture ($0.48 \pm 0.05 \text{ h}^{-1}$). As observed previously, in the co-cultures we also see higher butyrate

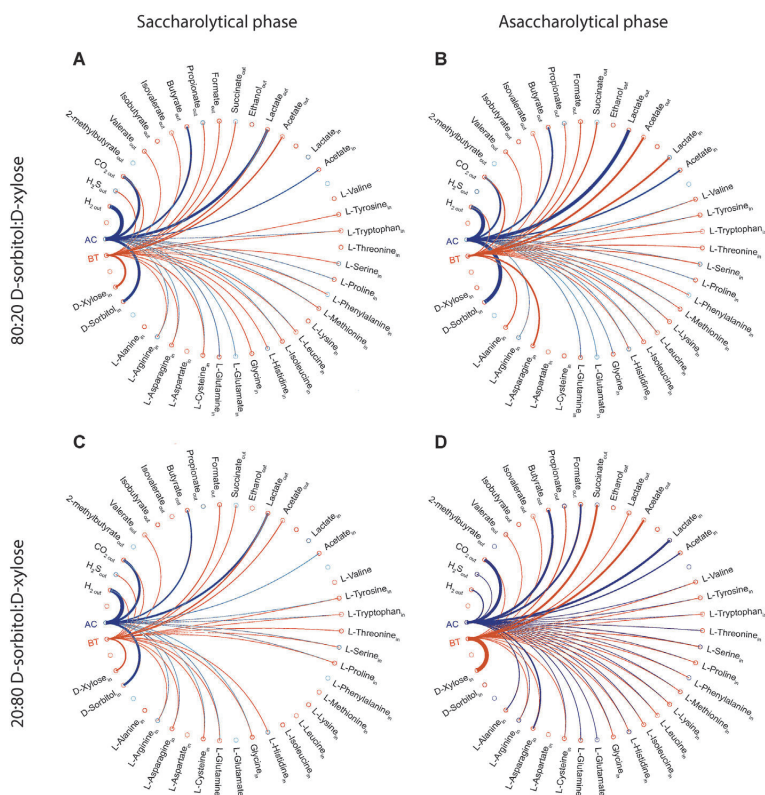


Fig. 3. Description of metabolic cross-feeding in *A. caccae* (AC) and *B. thetaiotaomicon* (BT) co-culture. Due to both species continuing growth after depletion of the main carbon source, growth was divided into saccharolytic and asaccharolytic phases. Since the initial concentration of the main carbon source was varied, different metabolic scenarios occurred. Metabolic fluxes in the 80:20 (D-sorbitol:D-xylose) experiment where both species are in the saccharolytic phase (A) and where BT is in the asaccharolytic phase (B) are depicted. In the asaccharolytic phase, BT is consuming lactate which is produced by AC while AC mainly utilizes D-sorbitol and acetate. Metabolic fluxes in the 20:80 (D-sorbitol:D-xylose) experiment where both species are in the saccharolytic phase (C) and where AC is in the asaccharolytic phase (D) are also depicted. In the asaccharolytic phase, AC is consuming acetate and lactate while BT mainly utilizes D-xylose. Orange lines represent AC's metabolic fluxes and blue lines BT's metabolic fluxes. The thickness of the line correlates with the flux value. Note that the compounds that are labeled as "in" are consumed and as "out" are produced. (For interpretation of the references to color in this figure legend, the reader is referred to the Web version of this article.)

Table 5

Production of major metabolites by monocultures of *A. caccae*, *B. thetaiotaomicron*, and *B. vulgatus*, and two-species co-cultures in bioreactor experiments. Average values (mM) \pm standard errors ($n \geq 2$) are presented. Statistical significance between co-culture and the sum of monocultures was calculated with a Student's *t*-test (* $p < 0.05$, ** $p < 0.01$, *** $p < 0.001$). ND – not detected.

	acetate	butyrate	formate	lactate	propionate	succinate
<i>A. caccae</i>	ND	4.31 \pm 0.03	0.45 \pm 0.01	13.40 \pm 0.29	ND	ND
<i>B. thetaiotaomicron</i>	9.24 \pm 0.10	ND	3.71 \pm 0.15	0.35 \pm 0.18	1.22 \pm 0.05	6.96 \pm 0.04
<i>B. vulgatus</i>	16.68 \pm 0.68	ND	2.74 \pm 0.04	0.05 \pm 0.05	0.62 \pm 0.01	2.78 \pm 0.22
<i>A. caccae</i> + <i>B. thetaiotaomicron</i> co-culture	3.11 \pm 0.34**	9.51 \pm 0.51**	2.52 \pm 0.11**	8.58 \pm 0.69**	1.85 \pm 0.21	5.48 \pm 0.62
<i>A. caccae</i> + <i>B. vulgatus</i> co-culture	6.11 \pm 1.02***	14.06 \pm 0.50***	4.82 \pm 1.17	3.80 \pm 0.59***	1.10 \pm 0.09***	2.03 \pm 0.23
Sum of <i>A. caccae</i> and <i>B. thetaiotaomicron</i>	9.24 \pm 0.10	4.31 \pm 0.03	4.17 \pm 0.15	13.76 \pm 0.34	1.22 \pm 0.05	6.96 \pm 0.04
Sum of <i>A. caccae</i> and <i>B. vulgatus</i>	16.68 \pm 0.68	4.31 \pm 0.03	3.20 \pm 0.04	13.45 \pm 0.30	0.62 \pm 0.01	2.78 \pm 0.22

and propionate concentrations, as well as lower acetate and lactate concentrations, compared to the monocultures (Table 5). Since we could not use qPCR for determining the species ratio, we took microscopy images from samples at the end of fermentation, and based on size, we could differentiate between *Bacteroides* spp. and *A. caccae*. In the *A. caccae* + *B. thetaiotaomicron* co-culture, we calculated the ratio as 43:57 (*A. caccae*:*B. thetaiotaomicron*), and in the *A. caccae* + *B. vulgatus* co-culture, we calculated the ratio 49:51 (*A. caccae*:*B. vulgatus*). This shows that the species control was maintained after the scale of the co-culture process was increased.

3.6. Demonstrating substrate control and its effect on metabolic interactions with FBA

Our co-culture production relies on the unique substrates and eliminating competition to the main carbon source between species. Additionally, we demonstrated that it is possible to change a species ratio by changing the substrate ratio. Instead of the initial 50:50 (percentage wise) (D-sorbitol:D-xylose), we changed the ratio to 80:20 (D-sorbitol:D-xylose) and vice versa, but we kept the species ratio in the inoculum at 50:50 (*A. caccae*:*B. thetaiotaomicron*). Firstly, we raised the amount of D-sorbitol (substrate for *A. caccae*) to 66.8 mM and kept the D-xylose (substrate for *B. thetaiotaomicron*) concentration at 16.7 mM. Compared to the 50:50 substrate ratio, the co-culture lag-phase was significantly longer. Most probably, *B. thetaiotaomicron* produced an insufficient amount of acetate (we did not detect acetate before 12.4 h, Table S7) to maintain the same high growth rate that was previously observed. As the D-sorbitol amount was higher than D-xylose, we measured hydrogen production throughout the growth, which is an indicator of the metabolic activity of *A. caccae*. At the end of fermentation, we determined the ratio of the cells to be 82:18 (*A. caccae*:*B. thetaiotaomicron*) using microscopy images.

Secondly, we raised the amount of D-xylose (substrate for *B. thetaiotaomicron*) to 66.8 mM and kept the D-sorbitol (substrate for *A. caccae*) concentration at 16.7 mM. Again, the co-culture lag-phase was significantly longer compared to the 50:50 substrate ratio experiment. At the end of fermentation, we determined the ratio of the cells to be 29:71 (*A. caccae*:*B. thetaiotaomicron*) using microscopy images. Hydrogen production stopped at 17.8 h, which indicates depletion of D-sorbitol and the start of the asaccharolytic phase for *A. caccae*.

For metabolic modeling, we divided the growth of the organisms into two phases: saccharolytic and asaccharolytic. The model calculations showed 2%–5% deviance between the experimentally determined metabolome and computational metabolome, resulting in a carbon balance error of 1%–4% surplus, being largest in the asaccharolytic growth phases of both species (Table S9).

Flux variability analysis revealed obligatory cross-feeding in several experimental conditions (Fig. 3). Using measured

exometabolome data, the model identified definite acetate cross-feeding by *A. caccae* in the 80:20 (D-sorbitol:D-xylose) experiment in the saccharolytic growth phase and definite lactate cross-feeding by *B. thetaiotaomicron* in the asaccharolytic growth phase. In the 20:80 (D-sorbitol:D-xylose) experiment, definite lactate cross-feeding by *A. caccae* in the asaccharolytic growth phase was also determined, thus confirming the existence of trophic interactions in co-culture.

Interactions between *A. caccae* and *B. thetaiotaomicron* have been studied before [11]. Chia et al. [11] detected several metabolite changes in co-culture compared to monoculture: depletion of lactate and decreases in acetate and malate concentrations. In accordance with their results, we also discovered changes in short-chain fatty acid concentrations. We detected a decrease in acetate and lactate; both can be utilized by *A. caccae* [39,49]. While the utilization of acetate has been shown with *B. thetaiotaomicron*, lactate utilization has not been reported before. On the contrary, with a different *B. thetaiotaomicron* strain (LMG 11262), it was reported that it cannot metabolize lactate [51]. In addition, our cultivation experiments showed a significant increase in butyrate and propionate concentrations, which additionally indicates that both species gained from co-cultivation, since only *A. caccae* can produce butyrate and *B. thetaiotaomicron* propionate.

4. Conclusions

Maintaining the stability of consortia in a manufacturing process is not a straightforward task. Even if stability is theoretically reached in complex media, the species ratios in experiments cannot be easily altered when needed. It is important to explore the substrate possibilities and investigate metabolic interactions for co-culture production. In this study, we demonstrated that it is possible to find unique carbon sources for controlling the final biomass concentrations in co-culture production. Interestingly, the growth dynamics of the studied species changed in co-cultivation conditions – the growth rates of all species were increased. Detailed analysis of substrates and metabolic by-products, together with co-culture growth metabolic modeling (FBA), revealed that *A. caccae* benefited from the acetate produced either by *B. thetaiotaomicron* or *B. vulgatus*. At the same time, both *Bacteroides* species benefited from the lactate produced by *A. caccae*. For fine control of co-culture growth, it is necessary to manage the available substrates for the species, but also understand the metabolic interactions.

Funding

This work was supported by the European Regional Development Fund (“High throughput platform for growth improvement of microorganisms”; NSP137, 2014-2020.4.02.17-0104). The funding organization is SA Archimedes.

Declaration of competing interest

All data generated and analyzed during this study will be made available to any scientist wanting to use them for non-commercial purposes upon reasonable request.

Data availability

Data will be made available on request.

Acknowledgments

The authors would like to thank Mary-Liis Kütt for her contributions in writing the project proposal and Aleksei Kaleda for microscopy image analysis. In addition, we would like to thank Taivo Lints for the support with statistical analysis.

Appendix A. Supplementary data

Supplementary data to this article can be found online at <https://doi.org/10.1016/j.anaerobe.2022.102680>.

References

- [1] G. Klein, A. Pack, C. Bonaparte, G. Reuter, Taxonomy and physiology of probiotic lactic acid bacteria, *Int. J. Food Microbiol.* 41 (2) (1998) 103–125, [https://doi.org/10.1016/S0168-1605\(98\)00049-X](https://doi.org/10.1016/S0168-1605(98)00049-X).
- [2] D. Almeida, D. Machado, J.C. Andrade, S. Mendo, A.M. Gomes, A.C. Freitas, Evolving trends in next-generation probiotics: a 5W1H perspective, *Crit. Rev. Food Sci. Nutr.* 60 (11) (2020) 1783–1796, <https://doi.org/10.1080/10408398.2019.1599812>.
- [3] C.W.Y. Ha, S. Devkota, Division of Gastroenterology, F. Widjaja Foundation Inflammatory Bowel and Immunobiology 1 Research Institute, Cedars-Sinai Medical Center, Los Angeles, CA vol. 11762, 2020, 90048.
- [4] T.P. Singh, B.H. Natraj, Next-generation probiotics: a promising approach towards designing personalized medicine, *Crit. Rev. Microbiol.* 47 (4) (2021) 479–498, <https://doi.org/10.1080/1040841X.2021.1902940>.
- [5] A. López-Moreno, et al., Next generation probiotics for neutralizing obesogenic effects: taxa culturing searching strategies, *Nutrients* 13 (5) (2021), <https://doi.org/10.3390/nu13051617>.
- [6] H. Sokol, et al., Faecalibacterium prausnitzii is an anti-inflammatory commensal bacterium identified by gut microbiota analysis of Crohn disease patients, *Proc. Natl. Acad. Sci. U. S. A.* 105 (43) (2008) 16731–16736, <https://doi.org/10.1073/pnas.0804812105>.
- [7] D. Jonkers, J. Penders, A. Masclee, M. Pierik, Probiotics in the management of inflammatory bowel disease: a systematic review of intervention studies in adult patients, *Drugs* 72 (6) (2012) 803–823, <https://doi.org/10.2165/11632710-000000000-00000>.
- [8] C. Depommier, et al., Supplementation with Akkermansia muciniphila in overweight and obese human volunteers: a proof-of-concept exploratory study, *Nat. Med.* 25 (7) (2019) 1096–1103, <https://doi.org/10.1038/s41591-019-0495-2>.
- [9] S. Wang, et al., Systematic review: adverse events of fecal Microbiota transplantation, *PLoS One* 11 (8) (2016) 1–24, <https://doi.org/10.1371/journal.pone.0161174>.
- [10] F. Kurt, et al., Co-cultivation is a powerful approach to produce a robust functionally designed synthetic consortium as a live biotherapeutic product (LBP), *bioRxiv* (2021), <https://doi.org/10.1101/2021.10.13.464188>.
- [11] L.W. Chia, M. Mank, B. Blijenberg, S. Aalvink, R.S. Bongers, Bacteroides thetaiotaomicron fosters the growth of butyrate-producing Anaerostipes caccae in the presence of early life carbohydrates, *Microorganisms* (2008) 1–15.
- [12] B.H. McGovern, et al., SER-109, an investigational microbiome drug to reduce recurrence after Clostridioides difficile infection: lessons learned from a phase 2 trial, *Clin. Infect. Dis.* 72 (12) (2021) 2132–2140, <https://doi.org/10.1093/cid/ciaa387>.
- [13] J. Huang, et al., Effects of microbiota on anticancer drugs: current knowledge and potential applications, *EBioMedicine* 83 (2022), 104197, <https://doi.org/10.1016/j.ebiom.2022.104197>.
- [14] W. Forrest, D.J. Walker, Calorimetric measurements of energy of maintenance of Streptococcus faecalis, *Biochem. Biophys. Res. Commun.* 13 (3) (1963) 217–222.
- [15] S. Gaisford, M.A.A. O'Neill, A.E. Beezer, Shelf life prediction of complex food systems by quantitative interpretation of isothermal calorimetric data, in: G. Kaletunç (Ed.), *Calorimetry in Food Processing: Analysis and Design of Food Systems*, John Wiley & Sons Publishers, New York, NY, USA, 2009, pp. 237–263.
- [16] O. Braissant, D. Wirz, B. Göpfert, A.U. Daniels, Use of isothermal microcalorimetry to monitor microbial activities, *FEMS Microbiol. Lett.* 303 (1) (2010) 1–8, <https://doi.org/10.1111/j.1574-6968.2009.01819.x>.
- [17] P. Louis, H.J. Flint, Diversity, metabolism and microbial ecology of butyrate-producing bacteria from the human large intestine, *FEMS Microbiol. Lett.* 294 (1) (2009) 1–8, <https://doi.org/10.1111/j.1574-6968.2009.01514.x>.
- [18] D.A. Ravcheev, A. Godzik, A.L. Osterman, D.A. Rodionov, Polysaccharides utilization in human gut bacterium Bacteroides thetaiotaomicron: comparative genomics reconstruction of metabolic and regulatory networks, *BMC Genom.* 14 (1) (2013) 1–17, <https://doi.org/10.1186/1471-2164-14-873>.
- [19] N.D. Schwalm, E.A. Groisman, Navigating the gut buffet: control of polysaccharide utilization in Bacteroides spp, *Trends Microbiol.* 25 (12) (2017) 1005–1015, <https://doi.org/10.1016/j.tim.2017.06.009>.
- [20] M.A. Mahowald, et al., Characterizing a model human gut microbiota composed of members of its two dominant bacterial phyla, *Proc. Natl. Acad. Sci. U. S. A.* 106 (14) (2009) 5859–5864, <https://doi.org/10.1073/pnas.0901529106>.
- [21] T.P.N. Bui, H.A. Schols, M. Jonathan, A.J.M. Stams, W.M. De Vos, C.M. Plugge, Mutual metabolic interactions in Co-cultures of the intestinal Anaerostipes rhamnosivorans with an acetogen, Methanogen, or Pectin-Degrader Affecting Butyrate Production, *Front. Microbiol.* 10 (November) (2019) 1–12, <https://doi.org/10.3389/fmicb.2019.02449>.
- [22] K. Adamberg, M. Jaagura, A. Aaspõllu, E. Nurk, S. Adamberg, The composition of faecal microbiota is related to the amount and variety of dietary fibres, *Int. J. Food Sci. Nutr.* 71 (7) (2020) 845–855, <https://doi.org/10.1080/09637486.2020.1727864>.
- [23] D.J. Gascoyne, M.K. Theodorou, Consecutive Batch Culture A Novel Technique for the in vitro Study of Mixed Microbial Populations from the Rumens, *Cultures* 21 (1988) 183–189.
- [24] S. Adamberg, et al., Degradation of fructans and production of propionic acid by Bacteroides thetaiotaomicron are enhanced by the shortage of amino acids, *Front. Nutr.* 1 (December) (2014) 1–10, <https://doi.org/10.3389/fnut.2014.00021>.
- [25] M. Kuhn, et al., Nutritional preferences of human gut bacteria reveal their metabolic idiosyncrasies, *Nat. Microbiol.* 3 (April, 2018), <https://doi.org/10.1038/s41564-018-0123-9>.
- [26] T. Brettin, et al., RASTtk: a modular and extensible implementation of the RAST algorithm for building custom annotation pipelines and annotating batches of genomes, *Sci. Rep.* 5 (2015), <https://doi.org/10.1038/srep08365>.
- [27] M. Kanehisa, S. Goto, KEGG: kyoto encyclopedia of genes and genomes, *Nucleic Acids Res.* 28 (1) (2000) 27–30, <https://doi.org/10.1093/nar/28.1.27>.
- [28] R. Caspi, et al., The MetaCyc database of metabolic pathways and enzymes and the BioCyc collection of Pathway/Genome Databases, *Nucleic Acids Res.* 42 (D1) (2014) 459–471, <https://doi.org/10.1093/nar/gkt1103>.
- [29] J. Schindelin, et al., Fiji: an open-source platform for biological-image analysis, *Nat. Methods* 9 (7) (2012) 676–682, <https://doi.org/10.1038/nmeth.2019>.
- [30] E. Kivima, K. Tanilas, K. Martverk, S. Rosenvall, L. Timberg, K. Laos, The composition, physicochemical properties, antioxidant activity, and sensory properties of Estonian honeys, *Foods* 10 (3) (2021) 1–14, <https://doi.org/10.3390/foods10030511>.
- [31] P.P.F. Hanegraaf, E.B. Muller, The dynamics of the macromolecular composition of biomass, *J. Theor. Biol.* 212 (2) (2001) 237–251, <https://doi.org/10.1006/jtbi.2001.2369>.
- [32] K. Mumm, K. Ainsaar, S. Kasvandik, T. Tenson, R. Hörak, Responses of Pseudomonas putida to zinc excess determined at the proteome level: pathways dependent and independent of ColRS, *J. Proteome Res.* 15 (12) (2016) 4349–4368, <https://doi.org/10.1021/acs.jproteome.6b00420>.
- [33] J. Soini, K. Ukkonen, P. Neubauer, High cell density media for Escherichia coli are generally designed for aerobic cultivations - consequences for large-scale bioprocesses and shake flask cultures, *Microb. Cell Factories* 7 (–11) (2008) 1, <https://doi.org/10.1186/1475-2859-7-26>.
- [34] J.D. Orth, I. Thiele, B.Ø. Palsson, What is flux balance? *Nat. Biotechnol.* 28 (3) (2010) 245–248, <https://doi.org/10.1038/nbt.1614.What>.
- [35] R. Mahadevan, C.H. Schilling, The effects of alternate optimal solutions in constraint-based genome-scale metabolic models, *Metab. Eng.* 5 (4) (2003) 264–276, <https://doi.org/10.1016/j.ymben.2003.09.002>.
- [36] H.J. Flint, S.H. Duncan, Bacteroides and Prevotella, second ed., vol. 1, Elsevier, 2014.
- [37] S.F. Kotarski, A.A. Salyers, Effect of long generation times on growth of Bacteroides thetaiotaomicron in carbohydrate-limited continuous culture, *J. Bacteriol.* 146 (3) (1981) 853–860, <https://doi.org/10.1128/jb.146.3.853-860.1981>.
- [38] N. Pan, J.A. Imlay, How does oxygen inhibit central metabolism in the obligate anaerobe Bacteroides thetaiotaomicron? *Mol. Microbiol.* 39 (6) (2001) 1562–1571, <https://doi.org/10.1046/j.1365-2958.2001.02343.x>.
- [39] S.H. Duncan, P. Louis, H.J. Flint, Lactate-utilizing bacteria, isolated from human feces, that produce butyrate as a major fermentation product, *Appl. Environ. Microbiol.* 70 (10) (2004) 5810–5817, <https://doi.org/10.1128/AEM.70.10.5810-5817.2004>.
- [40] G. Falony, A. Vlachou, K. Verbrugghe, L. De Vuyst, Cross-feeding between Bifidobacterium longum BB536 and acetate-converting, butyrate-producing colon bacteria during growth on oligofructose, *Appl. Environ. Microbiol.* 72 (12) (2006) 7835–7841, <https://doi.org/10.1128/AEM.01296-06>.
- [41] L.W. Chia, et al., Deciphering the trophic interaction between Akkermansia muciniphila and the butyrogenic gut commensal Anaerostipes caccae using a

- metatranscriptomic approach, *Antonie van Leeuwenhoek, Int. J. Gen. Mol. Microbiol.* 111 (6) (2018) 859–873, <https://doi.org/10.1007/s10482-018-1040-x>.
- [42] F. Li, J. Hinderberger, H. Seedorf, J. Zhang, W. Buckel, R.K. Thauer, Coupled ferredoxin and crotonyl coenzyme A (CoA) reduction with NADH catalyzed by the butyryl-CoA dehydrogenase/Etf complex from *Clostridium kluyveri*, *J. Bacteriol.* 190 (3) (2008) 843–850, <https://doi.org/10.1128/JB.01417-07>.
- [43] M.C. Weghoff, J. Bertsch, V. Müller, A novel mode of lactate metabolism in strictly anaerobic bacteria, *Environ. Microbiol.* 17 (3) (2015) 670–677, <https://doi.org/10.1111/1462-2920.12493>.
- [44] H.P. Blaschkowski, G. Neuer, M. Ludwig-Festl, J. Knappe, Routes of flavodoxin and ferredoxin reduction in *Escherichia coli* CoA-acylating pyruvate: flavodoxin and NADPH: flavodoxin oxidoreductases participating in the activation of pyruvate formate-lyase, *Eur. J. Biochem.* 123 (3) (1982) 563–569, <https://doi.org/10.1111/j.1432-1033.1982.tb06569.x>.
- [45] O.S. Venturelli, et al., Deciphering microbial interactions in synthetic human gut microbiome communities, *Mol. Syst. Biol.* 14 (6) (2018) 1–19, <https://doi.org/10.15252/msb.20178157>.
- [46] S. Oba, et al., Prebiotic effects of yeast mannan, which selectively promotes *Bacteroides thetaiotaomicron* and *Bacteroides ovatus* in a human colonic microbiota model, *Sci. Rep.* 10 (1) (2020) 1–11, <https://doi.org/10.1038/s41598-020-74379-0>.
- [47] L.W. Chia, et al., Cross-feeding between *Bifidobacterium infantis* and *Anaerostipes caccae* on lactose and human milk oligosaccharides, *Benef. Microbes* 12 (1) (2021) 69–83, <https://doi.org/10.3920/BM2020.0005>.
- [48] B.W. Mackenzie, D.W. Waite, M.W. Taylor, Evaluating variation in human gut microbiota profiles due to DNA extraction method and inter-subject differences, *Front. Microbiol.* 6 (FEB) (2015) 1–11, <https://doi.org/10.3389/fmicb.2015.00130>.
- [49] A. Schwieritz, et al., *Anaerostipes caccae* gen. nov., sp. nov., a new saccharolytic, acetate-utilising, butyrate-producing bacterium from human faeces, *Syst. Appl. Microbiol.* 25 (1) (2002) 46–51, <https://doi.org/10.1078/0723-2020-00096>.
- [50] J.E. Weiss, L.F. Rettger, The Gram-negative *Bacteroides* of the intestine, *J. Bacteriol.* 3 (1937) 423–434.
- [51] G. Falony, T. Calmeyn, F. Leroy, L. De Vuyst, Coculture fermentations of *bifidobacterium* species and *bacteroides thetaiotaomicron* reveal a mechanistic insight into the prebiotic effect of inulin-type fructans, *Appl. Environ. Microbiol.* 75 (8) (2009) 2312–2319, <https://doi.org/10.1128/AEM.02649-08>.

Appendix 4

Publication III

Kallastu, A., Malv, E., Aro, V., Meikas, A., Vendelin, M., Kattel, A., Nahku, R., & Kazantseva, J. (2023). Absolute quantification of viable bacteria abundances in food by next-generation sequencing: Quantitative NGS of viable microbes. *Current Research in Food Science*, 6(December 2022), 100443. <https://doi.org/10.1016/j.crf.2023.100443>



Contents lists available at ScienceDirect

Current Research in Food Science

journal homepage: www.sciencedirect.com/journal/current-research-in-food-science

Absolute quantification of viable bacteria abundances in food by next-generation sequencing

Quantitative NGS of viable microbes

Aili Kallastu^a, Esther Malv^a, Valter Aro^{a,b}, Anne Meikas^a, Mariann Vendelin^a, Anna Kattel^{a,b}, Ranno Nahku^a, Jekaterina Kazantseva^{a,*}

^a Center of Food and Fermentation Technologies, Mäealuse 2/4, Tallinn, 12618, Estonia

^b Department of Chemistry and Biotechnology, Tallinn University of Technology, Akadeemia tee 15, Tallinn, 12618, Estonia

ARTICLE INFO

Handling Editor: Siyun Wang

Keywords:

Viable bacteria
Bacteria abundances
Bacteria enumeration
16S rRNA gene amplicon next-generation sequencing
Taxonomical identification

ABSTRACT

Next-generation sequencing (NGS) is an important tool for taxonomical bacteria identification. Recent technological developments have led to its improvement and availability. Despite the undeniable advantages of this approach, it has several limitations and shortcomings. The usual outcome of microbiota sequencing is a relative abundance of bacterial taxa. The information about bacteria viability or enumeration is missing. However, this knowledge is crucial for many applications. In the current study, we elaborated the complete workflow for the absolute quantification of living bacteria based on 16S rRNA gene amplicon sequencing. A fluorescent PMAxx reagent penetrating a damaged cell membrane was used to discriminate between the total and viable bacterial population. Bacteria enumeration was estimated by the spike-in technique or qPCR quantification. For method optimization, twenty bacterial species were taken, and the results of the workflow were validated by widely accepted methodologies: flow cytometry, microbiological plating, and viability-qPCR. Despite the minor discrepancy between all methods used, they all showed compatible results. Finally, we tested the workflow with actual food samples and received a good correlation between the methods regarding the estimation of the number of viable bacteria. Overall, the elaborated and integrated NGS approach could be the next step in perceiving a holistic picture of a sample microbiota.

1. Introduction

The knowledge and reliability of quantitative data on viable microbes are crucial for decision-making in many fields. Whether the microbes are pathogenic, neutral or probiotic, the quantitative information and their viable state matter the most. Currently available methods have different limitations and biases and therefore do not provide enough essential knowledge. Despite the fast development of molecular techniques, the most widely accepted methodology in food microbiology is plating. Cell plating is an affordable and simple method that describes the number of cultivable organisms in the product. However, not all bacteria are cultivable, taxonomic characterization is often missing, and it might take up to a week to obtain the results (Stewart 2012). Modern molecular methods to detect bacteria or metabolites such as next-generation sequencing (NGS), PCR or immunoassays provide more extended information about the number of specific bacteria, but they

also have drawbacks (Fanning et al., 2017), (Muyzer and Ramsing 1995). ELISA and PCR methods are good choices for the detection of specific and preselected microorganisms. These techniques allow a quantitative approach and are quick, but usually sensitive only after the cultural enrichment stage and evaluate only predefined bacteria in a sample. The only method that has the potential to characterize the food microbiota in full is NGS (Mayo et al., 2014), (Jagadeesan et al., 2019). 16S rRNA gene (16S) amplicon NGS provides a relative abundance of all bacteria, but their quantification is often stalled by the large variety of 16S copy numbers in different taxonomic groups. The usage of the amplification step by PCR in library preparation creates a bias and raises the question about the specificity and threshold choice for data analysis. Thus, the development of a methodology for the quantification of NGS data will give us valuable information about the absolute abundances of all alive bacteria in a food sample.

Recent developments related to NGS and its increased availability

* Corresponding author.

E-mail address: jekaterina@tftak.eu (J. Kazantseva).

<https://doi.org/10.1016/j.crfs.2023.100443>

Received 9 September 2022; Received in revised form 15 December 2022; Accepted 10 January 2023

Available online 12 January 2023

2665-9271/© 2023 The Authors. Published by Elsevier B.V. This is an open access article under the CC BY-NC-ND license (<http://creativecommons.org/licenses/by-nc-nd/4.0/>).

make it an excellent tool for the identification of microbiological taxa. The standard amplicon sequencing pipeline gives extensive data about the relative abundances of bacteria. However, an absolute quantification is often necessary. The first mention of Quantitative Microbiome Profiling (QMP) based on absolute quantification of microbial abundances from NGS data was introduced by Vandeputte (Vandeputte et al., 2017). They applied flow cytometry (FC) for the normalization of 16S rRNA gene sequencing data to determine the bacterial load of the gut microbiome samples. Different methodologies have been employed to quantify the sequencing data so far (Galazzo et al., 2020), (Props et al., 2017), and (Jin et al., 2022). The most widely applied methods are based on quantitative PCR and the usage of internal controls (Smets et al., 2016), (Stämmli et al., 2016), (D. M. Tourlousse et al., 2017), (Azarbad et al., 2022).

Quantitative real-time PCR (qPCR) is an affordable and technologically simple method to move from relative to absolute data. However, it possesses the same biases during a sequencing library preparation – amplification of the specific region of the 16S rRNA bacterial gene by conservative primers. The most used primers for bacterial quantification often are the same ones that work at the library preparation stage, namely universal primers specific for the hypervariable region of the 16S rRNA gene (Liu et al., 2012), (Kim et al. 2013). Imbalance in the amplification of different taxa and variation of 16S gene copy number are the main sources of errors in this type of quantification. Droplet digital PCR (ddPCR) is the most effective existing technology to get absolute DNA values. It does not need controls and provides precise concentrations. Although ddPCR is an ideal choice in the case of single bacterial species quantification, it is not suitable for consortia enumeration. Moreover, the method is quite expensive and not every laboratory can afford it.

The addition of internal standards or spike-in controls already at the stage of DNA extraction might be an excellent approach to check the whole sequencing workflow from the beginning and eliminate all biases connected with the loss of DNA during the isolation from complex matrices. Besides, the spike-in might be used for data quantification. Two major types of spike-in controls have been implicated so far – synthetic DNA molecules (Zemb et al., 2020), (Di. M. Tourlousse et al. 2018), (Tkacz et al. 2018) or cells (Smets et al., 2016), (Piwosz et al., 2018). Synthetic DNAs are more accurate and versatile but do not tackle all of the issues, such as cell lysis efficiency during microbial DNA extraction or PCR-based bias. Spike-in cells usually represent a mixture of different proportions and amounts of Gram-positive and Gram-negative bacteria that are not specific to the studied environment. Knowing the input spike-in quantity and relative abundance of bacteria in the studied sample enables the calculation of the absolute numbers.

However, even obtaining the absolute NGS data is often misleading and does not show the real microbiological situation. Standard NGS pipeline provides information about the total microbiota yet does not provide the number of live bacteria in a food sample. At the same time, knowledge about the variety of viable microbial consortia is what most microbiological tasks are aimed at. For example, sterilization and pasteurization kill the majority of viable microbes but do not often affect spores, and the detection of total consortia says little about the food safety. Even a low number of viable pathogens could reach critical numbers and pose a health risk in an environment that supports their growth. With these data, a more accurate model for the spread of diseases and health prognoses could be done. Moreover, the exact enumeration of viable bacteria is valuable to estimate the health benefits of fermented foods.

Despite the obvious benefits and common use of culture-based methodology, it is not so sensitive and does not provide the exact information about the presence of definite taxonomic groups. The second type of technique for living microbes' detection is based on membrane integrity of bacteria. The membrane of dead cells is permeable, and the addition of fluorescent dyes such as propidium iodide (PI), ethidium monoazide (EMA), or propidium monoazide (PMA) can discriminate

between live and dead microorganisms. So-called viability staining can be evaluated further by epifluorescence microscopy, flow cytometry, or is applied in viability qPCR. The last possibility to describe viable microbes only is RNA-based transcriptomics. As RNAs are unstable molecules and present only in alive bacteria, thereby the whole sequencing pipeline can start from RNA isolation. However, due to the short lifespan of RNA and limitations connected with it, this method is not commonly used. Despite high resolution, sensitivity, and compatibility with low biomass samples, RNASeq is an expensive and time-consuming analysis and is not widely used as a routine approach.

In our study, we modified the NGS pipeline by applying the fluorescent permeable dye PMAxx (improved version of PMA) for the detection of viable microbes only and the NGS data quantification by spike-in controls or qPCR using 16S rRNA gene V4 region-specific primers. The simple and reliable approach that is based on modification of broadly accepted amplicon NGS technology would allow the accurate estimation of the absolute number of alive bacterial cells that will significantly improve the quality of future microbiome studies.

Table 1

Bacterial strains used in the study and their viability measured by flow cytometry and qPCR.

Acronym	Bacterial species	Gram stain	Viability by FC, %	Viability by qPCR, %
AM	<i>Akkermansia muciniphila</i>	negative	66.11 ± 0.03	81.22 ± 13.47
AS	<i>Alistipes shahii</i>	negative	62.40 ± 7.63	78.51 ± 12.18
AC	<i>Anaerostipes caccae</i>	variable	60.69 ± 9.86	90.01 ± 5.02
ACo	<i>Anaerotruncus colthominis</i>	positive	23.35 ± 0.90	40.15 ± 13.87
BC	<i>Bacteroides caccae</i>	negative	3.76 ± 2.16	9.28 ± 0.26
BT	<i>Bacteroides thetaiotaomicron</i>	negative	63.88 ± 8.26	56.87 ± 2.51
BU	<i>Bacteroides uniformis</i>	negative	88.59 ± 1.82	100.00 ± 8.84
BA	<i>Bifidobacterium adolecentis</i>	positive	83.72 ± 1.55	90.26 ± 7.07
BH	<i>Blautia hydrogenotrophica</i>	positive	35.06 ± 14.86	24.63 ± 1.62
BF	<i>Butyrivibrio faecihominis</i>	negative	95.88 ± 0.85	92.47 ± 27.24
CM	<i>Catenibacterium mitsuokai</i>	positive	6.14 ± 1.86	0.46 ± 0.01
ChM	<i>Christensenella minuta</i>	negative	40.40 ± 0.46	34.66 ± 7.18
CA	<i>Collinsella aerofaciens</i>	positive	4.31 ± 0.13	11.25 ± 1.51
DF	<i>Dorea formicigenerans</i>	positive	81.80 ± 1.19	90.18 ± 8.42
DL	<i>Dorea longicatena</i>	positive	14.91 ± 1.49	22.70 ± 0.89
ET	<i>Eisenbergiella tayi</i>	positive but Gram-stain negative	8.95 ± 1.57	43.96 ± 2.16
FP	<i>Faecalibacterium prausnitzii</i>	positive	72.23 ± 5.40	74.70 ± 14.27
OS	<i>Odoribacter splanchnicus</i>	negative	87.06 ± 0.54	93.38 ± 4.83
PC	<i>Prevotella copri</i>	negative	32.88 ± 4.00	73.56 ± 21.67
RF	<i>Roseburia faecis</i>	negative or variable	67.84 ± 4.32	87.07 ± 2.16
	Mix of 20 strains		68.41 ± 0.18	60.92 ± 3.98 ^a

^a Universal 16S rRNA gene V4 primers were used instead of specific ones.

2. Materials and methods

2.1. Bacterial strains

All 20 strains (Table 1) used in this study were purchased from DSMZ (German Collection of Microorganisms and Cell Cultures GmbH). The strains were grown on modified YCM (yeast extract, casitone, mucin) or MRS (de Man, Rogosa and Sharpe) medium until the stationary growth phase. Cells were harvested by centrifugation at 14 000×g for 5 min at 4 °C and washed once with DPBS (Dulbecco's phosphate-buffered saline, PAN-Biotech GmbH, Germany). Cell pellets were suspended in a solution of DPBS with 20% glycerol and 1% L-cysteine hydrochloride, frozen in liquid nitrogen and stored at −80 °C in aliquots. The number of cells in the stock culture was estimated by optical density at 600 nm (OD600) with the assumption that OD600 of 1 equates approximately cfu/mL. 5×10^8 cells were taken from each strain stock and added to the mixture. The final OD600 of the mixed stock culture was 0.98.

For the viability analysis by qPCR and NGS, five multi-strain glycerol stocks were prepared in aseptic conditions. For that, the stocks were centrifuged at 5000×g for 10 min at 4 °C and the supernatant was discarded. Each pellet was resuspended in 1 mL of 0.85% NaCl solution and centrifuged at 5000×g for 10 min at 4 °C. Then two pellets were suspended in 200 µl of 1 × PBS (Phosphate-buffered saline, BIO-RAD, CA, USA) and continued with genomic DNA (gDNA) extraction for the total cell analysis. The other three pellets were suspended in 400 µl of 0.85% NaCl solution for the following PMAxx treatment, spike-in control inserting and gDNA isolation to predict viable cells' presence.

2.2. Bacterial cells separation from kimchi and sauerkraut samples

Microbial cells from kimchi and sauerkraut were isolated in sterile conditions. 50 g of each sample were agitated in 50 ml of 0.85% NaCl, 0.05% Tween 20 solution (Sigma) at 200 rpm for 15 min at room temperature on Yellow Line OS 5 Basic Orbital Shaker (IKA Works Inc, Wilmington, NC, USA). The samples were filtered through the Whatman filter paper, and the filtrate was centrifuged at 5000×g for 15 min at 4 °C. The cell pellets were washed with 1 ml of 0.85% NaCl solution and centrifuged at 5000×g for 15 min at 4 °C. The final pellet was resuspended in 2 ml of 0.85% NaCl solution and divided into five 400 µl aliquots. The first aliquot was subjected to flow cytometry analysis. Another four aliquots were used for viable and total cell analysis with qPCR and NGS. Two of the four aliquots were centrifuged at 5000×g for 15 min at 4 °C, the supernatant was discarded, and the pellets were frozen at −20 °C until gDNA extraction for total cell number estimation. For the remaining two aliquots, the PMAxx treatment was applied for alive cell consortia analysis, then cells were frozen until gDNA extraction.

2.3. Flow cytometry analysis

Samples were diluted to a final cell concentration of approximately 1×10^6 cells/mL with filter-sterilized (0.22 µm) PBS (PAN-Biotech GmbH, Germany). Membrane integrity was evaluated using double staining with green fluorescent-dye SYTO24 (SYTO™ 24 Green Fluorescent Nucleic Acid Stain - 5 mM Solution in DMSO, Invitrogen, USA) labelling all bacteria, and red fluorescent propidium iodide (PI) (Propidium Iodide - 1.0 mg/mL Solution in Water, Invitrogen, USA), which permeates only cells with damaged membranes. The final concentrations of SYTO 24 and PI were 1 µM and 2 µM, respectively. For staining, the cells were incubated in the dark for 20 min at 37 °C and 10 min on ice. Analyses were performed using A50-Micro Flow Cytometer (Apogee Flow Systems, UK) with a 20 mW laser at 488 nm. Over 10 000 events were collected per sample at a flow rate set to 3 µL/min. Green fluorescence was acquired using a bandpass filter FL-2 (517–553 nm), and red fluorescence was acquired using a long-wavelength pass filter FL-3 (>575 nm). All parameters were collected as logarithmic signals. Thresholds

were adjusted for forward (FSC) and side scatter (SSC) to exclude noise and debris. Gating of red fluorescence versus green fluorescence dot plot was used to obtain cell count data. Event count was obtained for both dyes and was used to calculate the absolute number as well as the ratio of viable and dead cells.

2.4. Microscopy

Single-strain bacterial stock cultures were adjusted to OD 1 at 600 nm by DPBS solution with 1% L-Cysteine hydrochloride. Samples were vortexed and pipetted onto microscope slides followed by Gram staining by BioGram 4 kit (Biognost Ltd, Croatia) according to the manufacturer's instructions. The strains were examined under the Eclipse E200-LED microscope (Nikon, Minato City, Tokyo, Japan) equipped with a 100-fold magnifying oil immersion objective lens. Nikon D5200 camera was used to take brightfield images.

2.5. Plating

Five grams of kimchi and sauerkraut samples were diluted in 45 ml sterile 0.85% NaCl solution, subsequently, serial 10-fold dilutions of the samples were made. The number of bacteria was determined by plating 100 µl of kimchi and sauerkraut samples dilutions on PCA (Plate Count Agar, Neogen, Lansing, MI, USA) and incubating for 72 h at 30 °C. Plating was carried out in two technical replicates. Results were presented as colony-forming units per gram of the sample (cfu/g).

2.6. PMAxx treatment and addition of spike-in control

Twenty-strain consortia, isolated kimchi and sauerkraut cell cultures were prepared as aforementioned. For viability testing, PMAxx™ solution in H₂O (Biotium, Fremont, CA, USA) was added to 400 µL of the cell suspension to obtain a 25 µM final concentration. The PMAxx-cells suspension was incubated in dark for 10 min on a shaker. After that, the samples were exposed to blue light by PMA-Lite™ LED Photolysis device (Biotium) for 20 min with intermittent inversion. The samples were centrifuged at 5000×g for 15 min at 4 °C, the pellets were resuspended in 200 µL of 1 × PBS. If applicable, a defined number of ZymoBIOMICS™ Spike-in Control 1 (High Microbial Load, Zymo Research, Irvine, CA, USA) was added. For the titration experiment, the number of the added spike-in control is shown in Table 2; the for method validation study, 4×10^7 spike-in cells were added to each aliquoted kimchi/sauerkraut samples. The cells were then immediately subjected to DNA extraction.

2.7. DNA extraction

The gDNAs of the 20-strain consortia samples were isolated by ZymoBIOMICS™ DNA Miniprep Kit (Zymo Research) and of the kimchi/sauerkraut samples by Quick-DNA™ Fungal/Bacterial Miniprep Kit (Zymo Research) according to the manufacturer's instructions. The

Table 2
Application of the spike-in standard for cell number absolute quantification.

	20St	20St	20St	20St
		0.5%	1%	2.5%
Number of added spike-in cells	0.00	7.50×10^6	1.50×10^7	3.75×10^7
Calculated abundance of added spike-in, %	0.00	0.25	0.72	1.13
<i>Allobacillus halotolerans</i>				
<i>Imtechella halotolerans</i>				
SUM of spike-in, %	0.00	0.43	1.07	2.42
Calculated abundance of 20 species consortia, %	100	99.57	98.93	97.58
Calculated number of total cells in consortia	N/A	1.74×10^9	1.39×10^9	1.51×10^9

concentrations of the extracted DNAs were quantified by a Qubit™ 4 Fluorometer (Thermo Fisher Scientific, Waltham, MA, USA) using Qubit dsDNA BR Assay Kit (Thermo Fisher Scientific).

2.8. Quantitative real-time PCR

For the viability study, quantitative real-time PCR (qPCR) was performed using $5 \times$ HOT FIREPol® EvaGreen qPCR Mix Plus (no ROX, Solis BioDyne, Tartu, Estonia). The reaction was done in triplicates on qTOWER3 thermal cycler (Analytik Jena, Jena, Germany) using a qPCRsoft 4.0 software. Each qPCR run contained no-template control for checking external contaminations. The cycling conditions included a preliminary denaturation at 95 °C for 12 min, then 40 cycles of denaturation at 95 °C for 30 s, annealing at temperature corresponding used primer pair (Supplementary Table S1) for 30 s, and extension at 72 °C for 1 min. During qPCR cycles, the fluorescence was measured at the end of each annealing step, and a melting curve analysis step (at a ramp from 55 °C to 95 °C) was included to assess the specificity of the amplification.

Viability qPCR for single strains of the 20-strain consortia was performed using strain-specific primers (Supplementary Table S1). To evaluate the cell viability, the ΔCq based on the quantification cycle (Cq) of the PMAxx-treated and untreated sample was calculated as follows:

$$\Delta Cq = Cq_{PMAxx\text{-treated}} - Cq_{\text{non-treated}}$$

The percentage of the viable cells was computed based on the equation:

$$\% \text{ viable} = \frac{100}{2^{\Delta Cq}}$$

Total and viable cell gDNA concentrations were measured based on the standard calibration curve using 515F/806R primers, specific for the bacterial V4 region of the 16S rRNA gene (Caporaso et al., 2011) as used during the preparation of the sequencing libraries but without adapter nucleotides (Supplementary Table S1). ZymoBIOGENICS™ Microbial Community DNA Standard (Zymo Research) was used for calibration curve creation. The microbial cell number was calculated considering the amount of sample taken for the DNA extraction, a dilution factor and an approximation expressed as 1 ng of bacterial DNA $\approx 2\text{--}4 \times 10^5$ cells, if the average size of the bacterial genome is taken as 2.2 Mbp for LAB (lactic acid bacteria) (Klaenhammer et al., 2002) and 4.5 Mbp for bacteria of 20-strain consortia. The equation for single-cell bacterial DNA will be:

$$m = \frac{\text{Genome size} \times M}{N_A}$$

where M is the average molar mass of a base pair equal to 660 g/mol, and N_A is the Avogadro constant $6.02 \times 10^{23} \text{ mol}^{-1}$.

2.9. 16S rRNA gene amplicon sequencing

Amplicon libraries targeting the V4 region of the 16S rRNA gene by the primer pair 515F/806R were prepared according to Illumina's dual indexing protocol as published in Kazantseva et al., (2021) (Kazantseva et al., 2021). Multiplexed and normalized libraries were sequenced on iSeq 100 System using i2 kit (Illumina, San Diego, CA, USA). DNA sequence data were analyzed as published before (Kazantseva et al., 2021), (Espinosa-Gongora et al., 2016), (McDonald et al., 2016) by BION-meta program (<https://github.com/nielsl/mcdonald-et-al>, Danish Genome Institute, Denmark) according to the current instructions. All sequencing data are available on the SRA database with the PRJNA861123 reference.

2.10. Data processing

Statistical analysis and visualization were carried out using Excel software (Microsoft 365 Apps for business, Microsoft Corp., Redmond, WA). qPCR and FC experiments as well as spike-in sequencing protocol were performed in triplicate. All data were independently analyzed using paired Student's t -test and represented where appropriate as means \pm standard deviation.

3. Results and discussion

The aim of the study was to develop and validate the methodology for quantitative taxonomical determination of bacterial species that distinguishes between viable and the whole microbiota using next-generation sequencing approach. For that, PMAxx reagent that discriminates between alive and total bacteria consortia was validated for 16S library preparation and two ways of bacteria enumeration including qPCR and spike-in cell addition were applied.

3.1. Assessment of bacteria viability by PMAxx-qPCR

For the first viability step validation, twenty bacterial species that differ by their Gram-stain (Table 1) were chosen. To discriminate between viable and dead bacteria, a new generation viability fluorescent reagent PMAxx was used. This reagent is a photoreactive dye that selectively penetrates dead cells through compromised membrane and covalently binds DNA upon photolysis with visible blue light. Dye-modified DNA cannot be amplified by PCR and thereby is eliminated from the following procedure. Cells for the analysis were taken from glycerol stocks and due to specific features, their viability after the storage was variable. For viability control, convenient flow cytometry (FC) with SYTO24 and PI dyes was carried out. According to the FC analysis (Table 1), viability for individual species varied from 4 to 96%, but the mix of 20 strains consortia had the viability of 68%.

The next step was to estimate the bacteria viability by PMAxx reagent and qPCR. For that, cells from glycerol stocks were mixed in some proportion according to their OD and half of them were treated by PMAxx (viable cells), while another half stayed untreated (total cells). Extracted gDNA was analyzed by viability qPCR using strain-specific primers. Despite the relatively good correlation between FC and qPCR data (Fig. 1, $R^2 = 0.884$ with two outliers excluded and 0.789 when outliers are used), some differences were observed. Since microbial populations are usually heterogenic (Hewitt and Nebe-Von-Caron 2001), the FC data are not completely reliable. The formation of cellular chains and aggregates may lead to underestimation of cell number, but PCR enumeration depends on DNA amount only. Besides, both viability tests are based on the similar fluorescence dye penetration that could be a limitation for some bacterial species. This may be the reason why qPCR data using PMAxx reagent and strain-specific primers tended to show higher level of viable cells than FC.

To understand the nature of dissimilarities, microscopic evaluation of several bacterial strains was performed (Fig. 2). As seen from Fig. 2B, cells that showed a discrepancy between FC and qPCR data are more prone to generate clusters and fiber-like structures that can affect definite cloud formation and the subsequent FC data interpretation.

The study by Vandeputte et al. (2017) (Vandeputte et al., 2017) also showed that qPCR quantification is significantly comparable and negatively correlated with FC for absolute quantification of fecal microbiota by the same amplicon sequencing protocol. However, in the case of FC, when more than one cell population is observed, single microbial cells interact with each other forming aggregates, or cell and matrix debris are not completely excluded from the analyzed pellet. The obtained data are not entirely accurate and abnormal populations could be missed or misinterpreted. The complete dissociation of cells is not trivial for samples where bacteria are attached to each other or to the substrate, which makes an accurate counting by FC difficult. On the other hand,

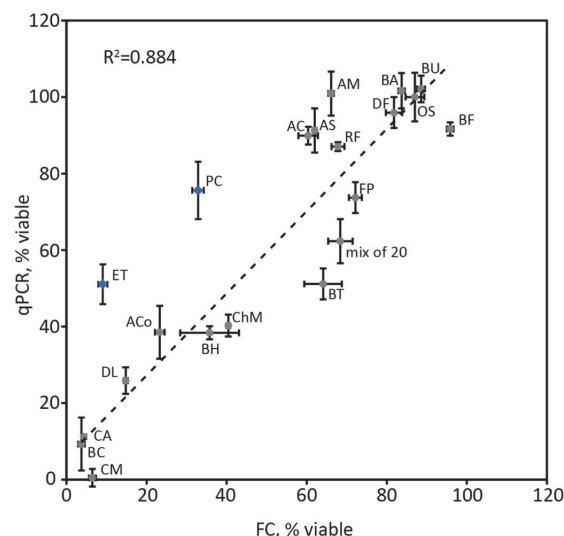


Fig. 1. Scatterplot for cell viability measured by FC and qPCR using strain-specific primers. The dotted line represents a linear regression trendline and R^2 shows the correlation. Bacterial strain acronyms can be found in Table 1. The grey circles represent points that were used for the trendline calculations, while the blue squares represent outliers. (For interpretation of the references to color in this figure legend, the reader is referred to the Web version of this article.)

the efficiency of PMAxx or any other reagent's penetration into a damaged cell could be limited. Also, the strength of dye-DNA covalent binding depends on the transparency of the cell's suspension. For colored matrices this efficiency could be decreased. At the same time, for not intensively colored matrixes, the covalent dye-DNA binding should be effective.

Overall, PMAxx dye is a reliable reagent that can be used to discriminate between viable and dead microbes in the NGS library preparation step, excluding damaged cells from the following analysis.

3.2. Bacterial enumeration of NGS

Next-generation sequencing is a powerful and reliable technology for taxonomic identification of bacteria. However, the common protocol

reveals only relative microbial distribution of the sample but does not provide information regarding absolute cell numbers. To evaluate the number of bacteria taken for sequencing, we applied spike-in cell control adding to the sample before DNA extraction procedure. We used commercial High-load Spike-in control from ZymoResearch with a defined amount of rarely occurred bacterial strains: *Imtechella halotolerans* and *Allobacillus halotolerans*. These spiked strains went through the whole NGS workflow and were used as *in situ* positive controls for the whole analysis. Knowing the exact amount of definite added cells, it is possible to recalculate the number of all bacteria in the sample.

First, we performed the titration of the spike-in control to confirm the linear dependence of the added cells in the number of the whole bacteria population. As seen from Fig. 3, a different percentage of added spike-in control linearly correlates ($R^2 = 0.9962$) with the total bacteria number. Thus, it is not necessary to add spike-in at an exact amount to obtain a reliable estimation of a microbial cell number in the sample.

According to the OD600 measurement of the cultures, the theoretical total number of consortia cells taken for analysis was about 1.50×10^9 . To estimate the total number of cells by the NGS, we used the number of reads of spike-in control related to the reads of consortia species from NGS data. Knowing the exact number of spike-in cells taken for analysis, we calculated the total bacterial cells in the sample (Table 2). Using a different amount of added spike-in cells (0.5, 1.0, and 2.5%), the average calculated total bacterial load was $1.55 \pm 0.18 \times 10^9$, which is quite accurate.

Adding the spike-in cells as an internal standard prior to the DNA extraction step is crucial as the standard is subjected to cell lysis and DNA extraction efficiency together with target bacteria by the same methodological workflow. Both are important for absolute quantification, especially the method of cell destroying for complex microbiota. The bead-beating step is recommended for full DNA recovery and is included in most reliable DNA extraction kits. Adding cells as a spike-in control for bacteria enumeration has one more universal merit – it is possible to use different regions or even the whole of 16S rRNA gene for sequencing and not be limited by 515F/806R primer pairs. This is important in the case of some species, where V4 region is not suitable for their identification and different fragments for higher resolution of lower-rank taxa should be used (Bukin et al., 2019).

It is important to mention that spike-in addition should be done before the DNA extraction step, which is not always possible, or the knowledge about the number of bacteria in a sample is necessary in retrospective. For that, the only chance to obtain an estimated bacterial concentration in the sample is from microbial gDNA concentration. Real-time PCR is an accepted methodology to obtain quantitative data

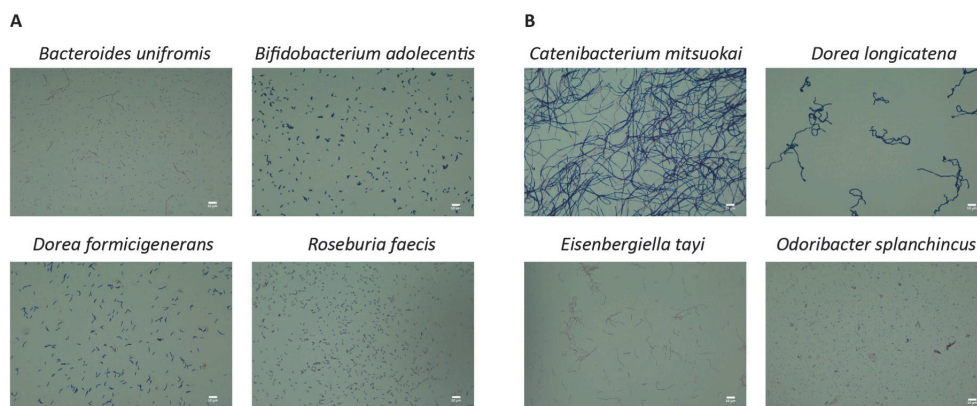


Fig. 2. Microscopy images of bacterial strains specific for (A) similar FC and qPCR data, and (B) different between FC and qPCR data. The white bar on the bottom right corner represents the length of 10 μ m.

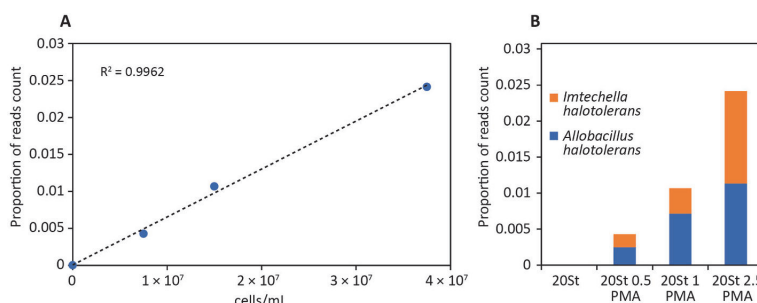


Fig. 3. Assessment of the quantitative performance of the spike-in standard for varying amounts of spike-in control added using 16S V4 amplicon NGS. (A) Dose-response correlation graph. (B) Relative abundance of spike-in species.

from DNA, as microbial gDNA concentration is directly proportional to bacteria cell number. To test the latter, we carried out qPCR using conservative 16S V4 region and degenerative primers for enumeration of bacteria in the samples (Table 3). Received by calibration curve methodology gDNA microbial concentration was converted to the total bacterial cell number which was $1.16 \pm 0.12 \times 10^9$ cells (20St qPCR). To compare with the theoretical value, the number of total cells calculated by the qPCR equation is of the same order but a lower number.

In our study, spike-in application led to very precise microbes' enumeration similar to FC, while data received by qPCR were slightly lower. Similar results were obtained by O. Zemb et al., (2020), where qPCR gave 1.9 times lower bacterial number estimates than artificial internal spike-in standard. In their work, qPCR allowed the increase of the sensitivity of the technology and minimize the amount of internal standard added when compared to the work published by Tkacz et al. (2018) (Tkacz et al. 2018), where they had to add 20–80% of the synthetic spike-in and thereby sacrifice the total sequencing input. The difference between qPCR and spike-in methodologies may be due to the degenerative primer usage, variances between 16S rRNA gene copy numbers for different species, or approximation between DNA mass and average cell number taken for analysis. Indeed, 16S rRNA gene copy number is determined by the dynamics of DNA replication and cell division (Cooper and Helmstetter 1968) and can change from 7 to 38 copies per cell even for *E. coli* (Bremer and Dennis 2008). It means that any estimation of cell number based on 16S rRNA gene copy number is biased if the population is growing, which should be considered for fast growing environments. Furthermore, PCR inhibitors would impact the bacterial estimation by qPCR, but it is fair to say that the same bias is appropriate for the whole amplicon-based sequencing pipeline. Despite all these bottlenecks, even qPCR combined with a standard curve quantification gave reliable data that can be considered as complementary quantification methods for bacterial count.

In general, both technologies showed comparable and reliable data, and thereby complemented each other.

3.3. Combined approach

The next step in the protocol development was to combine PMAxx treatment and bacteria enumeration procedures. For that, PMAxx-treated (for viable cell detection), and untreated (for total) microbial cells were subjected to spike-in addition, and the whole workflow of 16S amplicon sequencing was carried out. For alive bacteria enumeration, the analysis was performed in three parallels (20St 0.5PMA, 20St 1PMA, 20St 2.5PMA) that differed by the amount of *in situ* spike-in control added. The DNA sequencing data analysis showed that all 20 bacterial species were detected (Fig. 4). Moreover, the taxonomical distribution of viable bacteria performed in three parallels was consistent but differed from total bacteria profile. Thus, *Catenibacterium mitsuokai* and *Collinsella aerofaciens* were detected in total consortia but were absent among the viable cells, which correlates with FC and qPCR data (Fig. 4A, Table 1). Also, the number of *Bacteroides caccae* decreased in viable cells consortia in accordance with FC and qPCR analyses. In general, the viability of all members of 20-strain consortia assessed by NGS showed the pattern completely correlated with FC and qPCR data.

To represent results in absolute cell numbers, the data were normalized according to spike-in or qPCR quantification (Fig. 4B). The total amount of detected bacteria measured by spike-in control was $1.55 \pm 0.18 \times 10^9$ (Table 3), which is similar to that evaluated by FC quantity of 1.56×10^9 cells and close to the theoretical value. The average number of alive bacteria in the samples according to the spike-in control was $1.05 \pm 0.12 \times 10^9$ (20St alive Spike-in) while using qPCR approach – $7.03 \pm 0.25 \times 10^8$ cells (20St alive qPCR). FC data regarding bacterial viability estimation significantly correlated with spike-in enumeration and showed 1.06×10^9 alive cells in the sample. The calculated percentage of viability (Table 3) stayed in the range of 61–68% for all methods used.

Overall, for total and viable consortia, the cell number estimation was very similar between FC and spike-in sequencing methodology but the usage of qPCR as a method for cell number measurement resulted with slightly lower values.

3.4. Quantitative alive bacteria NGS for food samples

To demonstrate the potential of the methodology as applicable for real food samples, we chose three fermented foods for analysis – two kimchi prepared from Chinese and White cabbage (K4 and K5), and classical sauerkraut (K6). These food matrices can be considered complicated as they consist of plant material and are enriched with colorful tiny particles of spices that in case of kimchi gives an intensive color to cell pellets and interferes with DNA-PMAxx covalent binding. However, these are naturally fermented models and have enough bacteria for a proper analysis. Thus, the main task was to understand how our pipeline works for complex food matrices, describe their microbiological profiles, and find out the limitations and bottlenecks of the

Table 3

Assessment of various methods for cell number estimation for total and viable bacterial consortia.

Sample name	Cell number	Viability, %
20St theoretical	1.50×10^9	
20St FC	$1.56 \pm 0.17 \times 10^9$	68.41 ± 0.18
20St qPCR	$1.16 \pm 0.12 \times 10^9$	60.92 ± 3.98
20St spike-in	$1.55 \pm 0.18 \times 10^9$	67.79 ± 8.19
20St alive FC	$1.06 \pm 0.17 \times 10^9$	
20St alive qPCR	$7.03 \pm 0.25 \times 10^8$	
20St alive spike-in	$1.5 \pm 0.12 \times 10^9$	

*based on three parallel measurements.

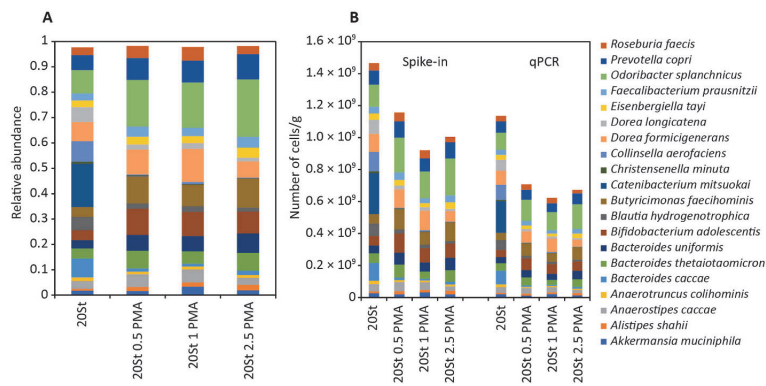


Fig. 4. Bacterial identification of total (20St) and alive (20St 0.5PMA, 20St 1PMA, 20St 2.5PMA) consortia samples based on 16S V4 amplicon NGS. (A) Relative abundance of bacterial distribution. (B) NGS data normalized to spike-in control and qPCR-based quantification.

technology.

For the method validation, classical microbiological methods such as PCA plating and FC were employed to estimate the number of viable bacteria and compared with the developed technology. Cells analyzed by NGS were divided by half and PMAxx treatment was applied for one part of the cell pellet (viable bacteria), while untreated cells were considered as total cell population. The results of the study represented in Table 4 show that the estimated number of cells measured by different methodologies does not differ significantly. In general, plating gave the lowest cell values, while spike-in technology operates with the highest numbers. As the majority of bacteria in the analyzed food samples belonged to LAB, for cell numbers calculation with qPCR we took the average genome size in the equation as 2.2 Mb (Klaenhammer et al., 2002). This led, in general, to similar values as for the spike-in approach. Thus, for kimchi samples, the numbers differed non-significantly but were lower in case of total bacteria number for sauerkraut (3.06×10^8 against 1.86×10^9 for qPCR and spike-in correspondingly), and higher for viable bacteria enumeration (Table 4). The common tendency is that the viable bacterial number was always lower compared to the total bacteria. The largest difference between all methodologies was observed for sauerkraut K6 samples, where the proportion of viable cell consortia was minimal for studied fermented food. In general, standard microbiological plating showed the lowest bacteria count. It is explained by the fact that not all bacteria are culturable or capable of growth on a specific unified medium within predefined conditions.

The whole elaborated sequencing pipeline that discriminates viable (PMA) and total (TOT) consortia and establishes bacteria enumeration (B) is introduced in Fig. 5. Analysis of viable and total bacterial distribution indicated that some bacteria disappeared from the total cell consortia. Thus, *Leuconostoc mesenteroides* was mainly detected among the total cells but not in viable cell profile. At the same time, the proportion of *Levilactobacillus* spp and *Lactiplantibacillus plantarum* were higher for viable bacteria. The differences between the total and viable taxonomical profiles are better evaluated by relative distribution analysis (Fig. 5A), while the real picture is clear only after the application of spike-in normalization methodology (Fig. 5B). This picture shows the actual pattern of total and viable bacteria in the samples. Overall, it means that both relative and absolute values must be evaluated and represented to make a conclusion regarding an analysis.

The next step for the method development could be the estimation of spike-in standard by qPCR with species-specific primers and assessment of more accurate DNA recovery yield. Another approach for more accurate qPCR quantification could be an application of individual genome sizes for identified bacteria instead of the average for the population for recalculating relative to absolute abundances. It will give more precise calculation of cell numbers in qPCR equation. It was shown in the case of kimchi and sauerkraut bacteria quantification, where the food samples contained mainly lactic acid bacteria. Correction of genome size for the LAB specific number in the equation led to more accuracy (similar to other methods of bacteria enumeration).

In summary, we can conclude that the introduced modifications are applicable to the real matrices. This complex technology is capable of differentiation between total and alive bacterial species and the acquisition of the absolute number of cells for the taxonomical description of food microbiota by NGS. This elaborated workflow provides much more information that can be used for technological process development, in shelf-life study, or for making decisions regarding safety issues.

Table 4
Bacterial enumeration of kimchi (K4 and K5) and sauerkraut (K6) microbiota by different methodologies.

Sample	Plating, cfu/g	Cell number by FC	Cell number by spike-in	Cell number by qPCR
K4 TOT		$1.49 \pm 0.26 \times 10^8$	8.56×10^8	$4.60 \pm 0.26 \times 10^8$
K4 PMA	$1.17 \pm 0.32 \times 10^8$	$2.61 \pm 0.05 \times 10^7$	3.97×10^8	$4.12 \pm 0.35 \times 10^8$
K5 TOT		$1.34 \pm 0.33 \times 10^8$	5.90×10^8	$5.66 \pm 1.65 \times 10^8$
K5 PMA	$3.64 \pm 0.12 \times 10^7$	$7.04 \pm 0.14 \times 10^7$	3.82×10^8	$3.73 \pm 0.16 \times 10^8$
K6 TOT		$1.26 \pm 0.05 \times 10^9$	1.86×10^9	$3.06 \pm 0.07 \times 10^9$
K6 PMA	$1.53 \pm 0.13 \times 10^7$	$5.96 \pm 0.02 \times 10^7$	1.28×10^8	$1.71 \pm 0.56 \times 10^8$

4. Conclusion

An integrated approach that combines new generation viability reagent usage and two alternative approaches for microbiological quantitative data assessment by spike-in control or qPCR with subsequent NGS analysis was elaborated. The full scheme of the workflow is indicated in Fig. 6. This modified sequencing workflow discriminates dead and viable microbial consortia and transforms sequencing-generated relative abundance data into a straightforward quantitative microbiota profile.

Although this method works well even in the case of real complex samples and can be routinely used for microbiological data acquisition and interpretation, it might need some further development and fine tuning. It should be noted that the methodology we proposed was tested on food samples but can be applied on any microbial sample. For example, this technology can be used for identification and evaluation of

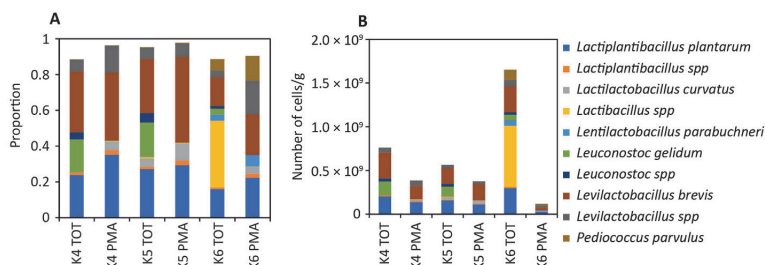


Fig. 5. The results of bacterial identification of total (TOT) and viable (PMA) kimchi and sauerkraut samples based on 16S V4 amplicon NGS. (A) Relative abundance of bacterial distribution. (B) NGS data normalized to spike-in standard.

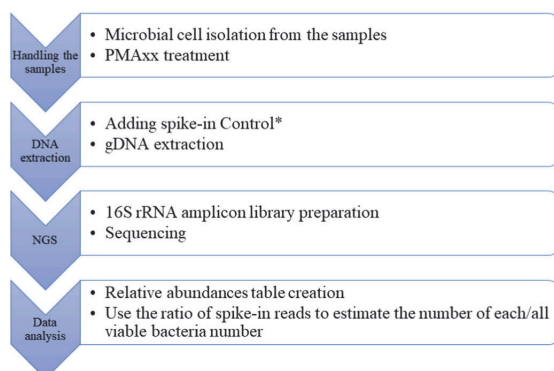


Fig. 6. The workflow used for identification and enumeration of viable microbiota by 16S rRNA NGS. *In case the spike-in control was not added, it is possible to estimate the bacterial load of the sample by qPCR approach.

viable pathogenic bacteria in any kind of environment, although it should be considered that sufficient sequencing depth per sample is designated, as NGS usually underestimates targets lower than 1% of relative abundance. Overall, an elaborated integrated workflow represents a further step in a complex approach for the application of next-generation sequencing for quantitative microbiota analysis.

Funding

This research was funded by EU European Regional Development Fund, grant number EU48667.

CRedit authorship contribution statement

Aili Kallastu: Methodology, Validation, Formal analysis, Investigation, Writing – review & editing, Visualization. **Esther Malv:** Methodology, Validation, Formal analysis, Investigation, Writing – review & editing, Visualization. **Valter Aro:** Formal analysis, Investigation, Writing – review & editing, Visualization. **Anne Meikas:** Methodology, Validation, Formal analysis, Investigation, Writing – review & editing. **Mariann Vendelin:** Validation, Investigation, Writing – review & editing. **Anna Kattel:** Validation, Investigation, Writing – review & editing. **Ranno Nahku:** Writing – review & editing. **Jekaterina Kazantseva:** Conceptualization, Methodology, Formal analysis, Data curation, Writing – original draft, Preparation, Writing – review & editing, Supervision, Project administration.

Declaration of competing interest

The authors declare that they have no known competing financial interests or personal relationships that could have appeared to influence the work reported in this paper.

Data availability

We uploaded data in public database and provided the link

Acknowledgments

The authors thank Johana Koppel for carrying out the bioinformatic analyses, and Ene Viirard and Tiina Kriscunaite for critical reading of the manuscript.

Appendix A. Supplementary data

Supplementary data to this article can be found online at <https://doi.org/10.1016/j.crfs.2023.100443>.

References

- Azarbad, Hamed, Tremblay, Julien, Bainard, Luke D., Yergeau, Etienne, 2022. Relative and quantitative rhizosphere microbiome profiling results in distinct abundance patterns. *Front. Microbiol.* 12 (January) <https://doi.org/10.3389/fmicb.2021.798023/FULL>.
- Bremer, Hans, Dennis, Patrick P., 2008. Modulation of chemical composition and other parameters of the cell at different exponential growth rates. *EcoSal Plus* 3 (1). <https://doi.org/10.1128/ecosal.5.2.3>.
- Bukin, Yu S., Galachyants, Yu P., Morozov, I.V., Bukin, S.V., Zakharenko, A.S., Zemskaya, T.I., 2019. The effect of 16S rRNA region choice on bacterial community metabarcoding results. *Sci. Data* 6. <https://doi.org/10.1038/sdata.2019.7>.
- Caporaso, J. Gregory, Lauber, Christian L., Walters, William A., Berg-Lyons, Donna, Lozupone, Catherine A., Turnbaugh, Peter J., Fierer, Noah, Knight, Rob, 2011. Global patterns of 16S rRNA diversity at a depth of millions of sequences per sample. *Proc. Natl. Acad. Sci. U.S.A.* <https://doi.org/10.1073/pnas.1000080107>.
- Cooper, Stephen, Helmstetter, Charles E., 1968. Chromosome replication and the division cycle of *Escherichia coli* B R. *J. Mol. Biol.* 31 (3) [https://doi.org/10.1016/0022-2836\(68\)90425-7](https://doi.org/10.1016/0022-2836(68)90425-7).
- Espinosa-Gongora, Carmen, Larsen, Niels, Schønning, Kristian, Fredholm, Merete, Guardabassi, Luca, 2016. Differential analysis of the nasal microbiome of pig carriers or non-carriers of *Staphylococcus aureus*. *PLoS One*. <https://doi.org/10.1371/journal.pone.0160331>.
- Fanning, Séamus, Proos, Sinéad, Jordan, Kieran, Srikanth, Shabarinath, 2017. A review on the applications of next generation sequencing technologies as applied to food-related microbiome studies. *Front. Microbiol.* <https://doi.org/10.3389/fmicb.2017.01829>.
- Galazzo, Gianluca, van Best, Niels, Benedikter, Birke J., Janssen, Kevin, Bervoets, Liene, Driessen, Christel, Oomen, Melissa, et al., 2020. How to count our microbes? The effect of different quantitative microbiome profiling approaches. *Front. Cell. Infect. Microbiol.* 10 <https://doi.org/10.3389/fcimb.2020.00403>.
- Hewitt, Christopher J., Nebe-Von-Caron, Gerhard, 2001. "An industrial application of multiparameter flow cytometry: assessment of cell physiological state and its application to the study of microbial fermentations." In: *Cytometry*, vol. 44 <https://doi.org/10.1002/1097-0320.2001070144:3<179::AID-CYTO1110>3.0.CO;2-D>.
- Jagadeesan, Balamurugan, Gerner-Smidt, Peter, Allard, Marc W., Leuillet, Sébastien, Winkler, Anett, Xiao, Yinghua, Chaffron, Samuel, et al., 2019. The use of next

- generation sequencing for improving food safety: translation into practice. *Food Microbiol.* 79 (June), 96–115. <https://doi.org/10.1016/J.FM.2018.11.005>.
- Jin, Jianshi, Yamamoto, Reiko, Takeuchi, Tadashi, Cui, Guangwei, Miyauchi, Eiji, Hojo, Nozomi, Ikuta, Koichi, Ohno, Hiroshi, Shiroguchi, Katsuyuki, 2022. High-throughput identification and quantification of single bacterial cells in the microbiota. *Nat. Commun.* 13 (1) <https://doi.org/10.1038/s41467-022-28426-1>.
- Kazantseva, Jekaterina, Malv, Esther, Kaleda, Aleksei, Kallastu, Aili, Meikas, Anne, 2021. Optimisation of sample storage and DNA extraction for human gut microbiota studies. *BMC Microbiol.* 21 (1) <https://doi.org/10.1186/s12866-021-02233-y>.
- Kim, Jaai, Lim, Juntaek, Lee, Changsoo, 2013. Quantitative real-time PCR approaches for microbial community studies in wastewater treatment Systems: applications and considerations. *Biotechnol. Adv.* <https://doi.org/10.1016/j.biotechadv.2013.05.010>.
- Klaenhammer, Todd, Altermann, Eric, Arigoni, Fabrizio, Alexander, Bolotin, Breidt, Fred, Broadbent, Jeffrey, Cano, Raul, et al., 2002. Discovering lactic acid bacteria by genomics. *Antonie van Leeuwenhoek, International Journal of General and Molecular Microbiology* 82 (1–4). <https://doi.org/10.1023/A:1020638309912>.
- Liu, Cindy M., Aziz, Maliha, Kachur, Sergey, Ren Hsueh, Po, Tsung Huang, Yu, Paul, Keim, Price, Lance B., 2012. "BactQuant: an enhanced broad-coverage bacterial quantitative real-time PCR Assay.". *BMC Microbiol.* 12 <https://doi.org/10.1186/1471-2180-12-56>.
- Mayo, Baltasar, Rachid, Caio, Alegria, Angel, Leite, Analy, Peixoto, Raquel, Delgado, Susana, 2014. Impact of next generation sequencing techniques in food microbiology. *Curr. Genom.* 15 (4) <https://doi.org/10.2174/1389202915666140616233211>.
- McDonald, James E., Larsen, Niels, Pennington, Andrea, Connolly, John, Wallis, Corrin, Rooks, David J., Hall, Neil, McCarthy, Alan J., Allison, Heather E., 2016. Characterising the canine oral microbiome by direct sequencing of reverse-transcribed RRNA molecules. *PLoS One.* <https://doi.org/10.1371/journal.pone.0157046>.
- Muyzer, Gerard, Ramsing, Niels B., 1995. Molecular methods to study the organization of microbial communities. *Water Sci. Technol.* 32 (8) [https://doi.org/10.1016/0273-1223\(96\)00001-7](https://doi.org/10.1016/0273-1223(96)00001-7).
- Piwoz, Kasia, Shabarova, Tanja, Tomasch, Jürgen, Šimek, Karel, Kopejtká, Karel, Kahl, Silke, Pieper, Dietmar H., Koblížek, Michal, 2018. Determining lineage-specific bacterial growth curves with a novel approach based on amplicon reads normalization using internal standard (ARNIS). *ISME J.* 12 (11) <https://doi.org/10.1038/s41396-018-0213-y>.
- Proops, Ruben, , Frederiek Maarten Kerckhof, Rubbens, Peter, De Vrieze, Jo, Hernandez Sanabria, Emma, Waegeman, Willem, Monsieurs, Pieter, Hammes, Frederik, Boon, Nico, 2017. Absolute quantification of microbial taxon abundances. *ISME J.* 11 (2) <https://doi.org/10.1038/ismej.2016.117>.
- Smets, Wenke, Leff, Jonathan W., Bradford, Mark A., McCulley, Rebecca L., Lebeer, Sarah, Fierer, Noah, 2016. A method for simultaneous measurement of soil bacterial abundances and community composition via 16S rRNA gene sequencing. *Soil Biol. Biochem.* <https://doi.org/10.1016/j.soilbio.2016.02.003>.
- Stämmeler, Frank, Gläsner, Joachim, Hiergeist, Andreas, Holler, Ernst, Weber, Daniela, Oefner, Peter J., Gessner, André, Spang, Rainer, 2016. Adjusting microbiome profiles for differences in microbial load by spike-in bacteria. *Microbiome* 4. <https://doi.org/10.1186/s40168-016-0175-0>.
- Stewart, Eric J., 2012. Growing unculturable bacteria. *J. Bacteriol.* <https://doi.org/10.1128/JB.00345-12>.
- Tkacz, Andrzej, Hortal, Marion, Poole, Philip S., 2018. Absolute quantitation of microbiota abundance in environmental samples. *Microbiome* 6 (1). <https://doi.org/10.1186/s40168-018-0491-7>.
- Tourlousse, Dieter M., Ohashi, Akiko, Yuji, Sekiguchi, 2018. Sample tracking in microbiome community profiling assays using synthetic 16S rRNA gene spike-in controls. *Sci. Rep.* 8 (1) <https://doi.org/10.1038/s41598-018-27314-3>.
- Tourlousse, Dieter M., Yoshiike, Satowa, Ohashi, Akiko, Matsukura, Satoko, Noda, Naohiro, Sekiguchi, Yuji, 2017. Synthetic spike-in standards for high-throughput 16S rRNA gene amplicon sequencing. *Nucleic Acids Res.* <https://doi.org/10.1093/nar/gkw984>.
- Vandeputte, Doris, Gunter, Kathagen, Kevin, D'Hoe, Vieira-Silva, Sara, Valles-Colomer, Mireia, Sabino, João, Wang, Jun, et al., 2017. Quantitative microbiome profiling links gut community variation to microbial load. *Nature* 551 (7681). <https://doi.org/10.1038/nature24460>.
- Zemb, Olivier, Achard, Caroline S., Hamelin, Jerome, Léa De Almeida, Marie, Gabinaud, Béatrice, Cauquil, Laurent, Lisanne, M., Verschuren, G., Godon, Jean Jacques, 2020. Absolute quantitation of microbes using 16S rRNA gene metabarcoding: a rapid normalization of relative abundances by quantitative PCR targeting a 16S rRNA gene spike-in standard. *MicrobiologyOpen.* <https://doi.org/10.1002/mbo3.977>.

Curriculum vitae

Personal data

Name: Anna Kattel
Date of birth: 19.11.1995
Place of birth: Põlva, Estonia
Citizenship: Estonian
ORCID: 0000-0002-8105-278X

Contact data

E-mail: anna.kattel11@gmail.com

Education

2019–2025 Tallinn University of Technology, Applied Chemistry and Biotechnology, PhD
2017–2019 Tallinn University of Technology, Applied Chemistry and Biotechnology, MSc
2014–2017 Tallinn University of Technology, Applied Chemistry and Biotechnology, BSc
2011–2014 Tartu Tamme Gümnaasium, High school

Language competence

Estonian Native
English Fluent

Professional employment

2024– ... Tallinn University of Technology, Specialist in valorisation of natural raw materials
2024 AS TFTAK, Senior research specialist
2022–2024 AS TFTAK, Project manager
2019–2022 AS TFTAK, Researcher

Supervised theses

2023 Liselle Kaldaru “Developing production of next-generation probiotic co-cultures using a unique substrate”

Publications

Kattel, A., Aro, V., Lahtvee, P. J., Kazantseva, J., Jöers, A., Nahku, R., & Belouah, I. (2024). Exploring the resilience and stability of a defined human gut microbiota consortium: An isothermal microcalorimetric study. *MicrobiologyOpen*, 13(4). <https://doi.org/10.1002/mbo3.1430>

Pismennõi, D., **Kattel, A.**, Belouah, I., Nahku, R., Vilu, R., & Kobrin, E. G. (2023). The Quantitative Measurement of Peptidoglycan Components Obtained from Acidic Hydrolysis in Gram-Positive and Gram-Negative Bacteria via Hydrophilic Interaction Liquid Chromatography Coupled with Mass Spectrometry. *Microorganisms*, 11(9). <https://doi.org/10.3390/microorganisms11092134>

Kattel, A., Morell, I., Aro, V., Lahtvee, P. J., Vilu, R., Jöers, A., & Nahku, R. (2023). Detailed analysis of metabolism reveals growth-rate-promoting interactions between *Anaerostipes caccae* and *Bacteroides* spp. *Anaerobe*, 79. <https://doi.org/10.1016/j.anaerobe.2022.102680>

Kallastu, A., Malv, E., Aro, V., Meikas, A., Vendelin, M., **Kattel, A.**, Nahku, R., & Kazantseva, J. (2023). Absolute quantification of viable bacteria abundances in food by next-generation sequencing: Quantitative NGS of viable microbes. *Current Research in Food Science*, 6(December 2022), 100443. <https://doi.org/10.1016/j.crfs.2023.100443>

Conferences

September 2023 Life Sciences Baltics; Vilnius, Lithuania

July 2022 Microbiome Connect: Europe; Amsterdam, Netherlands. Oral presentation

September 2019 Intensive course “Pro-, pre-, syn- and postbiotics: the effect on our microbiota and health”; Tartu, Estonia

Elulookirjeldus

Isikuandmed

Nimi: Anna Kattel
Sünniaeg: 19.11.1995
Sünnikoht: Põlva, Eesti
Kodakondsus: Eesti
ORCID: 0000-0002-8105-278X

Kontaktandmed

E-post: anna.kattel11@gmail.com

Hariduskäik

2019–2025 Tallinna Tehnikaülikool, Keemia ja biotehnoloogia PhD
2017–2019 Tallinna Tehnikaülikool, Rakenduskeemia ja biotehnoloogia, MSc
2014–2017 Tallinna Tehnikaülikool, Rakenduskeemia ja biotehnoloogia, BSc
2011–2014 Tartu Tamme Gümnaasium

Keelteoskus

Eesti keel Emakeel
Inglise keel Kõrgtase

Teenistuskäik

2024–... Tallinna Tehnikaülikool, biotoorme väärindamise ekspert
2024 AS TFTAK, vanemarendusspetsialist
2022–2024 AS TFTAK, projektijuht
2019–2022 AS TFTAK, nooremteadur

Juhendatud lõputööd

2023 Liselle Kaldaru “Uue põlvkonna probiootikumide koosluste tootmise arendamine kasutades unikaalsete substraatide lähenemist”

Publikatsioonid

Kattel, A., Aro, V., Lahtvee, P. J., Kazantseva, J., Jöers, A., Nahku, R., & Belouah, I. (2024). Exploring the resilience and stability of a defined human gut microbiota consortium: An isothermal microcalorimetric study. *MicrobiologyOpen*, 13(4). <https://doi.org/10.1002/mbo3.1430>

Pismennõi, D., **Kattel, A.**, Belouah, I., Nahku, R., Vilu, R., & Kobrin, E. G. (2023). The Quantitative Measurement of Peptidoglycan Components Obtained from Acidic Hydrolysis in Gram-Positive and Gram-Negative Bacteria via Hydrophilic Interaction Liquid Chromatography Coupled with Mass Spectrometry. *Microorganisms*, 11(9). <https://doi.org/10.3390/microorganisms11092134>

Kattel, A., Morell, I., Aro, V., Lahtvee, P. J., Vilu, R., Jöers, A., & Nahku, R. (2023). Detailed analysis of metabolism reveals growth-rate-promoting interactions between *Anaerostipes caccae* and *Bacteroides* spp. *Anaerobe*, 79. <https://doi.org/10.1016/j.anaerobe.2022.102680>

Kallastu, A., Malv, E., Aro, V., Meikas, A., Vendelin, M., **Kattel, A.**, Nahku, R., & Kazantseva, J. (2023). Absolute quantification of viable bacteria abundances in food by next-generation sequencing: Quantitative NGS of viable microbes. *Current Research in Food Science*, 6(December 2022), 100443. <https://doi.org/10.1016/j.crfs.2023.100443>

Konverentsid

September 2023 Life Sciences Baltics; Vilnius, Leedu

Juuli 2022 Microbiome Connect: Europe; Amsterdam, Holland. Suuline ettekanne

September 2019 Intensiivkursus “Pro-, pre-, syn- ja postbiootikumid: mõju meie mikrobiootale ja tervisele”; Tartu, Eesti

ISSN 2585-6901 (PDF)
ISBN 978-9916-80-359-2 (PDF)